UNIVERSITAT ROVIRA I VIRGILI

# ASSESSMENT OF THE HUMAN HEALTH RISKS AND TOXICITY ASSOCIATED TO PARTICLES (PM10, PM2.5 AND PM1), ORGANIC POLLUTANTS AND METALS AROUND CEMENT PLANTS

**Francisco Sánchez Soberón**

**ADVERTIMENT**. L'accés als continguts d'aquesta tesi doctoral i la seva utilització ha de respectar els drets de la persona autora. Pot ser utilitzada per a consulta o estudi personal, així com en activitats o materials d'investigació i docència en els termes establerts a l'art. 32 del Text Refós de la Llei de Propietat Intel·lectual (RDL 1/1996). Per altres utilitzacions es requereix l'autorització prèvia i expressa de la persona autora. En qualsevol cas, en la utilització dels seus continguts caldrà indicar de forma clara el nom i cognoms de la persona autora i el títol de la tesi doctoral. No s'autoritza la seva reproducció o altres formes d'explotació efectuades amb finalitats de lucre ni la seva comunicació pública des d'un lloc aliè al servei TDX. Tampoc s'autoritza la presentació del seu contingut en una finestra o marc aliè a TDX (framing). Aquesta reserva de drets afecta tant als continguts de la tesi com als seus resums i índexs.

**ADVERTENCIA.** El acceso a los contenidos de esta tesis doctoral y su utilización debe respetar los derechos de la persona autora. Puede ser utilizada para consulta o estudio personal, así como en actividades o materiales de investigación y docencia en los términos establecidos en el art. 32 del Texto Refundido de la Ley de Propiedad Intelectual (RDL 1/1996). Para otros usos se requiere la autorización previa y expresa de la persona autora. En cualquier caso, en la utilización de sus contenidos se deberá indicar de forma clara el nombre y apellidos de la persona autora y el título de la tesis doctoral. No se autoriza su reproducción u otras formas de explotación efectuadas con fines lucrativos ni su comunicación pública desde un sitio ajeno al servicio TDR. Tampoco se autoriza la presentación de su contenido en una ventana o marco ajeno a TDR (framing). Esta reserva de derechos afecta tanto al contenido de la tesis como a sus resúmenes e índices.

**WARNING**. Access to the contents of this doctoral thesis and its use must respect the rights of the author. It can be used for reference or private study, as well as research and learning activities or materials in the terms established by the 32nd article of the Spanish Consolidated Copyright Act (RDL 1/1996). Express and previous authorization of the author is required for any other uses. In any case, when using its content, full name of the author and title of the thesis must be clearly indicated. Reproduction or other forms of for profit use or public communication from outside TDX service is not allowed. Presentation of its content in a window or frame external to TDX (framing) is not authorized either. These rights affect both the content of the thesis and its abstracts and indexes.

Francisco Sánchez Soberón

# ASSESSMENT OF THE HUMAN HEALTH RISKS AND TOXICITY ASSOCIATED TO PARTICLES ($PM_{10}$, $PM_{2.5}$ AND $PM_1$), ORGANIC POLLUTANTS AND METALS AROUND CEMENT PLANTS

DOCTORAL THESIS

Supervisors:

Dra. Marta Schuhmacher Ansuategui

Dr. Joaquim Rovira Solano

CHEMICAL ENGINEERING DEPARTMENT

UNIVERSITAT
ROVIRA i VIRGILI

Tarragona 2017

UNIVERSITAT
ROVIRA i VIRGILI

FAIG CONSTAR que aquest treball, titulat “**Assessment of the human health risks and toxicity associated to particles (PM$_{10}$, PM$_{2.5}$ and PM$_{1}$), organic pollutants and metals around cement plants**”, que presenta **Francisco Sánchez Soberón** per a l’obtenció del títol de Doctor, ha estat realitzat sota la meva direcció al Departament d’Enginyeria Química d’aquesta universitat.

---

HAGO CONSTAR que el presente trabajo, titulado “**Assessment of the human health risks and toxicity associated to particles (PM$_{10}$, PM$_{2.5}$ and PM$_{1}$), organic pollutants and metals around cement plants**”, que presenta **Francisco Sánchez Soberón** para la obtención del título de Doctor, ha sido realizado bajo mi dirección en el Departamento de Ingeniería Química de esta universidad.

---

I STATE that the present study, entitled “**Assessment of the human health risks and toxicity associated to particles (PM$_{10}$, PM$_{2.5}$ and PM$_{1}$), organic pollutants and metals around cement plants**”, presented by **Francisco Sánchez Soberón** for the award of the degree of Doctor, has been carried out under my supervision at the Chemical Engineering Department of this university.

---

Tarragona, a 13 de Diciembre de 2017

El/s director/s de la tesi doctoral
El/los director/es de la tesis doctoral
Doctoral Thesis Supervisor/s

Marta Schuhmacher Ansuategui

Joaquim Rovira Solano

# ACKNOWLEDGEMENTS

I sincerely wanted to show my thankfulness to all the people that have helped me along this process of thesis development.

First of all, I would like to express my huge gratitude to my two supervisors, Professor Mrs. Marta Schuhmacher and PhD Mr. Joaquim Rovira for giving me the opportunity of being a PhD student and their guidance during all this time. Without them, none of this thesis would be possible.

Also, I would like to thank all the people who has been surrounding and enduring me in this laborious task. Since I know I will forget someone, I will be very coward here and generalize *ad libitum*. Thanks to all crew from AGA and Tecnatox group. Without your support and good vibes at work this last 4 years would have been a very tough time! Thanks also to all the people from Antwerp and Cardiff: this document would not be complete without you, and, apart from learning gigantically from you, I have to say that you know how to make a visitor feel at home.

I will be also right grateful to all those folks doing my life easier out of the job, and very specifically to Petra, who has been literally belaying me this entire big wall. Thanks for your patience!

And last, but not least, I owe a deep gratitude to my parents, siblings, and nephews. They have been suffering (with) me long before the development of this thesis, doing my life easier when staying by them.

# ABBREVIATIONS

BaP: Benzo[a]pyrene

COLD: Chronic Obstructive Lung Disease

CD: Cement Dust

EEA: European Environmental Agency

EC: Elemental Carbon

FESEM: Field Emission Scanning Electron Microscopy

GC-MS: Gas Chromatography coupled to Mass Spectrometry

HQ: Hazard Quotient

ICP-MS: Inductive Coupled Plasma Mass Spectrometry

ICP-OES: Inductive Coupled Plasma Optical Emission Spectrometry

IRMS: Isotope Ratio Mass Spectrometry

$LC_5$: Lethal Concentration eliciting 5% mortality

MCR-ALS: Multivariate Curve Resolution by Alternating Least Squares

NADPH: Nicotinamide Adenine Dinucleotide Phosphate

NOAEL: No-Observed-Adverse-Effect Level

NF-κB: Nuclear factor kappa-light-chain-enhancer of activated B cells

OC: Organic Carbon

LPS: Lipopolysaccharide

PAH: Polycyclic Aromatic Hydrocarbon

PCA: Principal Component Analysis

PCDD/Fs: Polychlorinated Dibenzo-p-dioxins and dibenzofurans

PM: Particulate Matter

RfC: Reference concentration

ROS: Reactive Oxygen Species

SOA: Secondary Organic Aerosols

TNFα: Tumor Necrosis Factor α

TOC: Total Organic Carbon

UF: Uncertainty Factor

USEPA: United States Environmental Protection Agency

WHO: World Health Organization

# TABLE OF CONTENTS

# SUMMARY

## Summary

Particulate Matter (PM) is considered the most hazardous air pollutant. Its effects are mainly focused on the respiratory and cardiovascular system, and range from increasing coughing and asthma, to lung cancer and heart attacks. These effects depend profoundly on the physicochemical properties of the PM. The smaller the size, and the higher the content in toxicants (i.e.: heavy metals, polycyclic aromatic hydrocarbons (PAHs), quinones, and endotoxins) the more hazardous the PM is. Since its composition is highly variable depending on sources and meteorological conditions, for regulatory purposes PM is usually classified into two categories attending to its size: $PM_{10}$ and $PM_{2.5}$ (smaller than 10 and 2.5 µm respectively). Besides these two fractions, it is lately becoming usual to focus also on those particles smaller than 1 µm ($PM_1$), since their small size allow them to get to deeper parts of the respiratory system.

Particulate matter is released as a consequence of several natural and anthropogenic activities, such as volcanoes, sea spray, traffic, and industries. One of the industrial activities historically recognized as a source of PM is the cement manufacture. In this industry, great amounts of raw materials and fuels are combusted together till reaching temperatures close to 1500ºC needed to form the clinker. In order to save energy and minimize production costs, different kinds of wastes and byproducts from other industries are used inside the cement kiln as both, alternative fuels and raw materials. The combination of this wide array of materials, joined with the high temperature processes undergoing inside the cement kiln introduces a high variability in the physicochemical characteristics of PM released from the stack of cement industries. Furthermore, storage, transport, and processing of raw materials and clinker could generate fugitive emissions of PM.

Despite the great body of knowledge already published focused on the hazardous potential of cement PM, most of it is focused on the study of $PM_{10}$. Furthermore, some aspects of these particles (such as their toxicity) have not been properly addressed. To surpass this gap we decided to study the physicochemical characteristics and toxicity of $PM_{10}$, $PM_{2.5}$, and $PM_1$ nearby a cement plant located in the outskirts of Barcelona (Spain) in different seasons. To know the environmental threats that population was facing, we calculated the exposure and human health risks derived from the inhalation of this pollutant. Finally, we elucidated the contribution from the cement plant to overall environmental PM levels.

Our results showed that around 60% of the $PM_{10}$ mass collected nearby the cement plant is comprised of $PM_1$ regardless of season. Winter registered the highest levels of PM, due to the increase in number and intensity of PM sources and meteorological conditions. Fine fractions ($PM_{2.5}$ and $PM_1$) showed a greater composition in most toxicants, such as some heavy metals (As, Pb, Cd, Mn, Cr (VI)) and PAHs. The microscopy study showed a great influence of combustion processes (i.e. traffic, domestic heating and cement plant) in $PM_{2.5}$, while a higher influence of mineral and biological sources was patent in bigger particles.

The toxicity studies carried out in this thesis showed that oxidative potential, mortality, and mucus secretion of tracheobronchial cells were higher after exposure to $PM_{2.5}$ than $PM_{10}$. On the other hand, cells exposed to $PM_{10}$ suffered a higher disruption of their cell barrier integrity. Histological observation of the tissues exposed to $PM_{2.5}$ showed a higher mucus release and greater size and density of vacuoles than tissues exposed to $PM_{10}$.

An infiltration model bound to a dosimetry model was used to study the exposure of population in different microenvironments, and to study deposition patterns of PM within the human respiratory tract. Despite the low share of time spent in the open, outdoor activities accounted for most of the deposited mass of PM in the respiratory tract. While $PM_{10}$ was mostly retained in the nasal area, $PM_{2.5}$ and $PM_1$ were able to get to lungs. Similar amounts of $PM_{2.5}$ and $PM_1$ reached the lung regardless of population group, which is especially concerning for children.

Non-carcinogenic risks were below the safety threshold (Hazard Quotient<1) for every measured toxicant (i.e. toxic metals and PAHs). Carcinogenic risks were below the threshold considered as acceptable (1 case of cancer every 100,000 inhabitants) for most metals and PAHs, except for Cr (VI), that reached a value of around 3 cases of cancer out of 100,000 inhabitants.

Finally, after applying complimentary tools of source apportionment it was seen that combustion sources were the majoritarian contributors to overall PM pool. By studying inorganic components it was possible to deduce that cement plant was the most prevalent source during winter. Subsequent application of Multivariate Curve Resolution by Alternating Least Squares (MCR-ALS) onto organic components of PM was used to confirm that, as seen in the chemical characterization and microscopy, contribution from combustion sources were higher when decreasing the PM size. Studying isotopic ratio of samples confirmed this trend.

# INTRODUCTION

# Introduction

## Particulate matter: definition, composition, sources, and health concerns

Particulate matter (PM) is a mixture of liquid droplets and solid fragments floating ubiquitously in the air. It is very variable in size, shape, and chemical composition, being included under this definition materials as heterogeneous as dust, smoke, pollen or soot (EEA, 2015). The breathable fraction of PM is referred as $PM_{10}$, since it has a size smaller than 10 µm. $PM_{10}$ could be then be divided into two categories attending to its size: "coarse" fraction (having a diameter between 10 and 2.5 µm), and "fine" fraction (also known as $PM_{2.5}$, having a diameter smaller than 2.5 µm) (Kelly and Fussell, 2012; USEPA, 2016). In addition to these two fractions, there is nowadays getting a higher attention the study of those particles in the nanometer (<100 nm) scale, denoted ultrafine particles or $PM_{0.1}$ (Nemmar et al., 2013). Since it is still challenging the collection of ultrafine particles, an usual approach is to focus on "quasy-ultrafine" particles (smaller than 1 µm, or $PM_1$) (Figure 1).

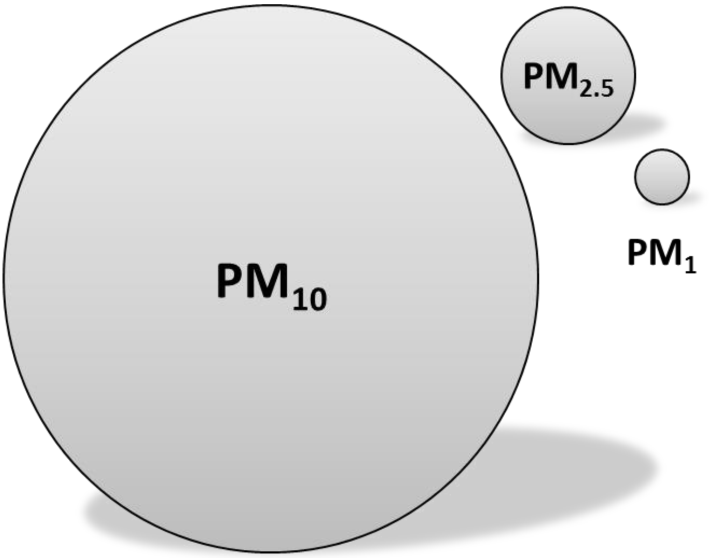

**Figure 1:** Representative sketch depicting the more relevant sizes of PM.

Coarse fraction includes particles related to natural origin, such as sea spray, pollen, and fungi spores. It also includes PM generated by anthropogenic activities, like grinding and crushing, and particles generated from soil and dust resuspension by traffic and agriculture (Cassee et al., 2013; Guevara, 2016). Due to its origins coarse fraction is usually rich in macroelements (Ni, Fe, Ca, Al) (Kim et al., 2003).

Fine ($PM_{2.5}$) and ultrafine ($PM_{0.1}$) are usually more related to combustion (traffic engines, domestic heating) and high temperature processes (industry, power plants) (Kelly and Fussell, 2012). Furthermore, fine particles comprises also most of the secondary particles, generated as consequence of gas-to-particle and condensation processes in the atmosphere (Hallquist et al., 2009). Consequently, these particles are richer in secondary compounds (i.e. nitrates, sulfates), organic carbon (OC), and elemental carbon (EC) (WHO, 2000).

Nowadays, PM is a concern due to its harmful potential for health, being involved in several diseases affecting the respiratory and cardiovascular systems (USEPA, 2016). Although coarse PM has been related to eyes, throat, and nose irritation, as well as asthma attacks, there is still a few studies focused on the pernicious effects of this pollutant (Adar et al., 2014; Lin et al., 2002; US EPA, 2017). Higher attention has been put on $PM_{2.5.}$ Due to its size, this fraction is able to get to the deepest parts of the respiratory system, and eventually pass the air-blood barrier (US EPA, 2016a). Consequently, long term exposures to this pollutant could lead to lung cancer and heart attacks (WHO, 2013). In fact, numerous studies state that $PM_{2.5}$ is the most dangerous air pollutant, responsible of 2 to 3 million premature deaths per year globally (Donahue et al., 2016).

### Mode of action of PM

In order to properly understand potential damage of PM it is important to know how it elicits toxicity inside the human body. Several studies dealing with this question agree that damage caused by the PM in the lung cells is linked to the capacity of generating reactive oxygen species (ROS) (Akhtar et al., 2010; Delgado-Buenrostro et al., 2013; Kelly and Fussell, 2012; von Moos and Slaveykova, 2014). The presence of ROS interacts with the NF-κB, which is a protein complex involved, among others, in the control of cell immunology, inflammatory response, growth, and apoptosis. As a consequence of that, this complex is active in several pulmonary diseases including lung cancer, chronic inflammation and asthma (Gilmore, 2009).

Mechanisms of ROS generation could be undertaken in two different places (Figure 2):

1. Extracellular location: This mechanism happens outside the cell. Extracellular ROS generation occurs in various ways including direct redox reactions between PM and

biomolecules present in the respiratory tract lining fluid. The presence of extracellular ROS can stimulate the intracellular generation of ROS in response (von Moos and Slaveykova, 2014).

2. Intracellular location: ROS damage is generated when PM get in contact with cells. Here we can find two different kind of damage:

   2.1. *Chemical damage*: Four main compounds are recognized as the main triggers of ROS generation:

- Redox active metals. Once into the lung, they can interact with intracellular biological reducing agents (such as glutathione or nicotinamide adenine dinucleotide phosphate (NADPH)) present in the cytoplasm (Faiola et al., 2011). The reduced metal can then return to its initial form by interacting with intracellular oxygen to yield the superoxide radical ($O_2^-$), hydrogen peroxide ($H_2O_2$), and hydroxyl radical (·OH).
- Same pathway is followed by quinones**,** that in presence of biological reductants can be reduced to form the semi-quinone radical ($SQ\cdot^-$) that will also yield $O_2^-$ and $H_2O_2$ in presence of oxygen (Kelly and Fussell, 2012).
- Bacterial endotoxins associated with the particle surface can trigger inflammation through its interaction with lipopolysaccharide (LPS) receptors. Once the receptor in engaged with a LPS (i.e. endotoxin), it activates the NF-κB complex (Calvano et al., 2003).
- Polycyclic aromatic hydrocarbons (PAHs) are not oxidative species *per se*, but they can undergo biotransformation in vivo into quinones (Moorthy et al., 2015).

   2.2. *Mechanical damage:* there are different physical mechanisms by which PM could induce toxicity to lung cells:

- Physical interactions of PM surface with the membranes of cells can induce direct ROS yielding mechanisms. PM with positive charge induced more toxic effects than their counterparts with negative charge, which might be attributed to the attractive or repulsive interaction between the positively or negatively charged PM and the negatively charged cell surface (Jiang et al., 2008; K. Li et al., 2012). Furthermore, interactions of PM with membrane-bound enzymes could lead to the formation of ROS (von Moos and Slaveykova, 2014).

- Same interactions than described above could be found between the particle surface and the membranes of subcellular compounds when the PM is able to get into the cell. Thus, electron transport chains in peroxisomes, mitochondria and the endoplasmic reticulum are disrupted after contact with PM surface, which produce ROS (Hou et al., 2010; Li et al., 2015).
- Interactions between organelle and PM can also cause a loss of integrity in the organelle membrane, releasing $Ca^{2+}$ to the cytoplasm. This increase in $Ca^{2+}$ levels activate some $Ca^{2+}$/calmodulin-dependent enzymes, which leads to the generation of ROS (Li et al., 2015; von Moos and Slaveykova, 2014).

So the way of action of PM is a mixture of several processes, where the whole picture should be taken into account. In order to properly address this, physicochemical characteristics of the PM should be taken into account.

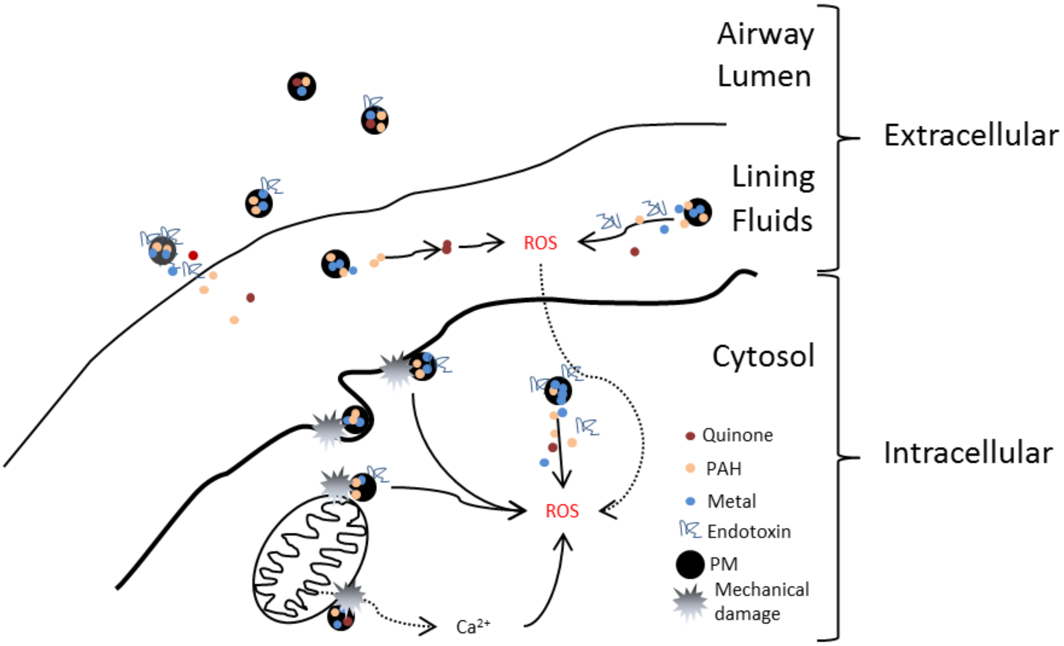

**Figure 2:** Sketch depicting PM way of action in pulmonary cells. Adapted from von Moos and Slaveykova (2014).

### PM sources: the case of cement industry

PM size, shape, and composition are conditioned by its source. PM has both, natural and anthropogenic origin. Among the natural origin of PM we can name pollen, mineral and soil resuspension, and wildfires (EEA, 2012). But nowadays, the most hazardous particles are those having human origin (Tainio et al., 2010). Road traffic, industry, power plants, and domestic heaters are amongst the main sources of anthropogenic PM (Figure 3, (EEA, 2017)).

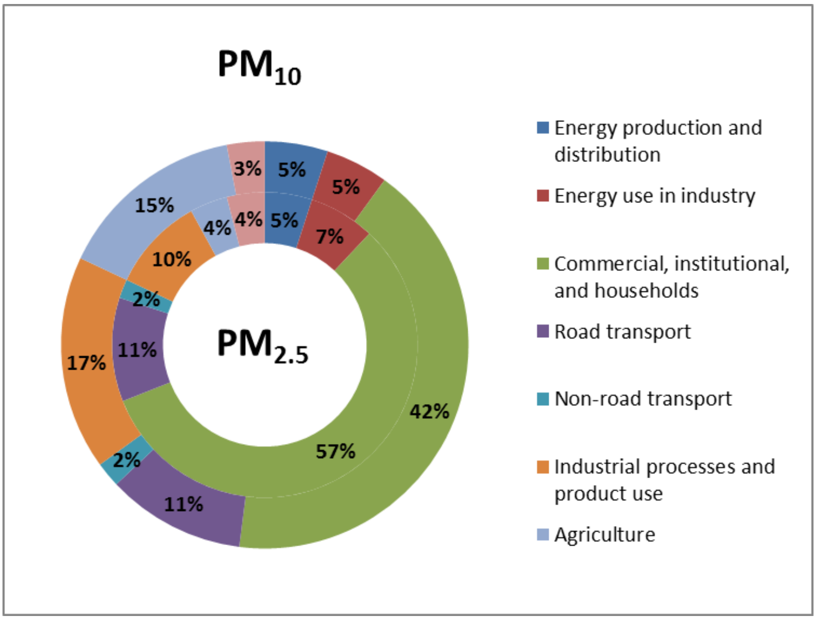

**Figure 3**: Share of anthropogenic $PM_{10}$ (outer circle) and $PM_{2.5}$ (inner circle) emissions in Europe (EEA, 2017).

Among the different economical activities performed in Spain, construction has historically played an important role. Nowadays more than 5% of the Spanish active population is employed on this sector (I.N.E., 2017). Consequently, manufacturing of cement is one of the most important industries in the country. According to data provided by Oficemen (Spanish Cement Manufacturers Association) the total production of clinker in 2016 was 17.3 millions of tons (Oficemen, 2016a).

A diagram of the cement manufacture dry process (the most used nowadays) can be seen in Figure 4. The cement manufacturing process consists in several stages. The first step in this procedure is the extraction of calcium carbonate ($CaCO_3$) from quarries. Lime, marl, or chalk deposits are suitable to obtain this raw material. Usually, in order to save costs, quarries are located as close as possible to the cement industry. Once having the carbonate, it is crushed into pieces of about 10 cm of diameter, and then they are grinded together with iron oxide ($Fe_2O_3$), alumina ($Al_2O_3$), and silica ($SiO_2$) to provide cement the needed characteristics, till providing a mixture of materials known as “raw meal”. This raw meal is then subjected to a preheating process before entering the kiln. This process undergoes in a preheating tower, comprising several cyclones in line. Exhaust gases from the kiln flow upstream, swirling through the cyclones, while the raw meal is transported the opposite way, to the kiln. In this process there is heat exchange, by which exhaust gases lost temperature in favor of a heat increase experienced by the raw meal. To ensure this heat, different kinds of fuel are fired in the kiln. To facilitate the movement of the raw meal through the kiln, it rotates at a pace between 3-5 rotations per minute. Since the meal is moving down in the kiln, the temperature of the mixture increases till reaching around 1500°C. At these temperatures the raw materials suffer physicochemical transformations leading to the formation of nodules smaller than 30 millimeter know as clinker. Clinker is composed of a mixture containing 50-70% of tricalcicum silicate (known as "alite", $Ca_3SiO_5$), 15-30% dicalcicum silicate (known as "belite"$Ca_2SiO_4$), 5-10% trycalcium aluminate ($Ca_3Al_2O_6$), and 5-15% of ferrite ($Ca_4Al_2Fe_2O_{10}$). Clinker is then cooled down to 100°C, and grinded with gypsum ($CaSO_4 \bullet 2H_2O$) in a ball mill, till reaching a homogenous cement powder. Final steps of this procedure comprises the storage and transportation of the product (Cembureau, 2017; Oficemen, 2017; Tokyay, 2016).

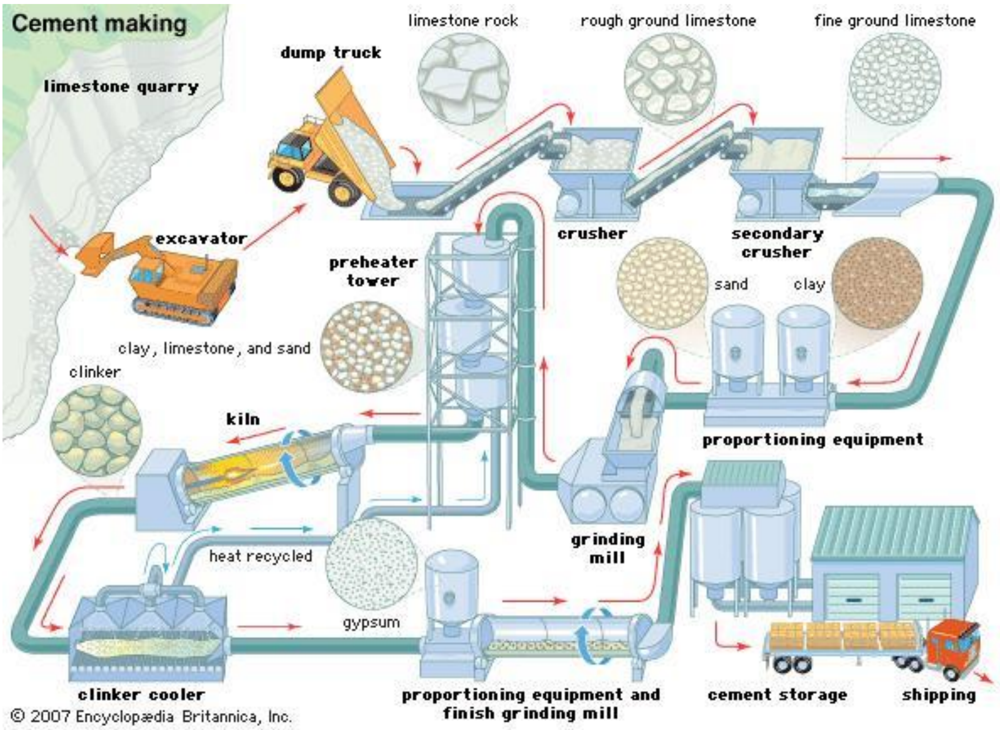

**Figure 4:** Cement production diagram (Enciclopædia Britannica, 2007)

Therefore, cement industry demands huge quantities of both, energy and raw materials. To reduce production costs, save energy, and avoid emissions of greenhouse gases, it is highly recommended the use of wastes as both, raw materials and fuels (Schorcht et al., 2013). Nowadays in Europe, 5% of raw materials and 37% of fuels have been substituted by different kind of wastes (Figure 5) (CEMBUREAU, 2016).

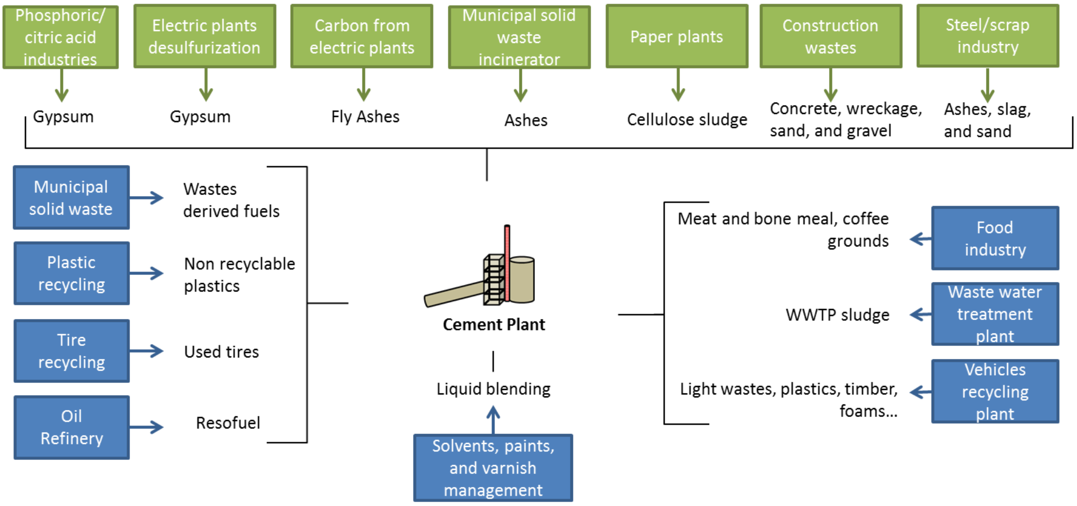

**Figure 5:** Alternative raw materials (Green) and fuels (blue) suitable to be used in a cement industry. Adapted from Oficemen (2016b)

### Environmental aspects in the cement industry.

As seen in Figure 4, cement manufacturing process has different steps that could be affecting the environment. Although quarrying activities have a local environmental impact, it is moderate in comparison with other mining activities, being paid most of the attention in cement industries in their emissions to air (Oss and Padovani, 2003). Among them, PM releases are recognized as the most concerning, due to both, their hazardous potential and their emission in different parts of the cement processing (Schorcht et al., 2013). While the release of other air pollutants is mainly happening in the combustion process, PM is being emitted into the environment also during crushing and grinding steps. Furthermore, there is also possible to register minor sources of PM during the processes of storage and transport (D. Brown et al., 2014; Schorcht et al., 2013).

Mechanical processes (crushing, grinding) could generate dust, including coarse PM. Storage, transport, and bagging of raw materials and cement powder could also lead to diffuse dust emissions (CPRAC, 2008). Both diffuse and mechanical generated dust include coarse PM rich in mineral components (silicates, aluminates, sulfates, carbonates)(Lafarge, 2011). Even though these PM are not able to travel long distances, they can become the main PM source in the nearby of cement plants if proper measures are not taken to abate these pollutants (Abdul-Wahab, 2006). Cover conveyors and elevators, as well as conducting exhaust gases from grinding and milling facilities through filters is a key strategy to avoid this kind of emissions (Schorcht et al., 2013).

However, kiln emissions are nowadays considered as a higher concern. Firstly, they are mostly fine PM, and, consequently, they can undergo to deeper parts of the respiratory tract (Dan et al., 2015; Ehrlich et al., 2007). Secondly, due to the high temperature combustion process and the great array of materials introduced in the kiln, chemical composition, size and shape of these PM is more complex than those coming from mechanical processes (Kim et al., 2015). The high temperatures reached in the kiln may favor the formation of different toxic by-products such as polychlorinated dibenzo-*p*-dioxins and dibenzofurans (PCDD/Fs) and PAHs, which may be adsorbed to particles (Ercan and Dinçer, 2016; Senthilkumar et al., 2014). Furthermore, the presence of heavy metals in both, fuels and raw materials used in the cement kiln enhances the emission of PM rich in these elements (Gupta et al., 2012).

To control these kiln emissions, the European Union has set a directive establishing emission limits for different pollutants (Table 1). In general terms, emission limits for the cement industry are related to 3 main pollutants: NOx, $SO_2$ and dust. In addition, the European directive (Directive 2010/75/EU, 2010) has also defined limits for metals, HCl, HF, total organic carbon (TOC), and PCDD/Fs.

Yet, some considerations should be taken into account when trying to cap the emissions from cement industries. First, the regulation contemplates the emission of total dust, but as we have seen size of dust is a highly important characteristic regarding toxicity of this material (Kelly and Fussell, 2016). Secondly, in the present normative, beryllium (Be) has not been taken into consideration, despite it is a compound that can be present in raw materials, and its inhalation toxicity has been previously recognized (Jakubowski and PałczyŃski, 2015; Schorcht et al., 2013). A third issue that should be faced in this normative is that established limits are applicable to the cement kiln, and not to the rest of the process.

**Table 1**: Emission limits from cement kilns co-incinerating wastes (Directive 2010/75/EU, 2010).

| **Pollutant** | **Limit (mg/Nm$^3$)*** |
|---|---:|
| Total dust | 30 |
| HCl | 10 |
| HF | 1 |
| NO$_x$ | 500 |
| Cd+Tl | 0.05 |
| Hg | 0.05 |
| Sb+As+Pb+Cr+Co+Cu+Mn+Ni+V | 0.5 |
| PCDD/Fs (ng/Nm$^3$) | 0.1 |
| SO$_2$ | 50 |
| TOC | 10 |

*Limits are expressed as daily average values for total dust, HCl, HF, NOx, SO$_2$ and TOC, as average values over the sampling period of a minimum of 30 minutes and a maximum of 8 hours for heavy metals, and as average values over the sampling period of a minimum of 6 hours and a maximum of 8 hours for PCDD/Fs. All values are standardized at 10% oxygen.

## Human health risk assessment: a tool to evaluate hazardous effects on population

As seen in the previous section, PM is a dangerous agent capable of provoking several adverse health effects as a consequence of complex processes underlying alveolar cells. Those effects depend not only in the composition of PM, but also on the exposure or the degree at which one individual or population is subjected to contact with this pollutant. In this regard, it is useful to introduce the concept of risk, which is defined as "the chance of harmful effects to human health or to ecological systems" (US EPA, 2016b). Going along with this definition, risk depends on two variables: adverse effects and likelihood of them to happen, as expressed in next equation:

$$R = F \cdot E$$

In which R is risk, F stands for frequency, and E represents the effect.

Taking into consideration this designation, we can consider risk assessment as a methodology to estimate the probability of suffering pernicious responses that may result from exposure to certain substances. In this discipline there are usually 4 steps to arrive to final risk management: Hazard identification, Exposure assessment, Dose-response assessment, and Risk characterization (Figure 6).

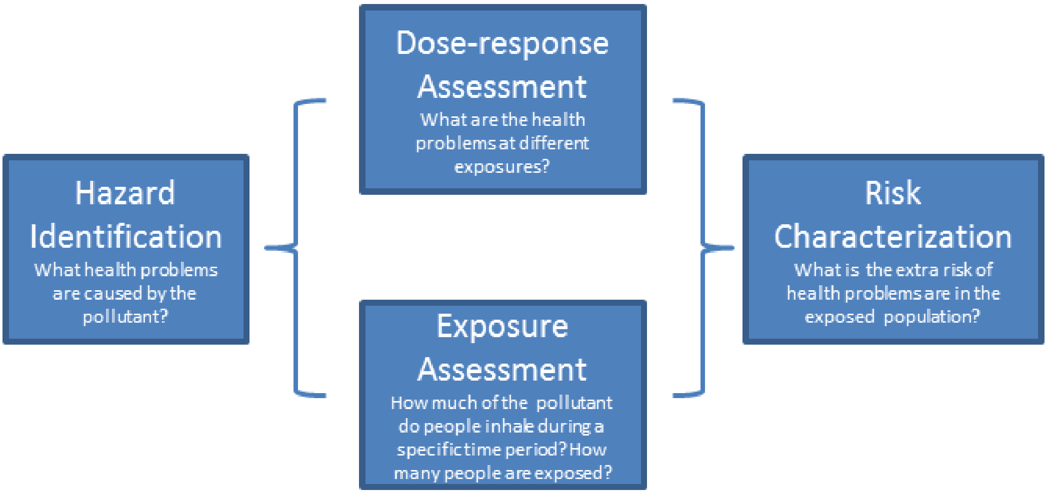

**Figure 6**: Risk assessment methodology steps.

The first stage, or **hazard identification**, consists on determining if exposure to a given stressor could generate adverse health effects. To do so, this step relies on three different kinds of data:

- Human epidemiology data: this is the most desirable data to start a risk assessment process. Unfortunately, this kind of data is rarely available, and causal relationship between pollutant and effects are only demonstrated on a qualitative basis.
- Animal bioassay data: the most frequent data used in the risk assessment procedures. When using this data, it is important to note that some differences could arise when extrapolating animal results to human scale
- Supporting data: like cell assays, or biochemical studies, is the last step in the hazard identification process. Having stablished a qualitative causality (epidemiology), and after seeing a quantitative relationship between exposure and effects in animals, *in-vitro* studies could help to find out the mechanisms by which the hazards is produced, and to adjust the differences in the effects between animal and human species.

Next stage consists on **dose-response assessment**, whose main goal is trying to find a relationship between probability and severity of adverse health effects (responses) and the different amounts and conditions of xenobiotic applied (doses). Usually, for a given effect, when rising the dose, the response also increases. At low doses it could be a lack of response but at some point, when increasing the dose, responses start to occur at low probability rate or in a small fraction of the population. The response occurring at the lowest level of dose among all the studies is taken as the critical effect, assuming that if this event is avoided, no other effects will happen.

This step begins with the analysis of the data gathered in the previous stage to understand the mechanisms underlying toxicity of a pollutant (mode of action), and covers all processes from agent-cell interaction to final pernicious effects. Besides, studies depicting dose-response experiments are reviewed, and in case the critical effect dose is not observed, data should be extrapolated following two different kinds of dose-response outlines:

- Non-linear:

This kind of relationship is characterized by the presence of a dose threshold that should be passed in order to observe adverse health effects. In as single experiment, the closest dose below this threshold is defined as No-Observed-Adverse-Effect Level (NOAEL) (Dorato and Engelhardt, 2005). For risk assessment purposes it is convenient to select the lowest NOAEL from a set of dose-response experiments dealing with same toxicant and effects in order to protect the most sensitive population.

From this NOAEL levels, USEPA has defined the reference concentration (RfC) to assess risks from airborne pollutants. RfC is defined as an estimated concentration below which not adverse effects are expected. Therefore, it is generally expressed in mg/m$^3$. RfC can be derived from NOAEL using the following equation:

$$RfC = NOAEL/UF$$

Where UF is the uncertainty factor, included to reflect variability and uncertainty between human and animals, and within human population. UF usually has a value of 100, but it can change depending on the experiment and effect studied.

- Linear

This dose response is characterized by not showing an effect threshold, but every dose elicits a consequent effect. This is the typical fitting used for carcinogenic risks. In the extrapolation of this kind of risks a line is drawn from the origin (zero dose and null response) to the closest dose-response spot. The slope of this straight line is known as inhalation unit risk (IUR) and it is used to estimate risks at doses entering into its domain.

In this case, risk is evaluated as the probability of suffering cancer over a lifetime exposed to a given concentration of a specific pollutant.

In this case, carcinogenic risk from pollutant inhalation is defined as

$$Cancer\ Risk = Exposure \cdot IUR$$

Exposure is expressed in concentration units (i.e. mg/m$^3$) while IUR is expressed in inverse of concentration, so cancer risk is dimensionless. Different thresholds of acceptable risks are set by diverse environmental agencies worldwide.

In the **exposure assessment** step the frequency, magnitude, and duration of exposure to a given pollutant is calculated. It can be measured directly in the population, but the most common approach is to by considering the environmental concentrations of a pollutant and estimating the human intake over time. For an accurate evaluation it is important to know the levels of pollutant in the different environments where population is developing their activities.

Thus, for airborne particles it is needed to know the habits of the population (time-activity patter), the places where these habits are taking place (home, outdoors, job), and the concentrations of the pollutant in every one of those environments. In advanced exposure assessments, population could be divided into different groups attending to age or lifestyle, adjusting the different inhalation rate to specific group patterns.

The last step is the **Risk Characterization** stage. In this step, the individual risk characterization derived from every step of the risk assessment process are integrated and analyzed together. This overall characterization should inform in a clear way, and should be comparable with previous published studies.

Performing a risk assessment of particulate matter has been considered a difficult question. Values of RfC and IUR are variable among particles, since its toxicity deeply depends on its physicochemical properties, and these are highly variable depending on weather and sources involved. To surpass this issue some epidemiological studies have used hazard ratio values (i.e. prevalence of a given sickness to appear in exposed versus control groups) as an approach to evaluate risks from PM inhalation (Beelen et al., 2014; Thurston et al., 2016). But the methodology usually followed is assessing the hazardous potential of the different constituents present within the PM.

### Risk assessment of toxic constituents of PM

As mentioned in the mode of action section, besides the mechanical PM properties, several substances within PM are able to generate damage:

Metals originate from natural (soil resuspension, volcanic eruptions) and anthropogenic sources (traffic and industries), and they are often referred as the most toxic constituent of PM (Kelly and Fussell, 2016; Popoola et al., 2017). Numerous studies have found evidence of the toxicity of these substances onto respiratory cells (Guan et al., 2016; Huang et al., 2015; Molinelli et al., 2006). Consequently, RfC and IUR for them are properly developed, and methodology to asses inhalation risks from metals is well defined (US EPA, 2009).

Endotoxins are biological compounds located in the cellular membrane of gram negative bacteria (Degobbi et al., 2011). They have been related with inflammation processes in human respiratory cells (Van Den Heuvel et al., 2016; B. Wang et al., 2016). However, toxicity of these compounds is highly focused on the upper parts of the respiratory tract, since they use to be associated to coarse PM (Thomson et al., 2015; Yang et al., 2016). Although some efforts have been made to establish a safety threshold for endotoxins inhalation, no RfC or IUR are found for these compounds (Thorn, 2001).

PAHs are a group of organic compounds having two or more fused aromatic rings having their origin in incomplete combustion processes (WHO, 2010). They are recognized as human carcinogens and mutagens, causing respiratory problems and bronchitis when inhaled (Tobiszewski and Namieśnik, 2012). Among them, benzo[a]pyrene (BaP) is considered the most toxic, being the only target PAH in European inmision air quality standards (EU Parliament, 2005). As in metals, there is nowadays a huge body of knowledge regarding toxicity and way of action of PAHs, and, therefore, risk assessment for these compounds is easy to undertake (IARC, 2012; Liao et al., 2011; Sarigiannis et al., 2015).

Quinones are chemicals comprising several aromatic rings released during incomplete combustion processes of fossil fuels, and also formed via photochemical conversions from PAHs in the atmosphere (Shang et al., 2014). Despite there is evidence of their toxic potential, few toxicological studies have been done to set RfC or IUR parameters for such pollutants (Y. Li et al., 2012; Sheng and Lu, 2017).

Since no parameters have been defined for assessing toxicity of quinones and endotoxins, and having into account that several studies recognize PAHs and metals as the most pernicious components of PM, the majority of the papers dealing with human health risk assessment from PM inhalation are focused on these two groups of compounds (Bonetta et al., 2009; MohseniBandpi et al., 2017; Raaschou-Nielsen et al., 2013).

### Previous studies

#### PM emissions in cement plants.

To date, several studies have been dedicdated to PM nearby cement plants. Most of the studies dealing with the cement emissions to air are focused in the release of several pollutants from the cement kilns. Thus, Gupta et al. (2012) analyzed the emission of a cement kiln using a low share (4%) of alternative fuels. After studying the distribution of PM sizes, described that 50% of the total PM emissions from the kiln were $PM_{2.5}$. The metallic composition of these PM was also analyzed, and a risk assessment using modelled concentrations showed not risk for the population.

Ehrlich et al. (2007) measured the emissions of three fractions of PM ($PM_{10}$, $PM_{2.5}$, and $PM_1$) in several steps of the cement process in different cement fabrics in Germany. In cement kilns, they found out that although the stack emissions of total dust was below the limit establish in the normative, $PM_{2.5}$ and $PM_1$ emissions represented around 65% and 35% of this pollutant. It was also observed that those clinker coolers using baghouse filters emitted a higher share of coarse PM than those equipped with electrostatic precipitators.

Aleksandar et al. (2010) measured the emission of PM and heavy metals in a couple of plants (A and B) with same state-of-the-art bag filters and different shares of tires co-incineration. Plant A, having a lower clinker production (2000 tons of clinker per day) showed a huge increase (from 0.7 to 56 mg/Nm$^3$) in total dust when replacing the fuel from 0% to 11.35% of used tires. Contrarily, PM emissions did not change significantly when replacing the share of tires up to 15.3% in the plant B (4000 tons of clinker per day). Same trend was found for heavy metals, concluding the study that the working volume of cement plant could have a significant effect in the PM emissions.

Asamany et al. (2017) investigated the effects of plastic waste burning in a cement kiln, concluding that the number of particulates generated did not show significant differences between burning standards and alternative fuels.

However, as described previously, emissions from cement plants are not only occurring during the combustion process. Although its importance has been recognized in several studies (Gupta et al., 2012; Santacatalina et al., 2010; Yubero et al., 2011) diffuse emissions from cement factories have not been properly addressed yet. To date, only Abdul-Wahab (2006) is devoted to the study of diffuse and fugitive emissions from the different steps of the cement manufacturing process. In this study, he took environmental samples of total suspended particles (TSP) in several parts of the cement facility, and through the use of a software model he calculated the emission rate of the different machinery. His results show that grinding operations and resuspension from trucks could have a similar or greater impact on the nearby atmosphere than the kiln itself.

### Epidemiological studies: occupational risks

A great bunch of knowledge has been generated regarding occupational risk of cement employees (Donato et al., 2016). Haxhiu et al. (1979) measured respiratory symptoms, smoking history, and duration of work and exposure among several cement plant workers, and compared it with non-exposed population. Results showed that long term workers experienced lower forced vital capacity (maximum quantity of air expelled after a maximum inhalation) and expiratory flow rate.

Amandus (1986) studied mortality from stomach cancer in cement workers. Although he found a significant increase in death in cement workers during 1965-69, he did not register the same trend during the whole studying term (1950-1980). However, (Jakobsson et al., 1990) when comparing cancer in digestive system between cement workers and nearby population found a correlation between probability of suffering gastrointestinal cancer and working in the cement plant.

Vestbo and Rasmussen (1990) studied hospitalizations from chronic obstructive lung disease (COLD) in working men of a cement plant. They concluded that long-term exposure to cement dust does not lead to higher morbidity of COLD. Similar study were developed by Giordano et al. (2012a), concluding that cement workers had significant lower risk of overall mortality and cancer probability than standard population. However, the authors speculated that it could be due to fact that medical data used was obtained at the beginning of the enrollment period in the cement plant, when workers exhibit a healthy overall condition.

Fell et al. (2003) measured spirometry and studied respiratory symptoms of former cement plant workers in Norway. They did not find any significant differences when comparing these variables to control group. A very comprehensive research was performed by Nordby et al. (2011) aimed to study lung function and airway symptoms among employees working in different jobs within the cement industry in 24 plants spread around Europe. To do that, they measured different pulmonary parameters in the workers during a four year period. Results concluded that those employees working in contact with cement dust were more willing to experience a decreased in forced vital capacity

Richard et al. (2016) performed a study comparing expiratory flow rate, transaminase content in liver and concentrations of heavy metals in workers, exposed population and controls. Workers and exposed population showed a significant higher content in transaminases and most heavy metals, while having a decrease in flow expiratory rate if compared to control groups. In this study it was also found that the higher the exposure time, the lower the expiratory flow rate.

Mirzaee et al. (2008) measured the concentrations of respirable dust in several parts of a cement industry using personal samplers. At the same time they measured lung function and interviewed 170 workers to gather information about their respirable health. Results showed that concentrations of cement respirable dust in the industry were extremely high (between 23-3.7 mg/m$^3$), and consequently, workers showed a significant lower expiratory volume and vital capacity than control groups (unexposed population). The paper finalizes recommending the use of personal protection devices and proper ventilation in the industry. Similar conclusions were achieved by (Mwaiselage et al., 2005), for a similar cement plant.

### Epidemiological studies: general population

Regarding general population nearby a cement plant, Brockhaus et al. (1981) studied the degree of thallium exposure in urine and hair of 1200 subjects. Average levels of thallium in the cohort's urine and hair were significantly higher than in the control group. Levels of thallium show good correlation with sleep disorders, headaches, fatigue, and muscle weakness within the population. It was also determined that ingestion was the major via of thallium exposure, since consumption of self-grown vegetables was quite habitual in the area. Same research group conducted a follow-up study focused on subjects with relatively high exposure or individuals (including children) and those suffering health disorders potentially related to thallium ingestion (Dolgner et al., 1983). The study noticed a decrease of thallium levels in urine after the publication of the first study, since population began to avoid consumption of home-grown vegetables. Although the population was concerned about children malformations, no causal relationship was found between thallium exposure and congenital malformations.

Ginns and Gatrell (1996) performed a study to determine whether there was a higher prevalence of respiratory illness in children living close to a cement industry. For that, they provided a questionnaire to parents that collected information about incidence of asthma, sore throat and eyes, and blocked nose. Incidence of asthma was similar between exposed and non-exposed groups, but the rest of symptoms studied showed significant higher occurrence among the exposed children. Same approach was developed by Nkhama et al. (2015) to evaluate eye and nose irritation trough analysis of questionnaires delivered to population living close to a cement plant in Zambia. They concluded that the odds of suffering these irritations were increased when living in the vicinity of a cement plant. However, both studies recommend that to state proper conclusions environmental (i.e. PM and $NO_X$ concentrations) and clinical data (i.e. hospitalizations) should be taken into account.

Işikli et al. (2006) measured Cadmium concentration in soils and vegetation at ranging distances from a cement plant. Furthermore, they also measured levels of this pollutant in blood of people living near the industry. Their results found higher concentrations of this metal than control samples, and found a relation between proximity to the plant and Cd concentration in these two matrixes. However, although levels of Cd within the exposed population were higher than control groups, they were still within the range of normal Cd reference levels.

Giordano et al. (2012) performed a study focused in mortality patterns of population living nearby a cement plant. It was found an increased mortality from respiratory diseases among males that were statistically significant during periods in which the plant increased its production. During these periods it was also recorded an increase in the decease from cerebrovascular and digestive diseases, as well as for injuries. Authors conclude that these increases could be attributed to occupational exposures, since the cement plant employed mainly males, and no prevalence of these illnesses were found among women.

Marcon et al. (2014) compared the children absences to school to $PM_{10}$ concentrations in an area influenced by the presence of a cement plant in Italy during a 3-year period. Average $PM_{10}$ concentrations were below European limits (34 $\mu g/m^3$). Even though, they conclude that increases in $10 \mu g/m^3$ leaded to a significant increase in the absenteeism ratio that was especially significant two days after exposure.

### Toxicity studies

Bibliography in this regard is scarcer than in case of epidemiology. Just a few examples of *in-vivo* or *in-vitro* toxicity of PM from cement facilities have been written to date. One study dealing with this topic was done by van Berlo et al. (2009). They exposed rat alveolar macrophages to a variety of cement dusts (CD), noticing an increase in production of macrophage tumor necrosis factor α (TNFα).

Bauer et al. (2012) aimed to understand the way of action of cement dust on human respiratory cells. For that, he studied the cytotoxicity and cytokine levels of two cell lines (alveolar epithelial cells (i.e. A549) and primary epithelial cells from oropharyngeal mucosa) after being exposed to different types of cement dust. Results showed a lack of significant cytotoxicity, and a decrease in one cytokine (IL-8). However, the study discusses that the decrease in IL-8 could be related with the affinity of this cytokine to be adsorbed by the PM surface, besides an inhibitory process underlying cell exposure to cement dust.

Roig et al. (2013) exposed A549 cells to aqueous extracts of $PM_{10}$ collected in different locations and season to compare their genotoxicity and cytotoxicity. Although no genotoxicity was observed, cytotoxicity results indicate that cement plant extracts posed the highest average mortality.

Senthilkumar et al. (2014) collected $PM_{10}$ up and down stream of dominant winds of several industries. Subsequently, they measured their content in heavy metals and PAHs, and exposed A549 cells to different doses of PM (from 1 to 10 $m^3$ of air) to measure cytotoxicity and mortality. Downstream samples were more toxic than upstream, having the same effect in the genotoxicity. However, cement PM was less pernicious than other industries (i.e. steel and sponge iron industry) having a higher richness in metals and PAHs.

### Risk assessment studies near cement plants

Regarding risk assessment for the general population nearby cement plant from PM, several studies can be found. The first study focused on $PM_{10}$ and its metallic content was developed by Schuhmacher et al. (2004). Atmospheric dispersion models were used to calculate the levels of $PM_{10}$ and metals in air, soil, and vegetation, showing that cement plant emissions did not provoke incremental health risks.

Same authors studied the effects of substituting 20% of the energy input in a cement plant from conventional to alternative fuels by collecting soil and vegetation samples nearby a cement facility (Schuhmacher et al., 2009). By studying the content of several metals and As, as well as PCDD/Fs, they concluded that levels of PCDD/Fs changed slightly, while concentrations of metals changed differently from one metal to another. To finish, a health risks assessment from inhalation, ingestion, and dermal contact showed a reduction in total carcinogenic risks. Same approach was followed by Rovira et al. (2014), but in a different cement plant and measuring also concentrations in air (gas and PM). Similar conclusions were found: no significant differences in carcinogenic and non-carcinogenic potential risks.

Probably, the most extended study regarding human health risk assessment nearby cement plants was done by J. Rovira in his PhD thesis (Rovira, 2013). He studied the temporal evolution of levels of PCDD/Fs and heavy metals measured in air (both gas and $PM_{10}$), soil, and, herbage nearby 4 different cement plants in Catalonia. After performing a risk assessment for the population living nearby these plants he concluded that the human risks were below the acceptable threshold of national and international standards. Likewise, he did not find significant differences when comparing the risk from plants using conventional or alternative fuels.

A follow-up study focused on the content of PCDD/Fs and heavy metals of one of these cement plants was performed after 5 years (Rovira et al., 2015). Only vanadium presented a significant increase during this period. Non-carcinogenic risks were below the safety threshold safety limit, while cancer risks were within the assumable range.

More recently, Dong et al. (2015) studied the metal content in the blood and hair of 185 individuals living within the influence of the emissions of a cement plant. They found out that metal levels in these two matrixes were comparable to U.S. general or regional population, stating that smoking and seafood consumption had a greater influence in these levels than exposition to the cement plant. Finally they concluded that this cohort was not at elevated health risk from metals.

Khwedim et al. (2015) collected soils nearby a cement plant in Iraq. After measuring the content of As and heavy metals, they calculated the potential non-carcinogenic human health risk that can overcome via ingestion, and applied a principal components analysis (PCA) to determine which soil compounds could be enriched by the cement plant. Although they found a high contribution on metals and As in soils surrounding the cement plant, they did not find significant non-carcinogenic risks for the population.

To evaluate not only health risks, but also to quantify their economical dimension Rovira et al. (2016) performed an evaluation of human risks including the costs on cancer to society. To do so, they conducted a long term monitoring of metals and PCDD/Fs around a cement plant gradually increasing its load of alternative fuels. Subsequently, they calculated years of life lost and years lost due to premature death for the population living nearby. They found out that premature deaths and years of life lost were reduced when increasing alternative fuels, involving a reduction in sanitarian costs of 31,000 € per year in the area.

Addo et al. (2016) collected total suspended PM at ranging distances (150-700m) from a cement plant stack. Then, they analyzed its content of some metals to perform a health risk assessment via ingestion, dermal absorption, and inhalation. Results indicated that average concentrations were very high (538.92 $\mu g/m^3$). Non-carcinogenic risk was insignificant, but carcinogenic risks via ingestion were probable (between 1 to 10 cases of cancer per 100,000 inhabitants) for the population living in the neighborhoods surrounding the facility.

### Summary of previous studies

From the bibliographical review undertook in the present section it is possible to conclude that cement workers could be more likely to suffer any kind of pulmonary disease, mainly related to pulmonary capacity. Epidemiological studies have found correlations between being exposed to a cement plant and showing higher-than-average levels of certain metals. However, adverse health effects related to those levels were not found, which are in line with the predictions exposed in risk assessment studies performed nearby cement plants. Bibliography regarding toxicity of PM nearby cement plants is still scarce, and focused on $PM_{10}$.

However, some issues should be properly addressed. Most of the studies reviewed were focused on $PM_{10}$ or total suspended particles, when it is already stated that more than 50% of PM from kiln combustion are $PM_{2.5}$. Risk assessment could be improved if having into account not only outdoor, but also indoor levels of PM. Furthermore, contribution from cement plants to environmental levels of PM should be stated in order to know the share of cement plant in total risks. Finally, toxicity regarding fine PM in the vicinity of cement industries is still a matter to deal with.

# HYPOTHESIS AND OBJECTIVES

# Hypothesis and objectives

Given the previous results in related recent studies, it is urgent to include the hazardous potential of fine and quasi-ultrafine particles in the risk evaluation process.

The general hypothesis of this thesis is that, in areas influenced by cement plants, composition and levels of fine ($PM_{2.5}$) and quasi-ultrafine particles ($PM_1$) are different from composition and levels of coarse particles ($PM_{10\text{-}2.5}$). These characteristics will depend on the contribution of cement plant and other sources to total environmental PM, and will affect the exposure, toxicity, and human health risks provoked by these PM.

Therefore, the general objective of this doctoral thesis is to assess the human health risk due to air pollution focusing a major attention to fine particles applied to the case study of the cement industry.

This main goal has been divided into four different specific objectives:

- Study the chemical characterization of coarse ($PM_{10\text{-}2.5}$), fine ($PM_{2.5}$), and quasi-ultrafine particles ($PM_1$) in environments influenced by cement plants.
- Study the human toxicity of breathable ($PM_{10}$) and fine ($PM_{2.5}$) PM using *in-vitro* technologies.
- Evaluate the exposure and human health risks derived from the inhalation of PM.
- Quantify the PM contribution from cement plant to the inmision.

# MATERIALS AND METHODS

# Materials and methods

## Site description

The cement plant object of investigation is located in Montcada i Reixac, a town situated in the north outskirts of Barcelona (41º 28' 30.88''N; 2º 11' 1.47''E) (MNT 421-1 Badalona). The ambient air in this area is influenced by an operational cement plant and two highways (C-33 and C-58) with dense traffic (Figure 7).

**Figure 7:** Location of the cement plant (blue) and the sampling school (green). Source: Google maps.

The cement plant has been working since 1917, and its current production is around 900,000 cement tons per year (Lafarge, 2016). This plant has a license to use up to 382,000 tons of wastes (e.g. slag, concrete wastes, paper mill sludge and fly ashes) as raw materials annually. Furthermore, sewage sludge, meat and bone meal, refuse-derived fuels, and biomass contribute up to 20% of the total energy consumed by the kiln (Generalitat de Catalunya, 2008)(Table 2).

**Table 2:** Description of alternative raw materials and fuels used in the cement kiln.

| **Raw materials** | | |
|---|---|---|
| **Material** | **European Waste Catalogue Code** | **Tons*10$^3$/yr.** |
| Mineral admixture | 190902; 100906 ;101304; 101313; 010409; 191209 | 100 |
| Lime admixture | 050113; 060201; 060314; 060316; 100104; 101110; 101120; 101208; 101311; 101314; 150203; 160304; 161103; 161104; 161106; 170101; 170103; 170107; 170504; 190206;191209; | 30 |
| Grinding aid | 070599; 161004 | 12 |
| Paper mill sludge | 030305; 030307; 030309; 030310; 030311 | 30 |
| Sewage sludge | 020502; 070112; 040220; 070312; 070512; 070612; 110110; 110114 ; 190813; 190814 ; 070712; 110109 | |
| Gypsum | 070610; 100105 | 40 |
| Coal fly ash | 100102 | 150 |
| Iron slag | 100201; 100202; 100210; 100299; 100903; 100908; 101006; 120117;100399; 100906 | 20 |
| **Total** | | **382** |
| **Fuels** | | |
| **Material** | **European Waste Catalogue Number** | **Tons*10$^3$/yr.** |
| Spent coffee grounds | 020301 | 40 |
| Sewage sludge | 190805 | |
| Meat and bone meal | 020203 | |
| Biodiesel | 130703 | 10 |
| Pruning and wood wastes | 170201; 030101; 030105; 030301; 020103 | 20 |
| Refuse derived fuel | 191210 | 30 |
| **Total** | | **100** |

## Sampling procedure

Sampling of ambient PM air pollution was performed on the roof of a two story primary school located 300 metres from the cement facility (41º 28’ 21.14’’N; 2º 11’ 9.47’’ E) (Figure 7). This point was selected since, according to previous studies, it reached the highest levels of PM in the area (Rovira et al., 2011). Two different kinds of samplers were used depending on the nature of the samples (Figure 8):

- High volume samplers: Three different high volume samplers were used to collect $PM_{10}$, $PM_{2.5}$ and $PM_1$ simultaneously for analytical purposes. Two TE-6070-DV (Tisch Environmental) and a CAV-A/mb (MCV S.A.) were used to sample $PM_{10}$ and $PM_{2.5}$, and $PM_1$. The samples were collected onto quartz fiber filters.
- Low volume sampler: A horizontal elutriator model 100 (Negretti) was used to collect PM onto polycarbonate filters for toxicological tests. Two fractions ($PM_{10}$ and $PM_{2.5}$) were collected alternatively by adjusting the flow to 10 or 5 L/min. respectively.

**Figure 8:** High volume TE-6070-DV (Tisch) and CAV-A/mb (MCV) samplers (left) and low volumen horizontal elutriator sampler (Negretti) (right).

Before sampling, collection filters were in an oven at 200ºC for 4 hours. Afterwards, they were conditioned under constant conditions of humidity and temperature (40% humidity and 20ºC) during three days. Subsequently, they were weighed till reaching a constant weight. This same procedure was followed after sampling, except for those samples set aside for organic components determination, since conditioning could cause loss of sample. Concentrations of PM were defined as the different between the initial and final weight divided by sampled volume.

## Analytical overview

Once the particles were collected, filters undergone two different protocols according to their objective. Quartz filters were cut in different portions. Each of them was subjected to different techniques depending on the objective (Figure 9):

- Most metals were determined by Inductively Coupled Plasma Mass Spectrometry (ICP-MS), except Ca, Fe, K, Mg, Na and P that were determined by Inductively Coupled Plasma Optical Emission Spectrometry techniques (ICP-OES).
- Organic compounds (PAHs, hopanes, saccharides and derivates, biomass combustion products, and dicarboxylic acids) were determined by Gas Chromatography coupled to Mass Spectrometry (GC-MS).
- Soluble ions ($Cl^-$, $SO_4^{2-}$, $NO_3^-$, and $NH_4^+$) were determined by Ionic Chromatography.
- Carbonaceous materials (total, organic, and elemental carbon) were determined by Pyrolysis.
- Carbon isotopes ($\delta^{13}C$) were determined by Isotope Ratio Mass Spectrometer (IRMS).

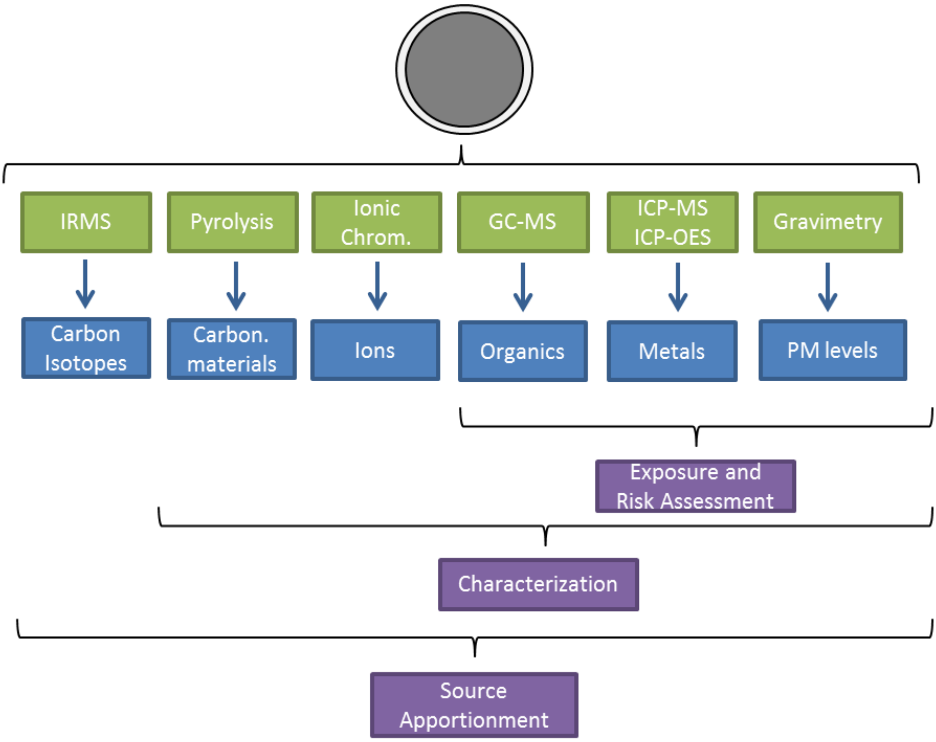

**Figure 9:** Sketch depicting the different techniques applied to quartz filters (green boxes), information obtained from each technique (blue boxes), and final outputs (purple boxes).

Polycarbonate filters underwent two different techniques depending on the objective (Figure 10):

- To obtain microscopic images and complete the characterization, a small portion of the filter was subjected to Field Emission Scanning Electron Microscopy (FESEM).
- The remaining filter was used to extract PM powder, which was then exposed to cells to study toxicity.

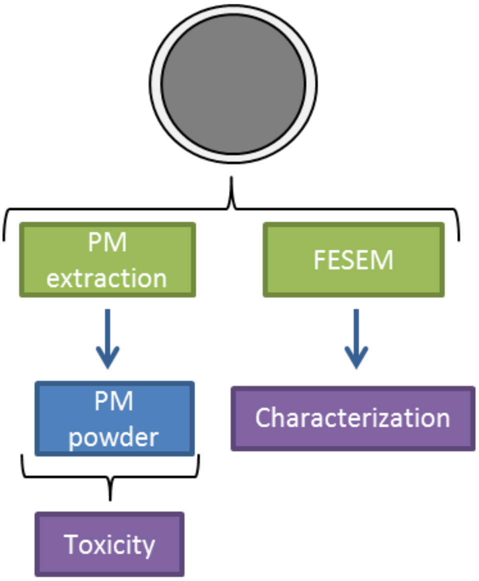

**Figure 10:** Sketch depicting the different techniques applied to polycarbonate filters (green boxes), information obtained from each technique (blue boxes), and final outputs (purple boxes).

Further details regarding techniques, reagents, and calculations are included in the different chapters of the thesis.

To accomplish the goals ascribed to the present thesis, our first step consisted on collecting and performing the chemical characterization of the particles (Chapters 1 and 2). These chapters were completed with an assessment of the human health risks derived from inhalation of PAHs and metals contained in the PM. To complete the characterization we wanted to include microscope imaging, which was done as depicted in Chapter 3. In this same chapter there is also a description of the toxicity studies undertaken with $PM_{10}$ and $PM_{2.5}$ to know their hazardous potential. To study the exposure of population living nearby the cement plant, we proposed the methodology explained in Chapter 4. On it, a combination of time activity pattern and simulated levels of PM in different microenvironments were used as inputs to calculate the deposition trend of PM along the respiratory tract of three population groups (kids, adults, and retired people). Afterwards, to know the contribution of different PM sources operating in the area, several receptor modelling techniques were applied together (Chapter 5). To finalize, we added chapter 6 to show how the combination and improvement of different aspects showed along this thesis can be suitable to evaluate toxicity of PM under realistic exposure scenarios.

# CHAPTER 1: Main components and human health risks assessment of PM$_{10}$, PM$_{2.5}$, and PM$_1$ in two areas influenced by cement plants

Francisco Sánchez-Soberón, Joaquim Rovira, Montse Mari, Jordi Sierra, Martí Nadal, José L. Domingo, Marta Schuhmacher (2015). Atmospheric Environment 120 (2015) 109-116.

# Main components and human health risks assessment of $PM_{10}$, $PM_{2.5}$, and $PM_1$ in two areas influenced by cement plants

Francisco Sánchez-Soberón, Joaquim Rovira, Montse Mari, Jordi Sierra, Martí Nadal, José L. Domingo, Marta Schuhmacher (2015). Atmospheric Environment 120 (2015) 109-116.

Abstract:

Particulate matter (PM) is widely recorded as a source of diseases, being more harmful those particles with smaller size. PM is released to the environment as a consequence of different activities, being one of them cement production. The objective of this pilot study was to characterize PM of different sizes around cement facilities to have a preliminary approach of their origin, and evaluate their potential health risks. For that purpose, three fractions of PM (10, 2.5, and 1) were collected in the nearby area of two cement plants with different backgrounds (urban and rural) in different seasons. Subsequently, main components, outdoor and indoor concentrations, exposure, and human health risks were assessed. Greatest levels of PM1, organic matter, and metals were found in urban location, especially in winter. Consequently, environmental exposure and human health risks registered their highest values in the urban plant during wintertime. Exposure was higher for indoor activities, expressing some metals their peak values in the $PM_1$ fraction. Non-carcinogenic risks were below the safety threshold (HQ<1). Carcinogenic risks for most of the metals were below the limit of $10^{-5}$, except for Cr (VI), which exceeded it in both locations, but being in the range considered as assumable ($10^{-6}$-$10^{-4}$).

*Key words*

Cement; Particulate matter fractions; Indoor and outdoor exposure; Human health risk

*Highlights*

- Characterisation of $PM_{10}$, $PM_{2.5}$, and $PM_1$ was carried out around two cement plants.
- Outdoor and indoor exposure and human health risk to toxic elements were assessed.
- Higher concentrations and human health risks were observed in urban site in winter.
- Maximum human health risk levels were found due to $PM_1$ fraction exposure.

## 1. Introduction

Air pollution is composed by a bunch of gases (ozone, nitrogen, and sulphur oxides) and particulate matter (PM). World Health Organization has recently estimated that ambient pollution is responsible for 3.7 million premature deaths yearly (WHO, 2014). Among the substances comprising air pollution, PM is seen by some studies as the most harmful (Cohen et al., 2005; EEA, 2013). PM can cause a wide variety of health impacts, such as asthma, bronchitis, cardiovascular diseases, and lung cancer (Čupr et al., 2013).

Most influent parameters in PM hazardous potential are size and chemical composition (Harrison and Yin, 2000). PM size range spreads from micrometers to nanometres. PM with a diameter smaller than 10 µm ($PM_{10}$) are able to enter into the respiratory tract and reach the lungs (US EPA, 2013). The coarse fraction of these particles, those with a diameter between 10 and 2.5 µm ($PM_{10-2.5}$), remains in the upper part of the respiratory tract, while the fine particles, those PM smaller than 2.5 µm ($PM_{2.5}$), can undergo deeper in the lung system, being the smallest fraction capable of reaching the bloodstream (Anderson et al., 2012). The potential effects that can be developed after entering into the circulatory system could be more pernicious, concluding several publications (Cifuentes et al., 2000; Schwartz et al., 1996) that the smaller the PM, the more harmful it is. Regarding their chemical composition, the presence of toxic substances (e.g. acids, metals, and PAHs), plays an important role in health impacts (Cassee et al., 2013). PM size and chemical composition depend on several parameters, such as the weather, period of the year, and emission source (Cassee et al., 2013).

One of the industrial activities that releases PM into the environment is the cement production (Gupta et al., 2012; Predicatori et al., 2009). In this activity, PM are generated as a consequence of subjecting lime to high temperatures (from 900 to 1,500ºC) for yielding cement (EU Comission, 2013). Furthermore, raw materials processing and clinker milling and packaging could lead to PM fugitive emissions (Abdul-Wahab, 2006). Currently, there are few papers focusing on the study of health risks produced by PM around cement facilities (Abdul-Wahab, 2006; Rovira et al., 2015, 2014, 2011a). Although it is stated that almost 50% of the PM emitted from the cement industry is smaller than 2.5 µm (Gupta et al., 2012), no one of the previous cited articles is focused on the fine fraction of particles.

The aim of this study is to characterize PM around cement facilities to have a preliminary approach of their origin and assess their potential risk for human health. For that purpose, three PM fractions (10, 2.5, and 1) were collected in the surrounding of two cement factories. Concentrations of metals, ions, and carbon were measured in order to better know the main PM components. Human health risks were evaluated having into account the carcinogenic and non-carcinogenic risks derived from the particles metal content. To our knowledge, this is the firsts study focused in revealing potential health effects of fine fraction of PM in the surrounding of cement facilities.

## 2. Materials and Methods

### *2.1. Site description and PM monitoring*

The two studied facilities are located in Catalonia (Northeast Spain). The first one (A) is placed in Barcelona metropolitan area, within an urban sector profoundly affected by a number of different industries. Moreover, the settlement is crossed by two highways with an average daily traffic of 49,199 and 160,558 vehicles per day, respectively (Ministerio de Fomento, 2012). The plant has been operating there since 1917, and as a consequence of the substantial development of the town in recent decades, the distance from the facility to some neighbourhoods has dramatically decreased to 300 m. According to the company ruling the installation, the plant has an annual production close to 1 million of cement tons. Non-conventional fuels (sewage sludge, animal flours, refuse derived fuels, biomass) account 20% of the total energy consumed. The second plant (B) is set in the coastline of southern Catalonia, integrated in a rural background. Apart from the cement manufacture process, limestone mining activities are performed in the nearby of the plant. Close to the cement plant there is a road with an average daily traffic of 12,380 vehicles per day, being 34.4 % of them considered as heavy vehicles (Ministerio de Fomento, 2012). It has been operating since 1968. The closest population nucleus is 3 km away from the plant. In the year 2012 the plant reached a production of 867,353 metric tons of cement. During the same year 31.9% of the total energy consumption came from alternative fuels, which means more than 85.5 thousands metric tons yearly. Half of this number is composed by biomass, while the other half is made from refused-derived-fuel. Both plants are 165 km away from each other, and they present similar air cleaning devices.

After running a dispersion model (AERMOD v.12345) (US EPA, 2012) for every cement plant, we assessed the area affected by the cement plume. Within this area, we chose a single sampling point for every location. These points were located into populated nuclei including especially sensitive groups of population (children, seniors, etc.). In location A the sampling point was located 300 m away from the cement plant, while in location B it was located 500 m away from the facility. To evaluate differences among seasons with different meteorological conditions, samples in location A were collected in three periods: autumn 2013 (AA), winter 2013/2014 (AW), and summer 2014 (AS). In location B samples were obtained during autumn 2014 (BA). For every period, samples were collected during five consecutive days. Samples were collected simultaneously with three high-volume active samplers, one for each analyzed fraction. $PM_{10}$ and $PM_{2.5}$ were sampled using two TE-6070-DV devices (Tisch Environmental), while $PM_1$ samples were collected using CAV-A/mb sampler (MCV SA). Volume sampled was around 1700 $m^3$ for $PM_{10}$ and $PM_{2.5}$ and around 600 $m^3$ for $PM_1$. All the three fractions were collected in quartz microfiber filters (QFF).

### *2.2. Analytical methods*

Before sampling, filters were heated at 200ºC for 4 h. PM levels were calculated by gravimetric determination. Filters were acclimated and weighted at constant humidity (40%) and temperature (20ºC) during consecutive days until constant weight before and after sampling campaign. Subsequently, filters were divided into three portions to perform different analytical determinations.

The first portion of filter was used for metals analysis. It was treated with a mixture of 2 mL of $HNO_3$ (65% Suprapur, E.Merck) and 3 mL of HF (37.5%, Panreac) in hermetic Teflon bombs for 8 h at room temperature, and 8 additional hours at 80°C. After cooling, extracts were filtered and made up to 25 mL with ultrapure water. They were kept frozen at -20 °C until further analysis (Mari et al., 2009). Contents of trace elements were determined by means of Inductively Coupled Plasma Mass Spectrometry (ICP-MS, Perkin Elmer Elan 6000), while major elements were determined by means of Inductively Coupled Plasma Optical Emission Spectrometry techniques (ICP-OES, Perkin Elmer, Optima 3200RL). A complete list with all the analyzed elements, as well as their corresponding limits of detection is included in supplementary materials.

Another portion of filter was used for the determination of soluble inorganic ions ($Cl^-$, $SO_4^{2-}$, $NO_3^-$, and $NH_4^+$). The piece of filter was cut in smaller portions and mixed with 15 mL of deionised water in a falcon tube. Then, it was shaken during 4 hours and submerged in a sonication bath at 60ºC during 1 hour. The extract was then filtered with a 250 µm sieve, and the filtered liquid analyzed by means of Ionic Chromatography and specific electrode (DX-300 Dionex) to elucidate the ionic content. For obtaining the total carbon (TC) content, the last portion of filter was submitted to pyrolysis with oxygen at 1,000 ºC. Resulting gases ($CO_2$ and $NO_X$) were driven by a helium flow, which was subsequently analyzed by means of gas chromatography (Thermo EA 1108 CHNS-O Carlo Erba Instruments) (Tiessen and Moir, 2000a, 2000b). To address the joint content of organic carbon (OC) and elemental carbon (EC), sample was previously exposed to a HCl enriched atmosphere in order to remove the carbon from carbonates. After that it was analyzed following the same methodology described for TC.

Laboratory reagents blanks and duplicates were performed in order to control the quality of the process. As external standard, Loamy clay soil (National Institute of Standards and Technology) was used for metal and sulphanilamide for carbonic content.

Some indirect calculations were performed in order to find out the contents of different compounds. To establish the OC content we solved the equation $OC = 0.7 \times (OC + EC)$ (Pérez et al., 2008). Organic matter (OM) was estimated by applying a factor of 1.6 to organic carbon concentrations (Pérez et al., 2008). Carbonate and $SiO_2$ content were estimated from Ca and Mg ($1.5 \times Ca + 2.5 \times Mg = CO_3^{2-}$) and $Al_2O_3$ concentrations ($2 \times Al_2O_3 = SiO_2$), respectively (Querol et al., 2001). We assume that the totality of Al analysed was in oxide form ($Al_2O_3$) (Querol et al., 2001).

### *2.3. Main components determination*

PM were divided in six main components: mineral matter (Sum of $CO_3^{2-}$, $SiO_2$, $Al_2O_3$, Ti, P, Mn, Mg, K, Fe, and Ca), sea spray (sum of $Na^+$ and $Cl^-$), organic matter and elemental carbon (OM+EC), secondary inorganic aerosols (sum of $SO_4^{2-}$, $NH_4^+$, and $NO_3^-$), trace elements (the sum of the rest of elements), and unaccounted (the difference between the PM concentration and the sum of the rest of fractions).

### *2.4. Exposure Model*

Concentrations of harmful metals (As, Be, Cd, Co, Cr, Hg, Mn, Ni, Pb, Se, V, and U) in the different PM fractions, seasons, and locations were used for assessing the human exposure. This metal selection was done according toxicological parameters availability in the risk assessment information system (RAIS, 2013). Exposure of the local population was estimated by considering only the inhalation route for an average adult individual (from 16 to 65 years old) in a mean daily routine based on annual data (Generalitat de Catalunya, 2012). Average exposure was calculated as divided in three different activities: sleeping, working/leisure, and outdoor time. Sleeping and working/leisure were considered as fully indoor activities. Numerical expression and parameters used to evaluate the exposure (Exp) for the different activities are shown in Equation 1:

$$Exp = \frac{C_{air} \times IR \times EF}{BW \times 365} \times \frac{AcT}{24} \qquad \text{(Eq. 1)}$$

Descriptions and values of the different parameters are presented in Table 1. $C_{air}$ used differed between indoor (sleeping and working/leisure) and outdoor activities. $C_{air}$ for outdoor activities was the obtained from analytical determinations. $C_{air}$ for indoor activities was calculated from outdoor $C_{air}$ through the software IAQX v 1.1, developed by the United States Environmental Protection Agency (US EPA, 2000). We set an average room volume of 30 $m^3$. Ventilation rates were taken according to the RD 1027/2007 specification for domestic and office buildings (IDA 2), published by the Spanish Ministry of Tourism, Energy, and Industry (MINETUR, 2013). Deposition and infiltration rates used in our simulations were obtained from previous studies (He et al., 2005; Hoek et al., 2008). Total exposure was calculated as the sum of every activity exposure (sleeping, work/leisure, and outdoor).

### *2.5. Human Health risks assessment*

Non-carcinogenic and carcinogenic risks calculations through inhalation were previously described (Rovira et al., 2010). Briefly, exposure concentrations (EC), Hazard Quotient (HQ) and cancer risk are described in equations 2, 3, and 4, respectively.

$$EC = \frac{C_{air} \times AcT \times EF \times ED}{AT \times 365 \times 24} \qquad \text{(Eq. 2)}$$

$$HQ = \frac{EC \times 10^6}{RfC} \qquad \text{(Eq. 3)}$$

$$CancerRisk = EC \times 10^6 \times IUR \qquad \text{(Eq. 4)}$$

All parameters used in these equations are depicted in Table 1.

**Table 1:** Parameters used for calculating human exposure and health risks.

| Parameter | Description | Value | | Units | Reference |
|---|---|---|---|---|---|
| IR | Inhalation rate | Sleeping | 7.58 | $m^3$/day | OEHHA 2012 |
| | | Work/Leisure | 38.8 | | |
| | | Outdoor | 38.8 | | |
| EF | Exposure frequency | 350 | | days/year | MAGRAMA, 2007 |
| BW | Body weight | 70 | | kg | US EPA, 1989 |
| AcT | Activity Time | Sleeping | 8.88 | hours/day | Generalitat de Catalunya, 2012 |
| | | Work/Leisure | 12.7 | | |
| | | Outdoor | 2.40 | | |
| ED | Exposure duration | 30 | | years | MAGRAMA, 2007 |
| AT | Averaging time | Carcinogenic: 70<br>Non-carcinogenic: 30 | | years | MAGRAMA, 2007 |
| RfC | Reference inhalation concentration | As | 1.50E+01 | ng/$m^3$ | RAIS, 2013 |
| | | Be | 2.00E+01 | | |
| | | Cd | 2.00E+01 | | |
| | | Co | 6.00E+00 | | |
| | | Cr | 1.00E+02 | | |
| | | Hg | 3.00E+02 | | |
| | | Mn | 5.00E+01 | | |
| | | Ni | 9.00E+01 | | |
| | | Se | 2.00E+04 | | |
| | | V | 1.00E+02 | | |
| | | U | 4.00E+01 | | |
| IUR | Inhalation Unit Risk | As | 4.3E-06 | $m^3$/ng | RAIS, 2013 |
| | | Be | 2.4E-06 | | |
| | | Cd | 1.8E-06 | | |
| | | Co | 9.0E-06 | | |
| | | Cr | 8.4E-05 | | |
| | | Ni | 2.6E-07 | | |
| | | Pb | 1.2E-08 | | |
| | Conversion factor | 365 | | days/year | |
| | Conversion factor | 24 | | hour/day | |
| | Conversion factor | $10^6$ | | ng/mg | |
| $C_{air}$ | Concentration in air | Site Specific | | mg/$m^3$ | Present study |

In order to know the carcinogenic potential of Cr, we assumed Cr (VI) concentration as 1/6 of the total Cr concentration (Brown et al., 2014; US EPA, 2011). It was also assumed that the totality of the As measured was inorganic (Huang et al., 2014).

### *2.6. Statistical Treatment*

For the statistical treatment we assumed a concentration equal to half the limit of detection for that species under the detection limit. Statistical processing was carried out by means of the statistical software package SPSS Statistics 20.0. For elucidating if the data present a parametric distribution a Levene test was performed. Subsequently, student T tests and ANOVA (parametric data), and Kruskall Wallis (non parametric data) tests were undergone. We considered difference as significant for those cases with a probability below 0.05 ($p<0.05$).

## 3. Results and discussion

### *3.1. PM concentrations*

Mean daily $PM_{10}$, $PM_{2.5}$, and $PM_1$ concentrations for the two plants (A and B) and for the different sampling periods: autumn (A), winter (W) and summer (S), are shown in Fig. 1. Statistically significant differences ($p<0.05$) were found between winter and the other seasons in plant A. The highest concentrations for the three fractions were reported during winter, with average values of 51.2 ± 13.9, 31.9 ± 9.9, and 31.3 ± 7.1 $\mu g/m^3$ for $PM_{10}$, $PM_{2.5}$, and $PM_{1,}$ respectively. Comparing the samples collected in summer and autumn, significantly ($p<0.05$) higher concentrations of $PM_{10}$ were recorded during autumn. No statistically significant differences were found between $PM_{10}$ and $PM_{2.5}$ concentrations obtained in plant B and those obtained in plant A in samples collected during autumn. However, regarding $PM_1$, statistically significant ($p<0.05$) smaller concentrations were found in plant B.

Mean values of the three particle fractions and the seasonal pattern obtained in plant A are similar to those reported previously in the metropolitan area of Barcelona (Pérez et al., 2008). In his turn, levels found in plant B are similar to those described in rural areas previously (Vicente et al. 2011; Pey et al. 2010c; Rodríguez et al. 2004). In our research, yearly limits established by the EU for $PM_{2.5}$ (25 $\mu g/m^3$), and yearly and daily values set for $PM_{10}$ (40 and 50 $\mu g/m^3$, respectively) (EU Parliament, 2008) were surpass only in the plant A in winter.

### *3.2. Main components of PM*

Fig. 2 shows the main components of the collected particles. The main components considered were organic matter and elemental carbon (OM+EC), sea spray (SS), mineral matter (MM), secondary inorganic aerosols (SIA), trace elements (TE), and unaccounted (U).

#### *3.2.1.Organic matter (OM) and elemental carbon (EC)*

OM+EC is mainly attributable to combustion sources (Pérez et al., 2008). Our results show that this component increases its contribution to the PM in the fine fraction of particles. This trend was described in previous studies (Pérez et al., 2008; Reche et al., 2012). Maximum levels of OM+EC were registered during winter, and reached their minimum in summer for every fraction. An increase in the use of heating systems and road traffic associated to low temperatures seems to be the cause for such result (Galindo et al., 2010). In our study, mean levels of OM+EC obtained during winter for $PM_{10}$ and $PM_{2.5}$ (19.8 and 16.8 µg/$m^3$, respectively) were higher than those recorded previously within the Barcelona metropolitan area (around 11.9 µg/$m^3$ for both fractions) (Viana et al., 2006). These differences could have their origin in different meteorological conditions during sampling collection, differences in heating systems between both places and/or combustion from cement facility. Comparing both cement plants, B location presented smaller values of OM+EC, explained by the lower traffic density.

#### *3.2.2.Sea spray (SS)*

Sea spray was mainly taking part into the $PM_{10}$ and $PM_{2.5}$ fractions, experiencing a great decrease in $PM_{1.}$ These results are in agreement with previous studies carried out by other authors (Kelly and Fussell, 2012; Mazzei et al., 2008). Higher contributions from this component are recorded in B location due to its proximity to the coastline.

#### *3.2.3.Mineral matter (MM)*

Maximum contributions of mineral matter are shown in $PM_{10}$ in winter. During this period, mineral matter contribution decreases notably when the particle size decreases to $PM_{2.5}$. In autumn, mineral matter shows similar contributions in $PM_{10}$ and $PM_{2.5}$, decreasing in $PM_1$. In summer, this component remains constant, between 10-20% for every fraction. Comparing both sites in autumn, cement plant B showed smaller contribution of this parameter in $PM_{10}$, but similar values to those experienced in plant for the rest of fractions.

### *3.2.4.Secondary Inorganic Aerosols (SIA)*

Ammonium and sulphate have been recorded to be present mainly in the fine fraction, while nitrate is usually part of the coarser fraction. For every season and location, SIA contributions show a homogeneous distribution among the three fractions, with values ranging between 12-22%. Comparing plant A and B in the same season, higher ammonium contributions are shown in location B, suggesting a bigger influence from farming activities (Pey et al., 2010b).

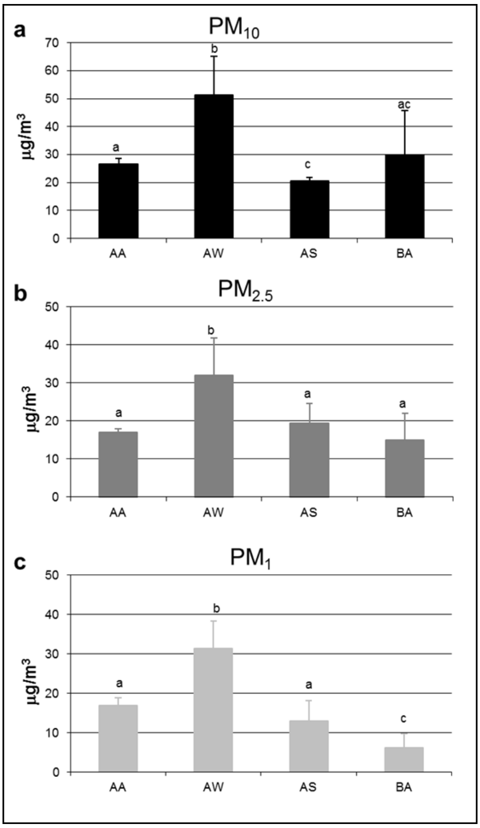

**Fig. 1:** Daily mean $PM_{10}$ (a), $PM_{2.5}$ (b), and $PM_1$ (c) levels for both cement plants (A and B), and sampling periods: autumn (A), winter (W), and summer (S). Different superscripted letters denote statistical significant differences (p<0.05).

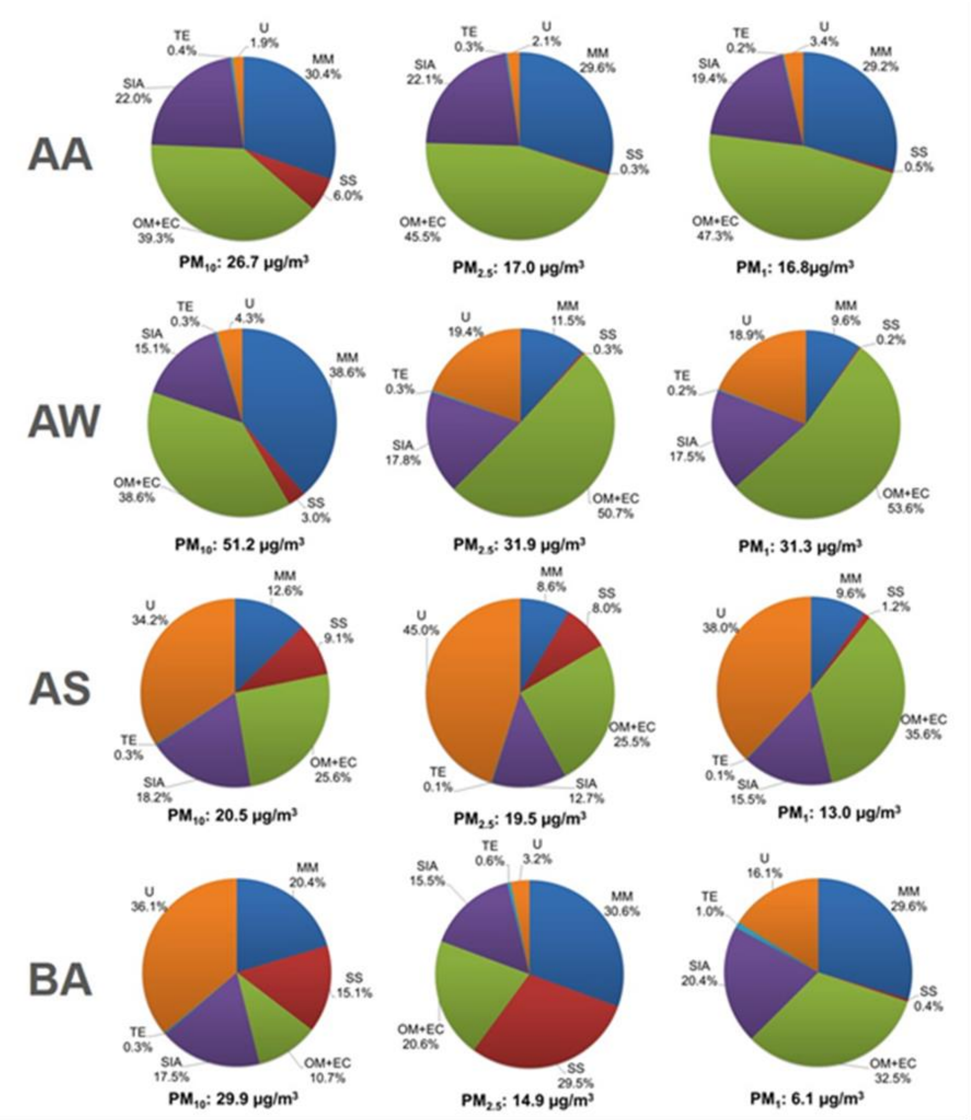

**Fig. 2:** Main components of collected PM for both cement plants (A and B), and sampling periods: autumn (A), winter (W), and summer (S). Results are expressed as percentage of the mass.

### *3.2.5.Trace elements (TE)*

Concentrations of all analysed elements for the three fractions can be seen in supplementary materials (Table S1). Levels of toxic metals regulated under the European legislation (As, Cd, Ni, and Pb) were much lower in our study (Table 2) than the annual average limits set by 2008/50/EC and 2004/107/EC Directives (EU Parliament, 2008, 2004). These regulations set mean annual air limits at 6, 5, 20, and 500 ng/m$^3$ for As, Cd, Ni, and Pb, respectively.

Statistically significant differences ($p<0.05$) were found during the winter period when comparing the levels of different trace elements with the rest of sampling periods. Higher concentrations for almost every metal were observed during the winter within the three analyzed fractions. Especially high are the levels of V within the PM$_{10}$ fraction in winter. This could be a result of changes in the composition of fuel used in the cement facility (Reche et al., 2012). Cu, Mn, and Sb in the coarser fraction (Pant and Harrison, 2013), which are used as traffic tracers, show similar levels in winter and autumn, experiencing a great decrease in summer. Comparing both plants in the same season, statistically significant higher ($p<0.05$) concentrations were recorded in A location for almost the totality of metals analyzed in every fraction. The only metals which registered higher significant levels in plant B were Sc, Mo, and V. These differences were especially clear in the PM$_{2.5}$ and PM$_1$ fractions, and could be a consequence of the differences in fuel composition between the two plants (Arbuzov et al., 2014; Lane et al., 2013; Santacatalina et al., 2010). Levels of Cu, Mn, and Sb were lower in the coarser fraction of B location, indicating a smaller contribution from traffic sources. Comparing our study with previous studies performed in the area (Pey et al., 2010c; Pérez et al., 2008; Minguillón et al., 2014), similar metal concentrations and seasonal patterns are observed. Plant A shows levels of metals similar to an urban-industrial site, while B presents a slightly higher metal concentrations than those reported for a rural background (Querol et al., 2007).

### *3.2.6. Unaccounted (U)*

This component expresses the difference between the PM levels and the sum of the rest of main components. Unaccounted contributions range between 2-46% for PM$_{2.5}$ and PM$_1$. This range decreases in the PM$_{10}$ fraction, having values between 2-35%. The origin of the unaccounted component is diverse. Previous studies have related this component with water bound to secondary inorganic aerosols, measurement errors or underestimations in the content of OM+EC (Pey et al., 2010a; Santacatalina et al., 2010).

.

**Table 2:** Levels (mean ± standard deviation) of toxic elements for both cement plants (A and B), and sampling periods: autumn (A), winter (W), and summer (S). Results are expressed in ng/m$^3$

| | AA | | | AW | | | AS | | | BA | | |
|---|---|---|---|---|---|---|---|---|---|---|---|---|
| | $PM_{10}$ | $PM_{2.5}$ | $PM_1$ | $PM_{10}$ | $PM_{2.5}$ | $PM_1$ | $PM_{10}$ | $PM_{2.5}$ | $PM_1$ | $PM_{10}$ | $PM_{2.5}$ | $PM_1$ |
| As | 0.63 ± 0.09 | 0.38 ± 0.07 | 0.36 ± 0.11 | 0.62 ± 0.13 | 0.59 ± 0.06 | 0.39 ± 0.21 | 0.19 ± 0.07 | ND | ND | 0.36 ± 0.16 | 0.30 ± 0.02 | 0.15 ± 0.10 |
| Be | 0.09 ± 0.03 | ND | ND | ND | ND | ND | ND | ND | ND | ND | ND | ND |
| Cd | 0.68 ± 0.35 | 0.31 ± 0.13 | 0.26 ± 0.05 | 0.47 ± 0.01 | 0.20 ± 0.01 | 0.20 ± 0.01 | ND | ND | ND | ND | ND | ND |
| Co | 0.33 ± 0.06 | 0.09 ± 0.03 | 0.08 ± 0.06 | 0.45 ± 0.27 | 0.15 ± 0.09 | 0.10 ± 0.02 | 0.15 ± 0.02 | ND | ND | 0.20 ± 0.10 | 0.11 ± 0.02 | 0.08 ± 0.01 |
| Cr | 7.28 ± 0.22 | ND | ND | 8.49 ± 3.09 | 4.20 ± 1.32 | 4.18 ± 3.26 | 3.26 ± 0.53 | ND | ND | 6.05 ± 0.70 | 6.02 ± 2.84 | ND |
| Mn | 6.98 ± 3.94 | 4.38 ± 1.02 | 3.32 ± 3.67 | 8.13 ± 2.82 | 7.48 ± 1.38 | 5.29 ± 2.47 | 7.85 ± 2.30 | 1.91 ± 0.91 | 1.89 ± 0.46 | 5.10 ± 3.32 | 2.83 ± 1.23 | 1.33 ± 0.70 |
| Ni | 4.07 ± 0.91 | 1.74 ± 0.14 | 1.6 ± 0.18 | 6.96 ± 2.42 | 5.94 ± 4.33 | 1.69 ± 0.94 | 7.0E ± 2.42 | ND | ND | 3.47 ± 0.47 | 3.24 ± 0.66 | 2.88 ± 0.69 |
| Pb | 11.9 ± 3.19 | 4.96 ± 1.76 | 4.07 ± 2.64 | 16.8 ± 3.03 | 13.2 ± 4.89 | 13.1 ± 3.88 | 3.16 ± 1.62 | 1.70 ± 2.21 | 1.29 ± 0.86 | 3.57 ± 2.57 | 2.88 ± 1.93 | 1.61 ± 0.96 |
| U | 0.11 ± 0.01 | 0.10 ± 0.01 | 0.10 ± 0.06 | 0.15 ± 0.04 | 0.15 ± 0.03 | 0.15 ± 0.07 | 0.02 ± 0.02 | ND | ND | 0.08 ± 0.06 | 0.08 ± 0.06 | ND |
| V | 6.87 ± 3.03 | 3.15 ± 0.57 | 2.22 ± 0.85 | 23.5 ± 8.95 | 9.09 ± 2.57 | 4.44 ± 1.02 | 6.57 ± 3.79 | 3.04 ± 0.05 | 2.85 ± 0.15 | 7.28 ± 1.02 | 6.36 ± 2.52 | 6.07 ± 1.85 |

ND: Not detected.

Except for the concentrations of OM+EC during winter, levels and seasonal patterns of the components in location A for every fraction present in this study are similar to those reported previously in the Barcelona metropolitan area (Pérez et al., 2008; Pey et al., 2010b, 2010c). Location A seems to be more influenced by traffic emissions than location B. Higher contributions in OM+EC could have their origin in traffic exhaust emissions, and contributions to coarse TE could have their source in traffic non-exhaust emissions.

### 3.3. Exposure Model

To quantify the exposure, outdoor and indoor (working/leisure and sleeping) activities were considered. To calculate indoor concentrations, IAQX model was run. Indoor PM levels and exposure values are shown in Table 3. In order to better assess the exposure to different size of particles, we calculated the health risks for three diameter ranges: $PM_{10-2.5}$ (result of subtracting $PM_{2.5}$ levels to $PM_{10}$ levels), $PM_{2.5-1}$ (result of subtracting $PM_1$ levels to $PM_{2.5}$ levels) and $PM_1$.

**Table 3:** Indoor and outdoor PM concentrations and exposure levels for both cement plants (A and B), and sampling periods: autumn (A), winter (W), and summer (S).

| | | PM concentration (µg/m$^3$) | | Exposure (mg/(kg·day)) | | |
|---|---|---|---|---|---|---|
| | | Outdoor | Indoor | Sleeping | Working/Leisure | Outdoor |
| AA | $PM_{10-2.5}$ | 9.68 | 4.36 | 1.7E-04 | 1.2E-03 | 5.1E-04 |
| | $PM_{2.5-1}$ | 0.16 | 0.10 | 4.0E-06 | 2.9E-05 | 8.5E-06 |
| | $PM_1$ | 16.8 | 10.9 | 4.2E-04 | 3.1E-03 | 9.0E-04 |
| | Total | 26.7 | 15.4 | 5.9E-04 | 4.3E-03 | 1.4E-03 |
| AW | $PM_{10-2.5}$ | 19.3 | 8.68 | 3.3E-04 | 2.4E-03 | 1.0E-03 |
| | $PM_{2.5-1}$ | 0.67 | 0.44 | 1.7E-05 | 1.2E-04 | 3.6E-05 |
| | $PM_1$ | 31.3 | 20.3 | 7.8E-04 | 5.7E-03 | 1.7E-03 |
| | Total | 51.2 | 29.4 | 1.1E-03 | 8.3E-03 | 2.7E-03 |
| AS | $PM_{10-2.5}$ | 1.04 | 0.47 | 1.8E-05 | 1.3E-04 | 5.5E-05 |
| | $PM_{2.5-1}$ | 6.51 | 4.23 | 1.6E-04 | 1.2E-03 | 3.5E-04 |
| | $PM_1$ | 13.0 | 8.42 | 3.2E-04 | 2.4E-03 | 6.9E-04 |
| | Total | 20.5 | 13.1 | 5.0E-04 | 3.7E-03 | 1.1E-03 |
| BA | $PM_{10-2.5}$ | 15.0 | 6.76 | 2.6E-04 | 1.9E-03 | 8.0E-04 |
| | $PM_{2.5-1}$ | 8.82 | 5.73 | 2.2E-04 | 1.6E-03 | 4.7E-04 |
| | $PM_1$ | 6.12 | 3.98 | 1.5E-04 | 1.1E-03 | 3.3E-04 |
| | Total | 30.0 | 16.5 | 6.3E-04 | 4.6E-03 | 1.6E-03 |

Indoor concentrations represent around 65% of the outdoor concentrations for $PM_{2.5-1}$ and $PM_1$, and around 45% of the outdoor $PM_{10}$ concentrations. In location A, the highest values of indoor concentrations are reached in the $PM_1$ fraction, while location B reaches its greatest values of indoor concentration in the $PM_{10-2.5}$ fraction. This result is a direct consequence of the higher proportion of $PM_1$ in $PM_{10}$ found in location A, and a bigger infiltration rate for fine PM. Regarding the activities, working and leisure showed the highest exposures for every period and PM fraction. Consequently, indoor exposure was the highest for every PM fraction due the most of time expended in indoor environment.

The results of specific metal exposure are shown in Fig. 3. Maximum exposure was reached by V in winter, with a value of $5.2 \cdot 10^{-6}$ mg/(kg·day). More than half of this value (54%) was reached in the $PM_{10-2.5}$. Se and Hg were not detected in any sampling period. Winter was the period that showed highest metal exposure for most of the metals analyzed. During this period, Pb and V levels of exposure were considerably higher (1.6 and 3.1 times respectively) than highest values for the rest of periods. Comparing the two sites in the same season, smaller levels of exposure were detected in location B. In this location, most of the exposure was addressed in the fine fraction, while in location A it was located in the $PM_{10-2.5}$ fraction. The higher metal content from traffic non-exhaust emissions in location A could explain this result.

Regarding the distribution of different metals, Co, Cd, and Be showed their maximum exposure values in the $PM_{10-2.5}$ fraction. U showed their maximum exposures in $PM_{2.5-1}$. As, Mn, and Pb experienced their peak exposure values in the $PM_1$ fraction. Apart from traffic, cement facilities could be also a supplementary source of Cd, Co, Cr, Mn, and Ni, and the main contributor for As, Pb, and V (Gupta et al., 2012; Santacatalina et al., 2010). Levels of exposure in plant A were similar to those reported before for the same area (Rovira et al., 2011b).

### *3.4. Human health risks assessment*

Regarding non-carcinogenic risks, HQ for all the chemicals was below the safety threshold, established in 1. Winter in plant A was the sampling period experiencing the highest levels of non-carcinogenic risks. Within this period, the highest HQ value corresponded to Mn allocated in $PM_1$, with a HQ value of 0.1. The rest of the HQ values were below 10% of the safety limit.

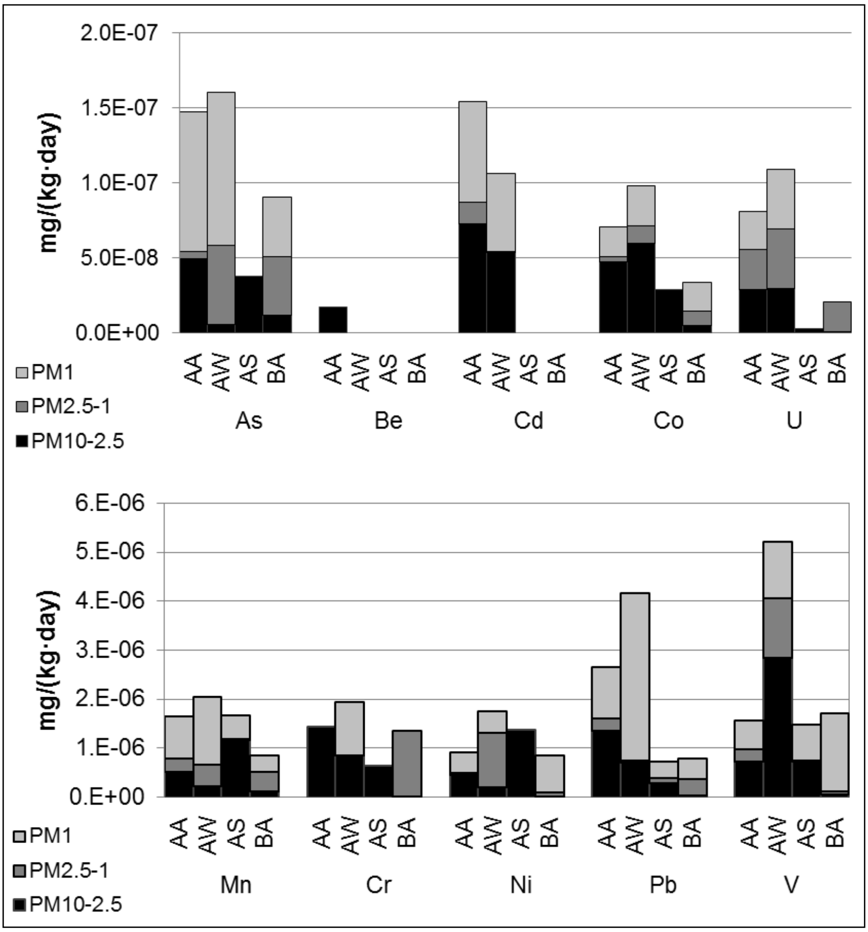

**Fig. 1:** Metal exposure levels for both cement plants (A and B), and sampling periods: autumn (A), winter (W), and summer (S).

Additional carcinogenic risks due to metal inhalation are depicted in Table 4. Cr (VI) was the only metal above the threshold for cancer risk established as $10^{-5}$ in Spain (MAGRAMA, 2007). This threshold was surpassed in every sampling period, except for plant A during summer. However, cancer values were assumable ($10^{-6}$–$10^{-4}$) depending on the variable characteristics of each individual (US EPA, 1996). The sampling period performed in winter experienced the highest levels of carcinogenic risk for most of metals. This period reached the highest overall value of additional cancer risk, with a value of 2.9 $10^{-5}$ for Cr (VI). In winter, most of the additional carcinogenic risks observed were part of the $PM_{2.5\text{-}1}$ or $PM_1$ fractions. Unlike winter, most of the additional carcinogenic risks observed in autumn and summer were located in the $PM_{10\text{-}2.5}$ fraction.

As observed with OM+EC, a higher contribution from combustion sources (such as heating systems) in winter could be the explanation to this fact.

**Table 4:** Carcinogenic risk due to the exposure to metals associated to different PM fractions for both cement plants (A and B), and sampling periods: autumn (A), winter (W), and summer (S).

| | | As | Be | Cd | Co | Cr (VI) | Ni | Pb |
|---|---|---|---|---|---|---|---|---|
| AA | PM$_{10-2.5}$ | 2.2E-07 | 4.3E-08 | 1.4E-07 | 4.5E-07 | 2.1E-05 | 1.3E-07 | 1.7E-08 |
| | PM$_{2.5-1}$ | 2.4E-08 | NC | 2.8E-08 | 3.4E-08 | NC | 1.0E-08 | 3.0E-09 |
| | PM$_1$ | 4.3E-07 | NC | NC | 1.3E-07 | NC | 1.2E-07 | 1.4E-08 |
| | Total | 6.8E-07 | 4.3E-08 | 1.7E-07 | 6.1E-07 | 2.1E-05 | 2.5E-07 | 3.4E-08 |
| AW | PM$_{10-2.5}$ | 2.5E-08 | NC | 1.0E-07 | 5.6E-07 | 1.2E-05 | 5.5E-08 | 8.8E-09 |
| | PM$_{2.5-1}$ | 2.4E-07 | NC | 1.4E-09 | 1.1E-07 | 6.5E-08 | 3.1E-07 | 4.7E-10 |
| | PM$_1$ | 4.7E-07 | NC | 1.0E-07 | 2.6E-07 | 1.6E-05 | 1.2E-07 | 4.4E-08 |
| | Total | 7.4E-07 | NC | 2.0E-07 | 9.4E-07 | 2.9E-05 | 4.9E-07 | 5.4E-08 |
| AS | PM$_{10-2.5}$ | 1.7E-07 | NC | NC | 2.8E-07 | 9.5E-06 | 3.8E-07 | 3.6E-09 |
| | PM$_{2.5-1}$ | NC | NC | NC | NC | NC | NC | 1.4E-09 |
| | PM$_1$ | NC | NC | NC | NC | NC | NC | 4.4E-09 |
| | Total | 1.7E-07 | NC | NC | 2.8E-07 | 9.5E-06 | 3.8E-07 | 9.4E-09 |
| BA | PM$_{10-2.5}$ | 5.4E-08 | NC | NC | 1.6E-07 | 7.9E-08 | 1.2E-08 | 1.7E-09 |
| | PM$_{2.5-1}$ | 1.8E-07 | NC | NC | 9.6E-08 | 2.0E-05 | 2.5E-08 | 4.3E-09 |
| | PM$_1$ | 1.8E-07 | NC | NC | 1.9E-07 | NC | 2.1E-07 | 5.4E-09 |
| | Total | 4.2E-07 | NC | NC | 4.5E-07 | 2.0E-05 | 2.5E-07 | 1.1E-08 |

NC: Not calculated. Values under the limit of detection

Carcinogenic risks were smaller in plant B if compared with plant A in the same season of the year. In this location, most of additional carcinogenic risks were in the PM$_1$ fraction. The presence of toxic metals in the fine fraction in location B suggests a higher contribution to metal content from combustion processes, such as the cement production (Kelly and Fussell, 2012).

PM$_1$ registers the maximum carcinogenic risk in the case of As and Pb, and the highest overall value for Cr (IV), evidencing thus the damage potential of PM$_1$. As said previously, As and Pb are elements suitable for coming principally from the cement plant. Although Cr (VI) is not an exclusive metal from cement production, it is feasible a contribution to this metal levels from the cement facility, especially in plant B, where traffic is less intense and no other industrial activities are developed. Levels of risks for most of the metals here described are similar to those previously reported in the same area (Rovira et al., 2011b).

## 4. Conclusions

In this study, three fractions of PM (10, 2.5, and 1) were collected in the nearby area of two cement plants in different seasons. Main components, exposure, and human health risks were calculated to preliminary know the main contributors to the PM mass and evaluate the potential health effects on the population. Our results show greatest levels of $PM_{10}$, $PM_{2.5}$, and $PM_1$ during winter. During this season, the highest levels of OM+EC and toxic metals were registered for every PM fraction. Consequently, exposure and human health risks experienced their highest values. Summer and autumn show similar levels of PM mass, but with a greater contribution from combustion sources in autumn. Comparing both plants in the same season, statistically significant differences were found in the levels of $PM_1$ and TE, presenting lower values plant B. Differences in the concentrations of Sc, Mo, and V between the two locations suggest the influence of the cement plant fuel used in the ambient particles composition, especially in the $PM_1$ fraction. Traffic had a major contribution to ambient PM in location A, while in location B, less impacted by traffic, cement plant had more influence, especially in the fine fraction.

Exposure values were higher for indoor activities (working/leisure and sleeping) due the most of time expended in indoor environment. Non-carcinogenic risks were below the safety threshold (HQ<1). Carcinogenic risks for most of the metals were below the limit of $10^{-5}$, except for Cr (VI), which exceeded it in both locations, but being in the range considered as assumable ($10^{-6}$-$10^{-4}$).

In this preliminary study, the importance of working on fine PM in areas influenced by cement plants is revealed. Maximum values of carcinogenic and non-carcinogenic risks were observed in the ambient $PM_1$. A possible contribution from cement plants to OM+EC and elements (especially As and Pb) in the ambient $PM_1$ is observed in this work. Further research, with greater number of samples and more detailed exposure evaluation for different ages and activities of indoor concentrations, is needed in order to elucidate the real contribution from different sources to human health damages.

### *Acknowledgments*

Financial support was received by the Spanish Ministry of Economy and Competitiveness (MINECO), through the project CTM2012-32778. F. Sánchez-Soberón received a doctoral scholarship as part of the project above mentioned. The authors also want to thank

Quentin Aiello for his collaboration through the investigation and LAFARGE CEMENTOS SAU and ADASA for their support during the sampling.

## References

Abdul-Wahab, S.A., 2006. Impact of fugitive dust emissions from cement plants on nearby communities. Ecol. Modell. 195, 338–348.

Anderson, J.O., Thundiyil, J.G., Stolbach, A., 2012. Clearing the air: a review of the effects of particulate matter air pollution on human health. J. Med. Toxicol. 8, 166–175.

Arbuzov, S.I., Volostnov, A.V., Mezhibor, A.M., Rybalko, V.I., Ilenok, S.S., 2014. Scandium (Sc) geochemistry in coals (Siberia, Russian Far East, Mongolia, Kazakhstan, and Iran). Int. J. Coal Geol. 125, 22–35.

Brown, R.J.C., Van Aswegen, S., Webb, W.R., Goddard, S.L., 2014. UK concentrations of chromium and chromium (VI), measured as water soluble chromium, in $PM_{10}$. Atmos. Environ. 99, 385–391.

Cassee, F.R., Héroux, M.-E., Gerlofs-Nijland, M.E., Kelly, F.J., 2013. Particulate matter beyond mass: recent health evidence on the role of fractions, chemical constituents and sources of emission. Inhal. Toxicol. 25, 802–812.

Cifuentes, L.A., Vega, J., Köpfer, K., Lave, L.B., 2000. Effect of the fine fraction of particulate matter versus the coarse mass and other pollutants on daily mortality in Santiago, Chile. J. Air Waste Manag. Assoc. 50, 1287–1298.

Cohen, A.J., Ross Anderson, H., Ostro, B., Pandey, K.D., Krzyzanowski, M., Künzli, N., Gutschmidt, K., Pope, A., Romieu, I., Samet, J.M., Smith, K., 2005. The global burden of disease due to outdoor air pollution. J. Toxicol. Environ. Health. A 68, 1301–1307.

Čupr, P., Flegrová, Z., Franců, J., Landlová, L., Klánová, J., 2013. Mineralogical, chemical and toxicological characterization of urban air particles. Environ. Int. 54, 26–34.

EU Comission, 2013. Best Available Techniques (BAT) Reference Document for the Production of Cement, Lime and Magnesium Oxide. EUR 26129 EN. European Commission Joint Research Centre.

EU Parliament, 2004. Directive 2004/107/EC of the European Parliament and of the Council of 15 December 2004 relating to arsenic, cadmium, mercury, nicker and polyciclic aromatic hydrocarbons in ambient air. Off. J. Eur. Communities. 23, 3–16.

EU Parliament, 2008. Directive 2008/50/EC of the European Parliament and of the Council of 21 May 2008 on ambient air quality and cleaner air for Europe. Off. J. Eur. Communities. 152, 1–44.

EEA, 2013. Air quality in Europe — 2013 report. EEA report 9/2013. European Environment Agency.

Galindo, N., Varea, M., Gil-Moltó, J., Yubero, E., Nicolás, J., 2010. The Influence of Meteorology on Particulate Matter Concentrations at an Urban Mediterranean Location. Water, Air, Soil Pollut. 215, 365–372.

Generalitat de Catalunya, 2012. Enquesta de l'ús del temps 2010-2011 [WWW Document]. URL http://www.idescat.cat/cat/idescat/publicacions/cataleg/pdfdocs/eut-pr2010-11.pdf (accessed 6.12.14)

Gupta, R.K., Majumdar, D., Trivedi, J.V., Bhanarkar, A.D., 2012. Particulate matter and elemental emissions from a cement kiln. Fuel Process. Technol. 104, 343–351.

Harrison, R.M., Yin, J., 2000. Particulate matter in the atmosphere: which particle properties are important for its effects on health? Sci. Total Environ. 249, 85–101.

He, C., Morawska, L., Gilbert, D., 2005. Particle deposition rates in residential houses. Atmos. Environ. 39, 3891–3899.

Hoek, G., Kos, G., Harrison, R., de Hartog, J., Meliefste, K., ten Brink, H., Katsouyanni, K., Karakatsani, A., Lianou, M., Kotronarou, A., Kavouras, I., Pekkanen, J., Vallius, M., Kulmala, M., Puustinen, A., Thomas, S., Meddings, C., Ayres, J., van Wijnen, J., Hameri, K., 2008. Indoor-outdoor relationships of particle number and mass in four European cities. Atmos. Environ. 42, 156–169.

Huang, M., Chen, X., Zhao, Y., Yu Chan, C., Wang, W., Wang, X., Wong, M.H., 2014. Arsenic speciation in total contents and bioaccessible fractions in atmospheric particles related to human intakes. Environ. Pollut. 188, 37–44.

Kelly, F.J., Fussell, J.C., 2012. Size, source and chemical composition as determinants of toxicity attributable to ambient particulate matter. Atmos. Environ. 60, 504–526.

Lane, S., Proemse, B.C., Tennant, A., Wieser, M.E., 2013. Concentration measurements and isotopic composition of airborne molybdenum collected in an urban environment. Anal. Bioanal. Chem. 405, 2957–2963.

MAGRAMA, 2007. Guía Técnica de aplicación del RD 9/2005, de 14 de enero, por el que se establece la relación de actividades potencialmente contaminantes del suelo y los criterios y estándares para la declaración de suelos contaminados. Ministerio de Agricultura, Alimentación y Medio Ambiente.

Mari, M., Nadal, M., Schuhmacher, M., Domingo, J.L., 2009. Exposure to heavy metals and PCDD/Fs by the population living in the vicinity of a hazardous waste landfill in Catalonia, Spain: health risk assessment. Environ. Int. 35, 1034–1039.

Mazzei, F., D'Alessandro, A., Lucarelli, F., Nava, S., Prati, P., Valli, G., Vecchi, R., 2008. Characterization of particulate matter sources in an urban environment. Sci. Total Environ. 401, 81–89.

MINETUR, 2013. Reglamento de Instalaciones Térmicas de los Edificios. Versión Consolidada. Instituto para la Diversificación y Ahorro de la Energía. Ministerio de Industria, Energía y Turismo.

Minguillón, M.C., Cirach, M., Hoek, G., Brunekreef, B., Tsai, M., de Hoogh, K., Jedynska, A., Kooter, I.M., Nieuwenhuijsen, M., Querol, X., 2014. Spatial variability of trace elements and sources for improved exposure assessment in Barcelona. Atmos. Environ. 89, 268–281.

Ministerio de Fomento, 2012. Mapa de Tráfico [WWW Document]. URL http://www.fomento.gob.es/NR/rdonlyres/6B349269-A03D-45CA-8AEC-0AF11A7EA168/119364/MapaIntensidad2012.pdf (accessed 4.17.14).

OEHHA, 2012. Hot Spots Exposure guidelines 3: Breathing rates [WWW Document]. URL http://oehha.ca.gov/air/hot_spots/pdf/2012tsd/Chapter3_2012.pdf (accessed 9.25.14).

Pant, P., Harrison, R.M., 2013. Estimation of the contribution of road traffic emissions to particulate matter concentrations from field measurements: A review. Atmos. Environ. 77, 78–97.

Pérez, N., Pey, J., Querol, X., Alastuey, A., López, J.M., Viana, M., 2008. Partitioning of major and trace components in $PM_{10}$–$PM_{2.5}$–$PM_1$ at an urban site in Southern Europe. Atmos. Environ. 42, 1677–1691.

Pey, J., Alastuey, A., Querol, X., Rodríguez, S., 2010a. Monitoring of sources and atmospheric processes controlling air quality in an urban Mediterranean environment. Atmos. Environ. 44, 4879–4890.

Pey, J., Pérez, N., Querol, X., Alastuey, A., Cusack, M., Reche, C., 2010b. Intense winter atmospheric pollution episodes affecting the Western Mediterranean. Sci. Total Environ. 408, 1951–1959.

Pey, J., Querol, X., Alastuey, A., 2010c. Discriminating the regional and urban contributions in the North-Western Mediterranean: PM levels and composition. Atmos. Environ. 44, 1587–1596.

Predicatori, F., Intini, B., Frontero, P., Martinelli, C., Culmone, L.R., Brunelli, S., Salomoni, A., Mosconi, C., Mattiolo, G., 2009. Influence of a cement industry on the fine and ultrafine particles composition in a rural area. Radiat. Prot. Dosimetry 137, 288–293.

Querol, X., Alastuey, A., Rodríguez, S., Plana, F., Ruiz, C.R., Cots, N., Massagué, G., Puig, O., 2001. $PM_{10}$ and $PM_{2.5}$ source apportionment in the Barcelona Metropolitan area, Catalonia, Spain. Atmos. Environ. 35, 6407–6419.

Querol, X., Viana, M., Alastuey, A., Amato, F., Moreno, T., Castillo, S., Pey, J., de la Rosa, J., Sánchez de la Campa, A., Artíñano, B., Salvador, P., García Dos Santos, S., Fernández-Patier, R., Moreno-Grau, S., Negral, L., Minguillón, M.C., Monfort, E., Gil, J.I., Inza, A., Ortega, L.A., Santamaría, J.M., Zabalza, J., 2007. Source origin of trace elements in PM from regional background, urban and industrial sites of Spain. Atmos. Environ. 41, 7219–7231.

RAIS, 2013. The Risk Assessment Information System [WWW Document]. URL http://rais.ornl.gov/ (accessed 10.13.14).

Reche, C., Moreno, T., Amato, F., Viana, M., van Drooge, B.L., Chuang, H.-C., Bérubé, K., Jones, T., Alastuey, A., Querol, X., 2012. A multidisciplinary approach to characterise exposure risk and toxicological effects of $PM_{10}$ and $PM_{2.5}$ samples in urban environments. Ecotoxicol. Environ. Saf. 78, 327–335.

Rodríguez, S., Querol, X., Alastuey, A., Viana, M.-M., Alarcón, M., Mantilla, E., Ruiz, C.R., 2004. Comparative $PM_{10}$-$PM_{2.5}$ source contribution study at rural, urban and industrial sites during PM episodes in Eastern Spain. Sci. Total Environ. 328, 95–113.

Rovira, J., Mari, M., Nadal, M., Schuhmacher, M., Domingo, J.L., 2010. Partial replacement of fossil fuel in a cement plant: risk assessment for the population living in the neighborhood. Sci. Total Environ. 408, 5372–5380.

Rovira, J., Mari, M., Nadal, M., Schuhmacher, M., Domingo, J.L., 2011a. Use of sewage sludge as secondary fuel in a cement plant: human health risks. Environ. Int. 37, 105–111.

Rovira, J., Mari, M., Schuhmacher, M., Nadal, M., Domingo, J.L., 2011b. Monitoring environmental pollutants in the vicinity of a cement plant: a temporal study. Arch. Environ. Contam. Toxicol. 60, 372–384.

Rovira, J., Nadal, M., Schuhmacher, M., Domingo, J.L., 2014. Environmental levels of PCDD/Fs and metals around a cement plant in Catalonia, Spain, before and after alternative fuel implementation. Assessment of human health risks. Sci. Total Environ. 485-486, 121–129.

Rovira, J., Flores, J., Schuhmacher, M., Nadal, M., Domingo, J.L., 2015. Long-Term Environmental Surveillance and Health Risks of Metals and PCDD/Fs Around a Cement Plant in Catalonia, Spain. Hum Ecol Risk Assess. 21, 514–532.

Santacatalina, M., Reche, C., Minguillón, M.C., Escrig, A., Sanfelix, V., Carratalá, A., Nicolás, J.F., Yubero, E., Crespo, J., Alastuey, A., Monfort, E., Miró, J. V, Querol, X., 2010. Impact of fugitive emissions in ambient PM levels and composition: a case study in Southeast Spain. Sci. Total Environ. 408, 4999–5009.

Schwartz, J., Dockery, D.W., Neas, L.M., 1996. Is daily mortality associated specifically with fine particles? J. Air Waste Manag. Assoc. 46, 927–939.

Tiessen, H., Moir, J., 2000a. Total and organic carbon., in: Carter, M.R., Gregorich, E.G. (Eds.), Soil Sampling and Methods of Soil Analysis. Canadian Society of Soil Science.

Tiessen, H., Moir, J., 2000b. Total nitrogen., in: Carter, M.R., Gregorich, E.G. (Eds.), Soil Sampling and Methods of Soil Analysis. Canadian Society of Soil Science.

US EPA, 1989. Risk assess ment guidance for superfund volume I: human health evaluation manual. EPA/540/1-89/002. United States Environmental Protection Agency.

US EPA, 1996. Soil screening guidance: technical background document. EPA/540/R-95/128. United States Environmental Protection Agency.

US EPA, 2000. Indoor Air Quality Modeling [WWW Document]. URL http://www.epa.gov/nrmrl/appcd/mmd/iaq.html (accessed 10.13.14).

US EPA, 2011. Methods to Develop Inhalation Cancer Risk Estimates for Chromium and Nickel Compounds. EPA/452/R-11/12. United States Environmental Protection Agency.

US EPA, 2012. Preferred/Recommended Models | TTN - Support Center for Regulatory Atmospheric Modeling | US EPA [WWW Document]. URL http://www.epa.gov/scram001/dispersion_prefrec.htm (accessed 1.21.15).

US EPA, 2013. Particulate Matter | Air & Radiation | US EPA [WWW Document]. URL http://www.epa.gov/pm/ (accessed 3.11.14).

Viana, M., Chi, X., Maenhaut, W., Querol, X., Alastuey, A., Mikuska, P., Vecera, Z., 2006. Organic and elemental carbon concentrations in carbonaceous aerosols during summer and winter sampling campaigns in Barcelona, Spain. Atmos. Environ. 40, 2180–2193.

Vicente, A.B., Sanfeliu, T., Jordan, M.M., 2011. Comparison Between Industrial–Urban and Rural Particle Stations in a Ceramic Cluster (NE, Spain). Water, Air, Soil Pollut. 215, 83–96.

WHO, 2014. Frequently Asked Questions: Ambient and Household Air Pollution and Health [WWW Document]. URL http://www.who.int/phe/health_topics/outdoorair/databases/faqs_air_pollution.pdf?ua=1 (accessed 6.12.14).

# CHAPTER 2: Size-distribution of airborne polycyclic aromatic hydrocarbons and other organic source markers in the surroundings of a cement plant powered with alternative fuels

Francisco Sánchez-Soberón, Barend L. van Drooge, Joaquim Rovira, Joan O. Grimalt, Martí Nadal, José L. Domingo, Marta Schuhmacher (2016). Science of the Total Environment 550 (2016) 1057–1064.

# Size-distribution of airborne polycyclic aromatic hydrocarbons and other organic source markers in the surroundings of a cement plant powered with alternative fuels

Francisco Sánchez-Soberón, Barend L. van Drooge, Joaquim Rovira, Joan O. Grimalt, Martí Nadal, José L. Domingo, Marta Schuhmacher (2016). Science of the Total Environment 550 (2016) 1057–1064

## Abstract

The distributions of polycyclic aromatic hydrocarbons (PAHs) and molecular tracer organic compounds for biomass combustion, traffic emissions, soil dust, and secondary aerosol processing have been studied in three fractions of ambient air particulate matter ($PM_{10}$, $_{2.5,}$ and $_1$) collected in the vicinity of a cement plant. PAH concentrations were used to estimate the carcinogenic risks in humans. Combustion related compounds, including PAHs, and those from secondary aerosol processing, predominated in the finest (PM<1) fraction, while saccharides related to organic soil dust predominated in the coarse fraction (<PM10). The molecular markers of biomass combustion were found in high concentrations, indicating the influence of biomass burning on PM. Most predominant PAHs were five and six rings species, related to a PAH profile characteristic of urban-industrial environments. The concentrations of benzo[a]pyrene varied between 0.2 and 1.0 ng/m$^3$, which is close but lower than the annual limit value of 1 ng/m$^3$ established by law. Exposure and inhalation carcinogenic risks from total PAHs were below the EPA threshold of acceptable risk ($1 \cdot 10^{-6}$).

*Keywords*

Cement; Particulate matter; Polycyclic aromatic hydrocarbons; Human health risk

*Highlights*

- Three fractions of PM (10, 2.5 and 1) were collected nearby a cement plant.
- Levels of PAHs and other organic compounds were analysed in these fractions of PM.
- Biomass combustion products were the most prevalent organic compounds.
- Levels of BaP were relatively high (0.6 ng/m$^3$), but lower than legislation limits.
- Carcinogenic risks for male and female individuals were considered acceptable.

## 1. Introduction

Polycyclic aromatic hydrocarbons (PAHs) are generated during incomplete combustion processes (Keyte et al., 2013). Their fused aromatic ring structure (Kamankesh et al., 2015) gives to some of them toxic properties such as cancer and birth failure (ATSDR, 2015; IARC, 2012; US EPA, 2008). Accordingly, outdoor levels of some of these compounds are restricted by legislation (EU Parliament, 2005; US EPA, 2007). Although natural processes such as volcanic eruptions and wildfires release PAHs, anthropogenic sources, such as road traffic, industry, power production, house heating, and incineration (Liao et al., 2011; Manoli et al., 2004; Zhou et al., 2015) are dominating contributors in densely populated areas (Lee and Van Tuan, 2010). The variety of sources, combustion processes, and environmental conditions result in a diversity of PAH distributions (Cecinato et al., 2014; Galarneau, 2008; Sicre et al., 1987). A potential industrial source for PAHs emissions is cement production (García-Pérez et al., 2015; Li et al., 2014). In this process, different amounts of fuel and raw materials are submitted to high temperatures and limited knowledge is available on the influence of different combustion sources, namely alternative fuels, such as sewage sludge or biomass, in the overall PAH production (Conesa et al., 2011).

Airborne PAHs can be present in the gas phase or bound to ambient air particulate matter (PM), depending on the physico-chemical properties of the compound and the meteorological conditions (van Drooge, 2013). Higher PAH levels in PM are typically observed in late autumn and winter, due to lower temperatures, which favours the adsorption of semi-volatile PAHs to PM. This effect, together with lower photo-chemical degradation of PAHs, and shallower atmospheric mixing layer, results in the accumulation of PAHs in a small air layer (Agudelo-Castañeda et al., 2014; Křůmal et al., 2013; van Drooge, 2013).

Concerning the PAH characteristics, those with highest molecular weight are preferentially linked to the finest PM fraction (Cecinato et al., 2014; Sarigiannis et al.,

---

*Abbreviations:* AT, averaging exposition time; ATSDR, Agency for Toxic Substances and Disease Registry; BaP, benzo[a]pyrene (BaP); BaPE, benzo[a]pyrene equivalent; BSFTA, bis(trimethylsilyl)trifluoroacetamide; C, concentration; Cal. EPA, Californian Environmental Protection Agency; CF, conversion factor; BW, body weight; ED, exposure duration; EF, exposure frequency; EU, European Union; GC/MS, Gas Chromatography coupled to Mass Spectrometry; IARC, International Agency for Research on Cancer; IR, inhalation rate; L/M , levoglucosan/mannosan ratio; PAH, polycyclic aromatic hydrocarbon; PM, particulate matter; QFF, quartz fibre filters; SF, slope factor; TEF, Toxicity Equivalency Factors; TMCS, trimethylchlorosilane ; USA; United States of America; US EPA, United States Environmental Protection Agency.

2015; Varea et al., 2011). Moreover, some of the higher molecular weight PAHs are the most toxic ones, i.e. benzo[a]pyrene (BaP). These two characteristics make PM-bound PAHs especially harmful for health, since submicron PM can enter deep into the respiratory system, and eventually cross the air-blood barrier (Kelly and Fussell, 2012).

Efforts have been made to elucidate source-dependent PAH distributions within different PM fractions, and assessment of their attributable risks to health. Studies in this field are mainly focused on urban-traffic influenced, industrial and indoor environments (Ladji et al., 2009; Liaud et al., 2014; Mesquita et al., 2014; Mirante et al., 2013; Sarigiannis et al., 2015). Only a few studies have considered PM-associated PAHs in the surrounding of cement facilities (Cho et al., 2014; Ercan and Dinçer, 2015; Senthilkumar et al., 2014), but they are focused on $PM_{10}$, which results in a significant lack of information concerning the PAH content and distribution among different sizes of PM, especially the submicron fraction, in areas receiving the emissions from these plants. The European policy promotes the use of alternative fuels for future industrial and domestic applications. (EU Comission, 2014). It is therefore important to study the emissions of installation such as cement plant and to investigate whether other local biomass burning sources may contribute to the particle-bounded PAHs in order to clarify their contributions to ambient PM.

The present study is aimed to improve the knowledge on the contribution of cement plants using alternative fuels to the ambient air PM-associated PAHs, and to assess their potential adverse effects on human health. Three PM fractions (<10, <2.5, and <1 µm) were collected during late autumn in the surroundings of a cement facility located in the outskirts of Barcelona. PAHs and molecular organic tracer compounds, i.e. hopanes for traffic, anhydro-saccharides and dihydroabietic acid for biomass burning, saccharides for organic soil dust, and dicarboxylic acids for secondary organic aerosol formation, were analysed in these three fractions in order to elucidate the origin of their organic matter constituents. Diagnostic ratios were used for source apportionment. Exposure and human health risks attributable to PAHs were calculated for average male and female adult individuals.

## 2. Materials and Methods

### *2.1. Site description and PM sampling*

Descriptions of the area have been provided in previous studies (Rovira et al., 2011; Schuhmacher and Domingo, 2006). Briefly, the studied cement facility is situated in the north of Barcelona. Several industries are active in the area, among them a waste treatment plant. Moreover, two highways with dense traffic in the vicinity of the area as well as the inhabited urban zone. The cement plant has been active since 1917, with a current annual production of about 1 million tons. Owing to the urban development in the surroundings, the distance from the facility to some neighbourhoods has decreased to less than 300 m in the recent years, which increases concern of the administration and public organizations on the possible health impacts of the kiln emissions. Besides fossil fuels, sewage sludge, meat and bone meal, refuse derived fuels, and biomass supply up to 20% of the total energy production are used to power this plant.

Three sampling devices were placed in the roof of a two storey school located 300 m from the cement plant. According to previous studies, this site registers the highest levels of PM in the area, and, therefore, the highest potential health risks (Rovira et al., 2011). Samples were collected during two consecutive weeks comprising the months of November and December of 2014. These days were selected having into consideration results from previous studies, in which major PAH concentrations, and, therefore, maximum risk levels were reached during these days (Mesquita et al., 2014). Meteorological data from this period was obtained from a nearby meteorological monitoring station. Three PM fractions (<10, <2.5 and <1 µm) were collected simultaneously with three high-volume active samplers. $PM_{10}$ and $PM_{2.5}$ were sampled using two TE-6070-DV devices (Tisch Environmental), while $PM_1$ samples were collected using CAV-A/mb sampler (MCV SA). Daily sampling volumes were 1700 $m^3$ for $PM_{10}$ and $PM_{2.5}$ and around 700 $m^3$ for $PM_1$. PM samples were collected on pre-heated quartz fibre filters (QFF). Before and after sampling, QFF were weighted at room conditions to have an approximate value of PM levels. This procedure was followed in order to minimise PAHs losses after sampling. Finally, filters were wrapped in aluminium foil, and stored at -20ºC until further analysis.

### *2.2. Analytical methods*

QFF were ultrasonically extracted in a mixture of dichloromethane and methanol (2:1 (v/v); 3× 20 mL; Merck, Germany) for 15 min. Before extraction 25 µL of surrogate standard succinic acid-D4, levoglucosan-D7 (Cambridge Isotopic Laboratories, UK), anthracene-D10, benz[a]anthrancene-D12, benzo[k]fluoranthene-D12, and benzo[ghi]perylene-D12 (Dr. Ehrenstorfer, Germany) were added to samples and blanks. Extracts were then passed through a 0.45-µm Teflon membrane filter (Whatman, USA) to remove particles. Finally, the extracts were concentrated by rotovap to 1 mL.

### *2.2.1. Analytical procedure for PAHs and hopanes.*

Half of the volume of the extract (0.5 mL) was cleaned up by adsorption column chromatography on 1 g of aluminium oxide (Merck, Germany), previously activated at 120 ºC overnight. The analytes were eluted with 5 mL of (9:1 v/v) hexane-dichloromethane and 15 mL of (1:2 v/v) hexane-dichloromethane, respectively (Merck, Germany). The collected fractions were concentrated by rotovap to 0.5 mL and further concentrated until almost dryness under a gentle stream of $N_2$ and diluted in 25 µL of iso-octane (Merck, Germany). An injection standard of 1-phenyldodecane was added before gas chromatographic analysis.

### *2.2.2. Analytical procedure for saccharides, and dicarboxylic acids.*

The analytical methods for these compounds were similar to those described elsewhere (Fontal et al., 2015; Medeiros and Simoneit, 2007). Aliquots of 25 µL of the extract were evaporated to dryness under a stream of $N_2$. Then, 25 µL of bis(trimethylsilyl)trifluoroacetamide (BSFTA) +1 % trimethylchlorosilane (TMCS) (Supelco, USA) and 10 µL of pyridine (Merck, Germany) were added for overnight derivation at room temperature. After that, an injection standard of 1-phenyldodecane was added before gas chromatographic analysis.

### *2.2.3. Instrumental analyses*

Instrumental analyses were carried out by gas chromatography coupled to mass spectrometry (GC/MS). Samples were injected in a Thermo GC/MS equipped with a 60-m fused capillary column (HP-5MS 0.25-mm×0.25-µm film thickness). The oven temperature program started at 60 °C held for 1 min, and then it was heated to 120 °C at 12 °C/min and to 310 °C at 4 °C/min where it was held for 20 min. The injector, ion source, quadrupole, and transfer line temperatures were 280 °C, 200 °C, 150 °C, and 280 °C, respectively. Helium was used as carrier gas at 0.9 mL/s. The MS selective detector operated in full scan (m/z 50–650) and electron impact (70 eV) modes.

PAHs were identified by the following ions: phenanthrene (*m/z* 178), anthracene (*m/z* 178), fluoranthene (*m/z* 202), pyrene (*m/z* 202), retene (m/z 219), benz[a]anthracene (*m/z* 228), chrysene (*m/z* 228), benzo[b]fluoranthene (*m/z* 252), benzo[k]fluoranthene (*m/z* 252), benzo[e]pyrene (*m/z* 252), benzo[a]pyrene (*m/z* 252), indeno[1,2,3-cd]pyrene (*m/z* 276), benzo[ghi]perylene (*m/z* 276), and coronene (*m/z* 300). Quantification was performed by calculating the concentrations of the analytes with the external standard calibration curve. The calculated concentrations were corrected for the recoveries of the above-mentioned surrogates: n-C24-$d_{50}$ (*m/z* 66), anthracene-$d_{10}$ (*m/z* 188), benz[a]anthrancene-$d_{12}$ (*m/z* 240), benzo[k]fluoranthene-$d_{12}$ (*m/z* 264), and benzo[ghi]perylene-$d_{12}$ (*m/z* 288). Hopanes were identified with the ion *m/z* 191 and quantified using the relative response of benzo[a]pyrene.

Biomass combustion products, and sugars and derivates were identified with ion *m/z* 204. Dicarboxylic acids were identified in their derivatized form from the *m/z* 73 and 147 fragmentograms, as well as the individual *m/z* 247, 261, 233, and 295 ions, respectively. Quantification was performed using the external standard calibration curves of levoglucosan and succinic acid. These concentrations were corrected by the recoveries of the surrogate standards $d_4$-succinic acid (*m/z* 251) and $d_7$-levoglucosan (*m/z* 206).

### 2.3. Risk assessment

Preliminary values of human exposure and carcinogenic risks derived from PAHs inhalation were calculated for average 35 years old male and female individuals. The benzo[a]pyrene equivalent (BaPE, in ng/m$^3$) levels for every carcinogenic compound were calculated multiplying concentration of different carcinogenic PAHs ($C_{i,}$ in ng/m$^3$) by Toxicity Equivalency Factors (TEF) provided by US EPA (1993), as expressed in Equation 1:

$$BaPE_i = C_i \times TEF_i \qquad \text{(Eq. 1)}$$

Exposure (mg/(kg·day)) was calculated as described in Equation 2:

$$Exp = \frac{BaPE_i \times IR \times EF}{BW \times 365} \times CF \qquad \text{(Eq. 2)}$$

where IR is the Inhalation Rate (m$^3$/day), EF is the Exposure Frequency (days/year), BW is the Body Weight (kg), and CF is the conversion factor (mg/ng). To know carcinogenic risks for the two assessed population groups we adapted equations from previous studies (Sarigiannis et al., 2015) into Equation 3:

$$\text{Cancer Risk} = Exp \times SF \times ED/AT \qquad \text{(Eq. 3)}$$

being ED the exposure duration (years), AT the averaging exposition time (years), and SF the Slope Factor ((kg·day)/mg) for benzo[a]pyrene (BaP) described by Cal. EPA (2011). All parameters used in the above equations are described in Table 1. To calculate the potentially highest carcinogenic risk the model assumed that the total amount of benz[b+j]anthracene was benz[b]anthracene.

**Table 1:** Parameters used in the exposure and cancer risk calculations.

| Parameter | Description | Value | | Units | Reference |
|---|---|---|---|---|---|
| IR | Inhalation rate | Male | 16.88 | $m^3$/day | US EPA, 2011 |
| | | Female | 13.68 | | |
| EF | Exposure frequency | 350 | | days/year | MAGRAMA, 2007 |
| BW | Body weight | Male | 71.5 | kg | US EPA, 2011 |
| | | Female | 58.7 | | |
| ED | Exposure duration | 35 | | years | MAGRAMA, 2007 |
| AT | Averaging time | 70 | | years | MAGRAMA, 2007 |
| TEF | Toxic Equivalent Factor | Benzo[a]pyrene | 1 | unitless | US EPA, 1993 |
| | | Benz[a]anthracene | 0.1 | | |
| | | Benzo[b]fluoranthene | 0.1 | | |
| | | Benzo[k]fluoranthene | 0.01 | | |
| | | Chrysene | 0.001 | | |
| | | Dibenz[a,h]anthracene | 1 | | |
| | | Indeno[1,2,3-cd]pyrene | 0.1 | | |
| SF | Slope Factor | Benzo[a]pyrene | 3.90 | (kg•day)/mg | Cal. EPA, 2011 |
| | Conversion factor | 365 | | days/year | |
| CF | Conversion factor | 10E-06 | | mg/ng | |
| $C_i$ | $PAH_i$ Concentration | Compound Specific | | ng/$m^3$ | Present study |

## *2.4. Statistical analysis*

Statistical processing was carried out using the statistical software package XLSTAT version 2015.2.02.18681. In order to study correlations among different compounds, Pearson coefficients were calculated. Levene test was performed to elucidate if the data present a parametric distribution. Subsequently, student T tests and ANOVA (parametric data), and Kruskall Wallis (non parametric data) tests were calculated. Correlations and differences were considered significant for probabilities below 0.05 ($p<0.05$).

## 3. Results and discussion

### *3.1. Meteorological conditions*

During the sampling days, temperatures ranged between 5.8 and 16.5 ºC, with an average value of 11.4 ºC, relative humidities ranged between 68.4 and 88.9 %, average 78.5 %, and wind speed ranged between 0.9 and 2.1 m/s, average 1.4 m/s. These values fall within the standard climate values recorded in the area for the season (AEMET, 2011). Average wind speeds were light and south west was the predominant direction. No precipitation was registered in sampling days.

### *3.2. Particulate matter*

The average PM concentrations are shown in Table 2. The daily threshold limits established by law are 50 µg/m$^3$ for $PM_{10}$ (EU Parliament, 2008). This value was exceeded in one sampling day (Fig. 1). Nevertheless, the average $PM_{10}$ and $PM_{2.5}$ levels for the sampling days were below the annual limit values. The PM concentrations obtained in this study were lower than those previously collected in the area (Sánchez-Soberón et al., 2015). About 50% of $PM_{10}$ were coarse particles ($2.5<PM<10$), while 60 % of $PM_{2.5}$ consisted of submicron particles ($PM<1$).

### *3.3. Organic compounds characterization*

The concentrations of PAHs and other organic compounds are reported in Table 2. The sampling variability of the different compounds is shown in Fig. 1. Except for the saccharides, no statistical significant differences were observed in the concentrations of the analysed organic compounds among the three PM fractions, indicating that they are predominantly present in the submicron fraction ($PM_1$), which is in agreement with other studies (Degrendele et al., 2014; Liaud et al., 2014), including those performed in the urban area of Barcelona (Aceves and Grimalt, 1993; van Drooge and Grimalt, 2015).

#### *3.3.1.PAHs*

The predominant PAHs in the PM samples contained five and six rings, namely benzo[b+j]fluoranthene and benzo[ghi]perylene. These compounds have also been identified as predominant PAH in other urban-industrial environments (Varea et al., 2011). No statistical significant differences (p>0.05) were found when comparing PAH distributions by number of rings in the three analyzed fractions, which is consistent with a predominance of all PAHs in the submicron fraction ($PM_1$). According to previous studies (Manoli et al., 2004), emissions from cement plants are characterized by a relatively high contribution of 3 rings compounds up to 30% of total PAHs mass. Previous studies

**Table 2:** Average levels of PM (µg/m$^3$) and organic compounds (ng/m$^3$) found in our study.

| | | | $PM_{10}$ | | $PM_{2.5}$ | | $PM_1$ | |
|---|---|---|---|---|---|---|---|---|
| | | rings | average | desvest | average | desvest | average | desvest |
| PM | | | 32.10 | 11.80 | 15.20 | 3.37 | 9.12 | 3.30 |
| PAH | phenanthrene | 3 | 0.14 | 0.07 | 0.10 | 0.05 | 0.12 | 0.05 |
| | retene | 3 | 0.26 | 0.22 | 0.19 | 0.15 | 0.15 | 0.11 |
| | fluoranthene | 4 | 0.32 | 0.16 | 0.23 | 0.12 | 0.24 | 0.09 |
| | pyrene | 4 | 0.41 | 0.23 | 0.29 | 0.17 | 0.42 | 0.21 |
| | benz[a]anthracene | 4 | 0.61 | 0.40 | 0.45 | 0.31 | 0.49 | 0.33 |
| | chrysene | 4 | 0.56 | 0.31 | 0.49 | 0.29 | 0.59 | 0.39 |
| | benzo[b+j]fluoranthene | 5 | 1.31 | 0.82 | 0.93 | 0.50 | 1.08 | 0.51 |
| | benzo[k]fluoranthene | 5 | 0.35 | 0.20 | 0.23 | 0.11 | 0.29 | 0.14 |
| | benzo[e]pyrene | 5 | 0.59 | 0.31 | 0.42 | 0.20 | 0.50 | 0.23 |
| | benzo[a]pyrene | 5 | 0.62 | 0.37 | 0.43 | 0.24 | 0.56 | 0.35 |
| | indeno[123cd]pyrene | 6 | 0.90 | 0.47 | 0.72 | 0.40 | 0.91 | 0.51 |
| | benzo[ghi]perylene | 6 | 1.05 | 0.51 | 0.84 | 0.42 | 1.15 | 0.58 |
| | coronene | 6 | 0.16 | 0.08 | 0.14 | 0.08 | 0.20 | 0.12 |
| | Total | | 7.28 | | 5.45 | | 6.69 | |
| Hopanes | 17(H)α-21(H)β-29-norhopane | | 0.20 | 0.09 | 0.12 | 0.05 | 0.13 | 0.04 |
| | 17(H)α-21(H)β-hopane | | 0.15 | 0.05 | 0.10 | 0.04 | 0.09 | 0.04 |
| | Total | | 0.35 | | 0.22 | | 0.23 | |
| Biomass combustion products | galactosan | | 61.17 | 45.19 | 43.76 | 32.81 | 46.71 | 38.06 |
| | mannosan | | 54.32 | 37.02 | 39.28 | 26.61 | 44.77 | 31.68 |
| | levoglucosan | | 518.97 | 421.59 | 349.62 | 278.27 | 342.75 | 271.06 |
| | dehydrabietic acid | | 57.97 | 43.14 | 42.77 | 30.58 | 47.32 | 33.69 |
| | Total | | 692.42 | | 475.43 | | 481.54 | |
| Saccharides and derivates | α-glucose | | 52.69 | 31.50 | 7.80 | 6.28 | 4.52 | 1.66 |
| | β-glucose | | 64.88 | 38.93 | 10.34 | 7.59 | 5.36 | 1.33 |
| | mannitol | | 52.62 | 26.65 | 9.00 | 7.72 | 3.63 | 1.44 |
| | Total | | 170.19 | | 27.14 | | 13.51 | |
| Dicarboxylic acids | succinic acid | | 15.65 | 4.20 | 13.61 | 2.51 | 14.00 | 4.96 |
| | glutaric acid | | 4.02 | 0.83 | 3.02 | 0.82 | 3.14 | 0.71 |
| | Total | | 19.66 | | 16.63 | | 17.14 | |

performed near cement plants (Ercan and Dinçer, 2015) also showed a high proportion of three ring PAHs. In the samples collected in the present study, this percent contribution of 3 rings PAHs (i.e. phenanthrene and retene) was 5%, indicating that PAH in the collected samples were likely exposed to atmospheric aging and partitioning between gas and particles. These processes are of high importance for lower molecular PAHs. Isomeric ratios of PAH can be used as diagnostic ratios for emissions, although caution should be taken on the interpretations due to the influence of environmental factors as well as variable emissions of PAHs from the same sources (Galarneau, 2008). Comparison of these values in $PM_{10}$ with previous studies, they were more similar to those reported for incinerators or gasoline cars than to cement plants (Table 3) (Cecinato et al., 2014; Sicre et al., 1987). This result could be a consequence of the use of alternative fuels (biomass, sewage sludge) in the cement plant. However, as mentioned before, the diagnostic ratios are variable depending on photooxidation rate, source type, and combustion conditions (Galarneau, 2008). They could also reflect that the PAH input from the cement plant do not predominate over other nearby sources such as the two highways, the waste treatment plant and several industries. Retene, a methyl-PAH and molecular tracer compound for (pine) wood combustion (Ramdahl, 1983), was found in all samples and at considerable concentrations ranging from 0.05 to 0.7 ng/m$^3$, and showing significant correlations with the other PAHs compounds ($0.18<R2<0.74$; $p<0.05$). The strongest correlation was observed for benz[a]anthracene, while the weakest correlation for benzo[ghi]perylene, which are two PAH compounds that are related to wood burning and (diesel) car emissions, respectively.

**Table 3:** $PM_{10}$-PAHs diagnostic ratios in present study and for different sources as reported previously (Cecinato et al., 2014).

| | Present Study | Cement stack | Incinerator stack | Straw burning | Pine wood burning | Diesel car | Gasoline car |
|---|---|---|---|---|---|---|---|
| BaA/(BaA+BaP) | 0.50 | 0.38 | 0.55 | 0.58 | 0.60 | 0.84 | 0.44 |
| Chy/(BaP+Chy) | 0.47 | 0.40 | 0.59 | 0.60 | 0.70 | 0.89 | 0.47 |
| BaA/(BaA+Chy) | 0.53 | 0.48 | 0.46 | 0.48 | 0.39 | 0.39 | 0.48 |
| Flu/(Flu+Pyr) | 0.44 | 0.68 | 0.56 | 0.55 | 0.54 | 0.52 | 0.49 |

BaA: benzo[a]anthracene; BaP: benzo[a]pyrene; Chy: chrysene; Flu: fluoranthene; Pyr: pyrene

Regarding weekly patterns, no statistical significant differences ($p>0.05$) were found in PAH concentrations when comparing weekdays and weekends. Previous studies performed in Barcelona showed the same trend (van Drooge et al., 2012b). The concentrations of total PAHs in this study were about two times higher than those observed in the urban background of the city of Barcelona in the same season (Mesquita et al., 2014). However, they were within the range of those recorded in other urban Mediterranean areas (Sarigiannis et al., 2015). In this study, the average levels of BaP (0.6 ng/m$^3$) and BaP-equivalents (0.9 ng/m$^3$) in PM$_{10}$ were slightly lower than the 1 ng/m$^3$ the annual limit established by the European Union in the directive 2004/107/EC (EU Parliament, 2005), indicating that despite an influence of additional emission sources, such as the cement plant, the limit values are not exceeded in the studied urban area. Nevertheless, the relatively high BaP levels justify a source apportionment study to estimate the contribution of the potential emission sources.

### *3.3.2. Hopanes*

Hopanes are found in lubricating oil of engines from diesel and gasoline powered vehicles and are used as traffic markers (Křůmal et al., 2013; van Drooge et al., 2012a). The concentrations of these compounds ranged between 0.1 and 0.2 ng/m$^3$, with no statistical significant differences ($p>0.05$) between weekdays and weekends. These levels were lower than those recorded previously in Barcelona in winter, suggesting a small influence from traffic sources in the collected particles (van Drooge et al., 2012a).

### *3.3.3. Biomass combustion products*

Levoglucosan, an anhydro-saccharide from thermal alternation of celluloses, was the prevalent organic compound in the analysed samples, showing about 8 times higher concentrations than its isomers (mannosan and galactosan). The concentrations of PM$_{10}$ levoglucosan ranged from 147 to 1300 ng/m$^3$, while mannosan and galactosan ranged from 19 to 150 ng/m$^3$. No statistical significant differences were observed among the three PM fractions, indicating that these compounds were predominantly in the submicron fraction. Levoglucosan, mannosan and galactosan have been identified as markers of biomass burning, essentially wood burning (Kourtchev et al., 2011). The ratio levoglucosan/mannosan (L/M) can be used to identify the wood type. In the present study, the L/M ratios ranged from 7.5-9.5 , which is intermediate between softwood (3.5-4.0) and hardwood (14-15) (Schmidl et al., 2008). The presence of dehydroabietic acid is characteristic of softwood combustion and is consistent with these intermediate levels. In any case, the concentrations of biomass combustion products were much higher than those observed in previous studies in Barcelona, but similar to those collected in regional areas of Catalonia and other Mediterranean cities during winter (Giannoni et al., 2012; Jedynska et al., 2015; Sarigiannis et al., 2014; van Drooge, 2013; van Drooge et al., 2012a) suggesting that biomass burning emissions are influencing air quality in the studied area, probably more than traffic emssions.

### *3.3.4. Saccharides and derivates*

Saccharides and derivates were mainly found in the coarse (2.5<PM<10) fraction. The concentrations of glucose (α and β) found in this study ranged from 43 to 259 ng/m$^3$ in PM$_{10}$, while PM$_{2.5}$ and PM$_1$ showed values between 6 and 52 ng/m$^3$. These levels were higher than those previously found in Mediterranean sites in winter (Pietrogrande et al., 2014). The lack of correlation between these components and the rest of the organic compounds suggests an origin different than combustion. Saccharides are related to wood smoke and soil resuspension (Schmidl et al., 2008). The lack of correlation between concentrations of saccharides and the other markers of biomass burning suggests a predominant source related with soil resuspension as the main origin of saccharides. Previous studies from this area (Sánchez-Soberón et al., 2015) showed that most mineral components of these airborne particles are found in the coarse fraction. Accordingly, soil resuspension is the main likely origin of these saccharides. Mannitol is a sugar alcohol used as marker of bioactivity, since it is a common storage substance in fungal spores (Bauer et al., 2008). The concentration of this component in our study were higher than registered previously in Barcelona during summer, but lower than those recorded in Easter Mediterranean regions in autumn (Burshtein et al., 2011; van Drooge et al., 2012b). These differences could be related to the life cycle of fungus, since autumn is the season of maximum fungal reproduction.

### *3.3.5. Dicarboxylic acids*

Dicarboxylic acids have been previously recognised as markers of secondary organic aerosols in the absence of biomass combustion (Hallquist et al., 2009). The concentrations of succinic acid were higher than glutaric acid (Table 2), since the former is one of the major acid compounds present in PM (Hsieh et al., 2008). The concentrations of this dicarboxylic acid were similar to those previously recorded in Barcelona in same season (van Drooge et al., 2012a). While secondary organic aerosols in this study were mainly located in the PM$_1$ fraction, secondary inorganic aerosols previously collected in the area had similar contribution for every PM fraction (Sánchez-Soberón et al., 2015). This could suggest different origins and formation processes between these two components or that part of the dicarboxylic acids could originate from primary sources such as biomass burning.

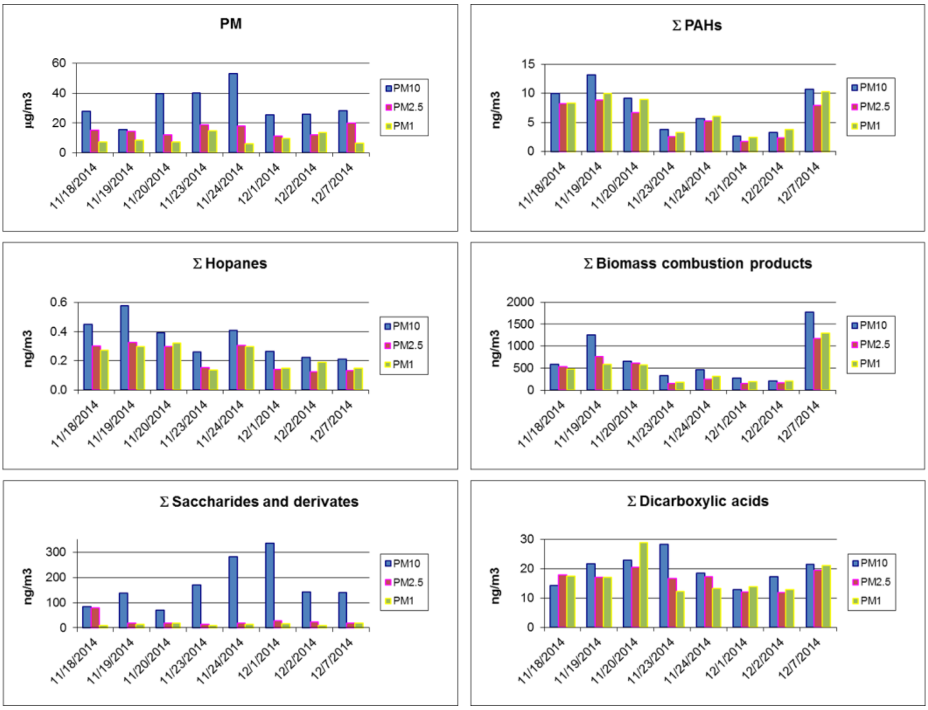

**Fig. 1:** Daily levels of PM, PAHs and other organic compounds.

### *3.4.* Risk assessment

Exposure and carcinogenic risk were evaluated for the seven carcinogenic PAHs recognized by the U.S. E.P.A (US EPA, 1993), among these dibenz[a,h]anthracene was not detected in the present study. Since PAHs were essentially in the $PM_1$ fraction, this fraction contributed the most to exposure and carcinogenic risk, reaching a value of $2.04\cdot10^{-7}$ mg BaPE/(kg·day). $PM_1$ was responsible of more than 94% of this value. Consequently, overall cancer risk were higher for male individuals, reaching a $PM_{10}$ value of $3.98\cdot10^{-7}$ (Fig. 2), involving about 4 cases of cancer due to PAH inhalation for every $10^7$ inhabitants. BaP was the compound that exhibited the highest exposure and carcinogenic activity, contributing about 70% of the overall exposure and cancer risk values. Carcinogenic risk due to PAHs inhalation was below the threshold of acceptable risk established by the U.S. E.P.A. as $1\cdot10^{-6}$ (one case of cancer for every $10^6$ inhabitants) (US EPA, 1996).

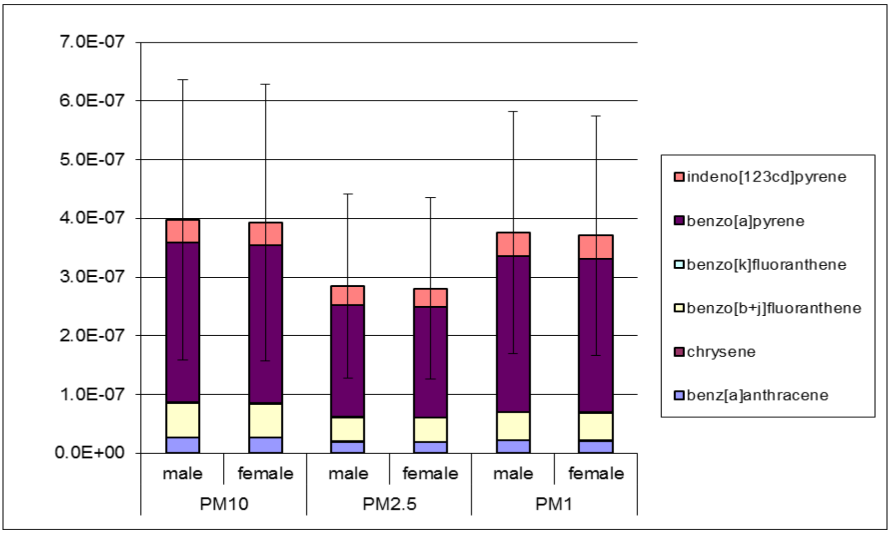

**Fig. 2:** Carcinogenic potential for the three PM fractions and PAHs compounds. Error bars depict total standard deviation.

## 4. Conclusions and implications

In this study three fractions of PM (<10, <2.5, and <1 µm) were collected in the vicinity (300 m) of a cement plant in late autumn, the period of the year in which highest PM levels are normally recorded. Daily limits of $PM_{10}$ were exceeded only one day, while the average levels of $PM_{10}$ and $PM_{2.5}$ were below the legal thresholds. Organic compounds (except saccharides) were predominantly found in the finest $PM_1$ fraction. Biomass combustion products were the most prevalent organic compounds, reaching higher levels than those found in Barcelona metropolitan area. This result evidences high contributions of local biomass burning in the studied area. The most predominant PAHs were five and six rings species with a PAH profile characteristic of a mixture of urban and industrial environments. The concentrations of benzo[a]pyrene were relatively high (0.6 ng/$m^3$), but below the limit set by the European Union (1 ng/$m^3$). Health risk to the population after exposure to ambient air PAHs in the area was 4 cases of cancer per $10^7$ inhabitants, which is below the EPA threshold ($1 \cdot 10^{-6}$).

*Acknowledgments*

This study was financed by the Spanish Ministry of Economy and Competitiveness (MINECO), as part of the project CTM2012-32778. F. Sánchez-Soberón received a doctoral scholarship as part of the project above mentioned. The authors also want to thank LAFARGE CEMENTOS SAU their help while sampling.

**Bibliography**

Aceves, M., Grimalt, J.O., 1993. Seasonally dependent size distributions of aliphatic and polycyclic aromatic hydrocarbons in urban aerosols from densely populated areas. Environ. Sci. Technol. 27, 2896–2908. doi:10.1021/es00049a033

AEMET, 2011. Standard climate Values: Barcelona, Fabra - Agencia Estatal de Meteorología - AEMET. Gobierno de España.

Agudelo-Castañeda, D.M., Teixeira, E.C., Calesso Teixeira, E., Teixeira, E.C., 2014. Seasonal changes, identification and source apportionment of PAH in PM1.0. Atmos. Environ. 96, 186–200. doi:10.1016/j.atmosenv.2014.07.030

ATSDR, 2015. Toxic Substances Portal - Polycyclic Aromatic Hydrocarbons (PAHs) [WWW Document]. URL http://www.atsdr.cdc.gov/PHS/PHS.asp?id=120&tid=25 (accessed 2.26.15).

Bauer, H., Claeys, M., Vermeylen, R., Schueller, E., Weinke, G., Berger, A., Puxbaum, H., 2008. Arabitol and mannitol as tracers for the quantification of airborne fungal spores. Atmos. Environ. 42, 588–593. doi:10.1016/j.atmosenv.2007.10.013

Burshtein, N., Lang-Yona, N., Rudich, Y., 2011. Ergosterol, arabitol and mannitol as tracers for biogenic aerosols in the eastern Mediterranean. Atmos. Chem. Phys. 11, 829–839. doi:10.5194/acp-11-829-2011

Cal. EPA, 2011. Technical Support Document for Cancer Potency Factors: Methodologies for derivation, listing of available values, and adjustments to allow for early life stage exposures. Appendix A.

Cecinato, A., Guerriero, E., Balducci, C., Muto, V., 2014. Use of the PAH fingerprints for identifying pollution sources. Urban Clim. 10, 630–643. doi:10.1016/j.uclim.2014.04.004

Cho, Y., Kim, G.-B., Cho, Y.-S., Choi, M.S., Ryu, S.-H., Choi, S.H., Park, Y.-K., Choi, J.W., 2014. Polycyclic aromatic hydrocarbons exposure in residents living near a cement factory with kilns. Int. Arch. Occup. Environ. Health 87, 889–896. doi:10.1007/s00420-014-0931-z

Conesa, J.A., Rey, L., Egea, S., Rey, M.D., 2011. Pollutant formation and emissions from cement kiln stack using a solid recovered fuel from municipal solid waste. Environ. Sci. Technol. 45, 5878–5884. doi:10.1021/es200448u

Degrendele, C., Okonski, K., Melymuk, L., Landlová, L., Kukučka, P., Čupr, P., Klánová, J., 2014. Size specific distribution of the atmospheric particulate PCDD/Fs, dl-PCBs and PAHs on a seasonal scale: Implications for cancer risks from inhalation. Atmos. Environ. 98, 410–416. doi:10.1016/j.atmosenv.2014.09.001

Ercan, Ö., Dinçer, F., 2015. Atmospheric concentrations of PCDD/Fs, PAHs, and metals in the vicinity of a cement plant in Istanbul. Air Qual. Atmos. Heal. doi:10.1007/s11869-015-0314-y

EU Comission, 2014. State of play on the sustainability of solid and gaseous biomass used for electricity, heating and cooling in the EU. Brussels.

EU Parliament, 2008. Directive 2008/50/EC of the European Parliament and of the Council of 21 May 2008 on ambient air quality and cleaner air for Europe. Off. J. Eur. Communities. 152, 1–44.

EU Parliament, 2005. Directive 2004/107/EC of the European Parliament and of the Council of 15 December 2004 relating to arsenic, cadmium, mercury, nicker and polyciclic aromatic hydrocarbons in ambient air. Off. J. Eur. Communities. 23, 3–16.

Fontal, M., van Drooge, B.L., López, J.F., Fernández, P., Grimalt, J.O., 2015. Broad spectrum analysis of polar and apolar organic compounds in submicron atmospheric particles. J. Chromatogr. A 1404, 28–38. doi:10.1016/j.chroma.2015.05.042

Galarneau, E., 2008. Source specificity and atmospheric processing of airborne PAHs: Implications for source apportionment. Atmos. Environ. 42, 8139–8149. doi:10.1016/j.atmosenv.2008.07.025

García-Pérez, J., López-Abente, G., Castelló, A., González-Sánchez, M., Fernández-Navarro, P., 2015. Cancer mortality in towns in the vicinity of installations for the production of cement, lime, plaster, and magnesium oxide. Chemosphere 128C, 103–110. doi:10.1016/j.chemosphere.2015.01.020

Giannoni, M., Martellini, T., Del Bubba, M., Gambaro, A., Zangrando, R., Chiari, M., Lepri, L., Cincinelli, A., 2012. The use of levoglucosan for tracing biomass burning in $PM_{2.5}$ samples in Tuscany (Italy). Environ. Pollut. 167, 7–15. doi:10.1016/j.envpol.2012.03.016

Hallquist, M., Wenger, J.C., Baltensperger, U., Rudich, Y., Simpson, D., Claeys, M., Dommen, J., Donahue, N.M., George, C., Goldstein, A.H., Hamilton, J.F., Herrmann, H., Hoffmann, T., Iinuma, Y., Jang, M., Jenkin, M.E., Jimenez, J.L., Kiendler-Scharr, A., Maenhaut, W., McFiggans, G., Mentel, T.F., Monod, A., Prévôt, A.S.H., Seinfeld, J.H., Surratt, J.D., Szmigielski, R., Wildt, J., 2009. The formation, properties and impact of secondary organic aerosol: current and emerging issues. Atmos. Chem. Phys. 9, 5155–5236. doi:10.5194/acp-9-5155-2009

Hsieh, L.-Y., Chen, C.-L., Wan, M.-W., Tsai, C.-H., Tsai, Y.I., 2008. Speciation and temporal characterization of dicarboxylic acids in PM2.5 during a PM episode and a period of non-episodic pollution. Atmos. Environ. 42, 6836–6850. doi:10.1016/j.atmosenv.2008.05.021

IARC, 2012. IARC Monographs - Volume 100F.

Jedynska, A., Hoek, G., Wang, M., Eeftens, M., Cyrys, J., Beelen, R., Cirach, M., De Nazelle, A., Keuken, M., Visschedijk, A., Nystad, W., Akhlaghi, H.M., Meliefste, K., Nieuwenhuijsen, M., de Hoogh, K., Brunekreef, B., Kooter, I.M., 2015. Spatial variations of levoglucosan in four European study areas. Sci. Total Environ. 505, 1072–81. doi:10.1016/j.scitotenv.2014.10.091

Kamankesh, M., Mohammadi, A., Hosseini, H., Modarres Tehrani, Z., 2015. Rapid determination of polycyclic aromatic hydrocarbons in grilled meat using microwave-assisted extraction and dispersive liquid-liquid microextraction coupled to gas chromatography-mass spectrometry. Meat Sci. 103, 61–7. doi:10.1016/j.meatsci.2015.01.001

Kelly, F.J., Fussell, J.C., 2012. Size, source and chemical composition as determinants of toxicity attributable to ambient particulate matter. Atmos. Environ. 60, 504–526. doi:10.1016/j.atmosenv.2012.06.039

Keyte, I.J., Harrison, R.M., Lammel, G., 2013. Chemical reactivity and long-range transport potential of polycyclic aromatic hydrocarbons--a review. Chem. Soc. Rev. 42, 9333–9391. doi:10.1039/c3cs60147a

Kourtchev, I., Hellebust, S., Bell, J.M., O'Connor, I.P., Healy, R.M., Allanic, A., Healy, D., Wenger, J.C., Sodeau, J.R., 2011. The use of polar organic compounds to estimate the contribution of domestic solid fuel combustion and biogenic sources to ambient levels of organic carbon and PM2.5 in Cork Harbour, Ireland. Sci. Total Environ. 409, 2143–55. doi:10.1016/j.scitotenv.2011.02.027

Křůmal, K., Mikuška, P., Večeřa, Z., 2013. Polycyclic aromatic hydrocarbons and hopanes in PM1 aerosols in urban areas. Atmos. Environ. 67, 27–37. doi:10.1016/j.atmosenv.2012.10.033

Ladji, R., Yassaa, N., Balducci, C., Cecinato, A., Meklati, B.Y., 2009. Distribution of the solvent-extractable organic compounds in fine (PM1) and coarse (PM1-10) particles in urban, industrial and forest atmospheres of Northern Algeria. Sci. Total Environ. 408, 415–24. doi:10.1016/j.scitotenv.2009.09.033

Lee, B.-K., Van Tuan, V., 2010. Sources, Distribution and Toxicity of Polyaromatic Hydrocarbons (PAHs) in Particulate Matter, in: Villanyi, V. (Ed.), Air Pollution. Sciyo. doi:10.5772/269

Li, C., Nie, Z., Cui, S., Gong, X., Wang, Z., Meng, X., 2014. The life cycle inventory study of cement manufacture in China. J. Clean. Prod. 72, 204–211. doi:10.1016/j.jclepro.2014.02.048

Liao, C.-M., Chio, C.-P., Chen, W.-Y., Ju, Y.-R., Li, W.-H., Cheng, Y.-H., Liao, V.H.-C., Chen, S.-C., Ling, M.-P., 2011. Lung cancer risk in relation to traffic-related nano/ultrafine particle-bound PAHs exposure: a preliminary probabilistic assessment. J. Hazard. Mater. 190, 150–158. doi:10.1016/j.jhazmat.2011.03.017

Liaud, C., Dintzer, T., Tschamber, V., Trouve, G., Le Calvé, S., 2014. Particle-bound PAHs quantification using a 3-stages cascade impactor in French indoor environments. Environ. Pollut. 195, 64–72. doi:10.1016/j.envpol.2014.08.007

MAGRAMA, 2007. Guía Técnica de aplicación del RD 9/2005, de 14 de enero, por el que se establece la relación de actividades potencialmente contaminantes del suelo y los criterios y estándares para la declaración de suelos contaminados. [WWW Document]. URL http://www.magrama.gob.es/es/calidad-y-evaluacion-ambiental/temas/suelos-contaminados/guia_tecnica_contaminantes_suelo_declaracion_suelos_tcm7-3204.pdf (accessed 9.25.14).

Manoli, E., Kouras, A., Samara, C., 2004. Profile analysis of ambient and source emitted particle-bound polycyclic aromatic hydrocarbons from three sites in northern Greece. Chemosphere 56, 867–878. doi:10.1016/j.chemosphere.2004.03.013

Medeiros, P.M., Simoneit, B.R.T., 2007. Analysis of sugars in environmental samples by gas chromatography–mass spectrometry. J. Chromatogr. A 1141, 271–278. doi:10.1016/j.chroma.2006.12.017

Mesquita, S.R., van Drooge, B.L., Reche, C., Guimarães, L., Grimalt, J.O., Barata, C., Piña, B., 2014. Toxic assessment of urban atmospheric particle-bound PAHs: relevance of composition and particle size in Barcelona (Spain). Environ. Pollut. 184, 555–562. doi:10.1016/j.envpol.2013.09.034

Mirante, F., Alves, C., Pio, C., Pindado, O., Perez, R., Revuelta, M.A., Artiñano, B., 2013. Organic composition of size segregated atmospheric particulate matter, during summer and winter sampling campaigns at representative sites in Madrid, Spain. Atmos. Res. 132-133, 345–361. doi:10.1016/j.atmosres.2013.07.005

Pietrogrande, M.C., Bacco, D., Visentin, M., Ferrari, S., Casali, P., 2014. Polar organic marker compounds in atmospheric aerosol in the Po Valley during the Supersito campaigns — Part 2: Seasonal variations of sugars. Atmos. Environ. 97, 215–225. doi:10.1016/j.atmosenv.2014.07.056

Ramdahl, T., 1983. Retene—a molecular marker of wood combustion in ambient air. Nature 306, 580–582.

Rovira, J., Mari, M., Schuhmacher, M., Nadal, M., Domingo, J.L., 2011. Monitoring environmental pollutants in the vicinity of a cement plant: a temporal study. Arch. Environ. Contam. Toxicol. 60, 372–384. doi:10.1007/s00244-010-9628-9

Sánchez-Soberón, F., Rovira, J., Mari, M., Sierra, J., Nadal, M., Domingo, J.L., Schuhmacher, M., 2015. Main components and human health risks assessment of PM10, PM2.5, and PM1 in two areas influenced by cement plants. Atmos. Environ. 120, 109–116. doi:10.1016/j.atmosenv.2015.08.020

Sarigiannis, D.A., Karakitsios, S.P., Kermenidou, M., Nikolaki, S., Zikopoulos, D., Semelidis, S., Papagiannakis, A., Tzimou, R., 2014. Total exposure to airborne particulate matter in cities: the effect of biomass combustion. Sci. Total Environ. 493, 795–805. doi:10.1016/j.scitotenv.2014.06.055

Sarigiannis, D.A., Karakitsios, S.P., Zikopoulos, D., Nikolaki, S., Kermenidou, M., 2015. Lung cancer risk from PAHs emitted from biomass combustion. Environ. Res. 137, 147–156. doi:10.1016/j.envres.2014.12.009

Schmidl, C., Marr, I.L., Caseiro, A., Kotianová, P., Berner, A., Bauer, H., Kasper-Giebl, A., Puxbaum, H., 2008. Chemical characterisation of fine particle emissions from wood stove combustion of common woods growing in mid-European Alpine regions. Atmos. Environ. 42, 126–141. doi:10.1016/j.atmosenv.2007.09.028

Schuhmacher, M., Domingo, J.L., 2006. Long-term study of environmental levels of dioxins and furans in the vicinity of a municipal solid waste incinerator. Environ. Int. 32, 397–404. doi:10.1016/j.envint.2005.09.002

Senthilkumar, S., Manju, A., Muthuselvam, P., Shalini, D., Indhumathi, V., Kalaiselvi, K., Palanivel, M., Chandrasekar, P.P., Rajaguru, P., 2014. Characterization and genotoxicity evaluation of particulate matter collected from industrial atmosphere in Tamil Nadu state, India. J. Hazard. Mater. 274C, 392–398. doi:10.1016/j.jhazmat.2014.04.017

Sicre, M.A., Marty, J.C., Saliot, A., Aparicio, X., Grimalt, J., Albaiges, J., 1987. Aliphatic and aromatic hydrocarbons in the mediterranean aerosol. Int. J. Environ. Anal. Chem. 29, 73–94. doi:10.1080/03067318708078412

US EPA, 2011. Exposure Factors Handbook: 2011 Edition, National Centre of Environmenatl Assessment, U.S. Environmental Protection Agency, Washington, D.C., U.S.A. Sept. 2011.

US EPA, 2008. Polycyclic Aromatic Hydrocarbons ( PAHs ) [WWW Document]. URL http://www.epa.gov/osw/hazard/wastemin/minimize/factshts/pahs.pdf

US EPA, 2007. Benzo(a)pyrene (BaP) TEACH Chemical Summary.

US EPA, 1996. Soil screening guidance: technical back- ground document.

US EPA, 1993. Provisional guidance for quantitative risk assessment of polycyclic aromatic hydrocarbons.

Van Drooge, B.L., 2013. Human Exposure to Polycyclic Aromatic Hydrocarbons in Urban and Rural Ambient Air, in: Occurrence, Fate and Impact of Atmospheric Pollutants on Environmental and Human Health. pp. 59–82. doi:10.1021/bk-2013-1149.ch004

Van Drooge, B.L., Crusack, M., Reche, C., Mohr, C., Alastuey, A., Querol, X., Prevot, A., Day, D.A., Jimenez, J.L., Grimalt, J.O., 2012a. Molecular marker characterization of the organic composition of submicron aerosols from Mediterranean urban and rural environments under contrasting meteorological conditions. Atmos. Environ. 61, 482–489. doi:10.1016/j.atmosenv.2012.07.039

Van Drooge, B.L., Grimalt, J.O., 2015. Particle size-resolved source apportionment of primary and secondary organic tracer compounds at urban and rural locations in Spain. Atmos. Chem. Phys. 15, 7735–7752. doi:10.5194/acp-15-7735-2015

Van Drooge, B.L., Lopez, J.F., Grimalt, J.O., 2012b. Influences of natural emission sources (wildfires and Saharan dust) on the urban organic aerosol in Barcelona (Western Mediterranean Basis) during a PM event. Environ. Sci. Pollut. Res. Int. 19, 4159–4167. doi:10.1007/s11356-012-0890-4

Varea, M., Galindo, N., Gil-Moltó, J., Pastor, C., Crespo, J., Gil-molt, J., Pastor, C., Crespo, J., 2011. Particle-bound polycyclic aromatic hydrocarbons in an urban, industrial and rural area in the western Mediterranean. J. Environ. Monit. 13, 2471–2476. doi:10.1039/c1em10163c

Zhou, H., Wu, C., Onwudili, J.A., Meng, A., Zhang, Y., Williams, P.T., 2015. Polycyclic aromatic hydrocarbons (PAH) formation from the pyrolysis of different municipal solid waste fractions. Waste Manag. 36, 136–46. doi:10.1016/j.wasman.2014.09.014

# CHAPTER 3: Physicochemistry and toxicity of inhalable particulate matter collected proximal to cement plants

Francisco Sánchez-Soberón, Matthew Lawson, Anna J. Wlodarczyk, Zoë C. Prytherch, Tim P. Jones, Kelly A. Bérubé, Marta Schuhmacher. Toxicology in vitro, in press.

# Physicochemistry and toxicity of inhalable particulate matter collected proximal to cement plants

Francisco Sánchez-Soberón, Matthew Lawson, Anna J. Wlodarczyk, Zoë C. Prytherch, Tim P. Jones, Kelly A. Bérubé, Marta Schuhmacher. Toxicology in vitro, in press.

Abstract

In this study two fractions of airborne particulate matter (smaller than 10μm and 2.5μm, respectively) were collected in an area influenced by a cement plant. These two fractions were analysed by Field Emission Scanning Electron Microscopy to determine particle morphology (e.g. size, shape, number). The oxidative damage to DNA by the particulate matter 10μm and 2.5μm fractions, along with a sample of cement dust were investigated using a Plasmid Scission Assay. Finally, an in-vitro cell culture model of the tracheobronchial epithelia (EpiAirwayTM) was exposed for 24 hours to particulate matter 10μm and 2.5μm fractions, and cement dust, as a mean to ascertain their potentials as inhalation hazards. Electron microscopy revealed that the 2.5μm fraction was richer in soot, while the 10μm fraction contained a higher proportion of mineral particles. Particulate matter of 2.5μm elicited a higher toxicity than the 10μm fraction with DNA damage, while no significant differences between these two fractions were found in total protein secretion, cell viability, and trans-epithelial electrical resistance. Qualitative observation revealed higher histopathological damage (i.e. vacuole formation and bronchial epithelial cell hyperplasia), in cells exposed to the 2.5μm fraction. Collective results from this study indicate that both particulate matter fractions and cement dust are able to generate respiratory damage, which is of special concern for the cement plant workers and population living nearby.

## Graphical abstract

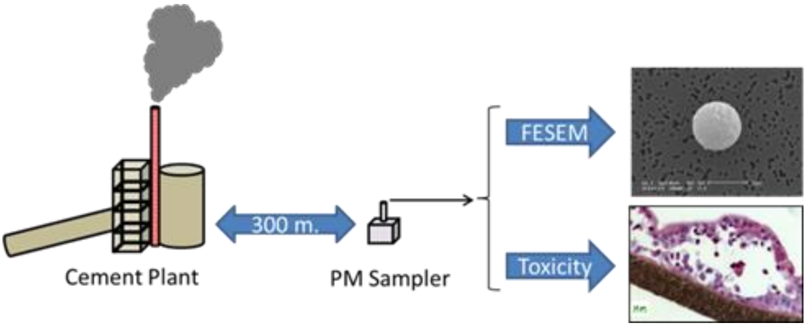

## 1. Introduction

Inhalable particulate matter (PM) is composed of solid and liquid droplets suspended in the ambient air, with variable sizes (from 10 µm to the nanometer [<0.01 µm] scale) and a composition consisting of ammonia, nitrates, sulfates, black carbon and mineral dusts[1,2]. In the 21st Century, PM is recognized as the most pervasive pollutant affecting the cardio-pulmonary health of mankind on a global scale[3,4]. For regulatory purposes, PM is divided in two categories: smaller than 10 µm ($PM_{10}$) or smaller than 2.5 µm ($PM_{2.5}$)[5,6]. The latter fraction is considered to be more dangerous than the former, since its smaller size facilitates its entrance to deeper points of the human respiratory tract (i.e. alveoli)[7–9].
To better understand the cellular mechanisms involved in PM toxicity, *in-vitro* toxicity assays have been extensively employed given their usefulness as biological tools to examine the oxidative potential on DNA, cell inflammation and cytotoxicity of PM[10,11]. To clarify the health effects caused by PM from different environments, numerous toxicological studies have been performed with PM collected in urban conurbations[12,13], shipping ports[14], subway platforms[15], heavily-trafficked vehicular zones[16,17], street canyons[18], indoor environments[8], or industry-influenced sites[19–21].

One of the industries widely recognized as a significant source of PM are cement factories[22–24]. In the cement process, clay and limestone react at temperatures between 1400-1500°C to form clinker. This clinker is then milled with gypsum to yield cement[25]. In order to reduce costs and minimize $CO_2$ emissions, the use of different proportions of wastes (e.g. fly ash, industrial and municipal sewage sludge, plastics or textiles) as both raw materials or fuels in cement kilns, is highly recommended by the European Commission[26].

Population health risks in environs influenced by PM emissions from cement plants have been extensively assessed[27–30], but there has been a paucity of experimental studies regarding the toxicity of these particles. To clarify the occupational hazards of the cement industry, van Berlo et al (2009)[31] elucidated the toxicity of a variety of cement dust (CD) using a cell culture of rat alveolar macrophages. These CDs were less than 10 µm in size, with at least 65% of them smaller than 2.5 µm. This study concluded that the CDs induced an activation of the macrophage tumor necrosis factor α (TNFα) production. For general public health risks, previous research by other investigators[32–34] has focused on the effects of whole $PM_{10}$ collected from near a cement plant on cultures of human alveolar basal epithelial cells (A549). Since $PM_{10}$ include particles whose size will restrict them penetrating into the lungs[35], those studies could be creating an unrealistic scenario.

To address this knowledge gap, and to better understand the mechanisms of toxicological action of PM on the general population, we present this study. Two fractions of PM (10 µm and 2.5 µm) were collected in the surroundings of a cement plant in Barcelona. The physicochemical characteristics of the two PM fractions were elucidated by means of Field Emission Scanning Electron Microscopy (FESEM) to evaluate the morphological organization of the PM and CD samples on a particle-by-particle basis. The relative bioreactivity (i.e. oxidative capacity to generate reactive oxygen species) of the two PM fractions were assessed by a Plasmid Scission Assay (PSA). Finally, well-established inhalation exposure protocols were employed by using an *in-vivo* like *in-vitro* model of the human bronchial epithelium to resolve any histopathological damage that may incur in humans post-exposure to a heterogeneous mixture of CD and local $PM_{10/2.5}$[36,37].

## 2. Materials and Methods

### 2.1. Site description, sampling and PM extraction

The geographical location of the experimental site has been described elsewhere[29,38]. In brief, the area of investigation was located in Montcada i Reixac, a town situated in the north outskirts of Barcelona (41º 28’ 30.88’’N; 2º 11’ 1.47’’E) (MNT 421-1 Badalona). The ambient air in this area is influenced by an operational cement plant and two highways (C-33 and C-58) with dense traffic (Figure S1). The cement plant has been working since 1917, and its current production is ~900,000 cement tons per year[39]. This plant has a license to use up to 382,000 tons of wastes (e.g. slag, concrete wastes, paper mill sludge and fly ashes) as raw materials annually. Furthermore, sewage sludge, meat and bone meal, refuse-derived fuels, and biomass contribute up to 20% of the total energy consumed by the kiln (Table S1)[40,41].

Sampling of ambient PM air pollution was performed on the roof of a two story primary school located 300 metres from the cement facility (41º 28’ 21.14’’N; 2º 11’ 9.47’’ E) (Figure S1). This point was selected since, according to previous studies, it reached the highest levels of PM in the area[38]. Samples were collected between March and April 2015. Two fractions of PM (10 µm and 2.5 µm) were gathered using alternatively the same low-volume air sampler (i.e. Negretti $PM_{10}$ selective inlet head[42]). $PM_{10}$ was collected at 10L /min for 6 hours, while $PM_{2.5}$ was collected at 5L/min for 8 hours. Ten samples were collected for every fraction. To cover the full length of a day, three samples were collected in morning, three in the afternoon and three during the night for each of the two fractions. Furthermore, one sample of every fraction was collected while the cement plant was not in operation for microscopic visualization purposes. Polycarbonate filters of

47 mm diameter and 0.22 µm pore size were used as collecting media[9]. Filters were weighed pre and post collection, using a micro-balance (Sartorius SC2) after neutralizing their static electricity by an ionizing blower (Sartorius YIB01-0UR). PM levels were calculated as the difference between these two measures (more information regarding meteorological data and PM levels while sampling can be found in Supporting Information). After weighing a small portion of each filter (5mm$^2$) was reserved for microscopy analysis.

The remaining filter fractions were weighted as explained above, and then particles were extracted from them according to methods reported in previous studies[18,43]. Briefly, filters were placed into 7 mL tubes and submerged in deionized water. Tubes were then shaken for 30 min. and sonicated for 10 min. Subsequently, filters were removed, and tubes were centrifuged for 10 minutes at 3500 RPM. Finally, centrifuged PM was submitted to lyophilization, at -40°C during 48 hours. In order to determine the extracted mass of PM, extracted filters fractions were air-dried for 24 hours and reweighed following the protocol outlined above.

### 2.2. *Electron Microscopy*

FESEM was employed to obtain 3-dimensional images of $PM_{10/2.5}$, following procedures described previously[18]. In brief, 5mm hole punches taken out of 47 mm round polycarbonate filters (Millipore, UK) were adhered onto 12.5 mm aluminum stubs (Agar Scientific, UK) using epoxy resin (Araldite™). The hole punches were coated with evaporated gold–palladium (Au–Pd 60:40; coat thickness of 20 nm) in an inert argon atmosphere using a Bio-Rad SC500 Sputter Coater. Coated samples were examined under a Veeco FEI Philips XL30 Environmental SEM with a field emission (FE) gun. FESEM parameters were set as per Jones et al. (2006)[44]: accelerating voltage 5 kV– 20 kV, working distance 5 mm–10 mm, magnification 50× to 200,000x.

### 2.3. *Plasmid Scission Assay (PSA)*

Details about the PSA protocol have been published previously[21,45]. Briefly, molecular grade water (Sigma, UK) was added to each type of PM sample to yield four replicates (n=4) for each dilution tested: 0.1, 1, 5, 10, 50, 100, 500 and 1000 µg PM/mL. Nineteen microliters of each one of the solutions were placed into 20 µl Eppendorf tubes. Then, 1 µL of solution containing 200 ng uX174 RF DNA (Promega, London, UK) was added to each sample to reach a final volume of 20 µl before 6 hours incubation at room temperature.

The same protocol was followed for molecular grade water and the restriction enzyme Pst I (Promega, Hampshire, UK); used as negative and positive controls, respectively. Also, 1000 µg/mL solutions of black carbon (M880; Cabot, US) and cement powder (i.e. Lafarge Ordinary Portland Cement; average particle diameter between 5-30 µm[46]) were used as PM reference materials. After incubation, 3.33 µl of orange/blue dye (Promega, Hampshire, UK) was added to every sample. Finally, samples were loaded and electrophoresed on a 0.6% gel and 0.00025 mg/mL of ethidium bromide (Sigma Aldrich, Dorset, UK) at 30 V for 16 hours in 1% Tris–Borate–EDTA buffer. VisionWorks (UVP, Cambridge, UK) and Genetools (Syngene, Cambridge UK) software packages were used for imaging and analyzing gels. DNA damage was calculated as the percentage of linear and relaxed forms in the total DNA according to previous studies[47] (Figure S2). $TD_{50}$ (i.e. toxic dose that causes damage on 50%) values were calculated by using second order polynomic regression lines after plotting the data on a dose-response graph with logarithmic X-axis.

### 2.4. *Lung cells exposure*

In order to determine the actual effects of PM on the human respiratory tract, a well-characterized commercial model of the tracheobronchial epithelium grown in the air-liquid-interface (ALI) (EpiAirway™, MatTek Corp., USA[48]) was employed. This model was derived by the differentiation of primary tracheobronchial epithelial cells into a pseudostratified epithelium featuring goblet, ciliated, basal and clara cells[49]. Tasks performed with this model, and subsequent cytotoxicity and histology assays have been described elsewhere[50]. In brief, once the cell cultures (n=6 inserts per 6-well plate) arrived, cell inserts were put on top of sterile washers in a 6 well plate containing 1 mL. of culture medium at 37°C. This plate was then placed in a sterile incubator at the same temperature with 5% $CO_2$. After 18 hours, cells were transferred to new 6-well plates with 3 mL of fresh pre-warmed media provided by MatTek. Samples of cement powder, $PM_{10}$ and $PM_{2.5}$ were diluted in Phosphate Buffered Saline (PBS, Sigma Aldrich) to a concentration of 1000µg/mL and a 50µL dose (per cell insert) was utilized from these stock solutions. PM/CD solutions (50µL dose for n=6 inserts per PM sample type) were delivered onto the apico-lateral surface of the EpiAirway ALI culture model. Six different inserts were committed for each PM sample category as follows: 4 inserts for cytotoxicity and 2 inserts for histological analyses. Furthermore, to assure GLP (good laboratory practice), six inserts exposed to PBS were used as control samples. After dosing, cell inserts were incubated at 37°C with 5% of $CO_2$ during 24h.

### *2.4.1. Cytotoxicity assays.*

Four replicates (n=4) of the tracheobronchial ALI model were subjected to three different conventional toxicology assays to identify different aspects of cytotoxicity[51].

2.4.1.1. Trans-Epithelial Electrical Resistance (TEER): performed to observe the integrity of the epithelial barrier by applying an electrical current before and after dosing. TEER is calculated from the difference between electrical resistances of these two measures. These resistances were measured using the epithelial volt/ohm meter EVOM$^2$ (World Precision Instruments, USA).

2.4.1.2. Adenosine triphosphate (ATP) assay: used to ascertain cell viability by measuring the luminescence produced by the reaction between ATP and D-luciferin in the presence of luciferase. The amount of light produced was proportional to the quantity of ATP produced by cells.

2.4.1.3. Bradford assay[52]: to determine the amount of protein secreted into the apico-basal surface of cells in response to the PM exposure. After the second TEER measurement, apical washes of PBS (Phosphate Buffered Saline) (150µL, n=4) were put in Eppendorf tubes and stored at 4°C. These washes were then mixed with Coomassie blue dye, and the absorbance of the mixture was measured at 595 nm. Relationships between absorbance and protein concentration are calculated from a regression line obtained by measuring absorbance at 595 nm of serial dilutions made from bovine serum albumin (BSA) and PBS at different known concentrations.

Results from these assays are presented as percentage of control (PBS), as expressed in the following equation:

$$\% \; \boldsymbol{of\ control} = \frac{\boldsymbol{Average\ value\ of\ samples}}{\boldsymbol{Average\ value\ of\ control}} \times \mathbf{100}$$

### *2.4.2. Histology assays*

Two of the inserts per each set of PM treatments (n=2) were designated for histology as described previously[37]. In brief, after exposure time, cells were subjected to subsequent stages of fixing, dehydration, clearing, and waxing. Then, tissues were cut into 10 µm thick sections (3 per sample) using a microtome (Leica RM2135). Subsequently, sections were submerged in 45ºC water to remove winkles and bubbles, and put at 37 – 45°C for 24 hours. Finally, sections were de-waxed and stained with Haematoxylin and Eosin before being dehydrated again. A Leica DFC 320 digital camera, attached to a Leica Phase Contrast Light Microscope (DM2500) was used for imaging.

### *2.5. Statistical analysis.*

Statistical treatment of data was undertaken using the software XLSTAT (version 2015.3.01.19349). Shapiro-Wilk was used to elucidate if the data present a normal distribution. In case of parametric data, ANOVA was used to study intergroup comparisons. Tukey's and Dunnett's tests were used to compare differences among groups and control respectively. In case of non-parametric data, differences among groups were assessed by Kruskall-Wallis tests. In those cases, Conover-Iman method was employed for multiple comparisons. We considered difference as significant for those cases with a probability below 0.05 ($P < 0.05$).

## 3. Results

### *3.1. Microscopy*

The PM collected in our study was highly influenced by the presence of soot, fly ash, mineral and unclassified particles (i.e. amorphous detritus; Figure 1a, d and f, respectively). During the days that the cement plant was operational, qualitative observations suggested an increased presence of gypsum particles (Figure 1h), in contrast to those days when the plant was not working (Figure 1e). Regardless of the cement plant's operational schedule, the presence of soot was higher in the $PM_{2.5}$ fraction, while mineral particles were more prevalent in $PM_{10}$ fraction.

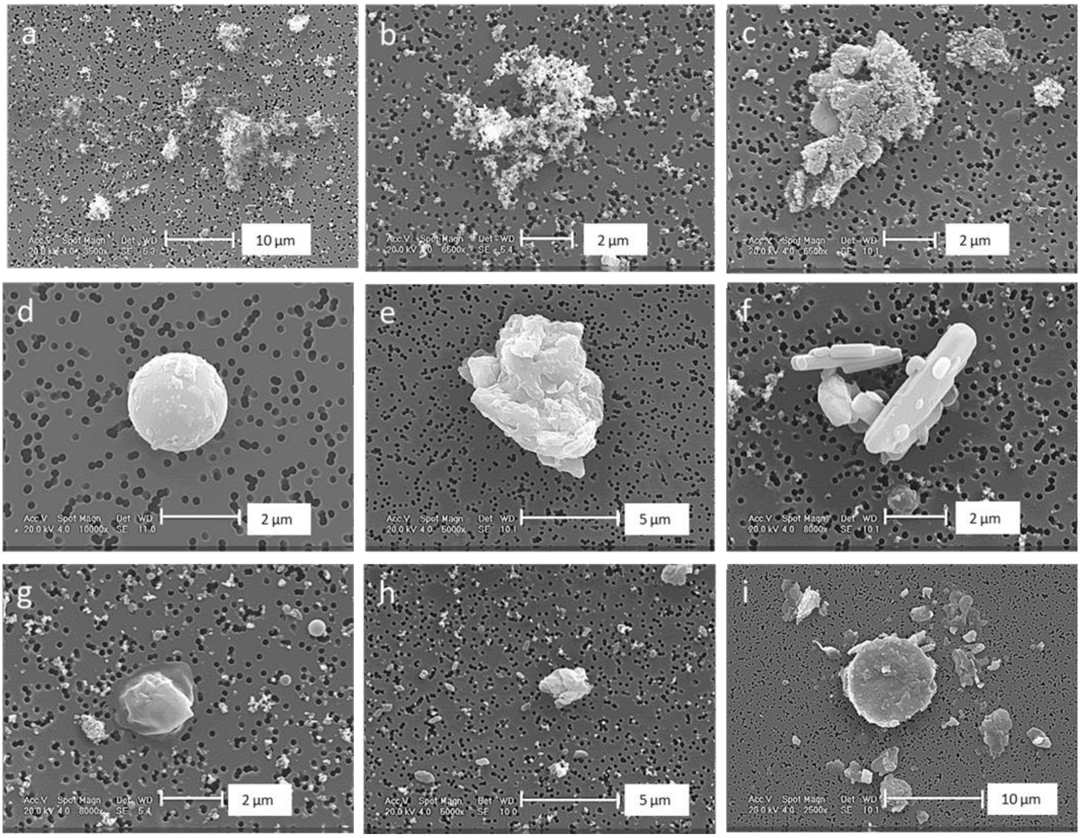

**Figure 1:** Examples of different kind of collected PM (n=9). a) Overview. b) Aggregate of soot particles c) Soot aggregate covering a mineral particle. d) Fly ash. e) Irregular mineral material. f) Elongated mineral particle g) Hydrocarbon particle (squashed). h) Mineral particle surrounded by gypsum particles (flat and hexagonal) i) Pollen spherical cap particle**.**

### *3.2. PSA*

Gel images are displayed in Figure 2, and dose-response curves for $PM_{10}$, $PM_{2.5}$, CD and Black carbon are shown in Figure 3. The linear form of DNA was observed only in those wells exposed to positive controls (Pst I). The $PM_{2.5}$ fraction elicited the greatest DNA damage, with a $TD_{50}$ value close to 50% the value of the $PM_{10}$ counterpart (i.e. 419.96 µg/mL and 777.28 µg/mL respectively). CD induced a high percentage of DNA damage, even at low concentrations (i.e. 23% at 1 µg/mL). Nonetheless, very similar damage values were observed when assessing concentrations between 5 and 500 µg/mL (≈30%), decreasing to 11% when challenged to 1000 µg/mL. The negative control, black carbon

(M880) induced minimal DNA damage (≈2%) but only at maximum concentrations, and therefore, deemed as a negligible effect.

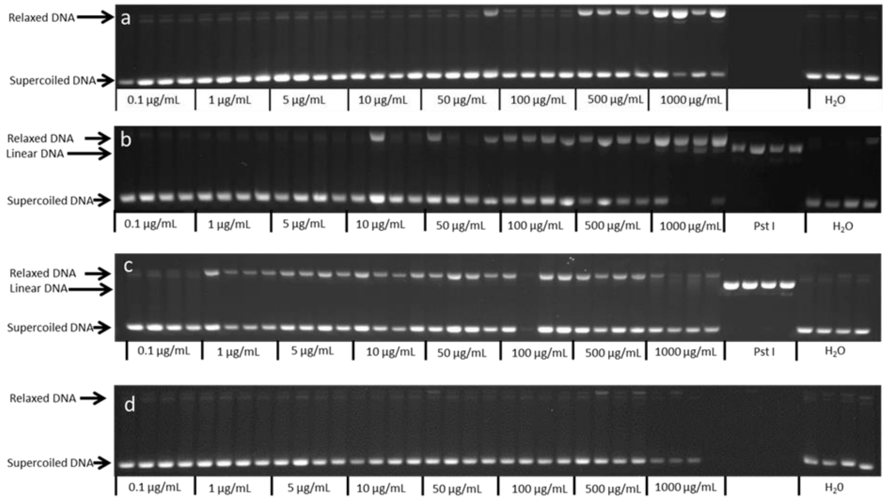

**Figure 2:** Gel images showing damage to supercoiled DNA caused by PM10 (a), PM2.5 (b), CD (c), and Black carbon (d).

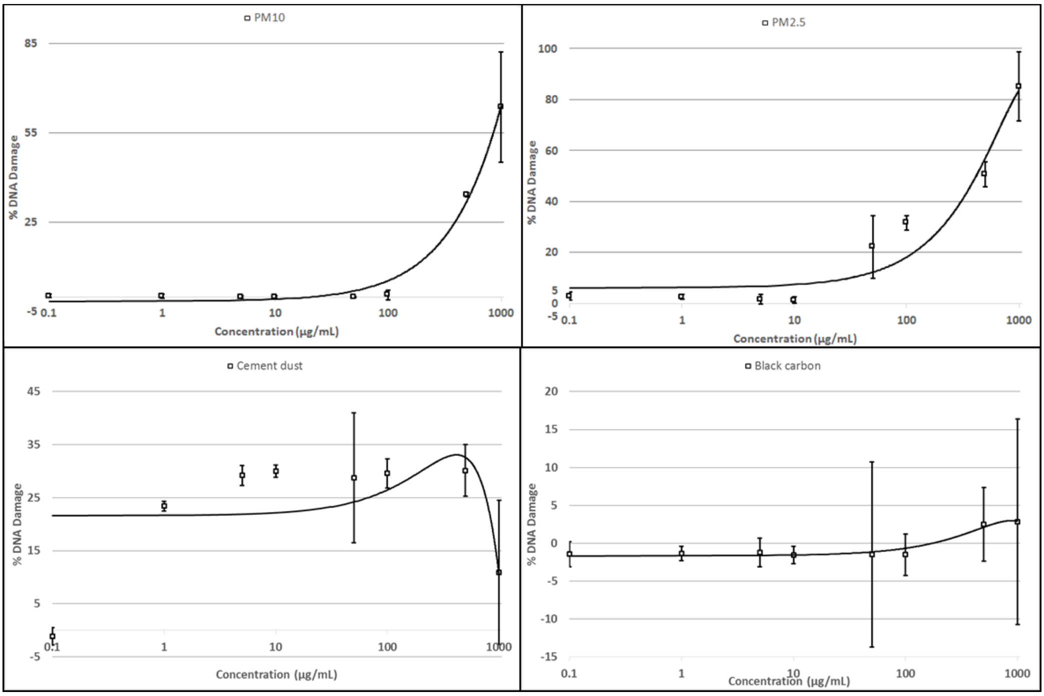

**Figure 3:** Dose-response plot graphs showing mean % DNA damage (n=4) versus concentration of different

materials: $PM_{10}$, $PM_{2.5}$ , CD, and Black carbon. Error bars show standard deviations. Second order polynomic regression lines were used as trend lines.

### *3.3. Lung cells exposure*

TEER values for $PM_{10}$, $PM_{2.5}$ and CD were significantly smaller ($P<0.05$) when compared to the control values (Figure 4). The average TEER values in cells exposed to these materials were between 70 to 80% of control TEER. Although there were no statically significant differences among the three toxicants, there was seen to be a tendency towards a higher TEER in those cells exposed to $PM_{2.5}$. With the ATP assay, no statistically significant differences ($P>0.05$) were found when comparing $PM_{10}$, $PM_{2.5}$ and CD to the control group. However, cells exposed to $PM_{2.5}$ showed a trend towards ATP decrease, while cells exposed to CD presented an average value above the control (114%). With respect to the protein content, no significant differences were observed after exposure to $PM_{10}$, $PM_{2.5}$ or CD compared to the control group. However, cells exposed to $PM_{2.5}$ and CD tended to show increased values of protein than the control.

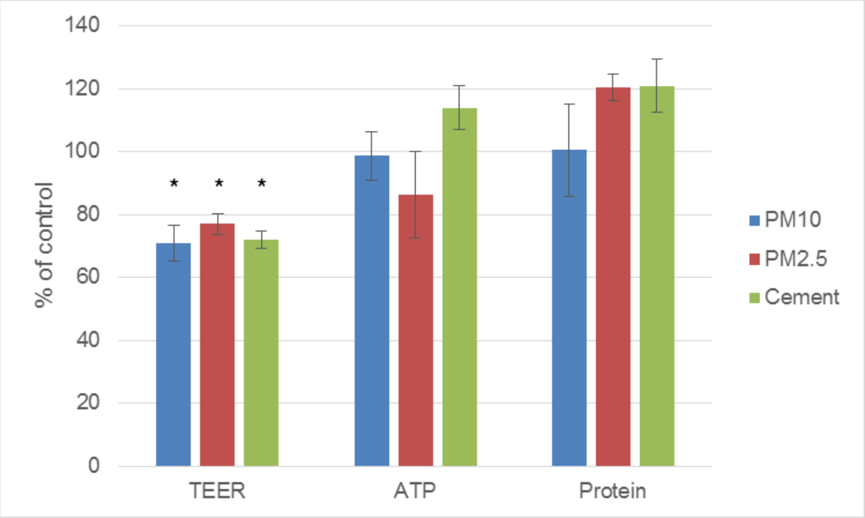

**Figure 4:** Mean results (n=4) from cytotoxicity assays at 1000µg/mL. Error bars show standard deviations. Asterisk (*) indicated significant differences ($P<0.05$) compared to control (PBS).

### *3.4. Histology*

A pseudostratified epithelium was observed in tissues exposed to PBS (i.e. control cell cultures) (Figure 5a).

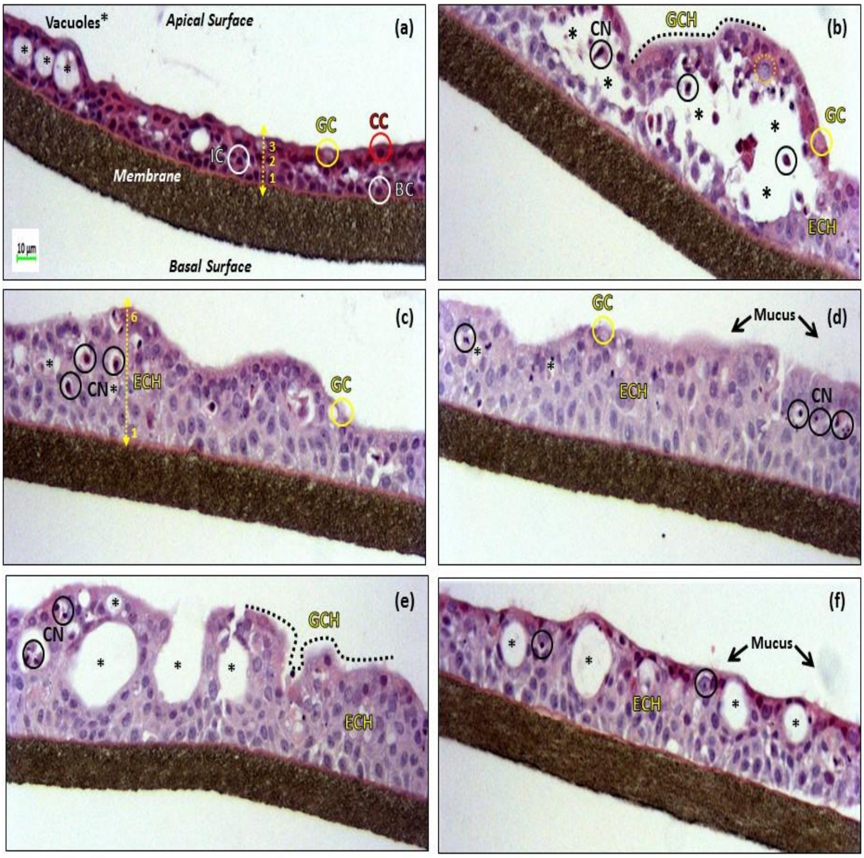

**Figure 5: Examples of histopathological changes observed *in vitro* following apical exposures to PM.** a) Control tissue (exposed to PBS), revealing small vacuoles (*) and compacted layers (i.e. 3-layers) of cells (i.e. goblet cell [GC], ciliated cell [CC], basal cell [BC], intermediate cell [IC]) supported on a PTFE (polytetrafluoroethylene) membrane for cells to access media from both their apical and basolateral sides. Cell growth, structure, and function more closely mimic what occurs *in vivo*. The cells were stained with H&E (Haemotoxylin and Eosin). b) Large gaps in cells exposed to $PM_{10}$ formed by fusion of multiple vacuoles in close proximity. There were focal regions of GC hyperplasia (GCH) and epithelial cell hypertrophy (ECH) featuring swollen cytoplasm and condensed nuclei (CN). Some nuclei have condensed chromatin attached to the inner nuclear envelope (orange dashed circle). c) EHP (i.e. 6-layers versus the 3-layers observed in control cell cultures) featuring cells with swollen cytoplasm and condensed nuclei (CN) after $PM_{10}$ exposure. Many regions containing small vacuoles or larger spaces between cells due to cell destruction. d) EC hyperplasia and hypertrophy (ECHH) after exposure to $PM_{2.5}$, in which was possible to observe mucus secretion, condensed nuclei and vacuolated spaces. e) Large vacuoles suggesting cell death in conjunction with ECHH and GCH discharging mucus following $PM_{2.5}$ exposure. f) Focal damage similar to the control cell cultures treated with PBS, visible mucus secretion and ECH after exposure to cement powder.

This anatomical aspect was characteristic of healthy cells, (Figure 5a) in which it was possible to observe a multi-layered (i.e. 3-layers), mixed muco-ciliary phenotype (i.e. goblet cells [GC], ciliated cells [CC], basal cells [BC] and intermediate cells [IC]). There was minor damage (i.e. vacuoles) caused by PBS. Cell cultures challenged with $PM_{10}$ demonstrated focal regions of damage. However, vacuoles in this case were noticeably larger when compared to PBS treatments (Figure 5b). A thicker cell membrane versus control tissues was also observed, meaning that the phenomenon of epithelial hyperplasia (EHP) had taken place (Figure 5c). Mucus hyper-secretion by goblet cells (i.e. goblet cell hyperplasia; GCH) was also observed, along with condensed nuclei.

## 4. Discussion

### *4.1. Microscopy*

The morphology of the analyzed samples was very similar to those reported previously in urban-industrial areas[21,53,54]. Fly ash particles were spherical in shape accompanied by a smooth surface; morphological features characteristic of high temperature combustion processes (Figure 1d)[55]. This type of PM has been universally recognized as a by-product from coal and industrial combustion processes[56,57]. In our study, the most probable origin of this contaminant was the cement factory due to both the use of petroleum coke as fuel and the addition of fly ash as raw material[41]. Soot particles appeared as small spheres forming 'bunch-of-grape' like aggregates, that sometimes coated mineral particles (Figure 1b and c). They most likely originated from incomplete combustion of different sources, i.e. diesel- and/or gasoline-engined vehicles[58,59]. Mineral PM was variable in shape and composition. Two main morphologies were recognized as follows: irregular- (Figure 1e) and/or elongated-shapes (Figure 1f). The former were usually composed of quartz and clays, and therefore, related with geological sources, while the latter were formed by secondary reactions, being rich in sulfates and nitrates[60]. Furthermore, it was possible to distinguish a third kind of mineral particle in the $PM_{10}$ collected while the cement plant was operational. These PM were characterized as having a flat rhomboid-shape (Figure 1h) that was suggestive of gypsum; one of the components involved in cement manufacture[25]. The unclassified PM includes the particles that could not be identified and thus included in any of the previous groups. There is also biogenic PM, such as pollen or vegetal debris (Figure 1i), but also hydrocarbon-based PM from incomplete combustion (tar balls) (Figure 1g).

### *4.2. PSA*

As seen in previous studies, size plays an important role in PM toxicity, it being more pernicious in those particles having smaller size[18]. $PM_{2.5}$ collected in the areas surrounding the cement plant previously showed higher contributions of polycyclic aromatic hydrocarbons (PAHs) and some transition metals (i.e. Mn, Pb, Ni) than those PM having a size between 10 and 2.5 µm ($PM_{10-2.5}$) [29,61]. These components could trigger the generation of reactive oxygen species[62,63]. Comparing our values with others documented in Barcelona at the same time[45], higher values of $TD_{50}$ were registered in our study, thus meaning toxicity of our PM is lower. However, $PM_{10}$ $TD_{50}$ values were similar to those registered in outdoor PM in rural areas of China[64], or smaller than PM recorded in other industrial areas of this same country in summer[21]. The plateau profile shown by CD indicated the possibility of aggregate formations between powder particles when concentrations were high. Cement particles are subjected to attractive forces between them after being mixed with water, favoring the formation of aggregates[65]. This, in conjunction with the wide range of particle size distributions of CD[66], could cause the cement particles to precipitate within the 96 plate wells, thus avoiding a proper interaction between the DNA and the CD. Low DNA damage caused by black carbon has been reported before[9], which is normal taking into account the low concentrations of transition metals or PAHs in this material.

### *4.3. Lung cells exposure*

The airway epithelium contributes significantly to the barrier function of human respiratory tract. The three critical components that maintain the barrier function of the airway epithelium include the muco-ciliary escalator, apical tight junctional complexes which regulate para-cellular permeability and the anti-microbial peptides secreted by the epithelial cells. These three components work in conjunction to clear inhaled pathogens, allergens and particulate matter without inducing inflammation and maintaining tissue homeostasis. Impairment of one or more of these essential components of barrier function may increase susceptibility to infection and promote exaggerated and prolonged innate immune responses to environmental factors such as air pollution, resulting in chronic inflammation; the hall mark for disease initiation[67]. Our well-established inhalation exposure protocols featuring an *in-vivo* like *in-vitro* model of the human bronchial epithelium was able to determine histopathological phenotypes (e.g. GCH, ECH, ECHH, condensed nuclei, apoptosis, etc.) that were in line with our previous work on ambient PM (both natural and anthropogenic)[14,18,50,51]. Thus inferring that acute (i.e. 24 hours) exposure to a heterogeneous mixture of CD and local $PM_{10/2.5}$ from cement factories is deleterious for the human respiratory system since it dysregulates the components of barrier function.

### *4.3.1. Cytotoxicity*

TEER values after the exposure to PM and CD were significantly lower ($P<0.05$) than control. This demonstrates that the three toxicants applied (i.e. $PM_{10}$, $PM_{2.5}$, and CD) are able to induce changes in the structural integrity of the epithelial barrier. Low TEER values are associated with significant damage of the epithelial continuum that has been observed in the pathogenesis of asthma and lung cancer[67]. This could happen in the presence of certain substances, such as cadmium or mannitol [68–70]. Previous PM monitoring and collection campaigns conducted in the same cement plant area[29,61] found an enrichment of these compounds in the particles having a diameter between 10 and 2.5 µm, which could suggest higher epithelial damage in cells exposed to $PM_{10}$. However, in the present study we did not see significant differences in TEER values between cells exposed to the different PM fractions. Nevertheless, some studies are skeptical about the suitability of TEER as a way of measuring epithelial permeability[70,71]. Usually, there are two manners of going through the cell junction: the pore pathway and the leak pathway[72]. The first mechanism is related with small ions, while the second one allows the movement of macro-molecules. Since the TEER assay gives information about the para-cellular flux of ions, macro-molecular flux (and therefore, permeability) could increase without decreasing TEER[70].

The ATP assay measures the cellular activity of a tissue, which is commonly used as an indicator of cell viability[73]. Both PM fractions showed smaller viabilities than the PBS control cultures, being opposite to the cellular responses following exposure to CD. This increase in ATP luminescence could suggest that tissues are experiencing the hormesis phenomenon. Hormesis has been the subject of a resurgence in interest, with reviews defining hormesis as a “dose-response phenomenon characterized by a low dose stimulation and a high dose-inhibition”[74]; whilst also being defined as an “adaptive response” of the organism to the effects of toxicant exposure[75]. Although this phenomenon was first observed over a century ago[76], this result is not commonly discussed in ecotoxicological monitoring studies, as the regulatory end-points emphasized are usually lethal or inhibitory effects. Nevertheless, this type of response has been previously reported by other investigators using the MatTek EpiAirway model[50,51,77]. To confirm that this phenomenon is taking place in our model more data is needed (i.e. a dose-response assay). Besides, since results were not statically significant ($P>0.05$), this response to CD could be within the range of normal output, given the demonstrated robustness of this cell model[78].

The Bradford assay provides information about total protein secreted onto the tissue surface in the form of cell debris and mucous. Low doses of toxicants increase the cellular activity (and therefore, the ATP) and the amount of secreted mucus. As the dose of a toxicant increases, so do these two parameters, until reaching a maximum, after which cell death is triggered[50]. Consequently, cell viability and mucus secretion decrease, while cellular debris increases its contribution towards total protein[50]. With regard to this current investigation of cement PM, the $PM_{2.5}$ fraction would be in this final step of this process, whilst the $PM_{10}$ fraction would be in the beginning, whereas CD would be located close to the maximum, before cell death begins to happen. Previous studies have shown this same trend, in which smaller PM sizes induce higher damage and mortality[79–82], while others present the opposite results[12,58,83,84]. Not only PM size, but also chemical composition seems to play an important role in determining cell mortality and inflammation[85,86]. As in the case of oxidative damage to DNA, some associations have been found between inflammation and some chemical compounds, such as the organic fraction and transition metals[7,87].

### *4.3.2.Histology*

The presence of little vacuoles was observed in the tissues when they were exposed to PBS, as observed previously in other studies[88]. This could be a consequence of normal cell excretion processes[89], or could be triggered by the difference in chemical composition between PBS and Respiratory Tract Lining Fluids (RTLN)[90]. However, the amount of damage generated is minor, supporting the idea that PBS was suitable for performing this type of assay. The use of PBS is a standard cell culture method[36,37]. $PM_{10}$ caused moderate focal damage (shown in Figure 5b) to human bronchial tissues. Observations in $PM_{2.5}$ exposed cells exhibited two different phenomena by releasing proteins into the lumen, i.e. mucus secretion and vacuolar cell debris discharge (Figure 5d and e, respectively). This was in line with the results obtained for the ATP and Bradford assays. Cells exposed to cement exhibited a thicker membrane (ECHH), as well as mucus release by goblet cells; supporting the hypothesis that these cells could be in some stage of the process of hormesis. The produced histological alterations may suggest that the PM2.5 samples interacted with proteins and enzymes of lung tissue interfering with the antioxidant defence mechanism and leading to reactive oxygen species (ROS) generation, which in turn may induce stress in the bronchial epithelial cells to undergo atrophy and necrosis[68]. Damaged epithelial cells can also release proteases such as elastin and MMPs (matrix metalloproteinases), growth factors and other matrix modifying enzymes that can further the release of TLR (toll-like receptors) ligands providing a feedforward inflammatory drive and enhanced tissue injury and airway remodelling[91].

The link between TEER measurements and histopathology was confusing. Some authors found a positive correlation between TEER values and thickening of the epithelial barrier[50,92], whereas a recent study performed with porcine oviduct epithelial cells demonstrated the opposite[93]. These different in outcomes could be the result of several factors affecting the measurement of TEER, such as the use of different cell lines, different cell culturing methods or cells coming from not ideal donors (damaged or diseased cells). In our case, we did not find any of these correlations. Maximum TEER values were reached in the case of control, which revealed the smallest tissue height. Cells exposed to $PM_{10}$, $PM_{2.5}$, and CD displayed similar values of TEER, despite presenting different stages of hyperplasia among them. Future studies measuring hyperplasia by quantitative means (i.e. ki67 staining[94]) could improve results in this regard. Overall, our results did not find significant differences in tracheobronchial damage between the two PM fractions. However, we found changes in some tests when comparing cells exposed to different materials and controls. Further research is needed to evaluate the harmful potential of cement factory generated PM on tracheobronchial cells at different application doses.

## Acknowledgements

Authors would like to thank Anthony Oldroyd and Derek Scarborough for their assistance in the processes of PM extraction from filters and histology imaging respectively. This study was financially supported by the Spanish Ministry of Economy and Competitiveness through the project CTM2015-65303-P. Francisco Sánchez-Soberón received a doctoral scholarship and an internship grant from the same organism.

## Author information

*Corresponding author: e-mail: marta.schuhmacher@urv.cat

## Competing interest

The authors declare that they have no competing interests.

## References

(1) Perez, L.; Medina-Ramón, M.; Künzli, N.; Alastuey, A.; Pey, J.; Pérez, N.; Garcia, R.; Tobias, A.; Querol, X.; Sunyer, J. Size Fractionate Particulate Matter, Vehicle Traffic, and Case-Specific Daily Mortality in Barcelona, Spain. *Environ. Sci. Technol.* **2009**, *43* (13), 4707–4714.

(2) Pérez, N.; Pey, J.; Querol, X.; Alastuey, A.; López, J. M.; Viana, M. Partitioning of major and trace components in PM10–PM2.5–PM1 at an urban site in Southern Europe. *Atmos. Environ.* **2008**, *42* (8), 1677–1691.

(3) US EPA. Health | Particulate Matter | Air & Radiation http://www3.epa.gov/pm/health.html (accessed Nov 6, 2015).

(4) WHO. Ambient (outdoor) air quality and health http://www.who.int/mediacentre/factsheets/fs313/en/ (accessed Nov 6, 2015).

(5) US EPA. Basic Information | Particulate Matter | Air & Radiation | US EPA https://www.epa.gov/pm-pollution/particulate-matter-pm-basics#PM (accessed May 31, 2015).

(6) EEA. *Air quality in Europe — 2015 report*; 2015.

(7) Kelly, F. J.; Fussell, J. C. Size, source and chemical composition as determinants of toxicity attributable to ambient particulate matter. *Atmos. Environ.* **2012**, *60*, 504–526.

(8) Shao, L.; Hou, C.; Geng, C.; Liu, J.; Hu, Y.; Wang, J.; Jones, T.; Zhao, C.; BéruBé, K. The oxidative potential of PM10 from coal, briquettes and wood charcoal burnt in an experimental domestic stove. *Atmos. Environ.* **2016**, *127*, 372–381.

(9) Chuang, H.-C.; Jones, T. P.; Lung, S.-C. C.; BéruBé, K. A. Soot-driven reactive oxygen species formation from incense burning. *Sci. Total Environ.* **2011**, *409* (22), 4781–4787.

(10) Akhtar, U. S.; Scott, J. A.; Chu, A.; Evans, G. J. In vivo and In vitro Assessment of Particulate Matter Toxicology. In *Urban Airborne Particulate Matter*; Zereini, F., Wiseman, C. L. S., Eds.; Environmental Science and Engineering; Springer Berlin Heidelberg: Berlin, Heidelberg, 2011; pp 427–449.

(11) Nemmar, A.; Holme, J. a; Rosas, I.; Schwarze, P. E.; Alfaro-Moreno, E. Recent advances in particulate matter and nanoparticle toxicology: a review of the in vivo and in vitro studies. *Biomed Res. Int.* **2013**, *2013*, 279371.

(12) Akhtar, U. S.; Rastogi, N.; McWhinney, R. D.; Urch, B.; Chow, C.-W.; Evans, G. J.; Scott, J. A. The combined effects of physicochemical properties of size-fractionated ambient particulate matter on in vitro toxicity in human A549 lung epithelial cells. *Toxicol. Reports* **2014**, *1*, 145–156.

(13) Jalava, P. I.; Happo, M. S.; Huttunen, K.; Sillanpää, M.; Hillamo, R.; Salonen, R. O.; Hirvonen, M.-R. Chemical and microbial components of urban air PM cause seasonal variation of toxicological activity. *Environ. Toxicol. Pharmacol.* **2015**, *40* (2), 375–387.

(14) Oeder, S.; Kanashova, T.; Sippula, O.; Sapcariu, S. C.; Streibel, T.; Arteaga-Salas, J. M.; Passig, J.; Dilger, M.; Paur, H. H.-R. H.-R.; Schlager, C.; et al. Particulate matter from both heavy fuel oil and diesel fuel shipping emissions show strong biological effects on human lung cells at realistic and comparable in vitro exposure conditions. *PLoS One* **2015**, *10* (6), e0126536.

(15) Moreno, T.; Pérez, N.; Reche, C.; Martins, V.; de Miguel, E.; Capdevila, M.; Centelles, S.; Minguillón, M. C.; Amato, F.; Alastuey, A.; et al. Subway platform air quality.Assessing the influences of tunnel ventilation, train piston effect and station design. *Atmos. Environ.* **2014**, *92*, 461–468.

(16) Wu, W.; Muller, R.; Berhane, K.; Fruin, S.; Liu, F.; Jaspers, I.; Diaz-Sanchez, D.; Peden, D. B.; McConnell, R. Inflammatory response of monocytes to ambient particles varies by highway proximity. *Am. J. Respir. Cell Mol. Biol.* **2014**, *51* (6), 802–809.

(17) Xia, M.; Viera-Hutchins, L.; Garcia-Lloret, M.; Noval Rivas, M.; Wise, P.; McGhee, S. A.; Chatila, Z. K.; Daher, N.; Sioutas, C.; Chatila, T. A. Vehicular exhaust particles promote allergic airway inflammation through an aryl hydrocarbon receptor-notch signaling cascade. *J. Allergy Clin. Immunol.* **2015**, *136* (2), 441–453.

(18) Price, H. D.; Jones, T. P.; BéruBé, K. A. Resolution of the mediators of in vitro oxidative reactivity in size-segregated fractions that may be masked in the urban PM(10) cocktail. *Sci. Total Environ.* **2014**, *485–486*, 588–595.

(19) Tarantini, A.; Douki, T.; Personnaz, M.-B.; Besombes, J.-L.; Jafrezzo, J.-L.; Maître, A. Effect of the chemical composition of organic extracts from environmental and industrial atmospheric samples on the genotoxicity of polycyclic aromatic hydrocarbons mixtures. *Toxicol. Environ. Chem.* **2011**, *93* (5), 941–954.

(20) Uzu, G.; Sauvain, J.-J.; Baeza-Squiban, A.; Riediker, M.; Hohl, M. S. S.; Val, S.; Tack, K.; Denys, S.; Pradère, P.; Dumat, C. In vitro assessment of the pulmonary toxicity and gastric availability of lead-rich particles from a lead recycling plant. *Environ. Sci. Technol.* **2011**, *45* (18), 7888–7895.

(21) Xiao, Z.; Shao, L.; Zhang, N.; Wang, J.; Chuang, H.-C.; Deng, Z.; Wang, Z.; BéruBé, K. A toxicological study of inhalable particulates in an industrial region of Lanzhou City, northwestern China: Results from plasmid scission assay. *Aeolian Res.* **2014**, *14*, 25–34.

(22) Abdul-Wahab, S. A. Impact of fugitive dust emissions from cement plants on nearby communities. *Ecol. Modell.* **2006**, *195* (3–4), 338–348.

(23) Brown, D.; Sadiq, R.; Hewage, K. An overview of air emission intensities and environmental performance of grey cement manufacturing in Canada. *Clean Technol. Environ. Policy* **2014**, *16* (6), 1119–1131.

(24) Li, C.; Nie, Z.; Cui, S.; Gong, X.; Wang, Z.; Meng, X. The life cycle inventory study of cement manufacture in China. *J. Clean. Prod.* **2014**, *72*, 204–211.

(25) CEMBUREAU. Cement manufacturing process http://www.cembureau.be/about-cement/cement-manufacturing-process (accessed Nov 6, 2015).

(26) EU Commission. *Best Available Techniques (BAT) Reference Document for the Production of Cement, Lime and Magnesium Oxide*; Seville, 2013.

(27) Wei, L.; Tang, H. L.; Guo, Y. Y.; Zou, Z. Y.; Liu, Y. S. Characteristics of PM2.5 emitted from cement kiln and the risk assessment of PAHs in PM2.5. *Zhongguo Huanjing Kexue/China Environ. Sci.* **2014**, *34* (5), 1113–1118.

(28) Oguntoke, O.; Awanu, A. E.; Annegarn, H. J. Impact of cement factory operations on air quality and human health in Ewekoro Local Government Area, South-Western Nigeria. *Int. J. Environ. Stud.* **2012**, *69* (6), 934–945.

(29) Sánchez-Soberón, F.; Rovira, J.; Mari, M.; Sierra, J.; Nadal, M.; Domingo, J. L.; Schuhmacher, M. Main components and human health risks assessment of PM10, PM2.5, and PM1 in two areas influenced by cement plants. *Atmos. Environ.* **2015**, *120*, 109–116.

(30) Shi, B. F.; Wu, Q. L.; Ouyang, H. X.; Liu, X. X.; Zhang, J. L.; Zuo, W. Y. Characteristics and sources of polycyclic aromatic hydrocarbons in surface soil from industrial areas of Baise, Guangxi. *Zhongguo Huanjing Kexue/China Environ. Sci.* **2014**, *34* (10), 2593–2601.

(31) van Berlo, D.; Haberzettl, P.; Gerloff, K.; Li, H.; Scherbart, A. M.; Albrecht, C.; Schins, R. P. F. Investigation of the cytotoxic and proinflammatory effects of cement dusts in rat alveolar macrophages. *Chem. Res. Toxicol.* **2009**, *22* (9), 1548–1558.

(32) Bauer, M.; Gräbsch, C.; Gminski, R.; Ollmann, A. I. H.; Borm, P.; Dietz, A.; Herbarth, O.; Wichmann, G. Cement-related particles interact with proinflammatory IL-8 chemokine from human primary oropharyngeal mucosa cells and human epithelial lung cancer cell line A549. *Environ. Toxicol.* **2012**, *27* (5), 297–306.

(33) Roig, N.; Sierra, J.; Rovira, J.; Schuhmacher, M.; Domingo, J. L.; Nadal, M. In vitro tests to assess toxic effects of airborne PM(10) samples. Correlation with metals and chlorinated dioxins and furans. *Sci. Total Environ.* **2013**, *443*, 791–797.

(34) Senthilkumar, S.; Manju, A.; Muthuselvam, P.; Shalini, D.; Indhumathi, V.; Kalaiselvi, K.; Palanivel, M.; Chandrasekar, P. P.; Rajaguru, P. Characterization and genotoxicity evaluation of particulate matter collected from industrial atmosphere in Tamil Nadu state, India. *J. Hazard. Mater.* **2014**, *274C*, 392–398.

(35) Brown, J. S.; Gordon, T.; Price, O.; Asgharian, B. Thoracic and respirable particle definitions for human health risk assessment. *Part. Fibre Toxicol.* **2013**, *10*, 12.

(36) Prytherch, Z. C.; Berube, K. A. A normal and biotransforming model of the human bronchial epithelium for the toxicity testing of aerosols and solubilised substances. *Altern. to Lab. Anim.* **2014**, *42* (6), 377–381.

(37) Prytherch, Z.; Job, C.; Marshall, H.; Oreffo, V.; Foster, M.; BéruBé, K. Tissue-Specific Stem Cell Differentiation in an in vitro Airway Model. *Macromol. Biosci.* **2011**, *11* (11), 1467–1477.

(38) Rovira, J.; Mari, M.; Schuhmacher, M.; Nadal, M.; Domingo, J. L. Monitoring environmental pollutants in the vicinity of a cement plant: a temporal study. *Arch. Environ. Contam. Toxicol.* **2011**, *60* (2), 372–384.

(39) Lafarge. Fábrica de Montcada http://www.lafarge.com.es/wps/portal/es/fabrica-de-montcada (accessed Jun 23, 2016).

(40) Generalitat de Catalunya. Expedient BA20100180: Incorporació d'un canvi no substancial consistent en la substitució de part del combustible fòssil utilitzat (coc de petroli) per CDR, combustible derivat de residus, amb el codi CER 191210 fins a 30.000 t/a. 2011.

(41) Generalitat de Catalunya. Expedient BA20060162: Autorització ambiental per a l'adequació a la Llei 3/1998 per a una activitat de fabricació de ciment. Barcelona 2008.

(42) Bérubé, K. A.; Jones, T. P.; Williamson, B. J.; Winters, C.; Morgan, A. J.; Richards, R. J. Physicochemical characterisation of diesel exhaust particles: Factors for assessing biological activity. *Atmos. Environ.* **1999**, *33* (10), 1599–1614.

(43) Berube, K. A.; Jones, T. P.; Housley, D. G.; Richards, R. J. The respiratory toxicity of airborne volcanic ash from the Soufriere Hills volcano, Montserrat. *Mineral. Mag.* **2004**, *68* (1), 47–60.

(44) Jones, T.; Moreno, T.; BéruBé, K.; Richards, R. The physicochemical characterisation of microscopic airborne particles in south Wales: a review of the locations and methodologies. *Sci. Total Environ.* **2006**, *360* (1–3), 43–59.

(45) Reche, C.; Moreno, T.; Amato, F.; Viana, M.; van Drooge, B. L.; Chuang, H.-C.; Bérubé, K.; Jones, T.; Alastuey, A.; Querol, X. A multidisciplinary approach to

characterise exposure risk and toxicological effects of $PM_{10}$ and $PM_{2.5}$ samples in urban environments. *Ecotoxicol. Environ. Saf.* **2012**, *78*, 327–335.

(46) Lafarge. *Health and Safety Information Portland cement*; 2011.

(47) Koshy, L.; Paris, E.; Ling, S.; Jones, T.; BéruBé, K. Bioreactivity of leachate from municipal solid waste landfills - assessment of toxicity. *Sci. Total Environ.* **2007**, *384* (1–3), 171–181.

(48) Bérubé, K.; Prytherch, Z.; Job, C.; Hughes, T. Human primary bronchial lung cell constructs: the new respiratory models. *Toxicology* **2010**, *278* (3), 311–318.

(49) Neilson, L.; Mankus, C.; Thorne, D.; Jackson, G.; DeBay, J.; Meredith, C. Development of an in vitro cytotoxicity model for aerosol exposure using 3D reconstructed human airway tissue; application for assessment of e-cigarette aerosol. *Toxicol. In Vitro* **2015**, *29* (7), 1952–1962.

(50) Balharry, D.; Sexton, K.; BéruBé, K. A. An in vitro approach to assess the toxicity of inhaled tobacco smoke components: nicotine, cadmium, formaldehyde and urethane. *Toxicology* **2008**, *244* (1), 66–76.

(51) Sexton, K.; Balharry, D.; BéruBé, K. a. Genomic biomarkers of pulmonary exposure to tobacco smoke components. *Pharmacogenet. Genomics* **2008**, *18* (10), 853–860.

(52) Bradford, M. M. A rapid and sensitive method for the quantitation of microgram quantities of protein using the principle of protein dye binding. *Anal. Biochem.* **1976**, *72*, 248–254.

(53) Feng, X.; Dang, Z.; Huang, W.; Shao, L.; Li, W. Microscopic morphology and size distribution of particles in PM2.5 of Guangzhou City. *J. Atmos. Chem.* **2010**, *64* (1), 37–51.

(54) Senlin, L.; Zhenkun, Y.; Xiaohui, C.; Minghong, W.; Guoying, S.; Jiamo, F.; Paul, D. The relationship between physicochemical characterization and the potential toxicity of fine particulates (PM2.5) in Shanghai atmosphere. *Atmos. Environ.* **2008**, *42* (31), 7205–7214.

(55) Xie, R. K.; Seip, H. M.; Leinum, J. R.; Winje, T.; Xiao, J. S. Chemical characterization of individual particles (PM10) from ambient air in Guiyang City, China. *Sci. Total Environ.* **2005**, *343* (1–3), 261–272.

(56) Brown, P.; Jones, T.; BéruBé, K. The internal microstructure and fibrous mineralogy of fly ash from coal-burning power stations. *Environ. Pollut.* **2011**, *159* (12), 3324–3333.

(57) Han, J. Chemical Characterizations of PM10 Profiles for Major Emission Sources in Xining, Northwestern China. *Aerosol Air Qual. Res.* **2014**, *14* (3), 1017–1027.

(58) Kim, Y. H.; Wyrzykowska-Ceradini, B.; Touati, A.; Krantz, Q. T.; Dye, J. A.; Linak, W. P.; Gullett, B.; Gilmour, M. I. Characterization of Size-Fractionated Airborne Particles Inside an Electronic Waste Recycling Facility and Acute Toxicity Testing in Mice. *Environ. Sci. Technol.* **2015**, *49* (19), 11543–11550.

(59) Popovicheva, O.; Kireeva, E. Microstructure and chemical composition of diesel and biodiesel particle exhaust. *Aerosol Air Qual. Res.* **2014**, *14*, 1392–1401.

(60) Song, X.; Shao, L.; Zheng, Q.; Yang, S. Mineralogical and geochemical composition of particulate matter (PM10) in coal and non-coal industrial cities of Henan Province, North China. *Atmos. Res.* **2014**, *143*, 462–472.

(61) Sánchez-Soberón, F.; van Drooge, B. L.; Rovira, J.; Grimalt, J. O.; Nadal, M.; Domingo, J. L.; Schuhmacher, M. Size-distribution of airborne polycyclic aromatic hydrocarbons and other organic source markers in the surroundings of a cement plant powered with alternative fuels. *Sci. Total Environ.* **2016**, *550*, 1057–1064.

(62) See, S. W.; Wang, Y. H.; Balasubramanian, R. Contrasting reactive oxygen species and transition metal concentrations in combustion aerosols. *Environ. Res.* **2007**, *103* (3), 317–324.

(63) Wilk, A.; Waligórski, P.; Lassak, A.; Vashistha, H.; Lirette, D.; Tate, D.; Zea, A. H.; Koochekpour, S.; Rodriguez, P.; Meggs, L. G.; et al. Polycyclic aromatic hydrocarbons-induced ROS accumulation enhances mutagenic potential of T-antigen from human polyomavirus JC. *J. Cell. Physiol.* **2013**, *228* (11), 2127–2138.

(64) Shao, L.; Hu, Y.; Wang, J.; Hou, C.; Yang, Y.; Wu, M. Particle-induced oxidative damage of indoor PM10 from coal burning homes in the lung cancer area of Xuan Wei, China. *Atmos. Environ.* **2013**, *77*, 959–967.

(65) Chougnet, A.; Palermo, T.; Audibert, A.; Moan, M. Rheological behaviour of cement and silica suspensions: Particle aggregation modelling. *Cem. Concr. Res.* **2008**, *38* (11), 1297–1301.

(66) Celik, I. B. The effects of particle size distribution and surface area upon cement strength development. *Powder Technol.* **2009**, *188* (3), 272–276.

(67) Sawada, N. Tight junction-related human diseases. *Pathol. Int.* **2013**, *63* (1), 1–12.

(68) Ganesan, S.; Comstock, A. T.; Sajjan, U. S. Barrier function of airway tract epithelium. *Tissue Barriers* **2013**, *1* (4), e24997.

(69) Cao, X.; Lin, H.; Muskhelishvili, L.; Latendresse, J.; Richter, P.; Heflich, R. H. Tight junction disruption by cadmium in an in vitro human airway tissue model. *Respir. Res.* **2015**, *16* (1), 30.

(70) Rezaee, F.; Georas, S. N. Breaking barriers. New insights into airway epithelial barrier function in health and disease. *Am. J. Respir. Cell Mol. Biol.* **2014**, *50* (5), 857–869.

(71) Georas, S. N.; Rezaee, F. Epithelial barrier function: at the front line of asthma immunology and allergic airway inflammation. *J. Allergy Clin. Immunol.* **2014**, *134* (3), 509–520.

(72) Shen, L.; Weber, C. R.; Raleigh, D. R.; Yu, D.; Turner, J. R. Tight junction pore and leak pathways: a dynamic duo. *Annu. Rev. Physiol.* **2011**, *73*, 283–309.

(73) Khalili Fard, J.; Jafari, S.; Eghbal, M. A. A Review of Molecular Mechanisms Involved in Toxicity of Nanoparticles. *Adv. Pharm. Bull.* **2015**, *5* (4), 447–454.

(74) Calabrese, E. J.; Baldwin, L. A. Hormesis: the dose-response revolution. *Annu Rev Pharmacol Toxicol* **2003**, *43*, 175–197.

(75) Stebbing, A. R. D. Hormesis: Interpreting the beta-curve using control theory. *J. Appl. Toxicol.* **2000**, *20* (2), 93–101.

(76) Christofi, N.; Hoffmann, C.; Tosh, L. Hormesis responses of free and immobilized light-emitting bacteria. *Ecotoxicol. Environ. Saf.* **2002**, *52* (3), 227–231.

(77) Koshy, L.; Jones, T.; BéruBé, K. Characterization and bioreactivity of respirable airborne particles from a municipal landfill. *Biomarkers* **2009**, *14 Suppl 1*, 49–53.

(78) Zavala, J.; O’Brien, B.; Lichtveld, K.; Sexton, K. G.; Rusyn, I.; Jaspers, I.; Vizuete, W. Assessment of biological responses of EpiAirway 3-D cell constructs versus A549 cells for determining toxicity of ambient air pollution. *Inhal. Toxicol.* **2016**, *28* (6), 251–259.

(79) Cao, L.; Zeng, J.; Liu, K.; Bao, L.; Li, Y. Characterization and Cytotoxicity of PM<0.2, PM0.2-2.5 and PM2.5-10 around MSWI in Shanghai, China. *Int. J. Environ. Res. Public Health* **2015**, *12* (5), 5076–5089.

(80) Halatek, T.; Stepnik, M.; Stetkiewicz, J.; Krajnow, A.; Kur, B.; Szymczak, W.; Rydzynski, K.; Dybing, E.; Cassee, F. R. The inflammatory response in lungs of rats exposed on the airborne particles collected during different seasons in four European cities. *J. Environ. Sci. Health. A. Tox. Hazard. Subst. Environ. Eng.* **2011**, *46* (13), 1469–1481.

(81) Ramgolam, K.; Favez, O.; Cachier, H.; Gaudichet, A.; Marano, F.; Martinon, L.; Baeza-Squiban, A. Size-partitioning of an urban aerosol to identify particle determinants involved in the proinflammatory response induced in airway epithelial cells. *Part. Fibre Toxicol.* **2009**, *6* (1), 10.

(82) Xu, W.; Jiang, J.; Yang, B.; Mei, D.; Dai, B. Comparison of the toxic effects in A549 cells induced by automobile exhaust particulates with different sizes. *Huanjing Kexue Xuebao/Acta Sci. Circumstantiae* **2013**, *33* (12), 3407–3412.

(83) Mirowsky, J. E.; Jin, L.; Thurston, G.; Lighthall, D.; Tyner, T.; Horton, L.; Galdanes, K.; Chillrud, S.; Ross, J.; Pinkerton, K. E.; et al. In vitro and in vivo toxicity of urban and rural particulate matter from California. *Atmos. Environ. (1994).* **2015**, *103*, 256–262.

(84) Thomson, E. M.; Breznan, D.; Karthikeyan, S.; MacKinnon-Roy, C.; Charland, J.-P.; Dabek-Zlotorzynska, E.; Celo, V.; Kumarathasan, P.; Brook, J. R.; Vincent, R. Cytotoxic and inflammatory potential of size-fractionated particulate matter collected repeatedly within a small urban area. *Part. Fibre Toxicol.* **2015**, *12* (1), 24.

(85) Cassee, F. R.; Héroux, M.-E.; Gerlofs-Nijland, M. E.; Kelly, F. J. Particulate matter beyond mass: recent health evidence on the role of fractions, chemical constituents and sources of emission. *Inhal. Toxicol.* **2013**, *25* (14), 802–812.

(86) Steenhof, M.; Gosens, I.; Strak, M.; Godri, K. J.; Hoek, G.; Cassee, F. R.; Mudway, I. S.; Kelly, F. J.; Harrison, R. M.; Lebret, E.; et al. In vitro toxicity of particulate matter (PM) collected at different sites in the Netherlands is associated with PM composition, size fraction and oxidative potential--the RAPTES project. *Part. Fibre Toxicol.* **2011**, *8*, 26.

(87) Lichtveld, K. M.; Ebersviller, S. M.; Sexton, K. G.; Vizuete, W.; Jaspers, I.; Jeffries, H. E. In Vitro Exposures in Diesel Exhaust Atmospheres: Resuspension of PM from Filters versus Direct Deposition of PM from Air. *Environ. Sci. Technol.* **2012**, *46* (16), 9062–9070.

(88) Sexton, K.; Balharry, D.; Brennan, P.; McLaren, J.; Brewis, I. A.; BéruBé, K. A. Proteomic profiling of human respiratory epithelia by iTRAQ reveals biomarkers of exposure and harm by tobacco smoke components. *Biomarkers* **2011**, *16* (7), 567–576.

(89) Dance, A. How Cells Take Out the Trash https://publications.nigms.nih.gov/insidelifescience/cells-take-out-trash.html (accessed Jun 1, 2017).

(90) Cross, C. E.; van der Vliet, A.; O'Neill, C. A.; Louie, S.; Halliwell, B. Oxidants, antioxidants, and respiratory tract lining fluids. *Environ. Health Perspect.* **1994**, No. Suppl 10, 185–191.

(91) Mortaz, E.; Barnes, P. J.; Heidarnazhad, H.; Adcock, I. M.; Masjedi, M. R. Immunological Features of Chronic Obstructive Pulmonary Disease (COPD) Induced by Indoor Pollution and Cigarette Smoke. *Tanaffos* **2012**, *11* (4), 6–17.

(92) Harrington, H.; Cato, P.; Salazar, F.; Wilkinson, M.; Knox, A.; Haycock, J. W.; Rose, F.; Aylott, J. W.; Ghaemmaghami, A. M. Immunocompetent 3D Model of Human Upper Airway for Disease Modeling and In Vitro Drug Evaluation. *Mol. Pharm.* **2014**, *11* (7), 2082–2091.

(93) Chen, S.; Einspanier, R.; Schoen, J. Transepithelial electrical resistance (TEER): a functional parameter to monitor the quality of oviduct epithelial cells cultured on filter supports. *Histochem. Cell Biol.* **2015**, *144* (5), 509–515.

(94) Atar, Y.; Salturk, Z.; Kumral, T. L.; Uyar, Y.; Cakir, C.; Sunnetci, G.; Berkiten, G. Effects of Smoke Generated by Electrocautery on the Larynx. *J. Voice* **2017**, *31* (3), 380.e7-380.e9.

# CHAPTER 4: An approach to assess the Particulate Matter exposure for the population living around a cement plant: modelling indoor air and particle deposition in the respiratory tract

Francisco Sánchez-Soberón, Montse Mari, Vikas Kumar, Joaquim Rovira, Martí Nadal, Marta Schuhmacher (2015). Environmental Research 143, 10-18.

# An approach to assess the Particulate Matter exposure for the population living around a cement plant: modelling indoor air and particle deposition in the respiratory tract

Francisco Sánchez-Soberón, Montse Mari, Vikas Kumar, Joaquim Rovira, Martí Nadal, Marta Schuhmacher (2015). Environmental Research 143, 10-18.

Abstract:

In this paper we studied the exposure to three size fractions of outdoor particulate matter ($PM_{10}$, $PM_{2.5}$, and $PM_1$) collected in an area influenced by a cement plant. For that purpose, three groups of population were evaluated (children, adults and retired) in two seasons (summer and winter). Outdoor measured PM concentrations, as well as physiological parameters and activity patterns of the three groups of population were used as input data in two different models. The first one was an indoor air quality model, used to elucidate indoor PM concentrations in different microenvironments. The second one was a dosimetry model, used to evaluate the internal exposure and the distribution of the different PM fractions in the respiratory tract. Result from the indoor air quality model showed that special attention must be paid to the finest particles, since they penetrate indoors in a greater degree. Highest pulmonary doses for the three PM sizes were reported for retired people, being the main contribution result of the high amount of time in outdoor environments exercising lightly. For children, the exposure was mainly influenced by the time they also spend outdoors, but in this case due to heavy intensity activities. It was noticed that deposition of fine particles was more significant in the pulmonary regions of children and retired people in comparison with adults, which has implications in the expected adverse health effects for those vulnerable groups of population.

*Key words*

Cement; Fine particulate matter; Indoor/outdoor exposure; Human respiratory tract model

*Abbreviations:* ARA, Applied Research Associates; BF, breathing frequency; DF, deposition fraction; FRC, functional residual volume; HRT, human respiratory tract; ICRP, International Commission on Radiological Protection; IEC, Statistical Institute of Catalonia; INE, Spanish Statistical Office; INSEE, French Institute of Statistics and Economy; ME, microenvironment; MPPD, multiple path particle dosimetry; P, pulmonary; PM, particulate matter; T, time; TB, tracheobronchial; TV, tidal volume; US EPA, United States Environmental Protection Agency; URT, upper respiratory tract; WHO, World Health Organization.

**Funding sources**

Two organizations were the main funding sources of the present study:

- The Spanish Ministry of Economy and Competitiveness (MINECO), through the project CTM2012-32778.
- The European Union, through the HEALS project FP7-ENV-2013-603946, included in the Seventh Framework Programme.

## 1. Introduction

Particulate matter (PM) is a complex mixture of extremely small particles and liquid droplets suspended in the atmosphere originated from a wide range of sources (such as traffic, industry, energy production or domestic combustion). Consequently, its composition and size is widely variable in space and time. Nowadays, PM is a concern because its inhalation is related with many adverse health effects (such as cardiovascular and pulmonary diseases), being estimated that this pollutant is responsible of around 2.1 million of premature deaths per year globally (Fantke et al., 2015; Kelly and Fussell, 2012; Kim et al., 2015).

The two more influent parameters in the damage potential of PM are its chemical composition and size. Common constituents of PM include sulphates, nitrates, ammonium, and other inorganic ions (such as ions of sodium, potassium, calcium, magnesium, and chloride), organic and elemental carbon, crustal material, particle-bound water and metals (including cadmium, copper, nickel, vanadium, and zinc). Furthermore, biological components such as allergens and microbial compounds are found in PM (WHO, 2013). Regarding PM size, literature discriminates between particles with a diameter of less than 10 µm ($PM_{10}$), and particles with a diameter smaller than 2.5 µm ($PM_{2.5}$). The fraction between $PM_{10}$ and $PM_{2.5}$ is usually known as “coarse particles” ($PM_{10-2.5}$), while $PM_{2.5}$ is often called “fine PM”. $PM_{2.5}$ also comprises ultrafine particles, which are those having a diameter of less than 0.1 µm. In most locations in Europe, $PM_{2.5}$ constitutes 50–70% of $PM_{10}$ (WHO, 2013). Size plays a key role on determining the part of the respiratory tract where particles deposit and, therefore, their potential of being harmful. Smaller particles, especially ultra-fines, penetrate into the interstitium and blood stream, being more hazardous (Hoek et al., 2008).

In order to control PM levels and protect the health of the population, outdoor concentrations of $PM_{10}$ and $PM_{2.5}$ are widely studied, especially in areas with heavy traffic, or with other significant sources, such as cement or power plants (Cheng et al., 2010; Marcon et al., 2014; Patton et al., 2014; Querol et al., 2014; Rovira et al., 2014; Wilkinson et al., 2013). In addition, ambient monitoring networks have been established all over Europe and the USA by national institutions and local councils. They are equipped with on-line monitors providing continuous data with sufficient time resolution (half-hourly values) (Monn, 2001). However, the monitoring of particles smaller than 2.5 µm is still very scarce. Although outdoor levels of $PM_{10}$ and $PM_{2.5}$ are usually used to estimate the human risks due to PM exposure, in developed countries population spend more than 80% of their time indoors (Hänninen et al., 2013). Furthermore, the different breathing patterns associated to the different activities performed both in and out doors are not taken into account when assessing human exposure. Therefore, risks due to PM exposure may be miscalculated.

Since data regarding indoor aerosol particles are not usually available, indoor aerosol models may be used as an alternative to estimate the amount of outdoor particles that penetrate indoors. Concerning the inhalation pattern issue, dosimetry models could be very useful to calculate the deposition of different PM sizes along the pulmonary region according to diverse breathing rates. Although some papers have addressed the simulation of indoor PM concentrations (McGrath et al., 2014; Sarigiannis et al., 2014) and some others the deposition in the human respiratory tract (Li et al., 2015; Patterson et al., 2014; Sarigiannis et al., 2015), studies joining the results from both kind of models are still sparse (Hussein et al., 2015).

The objective of this study was to evaluate the human PM exposure, in an industrial area where a cement plant is operating in Barcelona (Spain), as well as to assess the dose retained in the different parts of the human respiratory tract. To do that, outdoor concentrations of three PM fractions (10, 2.5, and 1 µm) were used as input in an indoor air quality model to calculate PM levels in indoor microenvironments. Furthermore, a dosimetry model was used to estimate the internal exposure and the distribution of the different PM fractions in the respiratory tract of three groups of population (children, adults and retired) in order to evaluate their potential hazard according to different patterns of exposure and conditions.

## 2. Methodology

### *2.1. Site description and PM outdoor concentrations*

The studied area is located in the north of the metropolitan area of Barcelona (Catalonia, Spain). Different PM sources are operating in the area, such as some industries and an important organic waste-treatment facility. In addition, the neighborhood is crossed by two highways with heavy traffic. However, in terms of sources of PM, the greatest attention is focused on the cement plant due to its proximity to nuclei of population. This plant has been operating in the area since 1917, and as a consequence of the substantial development of the town in recent decades, the distance from the facility to the dwellings has dramatically decreased to 300 m, meaning that some inhabitants are potentially being exposed to the emissions from the facility. Hence, not only residents but also local authorities are concerned about the potential health risks and environmental impact of the cement plant emissions (Rovira et al., 2011).

In order to know the composition of outdoor PM, and have a preliminary idea of the cement plant contribution to ambient PM, a previous study was performed in the area (Sánchez-Soberón et al., 2015). In that study, levels of $PM_{10}$, $PM_{2.5}$ and $PM_1$ were measured in a school placed 300 m away from the cement plant during different seasons.

This point was the only one selected in the evaluation since, according to previous studies performed in the area, highest concentrations of PM were registered there (Rovira et al., 2011). Those 24h-PM outdoor concentrations (shown in Table 1) were used in the present study as input to estimate indoor concentrations of PMs, and, therefore, assess the human exposure. Although we understand that the cement facility is not the only source of outdoor PM, outdoor PM could be used as an oversized approximation for cement emissions.

**Table 1**. Input parameters in the IAQX simulations.

| Parameter | Value | | | | Reference |
|---|---|---|---|---|---|
| ***Building*** | | | | | |
| Number of air zone | 1 | | | | |
| Volume (m$^3$) | 90m$^2$ x 2.5m=225m$^3$ | | | | |
| Do we consider deposition? | Yes | | | | |
| ***Ventilation*** | | | | | |
| Air exchange rate (h$^{-1}$) | Winter: 0.44; Summer: 1.30 | | | | (Wallace et al., 2002) |
| | Working: 1.00 | | | | (Orosa and Baaliña, 2008) |
| ***PM properties*** | | | | | |
| Number of size group | PM$_1$, PM$_{2.5-1}$, PM$_{10-2.5}$ | | | | |
| Deposition rate (h$^{-1}$) | 0.8, 1, 2.5 | | | | (He et al., 2005) |
| ***Outdoor sources*** | | | | | |
| Infiltration factor (IF) size (dimensionless) | 0.80, 0.60, 0.35 | | | | (Chen and Zhao, 2011) |
| Ambient particle concentration (µg/m$^3$) | | Mean | Min | Max | (Sánchez-Soberón et al., 2015) |
| | *Winter* | | | | |
| | PM$_1$ | 31 | 26 | 42 | |
| | PM$_{2.5-1}$ | 1.0 | 0.4 | 2.0 | |
| | PM$_{10-2.5}$ | 19 | 11 | 31 | |
| | *Summer* | | | | |
| | PM$_1$ | 13 | 9.0 | 20 | |
| | PM$_{2.5-1}$ | 7.0 | 0.0 | 14 | |
| | PM$_{10-2.5}$ | 1.0 | 0.0 | 6.0 | |

### *2.2. Exposure scenarios: Microenvironments (ME) and time patterns*

To evaluate the real human exposure it is important to know how people spend their time, which means knowledge regarding the contexts, circumstances, and durations of the exposures. A microenvironment (ME) is a generic location which may be assumed to have homogenous conditions (Monn, 2001). Exposures are then estimated using the concentrations, time spent, and activities performed in different MEs. In this study, we assumed three different microenvironments: Indoors (at home), workplace, and outdoors. Two seasons namely winter and summer were also considered. Time-activity profiles have been shown to be influenced by factors such as employment status and age, since these factors affect the relative proportion of time individuals spend indoors and outdoors (Schweizer et al., 2007). Regarding time activity profiles, the study was conducted to three population groups: children, adult employees, and retired person, all of them male (Table 2). Activity profiles for adults and retired were adapted from reports about time use (IEC, 2012; INSEE, 2010), while for children they were taken from (Cohen Hubal et al., 2000).

### *2.3. Indoor PM estimation: IAQX model*

The indoor concentrations were calculated using model for Indoor Particulate Matter (PM.exe) of US EPA's Indoor Air Quality simulation Tool Kit, IAQX v1.1 (US EPA, 2000a). This model was chosen according to its high accuracy, tested by the EPA by comparing indoor simulations and measures (US EPA, 2000b). Detail description of this generic indoor PM model can be found in Nazaroff and Cass (1989). The model takes into consideration: infiltration of ambient PM, interzone air movement, indoor sources, and deposition. Mean outdoor concentrations of $PM_{10\text{-}2.5}$, $PM_{2.5\text{-}1,}$ and $PM_1$ of two seasons (summer and winter) were used as constant input, while initial indoor concentrations were considered 0. Table 2 shows the values of the parameters considered for the simulations. Only one indoor air zone was considered since studies on air exchange rates have shown that generally air is well mixed in houses and minor differences are found between different rooms (Wallace et al., 2002). Different ventilation conditions were considered to simulate the PM levels in the indoor ME in winter and summer since amount of time that the windows are opened and the use of ventilation systems have been demonstrated to strongly influence the air exchange rates (Abt et al., 2000; Chen and Zhao, 2011; Korhonen et al., 2000; Wang et al., 2015). Home air exchange rates of 0.44 $h^{-1}$ for winter and 1.30 $h^{-1}$ for summer were taken from the comprehensive study of Wallace et al. (2002) monitored for a year under normal living conditions with more than 4500 measurements. Very limited information is available regarding ventilation rates in Spanish office workplaces (Dimitroulopoulou and Bartzis, 2014). Ventilation rate from workplace, 1.00 $h^{-1}$, was taken from the study by Orosa and Baaliña (2008), who evaluated 25 bank office buildings. Regarding indoor deposition rates, which are size

**Table 2**. Activity patterns and physiological/morphological parameters for children, adults and retired.

| | **Age (years)** | **Activity** | **Time (hours)** | **Height (cm)** | **BW (kg)** | **BF (breaths/min)**[f] | **TV (ml)**[g] | **FRC (ml)**[h] | **UTR (ml)**[i] |
|---|---|---|---|---|---|---|---|---|---|
| Child | 10 | Sleeping | 9.6[a] | 139.5[d] | 36[d] | 17 | 304 | 1484 | 25 |
| | | Sitting | 11.5[a] | | | 19 | 333 | | |
| | | Light indoor | 0.4[a] | | | 32 | 583 | | |
| | | Light outdoor | 0.5[a] | | | 32 | 583 | | |
| | | Heavy | 2.0[a] | | | 45 | 752 | | |
| Adult | 45 | Sleeping | 8.1[b] | 175[e] | 69.7[e] | 12 | 625 | 3455 | 50 |
| | | Sitting | 10.4[b] | | | 12 | 750 | | |
| | | Light indoor | 2.8[b] | | | 20 | 1250 | | |
| | | Light outdoor | 2.3[b] | | | 20 | 1250 | | |
| | | Heavy | 0.4[b] | | | 26 | 1920 | | |
| Retired | 75 | Sleeping | 8.6[c] | 175[e] | 69.2[e] | 9 | 625 | 3755 | 50 |
| | | Sitting | 7.8[c] | | | 9 | 750 | | |
| | | Light indoor | 3.7[c] | | | 22 | 1250 | | |
| | | Light outdoor | 3.7[c] | | | 22 | 1250 | | |
| | | Heavy | 0.2[c] | | | 25 | 1920 | | |

a: (Cohen Hubal et al., 2000); b: (IEC, 2012); c:(INSEE, 2010); d:(Carrascosa et al., 2008); e:(INE, 2012); f :(US EPA, 2011); g: (ICRP, 1994); h: (Stocks and Quanjer, 1995); i:(Brown et al., 2013).

dependent, have been estimated in many studies for different PM fractions. Results show substantial variability in the methods used and the type of particles examined (Wallace et al., 2002). In addition, other factors influence deposition, including near surface air flows, incomplete mixing of room air, and turbulence (Wallace et al., 2002). Infiltration factor, which is also size dependent, represents the equilibrium fraction of ambient particles that penetrates indoors and remains suspended. PM infiltration factors measured by different researchers also show great variability, since their measurement conditions are quite different as it was reviewed by Chen and Zhao (2011). They reported values ranging from 0.2 to 0.5 for $PM_{10}$ and from 0.5 to 0.8 for $PM_{2.5}$ (Chen and Zhao, 2011). According to those values, we assumed infiltration factors of 0.80, 0.60, and 0.35 for $PM_1$, $PM_{2.5-1}$ and $PM_{10-2.5}$, respectively. Since the main objective of the work was to evaluate the exposure to particles in an industrial area with a cement plant, no indoor sources were considered. Neither re-suspension and chemical reaction/dynamics were considered.

### *2.4. Multiple Path Particle Dosimetry model (MPPD2.11)*

The patterns of deposition after inhalation were estimated for the different sizes of PM in each region of the respiratory tract (head, tracheobronchial, and pulmonary) by Multiple Path Particle Dosimetry model (MPPD) developed by the Chemical Industry Institute of Toxicology (CIIT, USA). MPPD model is very trusted model in the area of airway particle dosimetry and used equally in research, education, industries and regulatory agencies. Model has gone through many years of development and test and validation cycle and currently one of the most mature model available in the market. There is detail and updated user help and documentation available on the model website (ARA, 2014). The use of this model is justified since the MPPD version 2.11 includes age-specific lung models and the possibility of assessing several sizes of particles (Winter-Sorkina and Cassee, 2002). Input parameters cover: 1) PM characteristics (size distribution, shape, and density), 2) Activity patterns, and 3) Exposed subject characteristics (age, height, and body weight of the subjects) as well as respiratory physiological parameters (such as tidal volume (TV), breathing frequency (BF), functional residual volume (FRC)). Particles were considered spherical (shape factor of 1) in the calculations. Although the density of particles is also variable depending on their composition, we assumed particles having a density of 1 g/cm$^3$ as it has been done in other studies with no site specific data (Hussein et al., 2015). Table 1 shows the activity patterns as well as physiological input parameters for the simulation of the deposition fraction of children, adults, and retired person. Mean body weights and heights for adults and retired were taken from INE (2012) while for children they were obtained from Carrascosa et al. (2008). Some physiological inputs were considered as age and activity dependent. Breathing frequencies for working adult, retired person, and children were obtained from ICRP (1994) and US EPA (2011). Default model values for Upper Respiratory Tract (URT) volumes were used. FRCs were calculated using following equations presented by Stocks and Quanjer (1995):

$$\text{Children: FRC (in milliliter)} = 0.125 \times 10^{-3} \times \text{Height (centimeters)}^{3.298}$$

$$\text{Adult and Retired: FRC (in liter)} = 2.34 \times \text{Height (meters)} + 0.01 \times \text{Age (years)} - 1.09$$

Deposited doses are function of ambient concentrations (indoor and outdoor), the deposition fractions (DF), the amount of time (T) spent in each activity during the day (classified as: sleeping, sitting, exercising lightly, and exercising heavily according to the different time patterns), as well as the BF and TV for the different aforementioned activities. The following equation was used to evaluate the deposited dose (Yeh and Schum, 1980):

$$\text{Deposited dose } (\mu g) = DF \times \text{ambient conc. } (\mu g/m^3) \times TV\ (m^3/\text{breath}) \times BF\ (\text{breath/min}) \times T\ (\text{min})$$

## 3. Results and discussion

### *3.1. Indoor concentrations*

The results of the simulated indoor concentrations of $PM_{10-2.5}$, $PM_{2.5-1}$ and $PM_1$ in the homes and workplaces defined by assumptions in Table 1 are presented in Fig. 1. As previously mentioned, for the simulations, mean outdoor concentrations were taken from a monitoring exercise in the case study area for two seasonal periods (winter and summer) (Sánchez-Soberón et al., 2015). Since it was assumed that initially indoor concentrations were zero, results of the simulation show how indoor concentrations increase until they reach a steady state value. For the three PM fractions, notable seasonal differences could be observed in home concentrations. These differences were directly related to the measured outdoor concentrations, higher in winter due to a higher contribution from traffic and heating systems, and the presence of anticyclonic conditions in the area (Pey et al., 2010; Rovira et al., 2011) ($PM_{10-2.5}$: 19 µg/$m^3$ , $PM_{2.5-1}$: 1 µg/$m^3$, and $PM_1$: 31 µg/$m^3$), with the exception of $PM_{2.5-1}$, which was larger in summer ($PM_{10-2.5}$: 1 µg/$m^3$, $PM_{2.5-1}$: 7 µg/$m^3$, and $PM_1$: 13 µg/$m^3$) (Sánchez-Soberón et al., 2015). Air exchange rate, which accounts for the airflows that can occur across buildings (leakage, natural ventilation, and mechanical ventilation), is considered one of the most important parameters to explain the indoor-outdoor PM relationship (Hussein et al., 2015). Although we assumed higher air exchange rates for summer, considering that windows are opened for more time in summer than in winter (Wallace et al., 2002), the estimated indoor $PM_{10-2.5}$ and $PM_1$ levels were still higher in winter, in line with the higher outdoor concentrations found. Regarding workplaces, winter concentrations were higher than that at home according to the higher air flow rates representative of an office (Orosa and Baaliña, 2008). Since the ventilation rate in an office remains almost constant over the year, PM levels in summer were lower than in winter, in consonance with the lower outdoor PM concentrations reported in summer.

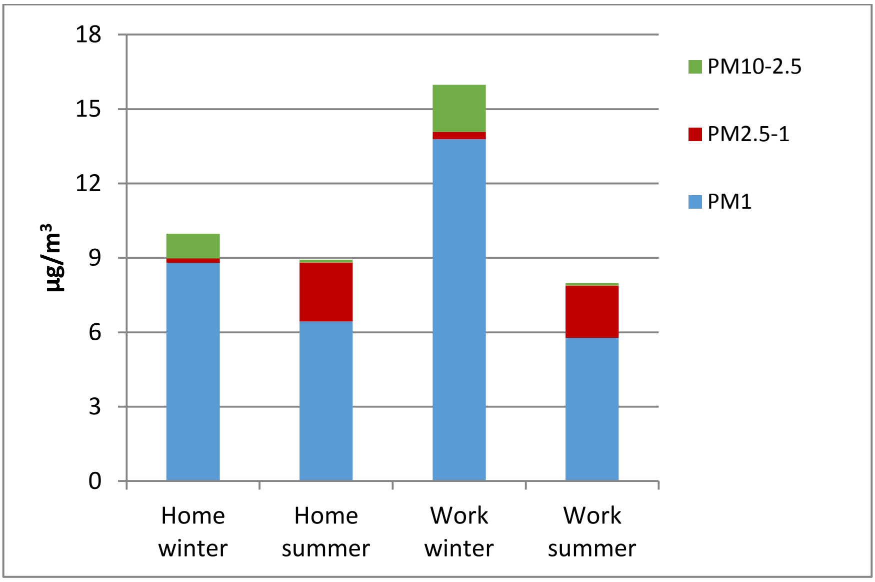

**Fig. 1.** Results of indoor $PM_{10-2.5}$, $PM_{10-2.5}$ , and $PM_1$ simulations.

With regard to the different PM sizes, $PM_1$ showed the highest concentrations in all the considered scenarios according not only to the higher outdoor concentrations, but also to the higher infiltration factors, since the smaller particles are those that mostly remain suspended once they penetrate indoors from outdoors. This is explained by their lower deposition rates and higher penetration factors in comparison with those of fine and coarse particles (Monn, 2001). In summer, the pattern indoors was $PM_1$>$PM_{2.5-1}$>$PM_{10-2.5}$ in both home and workplace. At home, PM levels were only slightly higher than that estimated in workplace according to the ventilation rates. In winter, in both environments the distribution was $PM_1$>$PM_{10-2.5}$>$PM_{2.5-1}$ in consonance with the outdoor concentrations.

**Table 3.** Deposition fractions for the different PM size fractions for child, adults and retired. Average values are calculated having into account the time spent in each activity on a daily basis.

| | **Child** | | | **Adult employee** | | | **Retired** | | |
|---|---|---|---|---|---|---|---|---|---|
| | **Head** | **TB** | **P** | **Head** | **TB** | **P** | **Head** | **TB** | **P** |
| **$PM_1$** | | | | | | | | | |
| Sleeping | 0.262 | 0.036 | 0.172 | 0.137 | 0.053 | 0.085 | 0.108 | 0.062 | 0.099 |
| Sitting | 0.269 | 0.037 | 0.164 | 0.158 | 0.051 | 0.101 | 0.126 | 0.058 | 0.118 |
| Light indoor | 0.317 | 0.047 | 0.108 | 0.347 | 0.038 | 0.076 | 0.367 | 0.038 | 0.068 |
| Light outdoor | 0.317 | 0.047 | 0.108 | 0.347 | 0.038 | 0.075 | 0.367 | 0.038 | 0.067 |
| Heavy | 0.345 | 0.065 | 0.075 | 0.535 | 0.036 | 0.046 | 0.526 | 0.036 | 0.046 |
| **Average** | **0.274** | **0.039** | **0.157** | **0.198** | **0.049** | **0.089** | **0.197** | **0.053** | **0.095** |
| **$PM_{2.5-1}$** | | | | | | | | | |
| Sleeping | 0.281 | 0.056 | 0.367 | 0.469 | 0.086 | 0.166 | 0.386 | 0.112 | 0.192 |
| Sitting | 0.292 | 0.056 | 0.357 | 0.509 | 0.075 | 0.185 | 0.430 | 0.097 | 0.216 |
| Light indoor | 0.354 | 0.132 | 0.226 | 0.773 | 0.032 | 0.103 | 0.793 | 0.030 | 0.091 |
| Light outdoor | 0.354 | 0.132 | 0.226 | 0.774 | 0.032 | 0.102 | 0.794 | 0.030 | 0.089 |
| Heavy | 0.362 | 0.340 | 0.094 | 0.894 | 0.021 | 0.046 | 0.891 | 0.021 | 0.048 |
| **Average** | **0.296** | **0.083** | **0.334** | **0.559** | **0.069** | **0.159** | **0.530** | **0.081** | **0.167** |
| **$PM_{10-2.5}$** | | | | | | | | | |
| Sleeping | 0.641 | 0.268 | 0.041 | 0.917 | 0.034 | 0.006 | 0.898 | 0.053 | 0.005 |
| Sitting | 0.667 | 0.270 | 0.022 | 0.924 | 0.027 | 0.007 | 0.909 | 0.041 | 0.006 |
| Light indoor | 0.796 | 0.192 | 0 | 0.949 | 0.008 | 0.001 | 0.951 | 0.007 | 0.001 |
| Light outdoor | 0.796 | 0.192 | 0 | 0.949 | 0.008 | 0.001 | 0.951 | 0.007 | 0.001 |
| Heavy | 0.855 | 0.139 | 0 | 0.955 | 0.004 | 0 | 0.955 | 0.004 | 0 |
| **Average** | **0.677** | **0.255** | **0.027** | **0.927** | **0.025** | **0.005** | **0.918** | **0.034** | **0.004** |

In our study to assess indoor exposure we only considered the infiltration of outdoor particles since our purpose was to assess the exposure to ambient PM in an area affected by a cement plant. However, particles are also originated from indoor sources (Ferro et al., 2004). Major indoor sources include combustion events (such as cooking, tobacco smoking, candle, and incense burning) and the use of gas and electric appliances as well as resuspension activities such as walking, dusting, and vacuum. Some studies point out that in homes major indoor sources of $PM_{2.5,}$ and even more of $PM_{1,}$ are originated outdoor (Hassanvand et al., 2014). Other studies, such as that by McGrath et al. (2014) show how indoor concentrations are highly modified by indoor activities. They reported mean $PM_{2.5}$ concentrations of 7.3 µg/$m^3$ in an indoor environment with no emission sources that were increased to 296 µg/$m^3$ when smoking 6 cigarettes, 289 µg/$m^3$ due to a frying event and 326 µg/$m^3$ as a result of burning an incense stick. Nevertheless, indoor sources are extremely variable according the human activities developed and their strength is still largely unknown since emission rates for the same process may be very different (Hussein et al., 2015).

### *3.2. Deposited fractions of PM in the HRT*

The average deposition fractions (DF) of $PM_{10-2.5}$, $PM_{2.5-1}$, and $PM_1$ in the head/throat (Head), pulmonary/tracheobronchial (TB), and pulmonary/alveolar (P) regions of the human respiratory system for children, adults, and retired during 24 hours are presented in Table 3. For each of the cohorts different DFs were obtained for each of the considered activities. Deposition fractions were estimated according to specific input parameters for Tidal volume (TV), functional residual volume (FRC), and breathing frequency (BF)) for each age and activity throughout the day (Table 2). As reported in previous studies using the same model (Li et al., 2015), there were no differences between summer and winter DFs. This is a direct consequence of the model here used, since it assumed that DFs does not depend on the PM concentrations. The head region was the part of the respiratory tract where higher percentages of deposition were calculated for all particle sizes and all age groups. Coarse particles addressed the highest deposition rates in this region. These values are in agreement with other studies where among all sizes, the coarse particles show the highest DFs in the head of the respiratory system (Behera et al., 2015; Sarigiannis et al., 2015; Winter-Sorkina and Cassee, 2002). That is explained by a combination of sedimentation and the impaction of particles onto the larynx and airway bifurcations (Behera et al., 2015). The DFs of coarse particles in the head region were higher for adults than for children. On the other hand, coarse particles DFs in the pulmonary TB region were significantly higher for children than for adults. These results are in agreement with those reported by Winter-Sorkina and Cassee (2002). Regarding $PM_{2.5-1,}$ head region addressed the highest deposition rates, being maximum in adults followed by retired and children. With respect to TB region, the percentage of $PM_{2.5-1}$ deposited fraction was significantly higher for children than for adults and retired, especially due to the characteristic heavy intensity activities of children (values of DFs were 0.340, 0.021 and 0.021, for children adults and retired, respectively). $PM_{2.5-1}$ DFs in P region were higher for children for all the activities. Regarding $PM_{1,}$ children experienced higher DFs than adults and retired for sleeping and sitting in head and P regions. The pattern of deposition for $PM_1$ was the same as for $PM_{2.5-1}$ for every population group, being the DFs higher in P than in TB regions. Differences in DFs among different age groups and respiratory regions described in the present study agree with the previously exposed by Watson et al. (1988). Higher ventilation rate per body weight in children, and differences in clearance patterns depending on the respiratory region could lead to a variable dose distribution from the childhood to the old age.

Data regarding different DFs according to different activities is sparse. Saber and Heydari (2012) calculated the DF for different particle sizes and breathing velocities in the head and the first three generations of branches in the tracheobronchial region. Their results showed that the bigger breathing intensity the higher deposition fraction in every respiratory region regardless of particle size. We found this same trend, but only in the head region, registering higher DFs in TB for sleeping or sitting activities. In the model used in the present study, TB region comprises 16 generations of branches. This greater number of bifurcations could lead to a higher deposition of particles by sedimentation under lower ventilation rates (Sarigiannis et al., 2015). It was not possible to compare our results of DF in the lung with those obtained by Saber and Heydari (2012), since they did not consider the deposition in the pulmonary region. Salma et al. (2015) studied the deposition of $PM_1$ in the respiratory tract of women within different environments and activities. They also observed that sleeping and sitting activities reached their maximum DFs in the head region. But unlike our study, light and heavy exercise experienced their maximum deposition fraction values in the pulmonary region. These results could be explained because oral breathing was taken into account under light and heavy exercise conditions, leading to a smaller deposition in the upper part of the respiratory tract. As in our study, DF was more affected by the type of activity (breathing frequency) than by locations (microenvironments). Hussein et al. (2015) also took into account time activity patterns to calculate the deposited doses of fine and ultrafine particles in the respiratory tract of adults exposed to indoor and outdoor environments. However, in that study the different DFs according to the activities were not discussed. In most studies deposition fractions are calculated by using the characteristics of the respiratory system of an average human adult with single values for tidal volume and breathing frequency (Ham et al., 2011). In other cases, deposition factors have been calculated with specific values for different groups of age for tidal volume, breathing frequency, functional residual volume and volume of the upper respiratory tract, but all those parameters are considered constant for the different activities (Sarigiannis et al., 2015; Winter-Sorkina and Cassee, 2002). The overall results show that the most sensible parameters that define the part of the tract where particles deposit are the particle size and the breathing rate. Therefore the consideration of different breathing rates according to pattern activities enhances the particle deposition assessment. FRC and URT could also be a source of variability for the DFs. Increases close to 65% of FRC could lead to decreases as far as 25% in pulmonary DFs, while increases of 40% URT could trigger decreases from 3-12% in the different parts of the respiratory system (Winter-Sorkina and Cassee, 2002).

### *3.3. Deposited doses of PM in the HRT*

Fig. 2 shows the estimated PM mass deposited in the different parts of the respiratory system (head/throat (Head), pulmonary/tracheobronchial (TB), and pulmonary/alveolar (P)) for children, adults, and retired people in the two periods (winter and summer) assessed. Notable differences could be noticed between summer and winter periods which were in accordance with the different outdoor PM concentrations measured in the area of study in TB region were nearly 15 and 12 times higher for children both periods and subsequently used to evaluate indoor concentrations. The accumulated doses of the three sizes of PM evaluated were mainly located in the head/throat part of the respiratory tract, being the values higher for the retired people followed by adults and children, respectively. The higher deposited doses of $PM_{10\text{-}2.5}$ in the head part of retired people were related to the high contribution (78%) of the light outdoor activities since they spend a high amount of time experiencing a high breathing rate in outdoor environments (in comparison with adults, that showed similar deposition fractions for the same activities and equal TV). For all three cohorts more than 80% of the $PM_{10\text{-}2.5}$ deposited dose in the head region were due to outdoor activities. In the case of children, this percentage increases till 90%, being in this case 80% of the dose attributable to heavy intensity activities. It has to be highlighted that as it can be observed in Fig. 2 children were reported as the group with the highest $PM_{10\text{-}2.5}$ dose deposited in the TB pulmonary region (being deposition winter values 16.8, 1.2, and 1.4 µg/day for children, adults, and retired, respectively). These means that deposited concentrations of $PM_{10\text{-}2.5}$ in than for

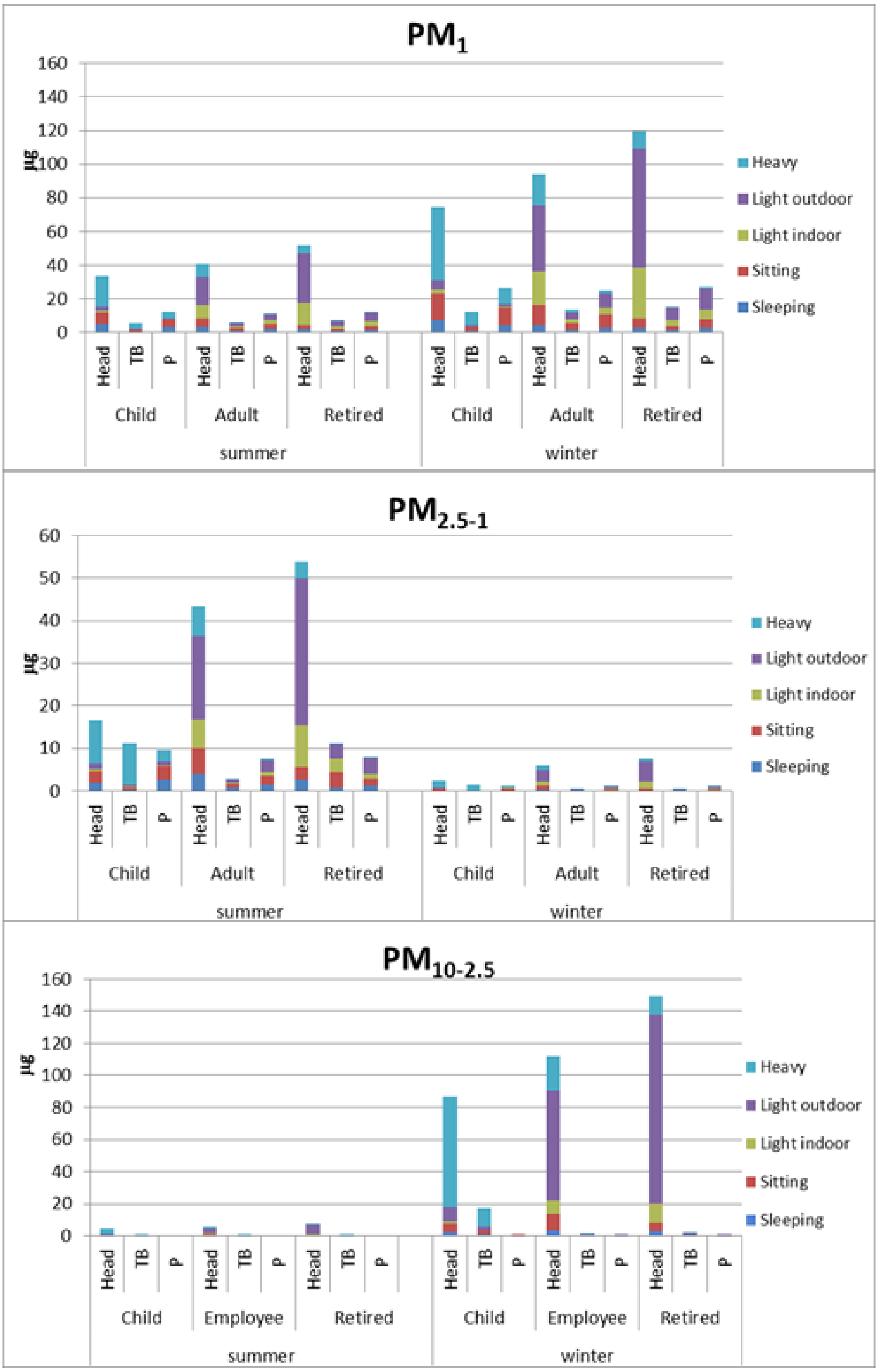

**Fig. 2.** Estimated PM deposited doses per day accumulated in the in the head, tracheobronchial (TB), and pulmonary/alveolar (P) regions of the human respiratory system.

adults and retired respectively. Regarding the amount of $PM_{2.5-1}$ deposited, it was higher in the P than in the TB area for the three groups evaluated. In the P region, children were the group with the highest amount of $PM_{2.5-1}$ deposited. As regards $PM_{2.5-1,}$ deposited in TB region was almost the same for adults, retired, and children. With respect to $PM_1$, similar accumulated values were calculated in the TB and P regions for adults, retired, and children, respectively. Maximum and minimum deposition doses followed the same trend than average values regarding population groups (retired>adults>children) and respiratory tract regions (head>TB>P) (Table 4). Higher variations were calculated in summer, when deposited mass could be close to six times higher than average values ($PM_{10-2.5}$), being in agreement with outdoor PM ranges. Apart from variations coming from the range of outdoor PM, some variability in results could be obtained depending on the assumptions made for the rest of inputs. In the present study we assumed the same activity pattern for summer and winter, since it was taken from studies based on annual data. However, activity patterns could be very different between these two seasons. Furthermore, ranges of FRC and UTR for the three population groups were not taken into consideration. Therefore, different results are expected when assessing the variability of all these parameters, being necessary future analyses in this field.

**Table 4**: Minimum, mean, and maximum calculated PM deposited doses for the totality of the respiratory tract

| | | **winter** | | | **summer** | | |
|---|---|---|---|---|---|---|---|
| | | **min** | **mean** | **max** | **min** | **mean** | **max** |
| **$PM_1$** | Child | 94.1 | 114 | 151 | 34.2 | 51.6 | 77.9 |
| | Adult Employee | 102 | 132 | 176 | 38.8 | 58.2 | 88.2 |
| | Retired | 114 | 162 | 208 | 45.5 | 70.7 | 103.6 |
| **$PM_{2.5-1}$** | Child | 2.01 | 5.07 | 10.1 | 0.00 | 37.5 | 75.0 |
| | Adult Employee | 2.88 | 7.27 | 14.4 | 0.00 | 53.7 | 107 |
| | Retired | 3.44 | 9.00 | 17.2 | 0.00 | 72.9 | 126 |
| **$PM_{10-2.5}$** | Child | 57.0 | 104 | 161 | 0.00 | 5.39 | 31.8 |
| | Adult Employee | 59.2 | 113 | 173 | 0.00 | 5.88 | 34.3 |
| | Retired | 72.3 | 151 | 218 | 0.00 | 7.75 | 39.5 |

Although we did not find any reference relating deposited doses and health problems, it is possible to have a preliminary idea of the effects by comparing our levels of outdoor concentrations with those limits established by the World Health Organization (WHO, 2005). According to this organization, mean annual guidelines for outdoor $PM_{10}$ and $PM_{2.5}$ are respectively 20 and 10 µg/$m^3$. These values are surpassed in both periods, meaning that some kind of long term adverse effects are expected. Since in our simulations most of the PM mass is deposited in the head region, diseases such as rhinitis, pharyngitis or sinusitis are the most likely (Vincent, 2005). Furthermore, due to the higher deposition mass of coarse PM in TB region in children, it is also expected a higher impact of asthma in this population group.

## 4. Conclusions

Human health risk assessment may be improved by a better knowledge of the total exposure. Integration of outdoor and indoor microenvironments concentrations and activity patterns can help to improve the information about real exposure. This approach however implies the availability of the reliable data for specific case studies. In this study, we implemented an indoor ambient model and a dosimetry model to evaluate the exposure to $PM_{10\text{-}2.5}$, $PM_{2.5\text{-}1}$ and $PM_1$ for the population living in the surroundings of a cement plant in Barcelona (Spain). The results of the IAQX model showed that $PM_1$ was the fraction with the highest indoor levels, at home and workplace, as a result of their higher infiltration factors and lower deposition rates. The indoor PM concentrations were in consonance with the outdoor concentrations, as well as the infiltration factors, which are higher in summer when windows are opened a higher percentage of time. It should be taken into account that we did not consider any emission from indoor sources which some studies point out that may be significant in some cases due to the activities of the inhabitants of the house, however they are still difficult to quantify. The results of the MPPD2.11 dosimetry model showed the different behaviour of the particles of different size in the human respiratory tract. Results showed that the activity pattern and physiological parameters have high impact on the deposited particles concentration in the human respiratory tract and the areas affected depending on their size. Age also plays important factor in the deposited dose as for all the three particle sizes, retired people have recorded higher doses. This fact was notably related to the activity pattern of retired people which spend significant amount of time in the light outdoor activities. For children, the exposure was mainly influenced by the time they spend outdoor doing heavy exercises. Results show that fine particles ($PM_{2.5\text{-}1}$ and $PM_1$) were more accumulated in the pulmonary regions (P and TB) of retired people and children which are more vulnerable groups of population. Particularly children are considered a risk group to environmental pollution since their immune system and lungs are not fully developed while old people are also more susceptible to respiratory disorders.

The integrated model showed to be suitable to evaluate the PM exposure and deposited doses in the different parts of the lung considering specific data for different exposure groups. However, for the two evaluated periods, high variability was reported in the deposited PM doses in the different parts of the lung, as result of the different outdoor PM concentrations considered. Ambient PM concentrations are very variable according to daily circumstances such as sources and meteorological conditions. The influence of the cement plant in ambient PM was noted in previous studies (Sánchez-Soberón et al., 2015), but contribution from this facility have not been quantified yet. However, the assessment here described could be used as a worst case scenario for the cement facility. Therefore, an extensive PM monitoring campaign in the area under study will be carried out. This will give us more accurately results that will help in the model validation, reduce uncertainty about the actual risk to the population, and clarify the contribution from cement plant to different health effects.

*Acknowledgments*

Financial support was received by the Spanish Ministry of Economy and Competitiveness (MINECO), through the project CTM2012-32778. F. Sánchez-Soberón received a doctoral scholarship as part of the project above mentioned. We also want to thank the European Union Seventh Framework Programme for the funding received through the HEALS project FP7-ENV-2013-603946. The authors also want to thank Quentin Aiello for his collaboration through the investigation.

## References

Abt, E., Suh, H., Catalano, P., Koutrakis, P., 2000. Relative contribution of outdoor and indoor particle sources to indoor concentrations. Env. Sci Technol 34, 3579–3587.

ARA, 2014. ARA :: Products :: MPPD [WWW Document]. URL http://www.ara.com/products/mppd.htm (accessed 8.24.15).

Behera, S., Betha, R., Huang, X., Balasubramanian, R., 2015. Characterization and estimation of human airway deposition of size-resolved particulate-bound trace elements during a recent haze episode in Southeast Asia. Environ. Sci. Pollut. Res. 22, 4265–4280. doi:10.1007/s11356-014-3645-6

Brown, J.S., Gordon, T., Price, O., Ashagarian, B., 2013. Thoracic and respirable particle definitions for human health risk assessment. Part. Fibre Toxicol. 10, 1-12. doi: 10.1186/1743-8977-10-12

Carrascosa, A., Fernández, J.M., Fernández, C., Ferrández, A., Longás, López-Siguero, J.P., Sánchez, E., Sobradillo, B., Yeste, F., 2008. Estudio transversal español de crecimiento 2008. Parte II: valores de talla, peso e índice de masa corporal desde el nacimiento a la talla adulta . An. Pediatría 68, 552–569.

Chen, C., Zhao, B., 2011. Review of relationship between indoor and outdoor particles: I/O ratio, infiltration factor and penetration factor. Atmos. Environ. 45, 275–288. doi:http://dx.doi.org/10.1016/j.atmosenv.2010.09.048

Cheng, K.-C., Goebes, M.D., Hildemann, L.M., 2010. Association of size-resolved airborne particles with foot traffic inside a carpeted hallway. Atmos. Environ. 44, 2062–2066. doi:http://dx.doi.org/10.1016/j.atmosenv.2010.02.027

Cohen Hubal, E.A., Sheldon, L.S., Burke, J.M., McCurdy, T.R., Berry, M.R., Rigas, M.L., Zartarian, V.G., Freeman, N.C., 2000. Children’s exposure assessment: a review of factors influencing Children's exposure, and the data available to characterize and assess that exposure. Environ. Health Perspect. 108, 475–486.

Dimitroulopoulou, C., Bartzis, J., 2014. Ventilation rates in European office buildings: A review . Indoor Built Environ. 23, 5–25.

Fantke, P., Jolliet, O., Evans, J.S., Apte, J.S., Cohen, A.J., Hänninen, O.O., Hurley, F., Jantunen, M.J., Jerrett, M., Levy, J.I., Loh, M.M., Marshall, J.D., Miller, B.G., Preiss, P., Spadaro, J. V., Tainio, M., Tuomisto, J.T., Weschler, C.J., McKone, T.E., 2015. Health effects of fine particulate matter in life cycle impact assessment: findings from the Basel Guidance Workshop. Int. J. Life Cycle Assess. 20, 276–288. doi:10.1007/s11367-014-0822-2

Ferro, A.R., Kopperud, R.J., Hildemann, L.M., 2004. Source Strengths for Indoor Human Activities that Resuspend Particulate Matter. Environ. Sci. Technol. 38, 1759–1764. doi:10.1021/es0263893

Ham, W.A., Ruehl, C.R., Kleeman, M.J., 2011. Seasonal Variation of Airborne Particle Deposition Efficiency in the Human Respiratory System. Aerosol Sci. Technol. 45, 795–804.

Hänninen, O., Sorjamaa, R., Lipponen, P., Cyrys, J., Lanki, T., Pekkanen, J., 2013. Aerosol-based modelling of infiltration of ambient PM2.5 and evaluation against population-based measurements in homes in Helsinki, Finland. J. Aerosol Sci. 66, 111–122. doi:http://dx.doi.org/10.1016/j.jaerosci.2013.08.004

Hassanvand, M.S., Naddafi, K., Faridi, S., Arhami, M., Nabizadeh, R., Sowlat, M.H., Pourpak, Z., Rastkari, N., Momeniha, F., Kashani, H., Gholampour, A., Nazmara, S., Alimohammadi, M., Goudarzi, G., Yunesian, M., 2014. Indoor/outdoor relationships of PM10, PM2.5, and PM1 mass concentrations and their water-soluble ions in a retirement home and a school dormitory. Atmos. Environ. 82, 375–382. doi:http://dx.doi.org/10.1016/j.atmosenv.2013.10.048

Hoek, G., Kos, G., Harrison, R., de Hartog, J., Meliefste, K., ten Brink, H., Katsouyanni, K., Karakatsani, A., Lianou, M., Kotronarou, A., Kavouras, I., Pekkanen, J., Vallius, M., Kulmala, M., Puustinen, A., Thomas, S., Meddings, C., Ayres, J., van Wijnen, J., Hameri, K., 2008. Indoor-outdoor relationships of particle number and mass in four European cities. Atmos. Environ. 42, 156–169.

Hussein, T., Wierzbicka, A., Löndahl, J., Lazaridis, M., Hänninen, O., 2015. Indoor aerosol modeling for assessment of exposure and respiratory tract deposited dose. Atmos. Environ. 106, 402–411. doi:http://dx.doi.org/10.1016/j.atmosenv.2014.07.034

ICRP, 1994. Human respiratory tract model for radiological protection: a report of a task group of the International Commission on Radiological Protection. Ann ICRP 24, 1–482.

IEC, 2012. Enquesta de l'ús del temps 2010-2011 : principals resultats. – (Estadística Social). Institut d'Estadística de Catalunya.

INE, 2012. Índice de masa corporal por grupos de edad. 2011-2012. Inst. Nac. estadística. Available http//www.ine.es/jaxi/tabla.do?type=pcaxis&path=/t00/mujeres_hombres/tablas_1/l0/&file=d06001.px.

INSEE, 2010. Conditions de vie-Société - Depuis 11 ans, moins de tâches ménagères, plus d'Internet. Insee. Available at: http://www.insee.fr/fr/themes/document.asp?ref_id=ip1377.

Kelly, F.J., Fussell, J.C., 2012. Size, source and chemical composition as determinants of toxicity attributable to ambient particulate matter. Atmos. Environ. 60, 504–526. doi:10.1016/j.atmosenv.2012.06.039

Kim, K.H., Kabir, E., Kabir, S., 2015. A review on the human health impact of airborne particulate matter. Environ. Int. 74, 136–143.

Korhonen, P., Kokotti, H., Kalliokoski, P., 2000. Survey and mitigation of occupational exposure of radon in workplaces. Build. Environ. 35, 555–562. doi:10.1016/S0360-1323(99)00048-7

Li, X., Yan, C., Patterson, R.F., Zhu, Y., Yao, X., Zhu, Y., Ma, S., Qiu, X., Zhu, T., Zheng, M., 2015. Modeled Deposition of Fine Particles in Human Airway in Beijing, China. Atmos. Environ. doi:10.1016/j.atmosenv.2015.06.045

Marcon, A., Pesce, G., Girardi, P., Marchetti, P., Blengio, G., de Zolt Sappadina, S., Falcone, S., Frapporti, G., Predicatori, F., de Marco, R., 2014. Association between PM10 concentrations and school absences in proximity of a cement plant in northern Italy. Int. J. Hyg. Environ. Health 217, 386–391. doi:10.1016/j.ijheh.2013.07.016

McGrath, J.A., Byrne, M.A., Ashmore, M.R., Terry, A.C., Dimitroulopoulou, C., 2014. Development of a probabilistic multi-zone multi-source computational model and demonstration of its applications in predicting PM concentrations indoors. Sci. Total Environ. 490, 798–806. doi:http://dx.doi.org/10.1016/j.scitotenv.2014.05.081

Monn, C., 2001. Exposure assessment of air pollutants: a review on spatial heterogeneity and indoor/outdoor/personal exposure to suspended particulate matter, nitrogen dioxide and ozone. Atmos. Environ. 35, 1–32. doi:10.1016/S1352-2310(00)00330-7

Nazaroff, W.W., Cass, G.R., 1989. Mathematical modeling of indoor aerosol dynamics. Environ. Sci. Technol. 23, 157–166. doi:10.1021/es00179a003

Orosa, J.A., Baaliña, A., 2008. Passive climate control in Spanish office buildings for long periods of time. Build. Environ. 43, 2005–2012. doi:http://dx.doi.org/10.1016/j.buildenv.2007.12.001

Patterson, R.F., Zhang, Q., Zheng, M., Yifang, Z., 2014. Particle Deposition in Respiratory Tracts of School-Aged Children. Aerosol Air Qual. Res. 14, 64–73.

Patton, A.P., Perkins, J., Zamore, W., Levy, J.I., Brugge, D., Durant, J.L., 2014. Spatial and temporal differences in traffic-related air pollution in three urban neighborhoods near an interstate highway. Atmos. Environ. 99, 309–321. doi:http://dx.doi.org/10.1016/j.atmosenv.2014.09.072

Pey, J., Pérez, N., Querol, X., Alastuey, A., Cusack, M., Reche, C., 2010. Intense winter atmospheric pollution episodes affecting the Western Mediterranean. Sci. Total Environ. 408, 1951–1959. doi:10.1016/j.scitotenv.2010.01.052

Querol, X., Alastuey, A., Pandolfi, M., Reche, C., Pérez, N., Minguillón, M.C., Moreno, T., Viana, M., Escudero, M., Orio, A., Pallarés, M., Reina, F., 2014. 2001-2012 trends on air quality in Spain. Sci. Total Environ. 490, 957–969.

Rovira, J., Mari, M., Schuhmacher, M., Nadal, M., Domingo, J.L., 2011. Monitoring environmental pollutants in the vicinity of a cement plant: a temporal study. Arch. Environ. Contam. Toxicol. 60, 372–384. doi:10.1007/s00244-010-9628-9

Rovira, J., Nadal, M., Schuhmacher, M., Domingo, J.L., 2014. Environmental levels of PCDD/Fs and metals around a cement plant in Catalonia, Spain, before and after alternative fuel implementation. Assessment of human health risks. Sci. Total Environ. 485-486, 121–129. doi:10.1016/j.scitotenv.2014.03.061

Saber, E.M., Heydari, G., 2012. Flow patterns and deposition fraction of particles in the range of 0.1–10&#xa0;µm at trachea and the first third generations under different breathing conditions. Comput. Biol. Med. 42, 631–638. doi:http://dx.doi.org/10.1016/j.compbiomed.2012.03.002

Salma, I., Füri, P., Németh, Z., Balásházy, I., Hofmann, W., Farkas, Á., 2015. Lung burden and deposition distribution of inhaled atmospheric urban ultrafine particles as the first step in their health risk assessment. Atmos. Environ. 104, 39–49. doi:10.1016/j.atmosenv.2014.12.060

Sánchez-Soberón, F., Rovira, J., Mari, M., Sierra, J., Nadal, M., Domingo, J.L., Schuhmacher, M., 2015. Main components and human health risks assessment of PM10, PM2.5, and PM1 in two areas influenced by cement plants. Atmos. Environ. in press.

Sarigiannis, D.A., Karakitsios, S.P., Kermenidou, M., Nikolaki, S., Zikopoulos, D., Semelidis, S., Papagiannakis, A., Tzimou, R., 2014. Total exposure to airborne particulate matter in cities: the effect of biomass combustion. Sci. Total Environ. 493, 795–805. doi:10.1016/j.scitotenv.2014.06.055

Sarigiannis, D.A., Karakitsios, S.P., Zikopoulos, D., Nikolaki, S., Kermenidou, M., 2015. Lung cancer risk from PAHs emitted from biomass combustion. Environ. Res. 137, 147–156. doi:10.1016/j.envres.2014.12.009

Schweizer, C., Edwards, R.D., Bayer-Oglesby, L., Gauderman, W.J., Ilacqua, V., Jantunen, M.J., Lai, H.K., Nieuwenhuijsen, M., Künzli, N., 2007. Indoor time–microenvironment–activity patterns in seven regions of Europe. J. Expo. Sci. Environ. Epidemiol. 17, 170–181.

Stocks, J., Quanjer, P.H., 1995. Reference values for residual volume, functional residual capacity and total lung capacity. ATS Workshop on Lung Volume Measurements. Official Statement of The European Respiratory Society. Eur Respir J 8, 492–506.

US EPA, 2011. Exposure Factors Handbook: 2011 Edition, National Centre of Environmenatl Assessment, U.S. Environmental Protection Agency, Washington, D.C., U.S.A. Sept. 2011.

US EPA, 2000a. Indoor Air Quality Modeling. IAQX v1.1 can be downloaded at: http://www.epa.gov/nrmrl/appcd/mmd/iaq.html.

US EPA, 2000b. Indoor Air Quality Modeling [WWW Document]. URL http://www.epa.gov/nrmrl/appcd/mmd/iaq.html (accessed 10.13.14).

Vincent, J.H., 2005. Health-related aerosol measurement: a review of existing sampling criteria and proposals for new ones. J. Environ. Monit. 7, 1037–1053.

Wallace, L., Emmerich, S., Howard-Reed, C., 2002. Continuous measurements of air change rates in an occupied house for 1 year: the effect of temperature, wind, fans, and windows. J Expo Anal Env. Epidemiol 12, 296–306.

Wang, J., Smedje, G., Nordquist, T., Norbäck, D., 2015. Personal and demographic factors and change of subjective indoor air quality reported by school children in relation to exposure at Swedish schools: A 2-year longitudinal study. Sci. Total Environ. 508, 288–296.

Watson, A.Y., Bates, R.R., Kennedy, D., 1988. Biological Disposition of Airborne Particles: Basic Principles and Application to Vehicular Emissions, in: Air Pollution, the Automobile, and Public Health. National Academies Press (US), Washington (DC).

WHO, 2013. Health effects of Particulate Matter. Policy implications for countries in eastern Europe, Caucasus and central Asia.

WHO, 2005. Air quality guidelines - global update 2005. World Health Organization.

Wilkinson, K.E., Lundkvist, J., Netrval, J., Eriksson, M., Seisenbaeva, G.A., Kessler, V.G., 2013. Space and time resolved monitoring of airborne particulate matter in proximity of a traffic roundabout in Sweden. Environ. Pollut. 182, 364–370. doi:http://dx.doi.org/10.1016/j.envpol.2013.07.043

Winter-Sorkina, R., Cassee, F.R., 2002. From concentration to dose: factors influencing airborne particulate matter deposition in humans and rats. RIVM Rep. 650010031/2002.

Yeh, H.-C., Schum, G.M., 1980. Models of human lung airways and their application to inhaled particle deposition. Bull. Math. Biol. 42, 461–480. doi:10.1007/bf02460796

# CHAPTER 5: Source apportionment of inorganic and organic PM in the ambient air around a cement plant: assessment of complementary tools

Montse Mari, Francisco Sánchez-Soberón, Carme Audí-Miró, Barend L. van Drooge, Albert Soler, Joan O. Grimalt, Marta Schuhmacher (2016). Aerosol and Air Quality Research 16 (12) 3230-3242.

# Source apportionment of inorganic and organic PM in the ambient air around a cement plant: assessment of complementary tools

Montse Mari, Francisco Sánchez-Soberón, Carme Audí-Miró, Barend L. van Drooge, Albert Soler, Joan O. Grimalt, Marta Schuhmacher (2016). Aerosol and Air Quality Research 16 (12) 3230-3242

Abstract:

In this study, we analyzed the sources of ambient PM inorganic and organic components near a cement plant using fossil fuels as well as alternative fuels, such as sewage sludge and biomass. Source apportionment methodologies, i.e., principal component analysis (PCA) and multivariate curve resolution by alternating least squares (MCR-ALS), and carbon isotope analysis ($\delta^{13}C$) were used to determine the potential sources and their contributions. Four sources of $PM_{10}$ main tracer compounds constituents were identified: marine and secondary inorganic aerosol, cement plant/industrial, traffic and crustal. The contributions of those sources varied significantly depending on the period of the year. However, the inorganic tracer PM species in the area were mainly released by combustion sources, namely traffic and the activity of the cement plant, especially in winter months. The analyses of tracer organic compounds also indicated combustion sources, i.e., biomass burning and fossil fuel combustion, as the predominant contributors to ambient air PM (62, 59 and 69%, in $PM_{10}$, $PM_{2.5}$ and $PM_1$, respectively). Organic dust was a significant source of $PM_{10}$ (33%) while its contribution was found to be minor in the finest fractions (9 and 2% in $PM_{2.5}$ and $PM_1$, respectively). Results of $\delta^{13}C$ corroborated a significant contribution of combustion sources, traffic or biomass fuel as well as a higher influence of mineral (calcite) powder in larger particles.

***Keywords:*** Particulate Matter, Cement plant, Principal Component Analysis (PCA), Multivariate curve resolution by alternating least squares (MCR-ALS), Carbon isotopes

## Introduction

Cement production is associated with the emission of a wide range of pollutants including gases (i.e., $NO_x$, $SO_x$, HF, HCl) and particle-bound pollutants such as metals (i.e., As, Cd, Pb, etc.) or organic compounds, (i.e., polycyclic aromatic hydrocarbons (PAHs), etc.). The emissions of particulate matter (PM) generates most of the noticeable impact and concern in the surroundings of cement plants and takes place at different points along the cement manufacturing process (quarrying of raw materials, packing of the product, combustion process, vehicle movements, etc.) (Marcon *et al.*, 2014). PM source apportionment of a cement plant becomes complex when this installation is located in the vicinity of other industrial and urban areas that have additional sources, such as traffic and power generation (Karagulian *et al.*, 2015). PM is associated with many health effects that include asthma, pulmonary injury, cardiorespiratory diseases and recently it was nominated as Group I carcinogen by the International Agency for Research on Cancer (IARC) (Hamra *et al.*, 2014). It is known that the size of particles plays a key role on determining their potential of being harmful. Due to the evidence of those adverse effects, in Europe the ambient air quality Directive (2008/50/EC) sets limits for particulate matter with aerodynamic diameter smaller than 10 and 2.5 µm (known as $PM_{10}$ and $PM_{2.5}$ respectively). Levels for smaller particles are not legislated yet, although it is known that the smaller particles, especially ultrafine particles (those with a diameter smaller than 100 nm), are the most hazardous ones since they may penetrate deeper into the lungs and eventually into the blood stream (Kelly and Fussell, 2012). Notwithstanding, PM-induced adverse health effects are linked to their chemical composition, particularly to trace metals and toxic organic compounds. However, data on PM composition is still limited for the smallest PM fractions (Tsai *et al.*, 2015).

Composition and levels of PM can vary dramatically among locations depending on the source emission strength as well as meteorological conditions and local topography. Nevertheless, in order to control levels to safeguard health and minimize environmental damage, it is necessary to determine the contribution of the different sources. Receptor models (RM) have been extensively used to apportion PM sources based on concentrations determined at monitoring sites (Karagulian *et al.*, 2015). The fundamental principle of receptor modelling is that mass and species conservation can be assumed and therefore a mass balance analysis can be used to identify and apportion sources of airborne PM in the atmosphere (Viana *et al.*, 2008b). Diverse RMs have been widely described (Belis *et al.*, 2013). Briefly, they can be classified as: 1) Chemical Mass Balance (CMB) models that require an input information of the emission profiles of the sources to identity their contributions to each sample, and 2) Multivariate Models (that include Principal Component Analysis (PCA), Multivariate Curve Resolution (MCR) and Positive Matrix Factorization (PMF)) that are able to identify the number of sources and the associated profiles of the sources based on marker species (Shi *et al.*, 2014). Other tools such as enrichment factors (EF) and diagnostic ratios (DR) may help to identify pollutant sources, however they are not able to reconstruct the sources contribution of the PM collected in a sampling site (Galarneau, 2008; Hernández-Mena *et al.*, 2011; Banerjee *et al.*, 2015). The DR consists on comparing the ratio of marker species in source profiles with those from ambient samples in order to identify the most important sources in a region (Robinson *et al.*, 2006). On the other hand, the EF compares the ratios of the atmospheric concentrations of various elements with the corresponding ratios in geological material to determine if a certain element has natural or anthropogenic origin (Enamorado-Báez *et al.*, 2015). Different authors have recently reviewed the use of receptor models to analyze the sources of PM and its organic fractions in Europe (Viana *et al.*, 2008a; Belis *et al.*, 2013; Karagulian *et al.*, 2015). They encourage the use of advanced factor analysis techniques that are able to deal with heterogeneous and complex data. In turn, they also note the common limitations in such type of analyses including the lack of markers for some sources, components or factors that may represent mixtures of emission sources, or source signatures that change with time. Another critical drawback is that a large number of samples are required for such kind of studies because although levels of $PM_{10}$ and $PM_{2.5}$ are currently widely monitored, their characterization is still limited due to the high cost that entails their chemical characterization. Thus, the combination of different types of receptor models is proposed to solve the limitations of each of the current models, by constructing a more robust solution based on their strengths (Viana *et al.*, 2008a; Zeng *et al.*, 2010). In turn, there are new tools such as stable isotopic analysis, that have been rarely used in receptor model studies and can also be used as complementary source identification technique (Pieri *et al.*, 2013).

In previous studies we evaluated the levels and composition, regarding inorganic and organic species of $PM_{10}$, $PM_{2.5}$ and $PM_1$ around a cement plant located in Barcelona (Sánchez-Soberón *et al.*, 2015; 2016). The objectives of the present study were: 1) to establish the most significant sources of PM in the area of study by applying PCA, MCR and isotopic analyses; and, at the same time, 2) to evaluate how these three methodologies can complement each other especially when dealing with relatively small data sets.

## Methods

### *Receptor Models*

*Principal Component Analysis (PCA)*

Principal component analysis (PCA) is a widely known technique of multivariate analysis that has been largely used for the identification of the potential sources of pollutants in the environment (Viana *et al.*, 2008a; Contini *et al.*, 2010; Mari *et al.*, 2010;

Contini *et al.*, 2012; Engelbrecht and Jayanty, 2013). The objective of a PCA is to derive principle components (PCs) as a linear combination of the original variables, which provides a description of the data structure with a minimum loss of information. These PCs are a set of orthogonal variables that best span the data variances in a way that they reflect the patterns of the correlations among the pooled initial variables (Zou *et al.*, 2015). In order to equally weight the data variance it is important to use an appropriate data pretreatment.

In this study, PCA was performed using XLStat software. The Pearson correlation was used in order to homogenize the variances of the data. Varimax rotation was used to maximize the sum of the variances of the squared loadings.

### *Multivariate Curve Resolution by Alternating Least Squares (MCR-ALS)*

Multivariate Curve Resolution– Alternating Least Squares method is similar to PCA (Jaumot *et al.*, 2005), basically, the main difference between PCA and MCR is that the latter method is based on the application of more natural constraints like non-negativity instead of the orthogonality constraints that are fixed in PCA. The variance explained by the different components is not orthogonal (non-overlapped) as in PCA (Jolliffe, 2002). Natural sources in the environment are rarely orthogonal; thus the MCR methods may have a physically sounder interpretation than orthogonal database decomposition methods. MCR-ALS was introduced for the first time as a multivariate analysis tool for PM source apportionment by Tauler *et al.* (2009) and has successfully been applied for environmental source apportionment (Terrado *et al.*, 2009) including organics in urban ambient air PM (Alier *et al.*, 2013; Elorduy *et al.*, 2016).

In our study, the MATLAB MCR-ALS toolbox interface was used for the analysis in order to obtain the loadings and scores of the components (Jaumot *et al.*, 2005). Individual concentrations were divided by the standard deviation of the variable in order to homogenize the variance. The component scores (potential sources) were used to regression analyses with respect to the PM mass concentrations to quantify the daily contributions of each of the identified sources.

### *Isotopic Analysis*

Stable isotope analysis is a tool capable of tracing the sources of atmospheric particles in urban air by comparing the carbon isotopic composition ($\delta^{13}C$) of ambient samples with those characteristic of potential sources (Widory *et al.*, 2004; Gorka and Jedrysek, 2008; Puig *et al.*, 2008; López-Veneroni, 2009). Carbon isotopic ($\delta^{13}C$) signature of total carbon in particulate matter can provide information about its origin as long as two premises are fulfilled: 1) the different potential sources have different carbon isotopic composition; 2) the carbon isotopic signature of the potential sources remain almost constant or vary in a known proportion throughout the processes they experience in the air (Boutton, 1991). The stable isotope composition of an element is expressed in delta (δ) notation, which is given in per mil (‰) units. For carbon, $\delta^{13}C$ is calculated as following:

$$\delta^{13}\mathrm{C}\ (‰) = \left[\left({}^{13}\mathrm{C}/{}^{12}\mathrm{C}\right)_{\mathrm{sample}} / \left({}^{13}\mathrm{C}/{}^{12}\mathrm{C}\right)_{\mathrm{standard}} - 1\right] \times 1000 \qquad (1)$$

where the carbon standard is a belemnite fossil (*Belemnitella americana*) from the Peedee Cretacic formation (North Carolina, United States), abbreviated as VPDB. Many authors have analyzed the carbon isotopic composition of the total carbon of ambient samples to discriminate the source of atmospheric particles by comparing the carbon isotopic composition of ambient samples with those of potential sources. The initial studies distinguished anthropogenic from natural particulate carbon emissions (Cheselet *et al.*, 1981; Cachier *et al.*, 1985). Later, Widory *et al.* (2004) differentiated between road traffic and industrial particle sources, and between diesel, fuel oil and several sources using both carbon and lead isotopes. Recently, Mkoma *et al.* (2014) studied the contribution of the burning of C3 and C4 plant species to the aerosols. Unlike PCA and MCR, isotopic analysis is a non-statistical fingerprinting technique and therefore only a few samples are required for the interpretation of the data.

### *Data Sets and Chemical Compounds Analyzed*

Chemical tracer compounds were previously determined in ambient air $PM_{10}$, $PM_{2.5}$ and $PM_1$ samples collected at a cement plant located in the surroundings of Barcelona (Sánchez-Soberón *et al.*, 2015; 2016). Details on the study area as well as on the sampling and analysis methodologies of major, inorganic and organic elements were previously described (Sánchez-Soberón *et al.*, 2015; 2016). In brief, 24-h samples were collected in quartz fibre filters (QFF) with high-volume active samplers. The studied facility is located within an urban area affected by a number of different industries. Moreover, two highways with heavy traffic cross the settlement. Fig. S1 of the study area is shown in the Supplementary Material. The plant has an annual production close to 1 million of cement tons and alternative fuels (they are authorized to use sewage sludge, meat and bone meal, refuse derived fuels and biomass) supply 20% of the total energy consumed. The first data set was composed by 23 variables, including the concentrations of 19 metals and metaloids (Al, As, Ca, Cd, Ce, Co, Cr, Cu, Fe, K, Li, Mn, Ni, Pb, Sb, Sn, Sr, Ti, V), OC + EC (Organic and Elemental Carbon) and 3 anions ($Cl^-$, $SO_4^{2-}$, $NO_3^-$) of 34 $PM_{10}$ samples that were collected in 4 different periods of time (October and December 2013, July and November-December 2014). The second data set consisted of 13 PAHs (phenanthrene, retene, fluoranthene, pyrene, benzo[a]anthracene, chrysene, benzo[b+j]fluoranthene, benzo[k]fluoranthene, benzo[e]pyrene, benzo[a]pyrene, inde[123cd]pyrene, benzo[ghi]perylene and coronene), 11 organic tracer compounds (2 hopanes (17(H)α-21(H)β-29-norhopane and 17(H)α-21(H)β-hopane), 4 organic biomass combustion products (galactosan, mannosan, levoglucosan, dehydrabietic acid), 3 saccharides and derivates (α-glucose, β-glucose, manitol) and 2 dicarboxylic acids (succinic acid, glutaric acid)), determined in $PM_{10}$, $PM_{2.5}$ and $PM_1$ samples (8 samples per mass fraction) collected in December 2014. Simultaneous data of inorganic and organic species was only available for 4 days in December 2014.

Apart from the chemical compounds described above, carbon isotopic composition was also measured in the $PM_{10}$, $PM_{2.5}$ and $PM_1$ samples collected in November-December 2014. For that purpose a piece of approximately 1 $cm^2$ of all the quartz filters containing the particulate matter of each different size was cut off. The filter piece was folded using a pair of flat tipped tweezers, placed into a tin cube together with vanadium pentoxide as a catalyser to achieve complete combustion. The tin cubes containing the samples were then analysed for their carbon isotopic composition using an Isotope Ratio Mass Spectrometer (Delta C Finnigan MAT) with an Elemental Analyser Carlo Erba Flash 1112 and an interface Conflo III (Finnigan MAT). Isotope data was reported as $\delta^{13}C$ values. A database with $\delta^{13}C$ values of the potential sources in the area was constructed and is shown in Fig. 1, comprising: 1) Mineral fraction sources, including cement and kiln dust, and street dust; 2) Combusted Biomass fuels from C3 plants; 3) Combusted fossil fuels; 4) Combusted sewage sludge; 5) Traffic sources; 6) Deposited particles on a Petri dish in the school sampling point. For street dust as well as from 2 to 4 sources, carbon isotopic fingerprints were obtained from bibliography (more details are given in section 3.3). Isotopic fingerprints for cement, kiln dust, traffic and total particles were characterized in this study. Cement and kiln dust were obtained from the studied plant. Traffic samples were collected by placing a quartz fiber filter in the tailpipe of both, diesel and gasoline cars. Deposited particles were collected in a Petri dish left during five days in the sampling location. Values of $\delta^{13}C$ on those samples were obtained with the same method than the one described for the ambient samples.

## Result and discussion

Particles of different sizes are released during different steps of the cement manufacturing process. In this study, the sources of $PM_{10}$, $PM_{2.5}$ and $PM_1$ in the neighborhood of a cement plant were inferred by considering its content of inorganic and organic species by means of two receptor model methodologies, PCA and MCR. The results are discussed and compared below. In turn, the $\delta^{13}C$ of the total carbon present in ambient PM samples was compared to the carbon isotopic signature of potential sources.

### *Sources of Major and Inorganic Elements of PM*

Although major and inorganic elements were determined in three PM fractions ($PM_{10}$, $PM_{2.5}$ and $PM_1$) (Sánchez-Soberón *et al.*, 2015), in this case the PCA was only performed to the $PM_{10}$ fraction since a significant number of tracers were found below the detection limit in $PM_{2.5}$ and $PM_1$ (40 and 50%, respectively). For calculations, when a concentration was below the LOD, the value was assumed to be half of that limit (ND = 1/2 LOD). Four components were resolved in such a way that they could explain the major variance while the loadings could be interpreted as profiles of the potential sources in the area. Components were sorted according to the amount of explained variances. Hence, the 4-dimensional model explained 86% of the variance. The Kaiser-Meyer-Olkin coefficient was 0.718 (higher than 0.5) indicating a good performance of the PCA analysis. Subsequently, MCR analysis was performed and again four components were selected. In this case, the model explained 90% of the variance. Figs. 2 and 3(a)–3(d) present the factor loadings obtained by means of PCA and MCR, respectively. It can be observed that in spite of the different constraints considered by the two models, orthogonality and non-negativity, respectively, similar loading profiles were found in both cases. The interpretation of the four components for PCA and MCR was as follows:

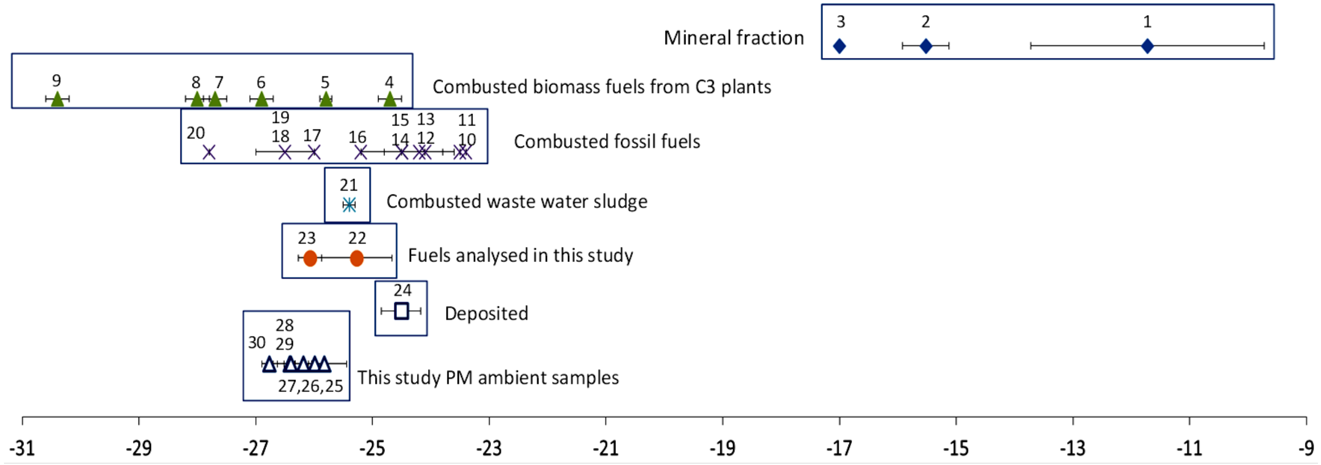

**Fig. 1.** $\delta^{13}C$ values of different sources, types of fuels and materials susceptible of being used as fuels together with $\delta^{13}C$ of the PM ambient samples. Error bars represent deviation between analytical duplicates. Description of each sample is listed in the supplementary material.

**C1: Cement plant/Industry.** This component was associated with two different emissions: mineral matter and combustion. PC1 showed high correlations with Al, Ca, Li and Ce. These elements, especially Al and Ca, are associated with crustal/mineral materials (Yatkin and Bayram, 2008; Belis *et al.*, 2013). They are characteristic not only of re-suspension of soil dust but also of mineral industries (ceramic or cement) as well as of quarries (Yatkin and Bayram, 2008). Therefore, the raw materials used in the cement plant located in the area may be responsible for the emissions of those elements. Correlations were observed between Ni and V which are typical tracers of fuel-oil/petcoke combustion (Viana *et al.*, 2008a). Those elements may be related to the cement plant activity together with other industrial activities in the same area (brick, plastics and packaging factories among others). The V/Ni ratio is normally within the range 0.5–2.0 at regional background air monitoring sites across Europe (Pey *et al.*, 2009; Moreno *et al.*, 2010). On the other hand, the ratio V/Ni from the combustion of refinery-produced materials may be highly variable, depending on the origin of the crude, and sometimes overlap with that from mineral dust (Moreno *et al.*, 2010). In our samples, the V/Ni value was higher than 2, being reasonable to associate the origin of those compounds in the area with petcoke and fuel oil combustion. In addition, K is an indicator of biomass combustion that could be correlated with the use of sewage sludge as alternative fuel in the cement plant as well.

**C2: Traffic**. This component was related to combustion processes and tire/break wear. PC2 is characterized by a high contribution of OC + EC (indicator of combustion processes) with a notable contribution of $NO_3^-$ that may derive from the oxidation of $NO_x$ emissions from traffic emissions. Regarding heavy metals, Cd is associated with the engine emissions of vehicles (Pey *et al.*, 2013), while As, Cu, Pb, Sb and Sn are associated with break wear (Belis *et al.*, 2013; Pey *et al.*, 2013).

**C3: Crustal.** This factor showed a high correlation with Mn and Fe (and Ti in the case of PCA). Those elements generally have a mineral origin and are generally correlated with other elements such as Al and Ca (Pey *et al.*, 2013). However, in our case, Al and Ca appeared more associated with the activity of the cement plant (component 1), that also entails the use of mineral materials. In any case, the EF values for Mn and Fe were < 5, indicating a geological origin (Hernández-Mena *et al.*, 2011).

**C4: Marine and Regional Secondary Inorganic Aerosol (SIA).** This component was characterized by $Cl^-$ and $SO_4^{2-}$, which suggests the contribution of marine aerosols. Regarding $SO_4^{2-}$, its origin is secondary aerosol (Viana *et al.*, 2008a). Since $SO_4^{2-}$ is related to $Cl^-$, and the plant is located at a distance of 8 km from the sea, we considered that the origin of this element may be linked to marine as well as aerosols of regional origin.

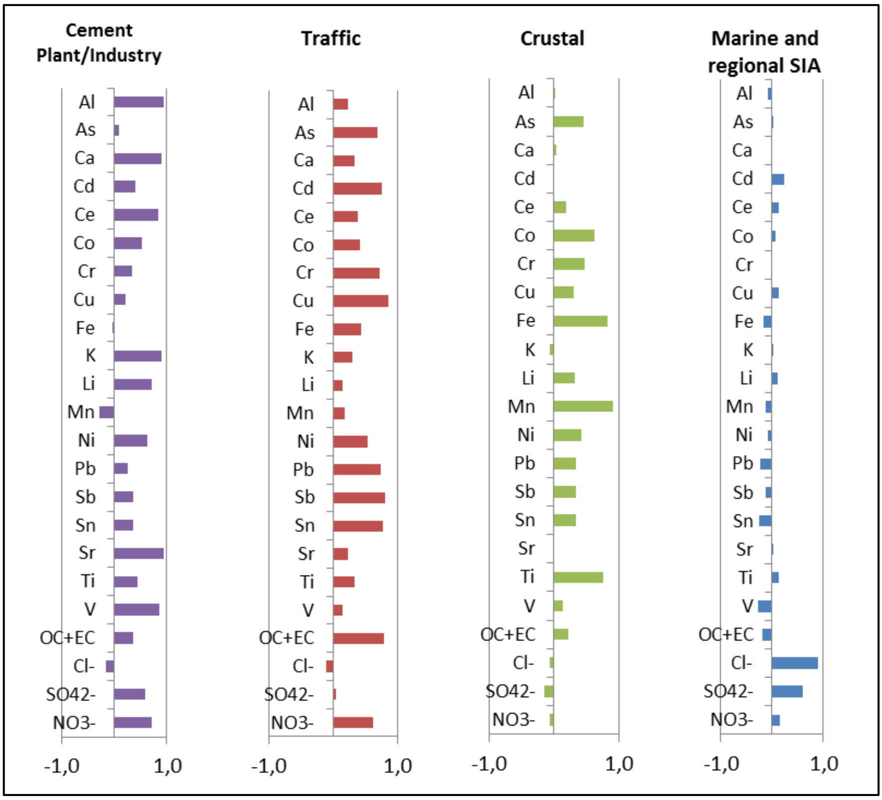

**Fig. 2.** Loading profiles for each component derived from PCA analysis of $PM_{10}$ inorganic species.

For the four sampling periods, the daily contributions of the four identified sources were evaluated by means of regression analysis of the component's score values with respect to the PM concentrations. Mean total concentrations of PM were 26, 51, 21 and 32 µg $m^{-3}$ in October 2013, December 2013, July 2014 and November/December 2014, respectively. Figs. 3(e)–3(h) shows the daily contributions of the four identified sources of inorganic species to $PM_{10}$. In turn, Fig. 4 shows the average contribution of the potential sources during the different sampling periods. It can be observed that the contribution of the sources varied significantly depending on the sampling period, showing that PM levels and composition depend not only on meteorological conditions but also on the intensity of irregular emissions such as traffic and some industrial activities. In October 2013, the contributions of traffic, marine and regional secondary aerosol and the cement plant/industry were similar (33, 29 and 26%, respectively), being those of crustal (12%) lesser. In December 2013, PM levels were clearly dominated by combustion sources namely, cement plant/industrial and traffic (66 and 22%, respectively), while crustal and marine and regional secondary aerosol were minor (9 and 3%, respectively). However, in July 2014 the highest contribution to total PM was associated with marine and regional secondary aerosol (50%), which was related to the active sea-breeze system in summer in this area. In the same period, a notable contribution was also observed for crustal, (35%), being low the contributions of the cement plant/industry (11%) and traffic (3%). Finally, in November/December 2014 the contribution of the cement plant/industry was the smallest (8%) of the four evaluated periods. The abated contribution of the cement plant to PM levels in this period is in agreement with the reduction of the production activity of the plant during the sampling period, since the plant was lessening its activity (from 25/11/14 to 08/12/14) until it was completely ceased (from 09/12/14 to 17/12/14). Therefore, crustal had a significant role as PM emitters (45%) followed by traffic (32%) and marine and regional secondary aerosol (15%). From these results, we can see that inorganic PM species in the area are mainly released by combustion sources, namely traffic and the activity of the cement plant, especially in winter months while in summer marine and regional secondary aerosol are more important. Nevertheless, during the last sampling period, in November/December 2014, the reduction of activity of the plant was noticeable in ambient inorganic PM components.

### *Sources of Organic PM*

PCA was applied on a matrix of scaled concentrations of 24 organic compounds (13 PAHs and 11 organic tracer compounds) measured in three PM mass fractions ($PM_{10}$, $PM_{2.5}$, $PM_1$) collected in November/December 2014 to explore the amount of variance that could be explained by a reduced number of components and to identify the most determinant associations among the organic tracer compounds analyzed in this study. A four-component solution was selected from the analysis involving a 93.5% of explained variance. Addition of a fifth component did not showed any further relevant environmental information. Following the optimal number of components obtained by PCA, MCR-ALS was applied to the scaled column-wise data matrix (i.e., without mean-centering) and non-negativity constraints, resulting in four components which accounted for 93.2% of the total data variance. Despite the limited size of our dataset as well as the different constraints considered by the two models; again, a good correlation between PCA and MCR-ALS models (Fig. S2 in the supplementary material). A reliable interpretation of sources according correlated molecular tracer compounds was found. Figs. 5(a)–5(d) shows the MCR loadings of the individual organic compounds in the components. Based on the abundance of molecular tracer compounds the four components were identified as:

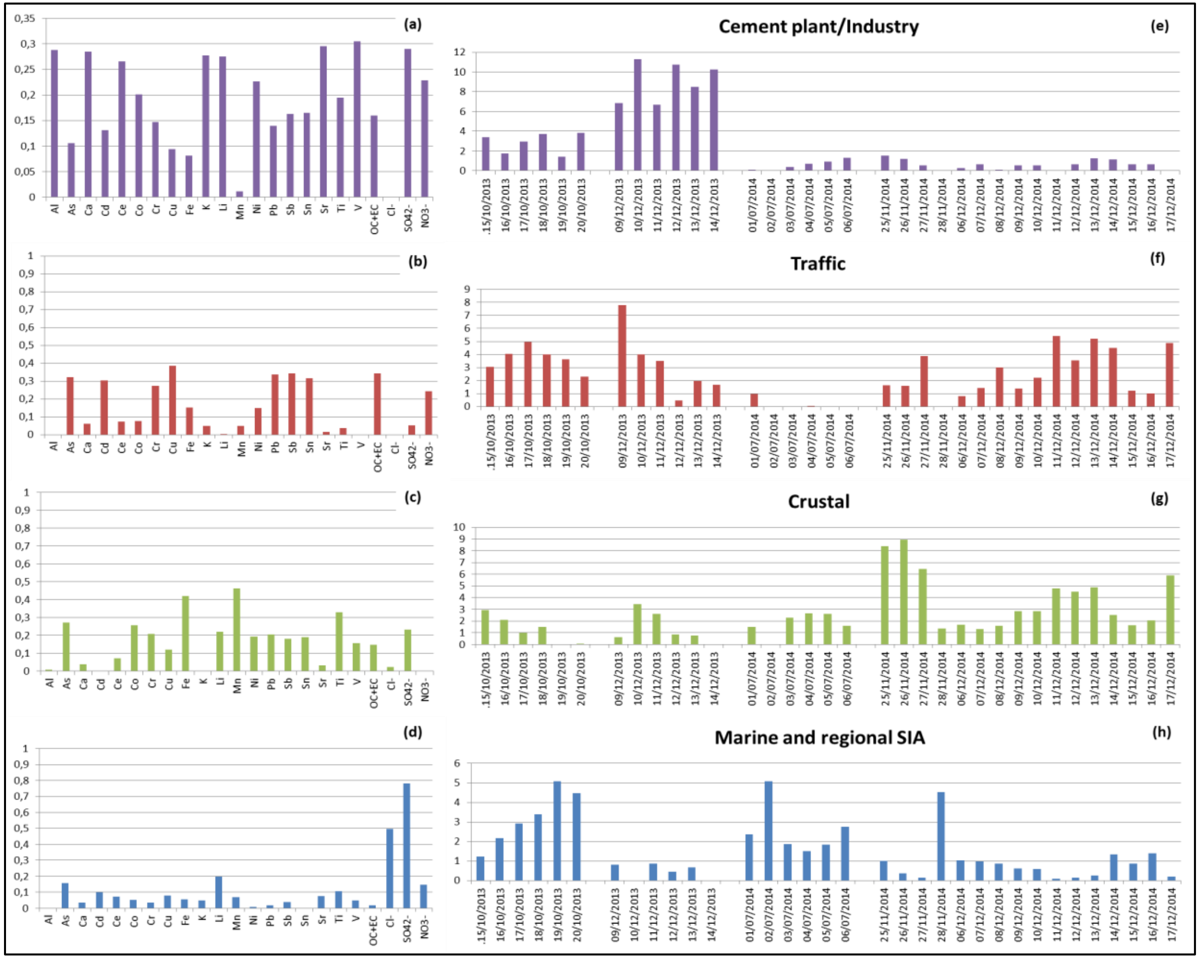

**Fig. 3.** Loadings (a–d) and daily contributions (e–h) of $PM_{10}$ inorganic species derived from MCR analysis.

**C1: Biomass burning.** This component was related to biomass burning due to the high correlation with well known tracers of biomass burning such as levoglucosan, and its isomers, dihydroabietic acid and retene (Kourtchev *et al.*, 2011; van Drooge *et al.*, 2014), as well as other PAHs.

**C2: Fossil fuel combustion.** This factor showed a high correlation with compounds characteristic of fossil fuel combustion such as hopanes, which are found in the lubricating oils used by both gasoline- and diesel-powered motor vehicles (Křůmal *et al.*, 2013) and some PAHs**.**

**C3: Soil dust.** This component was associated with soil dust resuspension due to the high contribution of glucose and mannitol as well as dicarboxylic acids and hopanes. Glucose is present in soil dust. Among the sugar alcohols, mannitol is one of the most abundant (Bauer *et al.*, 2008; Schmidl *et al.*, 2008). Mannitol is also associated with airborne fungal spores (Schmidl *et al.*, 2008).

**C4: Regional Secondary Organic Aerosols (SOA).** This component was characterized by a high contribution of secondary aerosol species (succinic and glutaric acid) (Hsieh *et al.*, 2008) together with traces of PAHs. In the atmosphere, non-methane volatile organic compounds from traffic

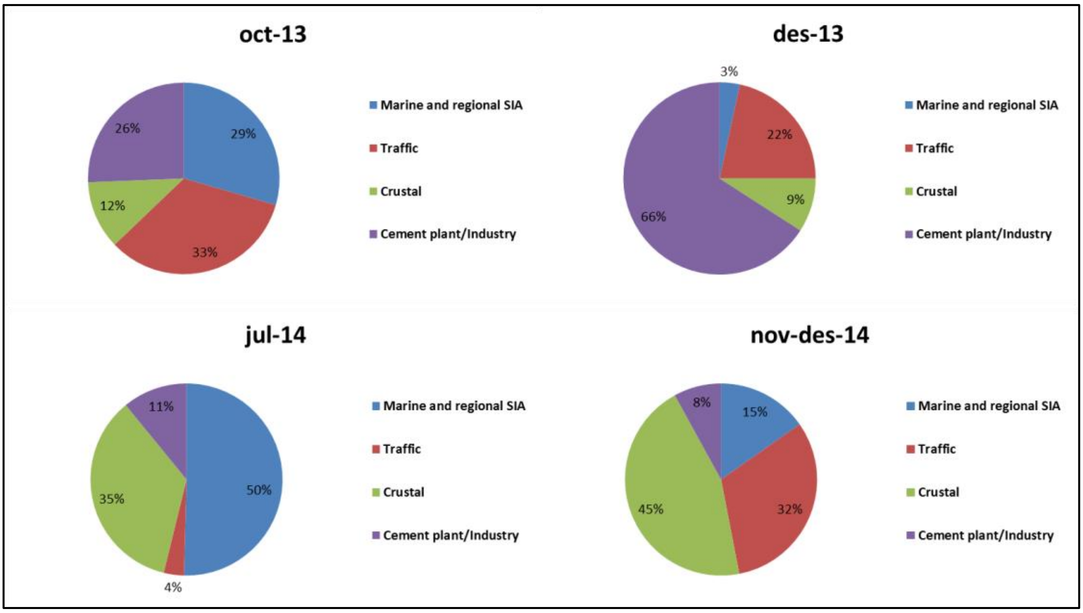

**Fig. 4.** Percentages of source contributions to main PM components of the four factors derived from MCR classified by 4 sampling periods.

emissions are transformed through photochemical reactions to dicarboxylic acids such as succinic and glutaric acids. Therefore, the origin of this component is probably from long- and middle-range atmospheric transport.

The loadings of the individual compounds in the components (Figs. 5(a)–5(d)) were used to estimate the daily contribution of the four identified sources of organic compounds in the studied area (Figs. (5e)–5(h)). Different sampling periods can be differentiated in the case of organic compounds: 1) when the plant was totally operative (from 18/11/14 to 24/11/2014), and 2) when the plant was reducing its activity (from 01/12/14 to 7/12/2014). Fig. 6 shows the average estimated contributions of identified sources and processes for each of the three PM mass fractions. Organic dust was the major contributor to the $PM_{10}$ fraction (33%), followed by biomass burning (29%), fossil fuel combustion (23%) and SOA + regional (15%). According to organic tracers, it was not possible to differentiate if biomass burning was related to the cement plant, which uses sewage sludge as alternative fuel, or to burning of pruning wastes in the area, neither if fossil fuel was related to the cement plant or to traffic. In $PM_{2.5,}$ biomass burning was dominant (34%) followed by regional Secondary Organic Aerosols (32%), fossil fuel combustion (25%) and organic dust (2%). Finally, $PM_1$ was dominated by combustion products from biomass combustion (37%) and fossil fuel (32%) origin followed by regional Secondary Organic Aerosols (29%) and organic dust (2%). As it has been found in other studies our results indicate that main sources of the finest PM components are linked with combustion processes. In fact, major sources of fine particles in urban areas are vehicular emissions especially of diesel vehicles (Shirmohammadi *et al.*, 2016). In our case, however biomass combustion also seems to have a considerable contribution in $PM_{2.5}$ and $PM_1$ levels what could be related to the plant activity.

### *Carbon Isotope Analysis*

Bulk carbon isotope analysis was applied in this study as a complementary source identification technique in order to explore its capacity to further refine the insight on the origin of the PM sampled in the vicinity of the cement plant. Despite the low number of samples, this method allows the fingerprinting of organic PM sources based on the carbon isotopic composition of the samples, which on its term can be compared to potential sources. For this purpose, the $\delta^{13}C$ was determined in the carbon content of the same $PM_{10}$, $PM_{2.5}$ and $PM_1$ samples, collected in November/December 2014, where organic compounds have also been determined, and compared with those of different types of potential contaminant sources in the area (Fig. 1). The potential sources included and indicated in Fig. 1 were: 1) Mineral fraction sources (cement and kiln dust measured in this study corresponding to points 1 and 2, respectively; and point 3 obtained from López-Veneroni (2009)), 2) Combusted biomass fuels of C3 plants origin (points 4 to 9, obtained from Garbaras *et al.* (2015)), 3) Combusted fossil fuels (points 10 to 23, being points 10, 11 and from 13 to 18 obtained from Widory *et al.* (2004) and 12, 19 and 20 from Andres *et al.* (1994)), 4) Combusted sewage sludge (point 21, obtained from Garbaras *et al.* (2015)), 5) Traffic sources (point 22, unleaded gasoline from an exhaust pipe; and point 23, diesel from an exhaust pipe, both analytically determined in this study), 6) Deposited particles on a Petri dish at a school located near the cement plant (point 24, analytically determined in this study). More details on the sources of Fig. 1 are indicated in the supplementary material. In Fig. 1 it can be observed that the $\delta^{13}C$ of the PM samples collected around the cement plant (points 25 to 30) were in the range of combustion sources. More specifically, the analyzed samples were within the range of two main groups of sources, namely group 1) biomass fuels, which include agricultural waste, wood pellets, as well as sewage sludge (points 5, 6 and 21, respectively) and group 2) fossil fuels, corresponding to domestic fuel oil, diesel particles, petroleum and unleaded gasoline (points 17, 18, 19, 22 and 23, respectively); while cement and kiln dust from the

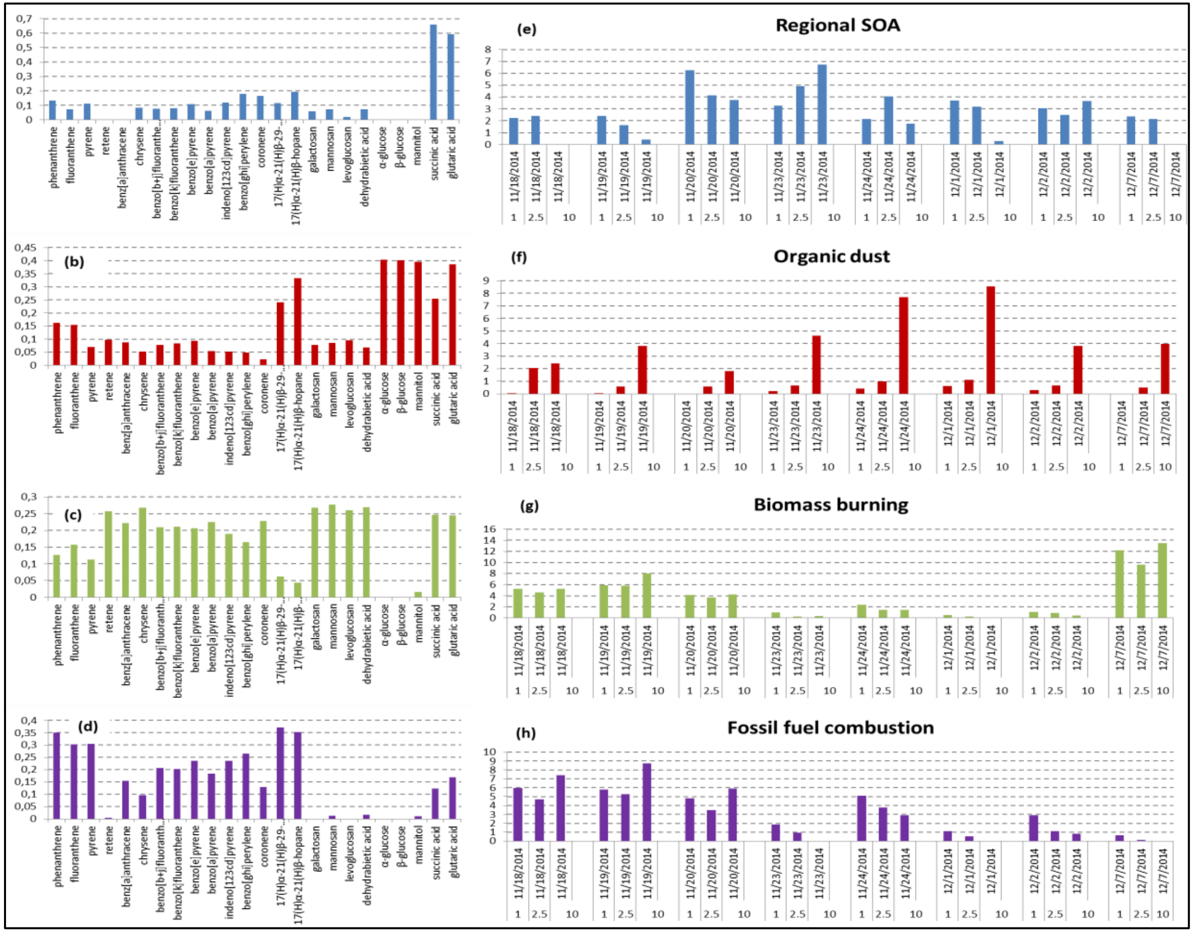

**Fig. 5.** Loadings (a–d) and daily contributions (e–h) of the analysed $PM_{10}$, $PM_{2.5}$ and $PM_1$ organic compounds in the identified components of the MCR-ALS.

plant (mineral fraction in Fig. 1) are far from the samples collected around the cement plant. Hence, fuel combustion and biomass combustion sources are clearly dominating in the ambient PM samples of study, which is consistent with the results of the source apportionment analysis of the organic compounds, which were determined in the same samples. The former analysis, however, was able to differentiate between biomass and fuel combustion sources, while the isotopic results are overlapping.

Although values of samples around the cement plant are far from the $\delta^{13}C$ of mineral fraction, if we take into account that the cement plant uses sewage sludge as alternative biomass fuel, the values of $\delta^{13}C$ in ambient PM were feasible with a contamination coming from the cement plant but also from traffic (diesel and gasoline combustion particles), domestic heating (domestic fuel oil) or fossil fuel used in the cement plant (petroleum). In order to discriminate the contribution of the cement plant, $\delta^{13}C$ values of samples collected when the cement plant was not operating were compared to those of operational days. It can be seen in Fig. 1, that point 26, which represents the average $\delta^{13}C$ value of samples collected when the cement plant was not operating, is within the range of $\delta^{13}C$ values obtained during the operational period. This result indicates that the cement plant emissions would not be significant in ambient PM during the overall sampling period or it could mean that the cement plant emissions cannot be detected since the $\delta^{13}C$ signature is very similar to the value of the average emissions from other sources.

Regarding differences in the $\delta^{13}C$ of PM according to size, a small but significant increase in the $\delta^{13}C$ value was noted when increasing PM size (Fig. 7). $PM_1$, $PM_{2.5}$ and $PM_{10}$ presented average $\delta^{13}C$ values of $-26.8 \pm 0.1‰$, $-26.4 \pm 0.1‰$ and $-25.8 \pm 0.4‰$, respectively. Results indicate that $PM_{2.5}$ is mainly composed of $PM_1$ while there is an enrichment of $^{13}C$ in the coarse fraction between 2.5 and 10 µm. This increase in $\delta^{13}C$ matches with the presence of calcite in $PM_{2.5}$ and $PM_{10}$, (revealed by DRX analyses, see Fig. S3 in the Supplementary Material) but not in $PM_1$. Hence, the differences in $\delta^{13}C$ observed in PM samples depending on the size (Fig. 7) indicate the effect of the mineral contribution in the coarser particle samples.

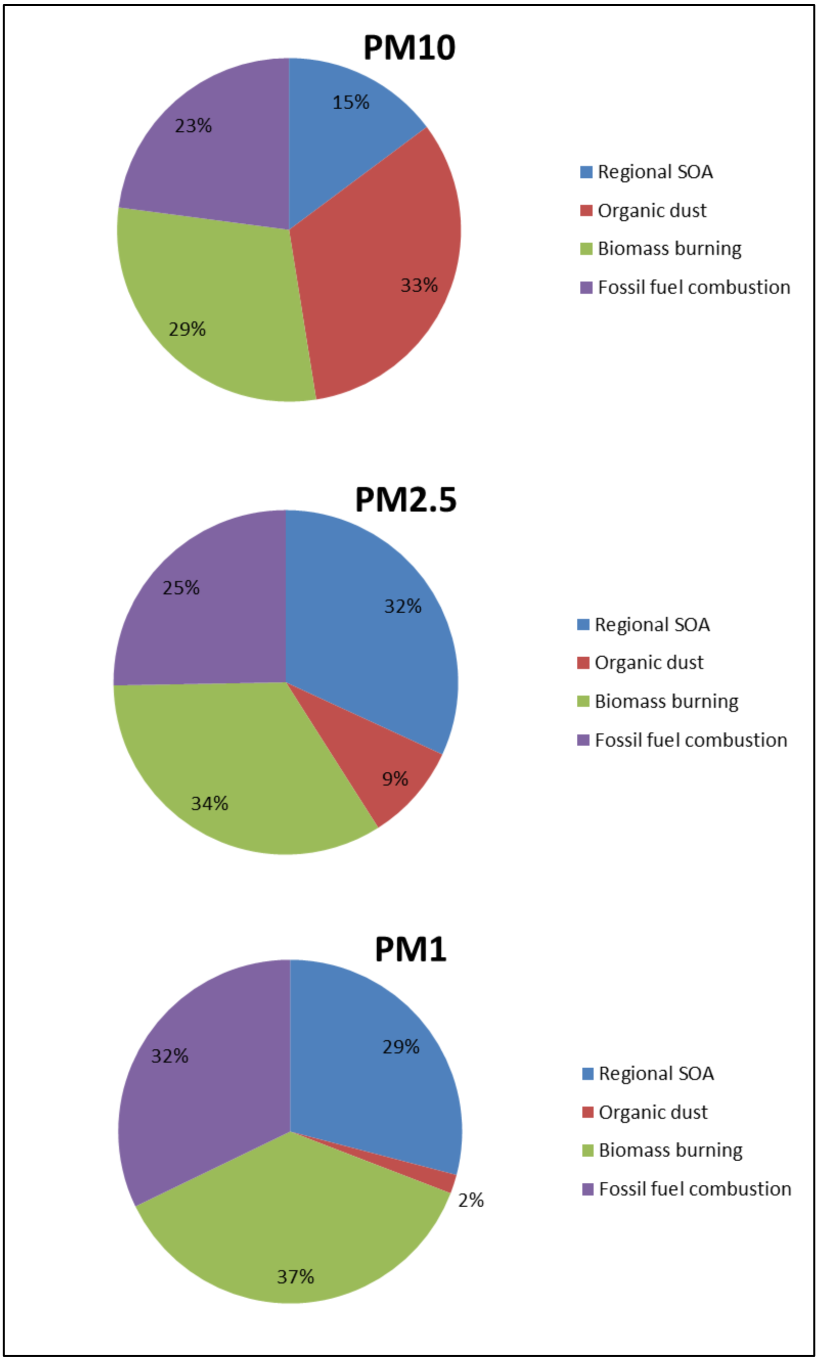

**Fig. 6.** Estimated contributions of identified sources and processes on the observed PM mass fractions in the vicinity of the cement plant.

These results are in agreement with the differences observed in the organic tracer composition of the different PM size fractions (Fig. 6), where higher contributions of organic dust were noted in $PM_{10}$ in comparison with the smaller $PM_{2.5}$ and $PM_1$ fractions. Geogenic calcite usually presents $\delta^{13}C$ values close to 0%. Moreover, sample point 24, that represented solid deposited material with no size selection and therefore containing larger particles, corroborates the influence of the mineral part on the $\delta^{13}C$ since it showed a $\delta^{13}C$ value of –24.5 ± 0.3‰ which is even higher than that found in $PM_{10}$ (–25.8 ± 0.4‰), in agreement with the presence of geogenic calcite. Therefore the mineral contribution of the cement plant starts to be visible when the particle size increases, however, its contribution to the total carbon in the ambient PM was always notably smaller than the contributions of the combustion sources that according to $\delta^{13}C$ analysis dominate in the vicinity of the cement plant.

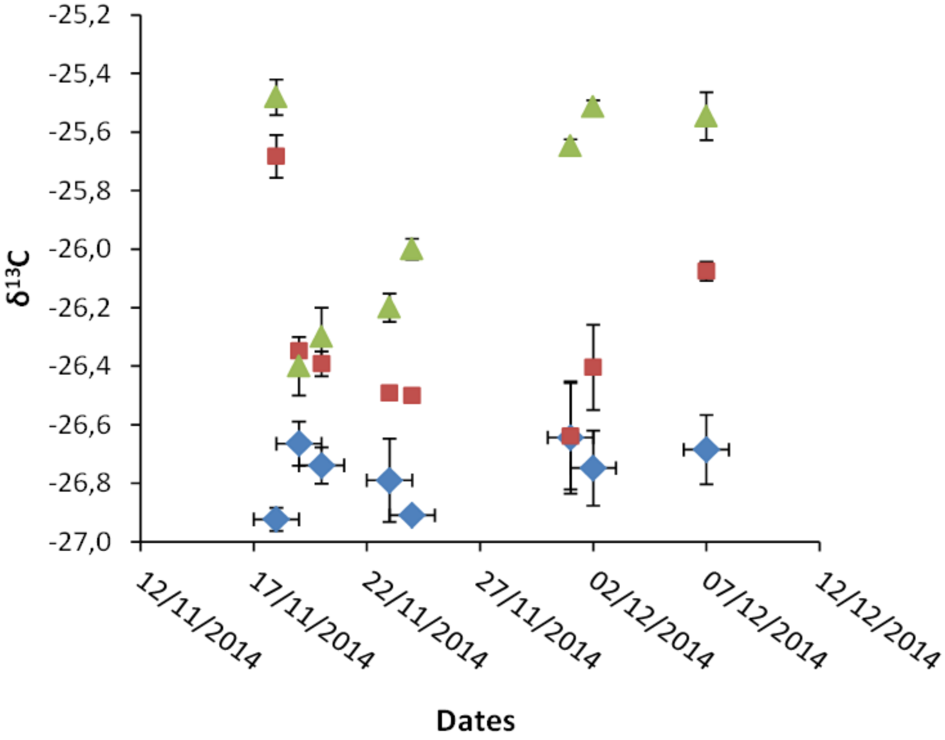

**Fig. 7.** Average $\delta^{13}C$ values in $PM_1$ (blue diamonds), $PM_{2.5}$ (red squares), and $PM_{10}$ (green triangles) samples collected around the cement plant while it was operating, from November 17th to December 7th, 2014. Error bars represent deviation between analytical duplicates.

## Conclusions

Particle matter is one of the pollutants that generate greatest concern around cement plants. Ambient PM is composed by inorganic and organic compounds and can be released from other sources that include combustion processes (traffic, power generation, etc.), mineral origins or secondary aerosols formation. These sources may be active simultaneously, resulting in a complex mixture of compounds difficult to appoint to one source. Moreover, external factors, such as meteorological conditions, may have equal influences on the compounds in the air shed, resulting in correlations among compounds that may not have the same emission source. It is therefore complex to apply source apportionment tools on a dataset. In addition, receptor models require large databases that, such as in our case, are not always available because of the high costs that entail the collection of the large number of samples as well as the analysis of the numerous tracers required. In our case, we used available PM ambient data regarding inorganic and organic compounds near a cement plant to establish the most significant sources of those pollutants by applying source apportionment methodologies PCA and MCR. In addition, we analyzed the $\delta^{13}C$ in the carbon content of PM ambient samples to identify sources by comparing with the $\delta^{13}C$ of potential contaminant sources. In spite of the different constraints considered by PCA and MCR-ALS and the the small datasets available, similar sources could be identified by both methodologies according to the correlations found between tracer compounds: marine and secondary inorganic aerosol, cement plant/industrial, traffic and crustal. MCR-ALS allowed quantifying those sources. The contributions of those sources varied significantly depending on the period of the year and even the year of collection. However, it could be noted that tracer PM species in the area were mainly released by combustion sources, namely traffic and the activity of the cement plant/industry, especially in winter months while in summer marine and secondary inorganic aerosol were more important. The reduction of activity of the plant was noticeable in ambient inorganic PM components. PCA, MCR-ALS and $\delta^{13}C$ on the organic dataset indicated that PM around the cement plant was mainly influenced by combustion sources, biomass burning and fossil fuel combustion. However, according to MCR-ALS and $\delta^{13}C$ it was not clear if all was emitted by the cement plant (burning fossil and sewage sludge as alternative fuel), since other activities, such as traffic, domestic heating and biomass removal from fields could also be involved. In spite of the limitations of our datasets regarding their size in comparison with traditional source apportionment studies, the overall results indicate that the three studied techniques, PCA, MCR and $\delta^{13}C$

agree between each other, even though they have been applied by using different type of data. PCA and MCR-ALS allowed differentiating cement plant emissions from traffic by means of correlations found between tracers of combustion and mineral matter, in the case of the cement activity, and between tracers of combustion and engine emissions and tire/break, in the case of traffic. On the other hand, PCA, MCR and $\delta^{13}C$ on the organic dataset empathized the significance of combustion sources in the area from both biomass burning and fossil fuel combustion. In the case of carbon isotopes, the lack of differences between operational and non-operational days of the plant showed the significant impact of traffic during the sampling period. These results confirm that the different techniques can be used together to corroborate each other and to give more reliability to the results; or, they can also be used separately in studies where only few data is available or there is some design limitation.

## Acknowledgments

This study was financed by the Spanish Ministry of Economy and Competitiveness (MINECO), as part of the projects CTM2012-32778 (F. Sánchez-Soberón received a doctoral scholarship as part of the project above mentioned), CTM2015-65303 and CGL2014-57215-C4-1-R, as well as by the Catalan Government, through the projects 2014SGR90 and 2014SGR1456. The authors also want to thank LAFARGE CEMENTOS SAU for their help during the sampling.

## Supplementary material

Supplementary data associated with this article can be found in the online version at http://www.aaqr.org.

## References

Alier, M., van Drooge, B.L., Dall'Osto, M., Querol, X., Grimalt, J.O. and Tauler, R. (2013). Source apportionment of submicron organic aerosol at an urban background and a road site in Barcelona (Spain) during SAPUSS. *Atmos. Chem. Phys.* 13: 10353–10371.

Andres, R., Marland, G., Boden, T. and Bischof, S. (1994). Carbon Dioxide Emissions from Fossil Fuel Consumption and Cement Manufacture, 1751-1991; and an Estimate of Their Isotopic Composition and Latitudinal Distribution. In *The Carbon Cycle*, Wigley, T.M.L. and

Schimel, D. (Eds.), Cambridge University Press.

Banerjee, T., Murari, V., Kumar, M. and Raju, M.P. (2015). Source apportionment of airborne particulates through receptor modeling: Indian scenario. *Atmos. Res.* 164–165: 167–187.

Bauer, H., Claeys, M., Vermeylen, R., Schueller, E., Weinke, G., Berger, A. and Puxbaum, H. (2008). Arabitol and mannitol as tracers for the quantification of airborne fungal spores. *Atmos. Environ.* 42: 588–593.

Belis, C.A., Karagulian, F., Larsen, B.R. and Hopke, P.K. (2013). Critical review and meta-analysis of ambient particulate matter source apportionment using receptor models in Europe. *Atmos. Environ.* 69: 94–108.

Boutton, T. (1991). Stable carbon isotope ratios of natural material: II. Atmospheric, terrestrial, marine and freshwater environments. In *Carbon Isotope Techniques*, Coleman, D.C. and Fry, B. (Eds.), Academic Press, pp. 172–185.

Cachier, H., Buat-Menard, P., Fontugne, M. and Rancher, J. (1985). Source terms and source strengths of the carbonaceous aerosol in the tropics. *J. Atmos. Chem.* 3: 469–489.

Cheselet, R., Fontugne, M., Buat-Ménard, P., Ezat, U. and Lambert, C. (1981). The origin of particulate organic carbon in the marine atmosphere as indicated by its stable carbon isotopic composition. *Geophys. Res. Lett.* 8: 345–348.

Contini, D., Belosi, F., Gambaro, A., Cesari, D., Stortini, A.M. and Bove, M.C. (2012). Comparison of $PM_{10}$ concentrations and metal content in three different sites of the Venice Lagoon: An analysis of possible aerosol sources. *J. Environ. Sci.* 24: 1954–1965.

Contini, D., Genga, A., Cesari, D. and Guascito, M. (2010). Characterisation and source apportionment of $PM_{10}$ in an urban background site in Lecce. *Atmos. Res.* 95: 40–54.

Elorduy, I., Elcoroaristizabal, S., Durana, N., García, J.A. and Alonso, L. (2016). Diurnal variation of particle-bound PAHs in an urban area of Spain using TD-GC/MS: Influence of meteorological parameters and emission sources. *Atmos. Environ.* 138: 87–98.

Enamorado-Báez, S.M., Gómez-Guzmán, J.M., Chamizo, E. and Abril, J.M. (2015). Levels of 25 trace elements in high-volume air filter samples from Seville (2001–2002): Sources, enrichment factors and temporal variations. *Atmos. Res.* 155: 118–129.

Engelbrecht, J.P. and Jayanty, R.K.M. (2013). Assessing sources of airborne mineral dust and other aerosols, in Iraq. *Aeolian Res.* 9: 153–160.

Galarneau, E. (2008). Source specificity and atmospheric processing of airborne PAHs: Implications for source apportionment. *Atmos. Environ.* 42: 8139–8149.

Garbaras, A., Masalaite, A., Garbariene, I., Ceburnis, D., Krugly, E., Remeikis, V., Puida, E., Kvietkus, K. and Martuzevicius, D. (2015). Stable carbon fractionation in size-segregated aerosol particles produced by controlled biomass burning. *J. Aerosol Sci.* 79: 86–96.

Gorka, M. and Jedrysek, M. (2008). $\delta^{13}C$ in organic atmospheric dust deposited at Wroclaw (SW) Poland: Critical Remarks on the passive method. *Geol. Q.* 52: 115–126.

Hamra, G., Guha, N., Cohen, A., Laden, F., Raaschou-Nielsen, O., Samet, J., Vineis, P., Forastiere, F., Saldiva, P., Yorifuji, T. and Loomis, D. (2014). Outdoor particulate matter exposure and lung cancer: A systematic review and meta-analysis. *Environ. Health Perspect.* 122: 906–911.

Hernández-Mena, L., Murillo-Tovar, M., Ramírez-Muñíz, M., Colunga-Urbina, E., de la Garza-Rodríguez, I. and Saldarriaga-Noreña, H. (2011). Enrichment factor and profiles of elemental composition of $PM_{2.5}$ in the city of Guadalajara, *Mexico. Bull. Environ. Contam. Toxicol.* 87: 545–549.

Hsieh, L.Y., Chen, C.L., Wan, M.W., Tsai, C.H. and Tsai, Y.I. (2008). Speciation and temporal characterization of dicarboxylic acids in $PM_{2.5}$ during a PM episode and a period of non-episodic pollution. *Atmos. Environ.* 42: 6836–6850.

Jaumot, J., Gargallo, R., de Juan, A. and Tauler, R. (2005). A graphical user-friendly interface for MCR-ALS: A new tool for multivariate curve resolution in MATLAB. *Chemom. Intell. Lab. Sys.* 76: 101–110.

Jolliffe, I. (2002). *Principal Component Analysis*, 2nd Edition ed, New York, USA.

Karagulian, F., Belis, C.A., Dora, C.F.C., Prüss-Ustün, A.M., Bonjour, S., Adair-Rohani, H. and Amann, M. (2015). Contributions to cities' ambient particulate matter (PM): A systematic review of local source contributions at global level. *Atmos. Environ.* 120: 475–483.

Kelly, F.J. and Fussell, J.C. (2012). Size, source and chemical composition as determinants of toxicity attributable to ambient particulate matter. *Atmos. Environ.* 60: 504–526.

Kourtchev, I., Hellebust, S., Bell, J.M., O'Connor, I.P., Healy, R.M., Allanic, A., Healy, D., Wenger, J.C. and Sodeau, J.R. (2011). The use of polar organic compounds to estimate the contribution of domestic solid fuel combustion and biogenic sources to ambient levels of organic carbon and $PM_{2.5}$ in Cork Harbour, Ireland. *Sci. Total Environ.* 409: 2143–2155.

Křůmal, K., Mikuška, P. and Večeřa, Z. (2013). Polycyclic aromatic hydrocarbons and hopanes in $PM_1$ aerosols in urban areas. *Atmos. Environ.* 67: 27–37.

López-Veneroni, D. (2009). The stable carbon isotope composition of $PM_{2.5}$ and $PM_{10}$ in Mexico City Metropolitan Area air. *Atmos. Environ.* 43: 4491–4502.

Marcon, A., Pesce, G., Girardi, P., Marchetti, P., Blengio, G., de Zolt Sappadina, S., Falcone, S., Frapporti, G., Predicatori, F. and de Marco, R. (2014). Association between $PM_{10}$ concentrations and school absences in proximity of a cement plant in northern Italy. *Int. J. Hyg. Environ. Health* 217: 386–391.

Mari, M., Harrison, R.M., Schuhmacher, M., Domingo, J.L. and Pongpiachan, S. (2010). Inferences over the sources and processes affecting polycyclic aromatic hydrocarbons in the atmosphere derived from measured data. *Sci. Total Environ.* 408: 2387–2393.

Mkoma, S., Kawamura, K., Tachibana, E. and Fu, P. (2014). Stable carbon and nitrogen isotopic compositions of tropical atmospheric aerosols: Sources and contribution from burning of $C_3$ and $C_4$ plants to organic aerosols. *Tellus Ser. B* 66: 20176.

Moreno, T., Querol, X., Alastuey, A., de la Rosa, J., Sánchez de la Campa, A.M., Minguillón, M., Pandolfi, M., González-Castanedo, Y., Monfort, E. and Gibbons, W. (2010). Variations in vanadium, nickel and lanthanoid element concentrations in urban air. *Sci. Total Environ.* 408: 4569–4579.

Pey, J., Pérez, N., Castillo, S., Viana, M., Moreno, T., Pandolfi, M., López-Sebastián, J.M., Alastuey, A. and Querol, X. (2009). Geochemistry of regional background aerosols in the Western Mediterranean. *Atmos. Res.* 94: 422–435.

Pey, J., Alastuey, A. and Querol, X. (2013). $PM_{10}$ and $PM_{2.5}$ sources at an insular location in the western Mediterranean by using source apportionment techniques. *Sci. Total Environ.* 456–457: 267–277.

Pieri, F., Katsoyiannis, A., Martellini, T., Hughes, D., Jones, K.C. and Cincinelli, A. (2013). Occurrence of linear and cyclic volatile methyl siloxanes in indoor air samples (UK and Italy) and their isotopic characterization. *Environ. Int.* 59: 363–371.

Puig, R., Àvila, A. and Soler, A. (2008). Sulphur isotopes as tracers of the influence of a coal-fired power plant on a Scots pine forest in Catalonia (NE Spain). *Atmos. Environ.* 42: 733–745.

Robinson, A.L., Subramanian, R., Donahue, N.M. and Rogge, W.F. (2006). Source apportionment of molecular markers and organic aerosol. 1. Polycyclic aromatic hydrocarbons and methodology for data visualization *Environ. Sci. Technol.* 40: 7803–7810.

Sánchez-Soberón, F., Rovira, J., Mari, M., Sierra, J., Nadal, M., Domingo, J.L. and Schuhmacher, M. (2015). Main components and human health risks assessment of $PM_{10}$, $PM_{2.5}$, and $PM_1$ in two areas influenced by cement plants. *Atmos. Environ.* 120: 109–116.

Sánchez-Soberón, F., van Drooge, B., Rovira, J., Grimalt, J., Nadal, M., Domingo, J. and

Schuhmacher, M. (2016). Size-distribution of airborne polycyclic aromatic hydrocarbons and other organic source markers in the surroundings of a cement plant powered with alternative fuels. *Sci. Total Environ.* 550: 1057–1064.

Schmidl, C., Marr, I.L., Caseiro, A., Kotianová, P., Berner, A., Bauer, H., Kasper-Giebl, A. and Puxbaum, H. (2008). Chemical characterisation of fine particle emissions from wood stove combustion of common woods growing in mid-European Alpine regions. *Atmos. Environ.* 42: 126–141.

Shi, G.L., Liu, G.R., Peng, X., Wang, Y.N., Tian, Y.Z., Wang, W. and Feng, Y.C. (2014). A comparison of multiple combined models for source apportionment, including the PCA/MLR-CMB, Unmix-CMB and PMF-CMB models. *Aerosol Air Qual. Res.* 14: 2040–2050.

Shirmohammadi, F., Hasheminassab, S., Saffari, A., Schauer, J.J., Delfino, R.J. and Sioutas, C. (2016). Fine and ultrafine particulate organic carbon in the Los Angeles basin: Trends in sources and composition. *Sci. Total Environ.* 541: 1083–1096.

Tauler, R., Viana, M., Querol, X., Alastuey, A., Flight, R.M., Wentzell, P.D. and Hopke, P.K. (2009). Comparison of the results obtained by four receptor modelling methods in aerosol source apportionment studies. *Atmos. Environ.* 43: 3989–3997.

Terrado, M., Barceló, D. and Tauler, R. (2009). Quality assessment of the multivariate curve resolution alternating least squares method for the investigation of environmental pollution patterns in surface water. *Environ. Sci. Technol.* 43: 5321–5326.

Tsai, M.Y., Hoek, G., Eeftens, M., de Hoogh, K., Beelen, R., Beregszászi, T., Cesaroni, G., Cirach, M., Cyrys, J., De Nazelle, A., de Vocht, F., Ducret-Stich, R., Eriksen, K., Galassi, C., Gražuleviciene, R., Gražulevicius, T., Grivas, G., Gryparis, A., Heinrich, J., Hoffmann, B., Iakovides, M., Keuken, M., Krämer, U., Künzli, N., Lanki, T., Madsen, C., Meliefste, K., Merritt, A.S., Mölter, A., Mosler, G., Nieuwenhuijsen, M.J., Pershagen, G., Phuleria, H., Quass, U., Ranzi, A., Schaffner, E., Sokhi, R., Stempfelet, M., Stephanou, E., Sugiri, D., Taimisto, P., Tewis, M., Udvardy, O., Wang, M. and Brunekreef, B. (2015). Spatial variation of PM elemental composition between and within 20 European study areas — Results of the ESCAPE project. *Environ. Int.* 84: 181–192.

van Drooge, B.L., Fontal, M., Bravo, N., Fernández, P., Fernández, M.A., Muñoz-Arnanz, J., Jiménez, B. and Grimalt, J.O. (2014). Seasonal and spatial variation of organic tracers for biomass burning in $PM_1$ aerosols from highly insolated urban areas. *Environ. Sci. Pollut. Res.* 21: 11661–11670.

Viana, M., Kuhlbusch, T.A.J., Querol, X., Alastuey, A., Harrison, R.M., Hopke, P.K., Winiwarter, W., Vallius, M., Szidat, S., Prévôt, A.S.H., Hueglin, C., Bloemen, H., Wåhlin, P., Vecchi, R., Miranda, A.I., Kasper-Giebl, A., Maenhaut, W. and Hitzenberger, R. (2008a). Source apportionment of particulate matter in Europe: A review of methods and results. *J. Aerosol Sci.* 39: 827–849.

Viana, M., Pandolfi, M., Minguillón, M.C., Querol, X., Alastuey, A., Monfort, E. and Celades, I. (2008b). Inter-comparison of receptor models for PM source apportionment: Case study in an industrial area. *Atmos. Environ.* 42: 3820–3832.

Widory, D., Roy, S., Le Moullec, Y., Goupil, G., Cocherie, A. and Guerrot, C. (2004). The origin of atmospheric particles in Paris: A view through carbon and lead isotopes. *Atmos. Environ.* 38: 953–961.

Yatkin, S. and Bayram, A. (2008). Source apportionment of $PM_{10}$ and $PM_{2.5}$ using positive matrix factorization and chemical mass balance in Izmir, Turkey. *Sci. Total Environ.* 390: 109–123.

Zeng, F., Shi, G.L., Li, X., Feng, Y.C., Bi, X.H., Wu, J.H. and Xue, Y.H. (2010). Application of a combined model to study the source apportionment of $PM_{10}$ in Taiyuan, China. *Aerosol Air Qual. Res.* 10: 177–184.

Zou, Y., Wang, L. and Christensen, E.R. (2015). Problems in the fingerprints based polycyclic aromatic hydrocarbons source apportionment analysis and a practical solution. *Environ. Pollut.* 205: 394–402.

# CHAPTER 6: In-vitro metabolomics to evaluate toxicity of PM nearby a petrochemical complex

Francisco Sánchez-Soberón, Matthias Cuykx, Noemi Serra, Victoria Linares, Montserrat Bellés, Adrian Covaci, Marta Schuhmacher

# *In-vitro* metabolomics to evaluate toxicity of PM nearby a petrochemical complex

Francisco Sánchez-Soberón, Matthias Cuykx, Noemi Serra, Victoria Linares, Montserrat Bellés, Adrian Covaci, Marta Schuhmacher

## Abstract

The objective of the present study is to evaluate the toxicity of particulate matter (PM) under realistic exposure scenarios in children. To do so, three fractions of PM ($PM_{0.25}$, $PM_{2.5-0.25}$, and $PM_{10-2.5}$) were collected in a village located nearby a petrochemical complex. The particles were sampled in three different environments: classroom, home, and outdoors. While sampling, time activity pattern of 20 students attending the classroom was obtained, and the daily mass of particles reaching the lungs was calculated via dosimetry model (MPPD). To study the hazardous potential of these material, two toxicity assays were performed onto alveolar cells (A549) exposed to PM. Firstly, to have an overview of the overall PM toxicity after 72 hours exposure, a cytotoxicity dose-response assay was conducted. Subsequently, to study changes in the metabolic profile of these cells under same exposure time, a metabolomic assay was performed at two doses ($LC_5$ and real dose). Levels of PM in every environment were below the limits established by the current normative, being classroom the microenvironment registering highest values. Despite occupying only 8% of the daily routine of kids, heavy intensity activities performed outdoors played a major role in PM deposition, especially in the upper part of the respiratory tract. Since most of $PM_{10-2.5}$ got retained in the upper part of the respiratory tract, toxicity assays on A549 cells were performed for $PM_{2.5-0.25}$ and $PM_{0.25}$. Lower $LC_5$ value was obtained for $PM_{0.25}$ than $PM_{2.5-0.25}$ (0.00808 and 0.07370 µg/mL respectively). Although the number of features affected by particles was similar in the $LC_5$ experiment, the number of altered metabolites under real dose exposition was higher for $PM_{0.25}$ than $PM_{2.5-0.25}$ (10 and 5 respectively). These changes were mostly in compounds dealing with cell and mitochondrial membrane functions

Despite the present chapter was not focused on PM collected nearby cement plants, we wanted to include it as part of the thesis since it combines and improves sampling procedures (Chapter 1 and 2), exposure calculation (Chapter 4) and toxicity assays (Chapter 3).

## 1. Introduction

Particulate matter (PM) is recognized as one of the most harmful air pollutants (Kim et al., 2015). PM consists of liquid droplets and solid fragments smaller than 10 µm suspended in the air, whose size, chemical composition, and shape are varied (WHO, 2014). For regulatory purposes, environmental agencies all over the world usually classify PM into two groups according to its size: $PM_{10}$ (those particles having a diameter smaller than 10 µm, sometimes named as respirable) and $PM_{2.5}$ (smaller than 2.5 µm, also referred as fine) (EU Parliament, 2008; US EPA, 2016). Several studies coincide that the smaller the PM, the more harmful it is, since it can reach deeper parts of the respiratory system (Kelly and Fussell, 2016). In fact, it is estimated that $PM_{2.5}$ is responsible of more than 2 million premature deaths per year globally (Donahue et al., 2016).

Due to the importance of this pollutant, *in vitro* tests have been useful tools to assess the toxicity of PM (Nemmar et al., 2013). The classical approach in these assays consists on applying different doses of toxicant on different kind of pulmonary cells, and study parameters such as cytotoxicity, genotoxicity, strength of cell junction or the presence of inflammatory mediators (Akhtar et al., 2010; L. Cao et al., 2015a; X. Cao et al., 2015). Consequently, these studies are conceived as a way of studying short times effects under PM doses much higher than those experienced under real conditions.

To have a better approach of changes in cells at low and real doses, omic sciences seem to be a powerful tool. Omics are a series of disciplines focused on studying the complete profile of genes (genomics), mRNA (transcriptomics), proteins (proteomics), or metabolites (metabolomics) for a given cell type or organism (Horgan and Kenny, 2011). Although nowadays it is possible to find papers applying different omics methods on lung cells, the amount number of studies assessing toxicity of ambient PM by omics means is still low (Q. Huang et al., 2015; Líbalová et al., 2012; Longhin et al., 2016; Vaccari et al., 2015; Wheelock et al., 2013; Zhang et al., 2017).

The aim of the present study is to have a deeper understanding of health effects on human lung cells when exposed to PM under environmental-like conditions. To do so, three fractions of fine PM ($PM_{10-2.5}$, $PM_{2.5-0.25}$ and $PM_{0.25}$) were collected nearby a petrochemical area in the Tarragona County. To have an overview of total toxicity of PM, a cytotoxicity assay was performed after exposing human alveolar cells (A549) to different doses of fine PM fractions ($PM_{2.5-0.25}$ and $PM_{0.25}$). Finally, to have a better insight of health effects of these materials, a metabolomic assay was performed using same cells at low PM doses and mid-term exposure time.

## 2. **Methods**

### *2.1. PM sampling and extraction*

Samples of $PM_{10\text{-}2.5}$, $PM_{2.5\text{-}0.25}$ and $PM_{0.25}$ were collected simultaneously from 2nd to 6th of May 2016 in Perafort (Tarragona province, Spain). This location is settled in a suburban area, where the main PM source in the surrounding is a petrochemical industry located 3 km south-west (**Figure 1**). Samples were collected in three different microenvironments within the village: inside a classroom, inside a living room in a house, and outdoors. The volume of the classroom was 173.25 $m^3$, and 20 students were attending the class while sampling. The house living room had 40.43 $m^3$, and was occupied by three nonsmoking people. No ventilation was registered during the sampling period in none of the indoor environments. Samples were collected onto polycarbonate (PC) filters using two personal cascade impactors (Siotuas$^{TM}$, SKC Inc. Eighty Four, PA, USA) connected to a pump (Leland Legacy, SKC) working simultaneously in every microenvironment at a flow rate of 9 L/min. PC filters were weighted on a microbalance before and after sampling, to elucidate the masses of PM. PM concentrations were then calculated by dividing theses mases by the total sampled volume.

Extraction of $PM_{2.5\text{-}0.25}$ and $PM_{0.25}$ from filters was done according to the protocol previously described (Chapter 3 of the present thesis). In brief, filters were submerged into tubes containing deionized water. Then they were shaken for 20 minutes and sonicated during 10 minutes. Subsequently, filters were removed from the tubes, and the supernatant was centrifuged at 3500 rpm. Finally, the tubes were freeze dried and stored at -20ºC until further analysis. Having into consideration that the objective of the present chapter was to assess toxicity of PM within lung cells, $PM_{10\text{-}2.5}$ was not used for toxicology purposes, since this fractions is mostly retained in the upper and tracheobronchial regions of the respiratory tract (Sánchez-Soberón et al., 2015).

**Figure 1**: Sampling location

### *2.2. Children activity pattern:*

To calculate real dose inhaled by children it is necessary to know the physical activities performed in every microenvironment as well as the duration of these activities. To get that information, 20 students attending the sampling room were asked to explain how their daily routine was. Once this information was obtained we classified their routine into 6 different activities: heavy exercise outdoors, light exercise outdoors, light exercise at home, sitting at school, sitting at home, and sleeping time. This last activity was considered as fully performed at home.

### *2.3. Calculation of real doses*

Using PM levels and kids activity patter as inputs, we calculated the deposition of the two PM fractions within three regions of the respiratory tract (Head, Tracheobronchial (TB), and Pulmonary (P)) by the use of a dosimetry model (MPPD v 2.11 (ARA, 2014)). Simulation was conducted for an 8 years old kid having a total alveolar air-tissue interface of 32 m² (Dunnill, 1962). Values of the rest of parameters needed for the simulation were remained as described previously (Chapter 4 of this thesis).

### *2.4. Cell line and cytotoxicity assay:*

Lung carcinoma cells A549 (ATCC® CCL-185™) were used in this study. These cells have been extensively used in toxicity of lung cells (L. Cao et al., 2015a; Xu et al., 2013). To study the cytotoxicity of collected PM, an MTT assay was performed (Roig et al., 2013). Cells were grown in Dulbecco's Modified Eagle's Medium, supplemented with 10 % inactivated Fetal Bovine Serum and 1 % penicillin in an incubator at 37 °C, 5 % $CO_2$ and saturating humidity. Following manufacturer recommendations, cells were seeded at a concentration of $4\times10^3$ cells/$cm^2$ in 96-well plates. After 48 h, cell medium was absorbed, and replenished with fresh medium containing different concentrations of PM. (500, 100, 50, 10, 5, 1, 0.5 and 0.1 µg/mL). Four replicates were used for every concentration, including negative controls. After exposure, cells were left in contact with the medium containing the particles during 72 h.

After exposure, MTT reagent [3-(4,5-dimethylthiazol-2-yl)-2,5-diphenyltetrazolium bromide] was added to the wells to a final concentration of 5 %. Then, samples were incubated until purple precipitate was visible (from 2 to 4 hours). Subsequently, detergent was added to a final concentration of 50% and samples were left in dark for 2 hours. Absorbance was then measured at 570 nm using an Epoch 2 microplate spectrophotometer (BioTek, USA). To ensure reproducibility of the procedure, this experiment was done twice. $LC_5$ doses were calculated by calculating a biphasic equation from the dose-response scatter plot using the software Dr. Fit (Di Veroli et al., 2015).

### *2.5. Exposure strategy and metabolite extraction:*

Cells were seeded and grown in 4.2 $cm^2$ chamber slides under the same conditions described for the cytotoxicity assay. After 48 hours of cell proliferation, medium was extracted, and cells were exposed to media containing solutions of the two PM fractions. Chamber slides were randomly provided with these solutions under three exposure conditions: $PM_{2.5-0.25}$, $PM_{0.25}$ and control. Six replicates were done for every PM group. Three independent experiments were conducted: one experiment where the real dose was applied and two experiments where the $LC_5$ was applied.

To extract metabolites, we followed procedures previously published (Cuykx et al., 2017). In brief, after 72 hours of exposure, cells were washed twice with PBS and cell metabolism was quenched by submerging cells into liquid nitrogen. Chamber slides were then scraped three times with 200 µL of 80% (v/v) methanol (MeOH)/MilliQ-water and the content was transferred to a vial containing 420 µL of chloroform and 500 µL of milliQ-water, having a final solvent ratio of 2/3/2 water/MeOH/$CHCl_3$. The vials were then spiked with internal standards: 200 ng cholesterol-d4, and 100 ng TEHP and lauric acid-d3 for non-polar fraction, and 200 ng tryptophane-d5 and succinic acid-d4 for the polar fraction. Vials were then vortexed three times for 30 seconds, and equilibrated for 10 minutes at 4 °C. Subsequently they were centrifuged at 3500 rpm during 7 minutes. After this, two phases were present in the vial: an upper polar phase and a lower non polar phase, separated by a protein disk. Upper phase was transferred to pre cooled Eppendorf tubes, while lower phase was transferred to vials containing chloroform. Quality control (QC) pools for polar compounds were made by pouring 20 µl of each sample in 4 Eppendorfs. QC for non-polar fraction were made by pouring 20 µl of each sample into 2 vials. Samples and QC were then evaporated with nitrogen (non-polar phase) or using a rotavap for 2.5 hours (polar phase). Both, polar and non-polar samples were stored at -80ºC prior to analysis.

## *2.6. Metabolomics Set-up:*

### 2.6.1.Non-polar fraction, positive ionization mode

Cell extracts were reconstituted using 35/65 isopropanol (IPA)/MeOH. Liquid Chromatography separation was undertaken using a Kinetex XB-C18 100 Å (150 × 2.1 mm; 1.7 µm particle size) RP-column. A buffer solution comprising 10 mM ammonium acetate ($NH_4Ac$) and 0.1% acetic acid (HAc) in milliQ water (pH 4.2) was added to mobile phases to keep their pH stable. Two mobile phases were used: mobile phase A was composed of Acetonitrile (ACN)/buffer (1/1), mobile phase B was made of 2/10/88 buffer/ACN/IPA. Elution took 40 min per sample, and the procedure was developed as follows: first, 55% of phase B was run for 1 min. Subsequently, contribution of phase B was increased to 70% at 5 min, and 98% at 25 mins. Then, a 4 min rinse at 100% of phase B was performed. Finally, starting conditions were set again for 9 min to equilibrate the column. Column temperature was set at 55 ºC, and flow rate remained constant at 0.25 mL/min. MS drying gas temperature (325 °C) and flow (8 L/min) were constant during the entire run. Capillary, nozzle and fragmentor voltage were 3500 V, 500 V and 175 V, respectively.

### 2.6.2.Non-polar fraction, negative ionization mode

Cell reconstitution and column used were the same as described for positive ionization mode. In this case, mobile phase A was composed of 1/1 MeOH and 10 mM $NH_4Ac$ in milliQ water to reach a pH of 6.7, and mobile phase B comprised 10 mM NH4Ac in milliQ water/MeOH/IPA (2/10/88). Elution was performed gradually, starting by running 55% of phase B for 1 min, and increasing it to 70% B at 5 min. Afterwards, percentage of B was augmented to 91% at 20 min and 6 min rinse at 100% B to complete the analytical separation. Re-equilibration of the column consisted in applying starting conditions for 9 min. Column temperature and flow remained equal as in positive ionization mode (55 °C and 0.25 mL/min. respectively). MS source conditions were constant during the entire run: drying gas temperature and flow were 350 °C and 8 L/min respectively. Capillary, nozzle and fragmentor voltage were 3750 V, 0 V and 175 V, respectively. After 21 min, the capillary and nozzle voltage were slightly altered to 3500 V and 500 V, respectively.

#### 2.6.3.Polar fraction, positive ionization mode

Cells extract were solubilized in 60% ACN. An iHILIC Fusion (100 × 2.1 mm; 1.8 µm particle size) column was used at 30ºC. Mobile phase A was made of 10 mM ammonium formate ($NH_4F$) and 0.1% formic acid (FA) v/v till reaching a pH of 3.15. Mobile phase B was made of ACN/MeOH (98/2, v/v). Flow rate was set at 0.3 mL/min. Elution started with 95% of phase B. Two minutes later, contribution of phase B decreased linearly to 65% at 8 min. A further decrease till 25% was experienced at 13 min, and a rinse was performed using 25% of phase B for 2 mins. Finally, the column was re-equilibrated at starting conditions during 6 min. Regarding MS, drying gas parameters (250ºC; 8 L/min), as well as sheath gas parameters (350ºC; 11 L/min) remained constant during the experiment. Capillary and fragmentor voltages were 2000 V and 150 V, respectively, and the nebulizer was set at 45 psig.

#### 2.6.4. Polar fraction, negative ionization mode

Cells extracts were resuspended in 20% MeOH. A Gemini® Phenyl-hexyl column (150 × 2 mm, 3 µm particle size) was used in this case. To prevent pairing agent contamination of apparatus, an isocratic pump with separate tubing system was used. Mobile phase was made of 25% MeOH with 10 mM tributylamine (TBA) and 0.02% FA (v/v) to a pH of 9. It was pumped through the column at a flow rate of 0.2 mL/min. Runtime was set at 20 min. Drying and sheath gases were set at similar temperature (250ºC) and flow rate (10 L/min). Capillary and fragmentor voltages were 2000 V and 100 V, respectively. The nebulizer was set at 45 psig.

### *2.7. Data treatment:*

Mass-Hunter qualitative software (version 2.06.00, Agilent technologies) was used to evaluate LC and MS parameters. To extract standards from the chromatogram, the “Find by Formula”-algorithm (FBF) was used. Deconvolution algorithm was set to retain peaks having a quality score higher than 80% and abundance greater than 3000. These signals were then grouped into molecular features according to their m/z, retention time, and correspondence to isotopes or adducts. Extracted features represent thus the different m/z signals of a metabolite. Mass Profiler (v12.5, Agilent Technologies) was used to merge data coming from consecutive runs, being the sum of the areas of all ions the dependent value of the variable.

Features present in at least 80 % of the samples were retained for statistical analysis and EZ info were used. Principal Component Analysis (PCA) and Orthogonal Partial Least Squares-Discriminant Analysis (OPLS-DA) techniques were applied to estimate the quality of the dataset and detect molecular features of interest respectively. Welch T tests with Benjamini-Hochberg correction were used to evaluate the significance of differences between exposed and control groups. Differences between control and exposed cells were considered when having a corrected p value smaller than 0.05.

Provisional identification of significant features was performed using Molecular Formula Generator algorithm from Mass-Hunter software. Tentative formulas were calculated having into account a mass error of 10 ppm, isotope spacing of 5 ppm, and a maximal 5 % difference in abundance compared to the calculated isotopic pattern. To find structures for these features, a search was performed in LipidMaps, Metlin, and Human Metabolome Database (HMDB) (Fahy et al., 2007; Smith et al., 2005; Wishart et al., 2013).

## 3. Results and discussion

### *3.1. PM levels and time activity pattern:*

Concentrations of the three PM fractions measured in the different microenvironments can be seen in Figure 2. Average daily concentrations of PM were below the threshold set by the European legislation (EU Parliament, 2008). Classroom registered the highest concentrations for every PM fraction, while home registered the lowest. These results could be highly related with the occupancy of these microenvironments. The higher the human activity, the greater the resuspension and contribution of organic PM (textile fibers and skin debris) (Serfozo et al., 2014; Viana et al., 2014). The low occupancy at home, joined to lack of ventilation and absence of other indoor sources in the room (i.e. tobacco, gas stove) could be the cause of experiencing lower PM levels at home than outdoors (Romagnoli et al., 2015).

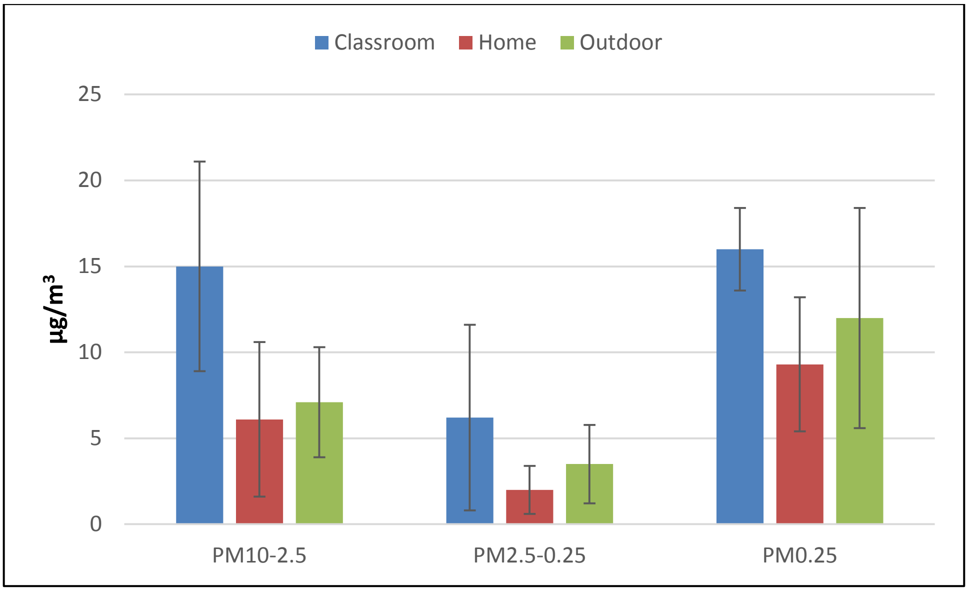

**Figure 2:** Average levels of PM within the three microenvironments. Error bars denote standard deviations.

Regarding time activity patterns, share of time spent by alums in the different microenvironments and performing the different activities can be seen on Figure 3:

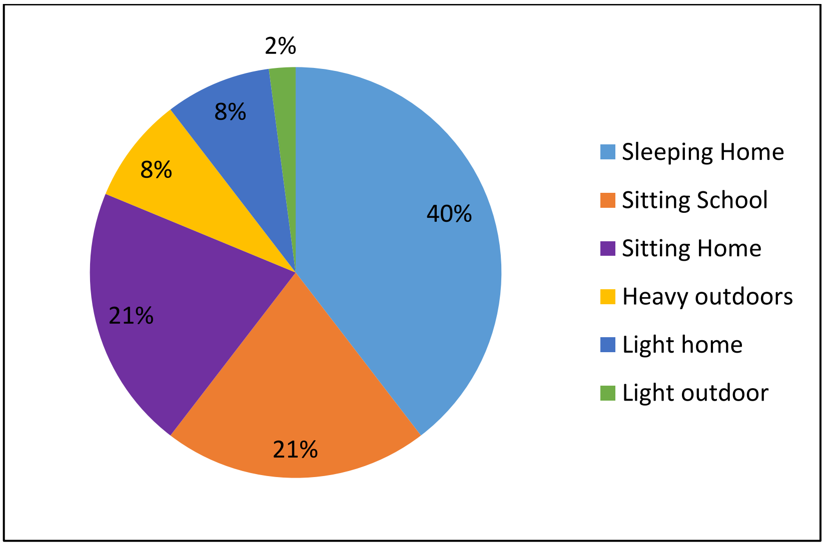

**Figure 3**: Average daily share of time of the students attending to the school

Kids spent most of their time (90%) indoors, while outdoor time is mostly used in heavy intensity activities. The most time demanding activity was sleeping, while same share of time was spent sitting in school and at home. Results obtained in the present study were similar to those obtained by other researchers in western countries (Cohen Hubal et al., 2000; Matz et al., 2015).

### *3.2. Deposition pattern of particles and real dose calculation:*

Daily deposited mass of the three sampled PM fractions can be seen in Table 1. Regardless of PM fraction, the head was region registering the highest deposition masses. The PM fraction registering the highest overall deposition masses was PM10-2.5. This fraction registered most its deposition in the tracheobronchial and head regions of the respiratory tract, while, as seen in previous studies, the amount of coarse particles reaching the lung were minor (Sánchez-Soberón et al., 2015). Despite the scarce amount of time spent outdoor performing high intensity activities (2 hours per day), this activity reached the highest share of $PM_{10\text{-}2.5}$ deposition. Fine fractions ($PM_{2.5\text{-}0.25}$ and $PM_{0.25}$) followed a different trend. Between 30 and 40 % of the total deposited mass of these fractions was addressed in the lung. However, heavy intensity deposition is maximum in every region of the respiratory tract for $PM_{0.25}$, while $PM_{2.5\text{-}0.25}$ reaches its maximum deposition in lung during class time.

**Table 1:** Daily deposited doses calculated for every PM fraction, activity, and respiratory region (µg/day).

| | | **$PM_{10\text{-}2.5}$** | | | **$PM_{2.5\text{-}0.25}$** | | | **$PM_{0.25}$** | | | **Total** |
|---|---|---|---|---|---|---|---|---|---|---|---|
| **Activity** | **Environment** | **Head** | **TB[1]** | **P[2]** | **Head** | **TB[1]** | **P[2]** | **Head** | **TB[1]** | **P[2]** | |
| Sleeping | Home | 11.24 | 5.44 | 0.30 | 1.60 | 0.34 | 2.40 | 4.98 | 1.30 | 5.70 | 33.31 |
| Sitting | Classroom | 18.88 | 8.51 | 0.17 | 3.21 | 0.71 | 4.45 | 5.86 | 1.46 | 6.35 | 49.60 |
| Sitting | Home | 7.55 | 3.41 | 0.07 | 1.07 | 0.24 | 1.48 | 3.30 | 0.82 | 3.57 | 21.50 |
| Light intensity | Home | 10.67 | 2.63 | 0.00 | 1.50 | 1.00 | 0.91 | 4.51 | 1.01 | 3.34 | 25.57 |
| Light intensity | Outdoors | 3.11 | 0.77 | 0.00 | 0.56 | 0.38 | 0.34 | 1.50 | 0.34 | 1.11 | 8.11 |
| Heavy intensity | Outdoors | 24.28 | 4.01 | 0.00 | 3.97 | 6.09 | 0.66 | 11.89 | 2.68 | 6.63 | 60.20 |
| **Total** | | 75.72 | 24.77 | 0.54 | 11.91 | 8.75 | 10.25 | 32.05 | 7.60 | 26.70 | 198.29 |

[1] TB: Tracheobronchial; [2] P: Pulmonary (Lung).

These differences in deposition patterns of the three PM fractions are related to the different levels of PM experienced in every environment, but also by the deposition mechanisms considered in the MPPD model: inertial impaction, sedimentation (gravitational setting), and diffusion (Brown et al., 2013). Impaction and sedimentation are the dominant mechanisms in particles bigger than 1 µm (Salma et al., 2015). These mechanisms are highly dependent on the air speed on the respiratory tract (Hussain et al., 2011). Thus, high air speeds will favor the impaction, while low velocities will favor sedimentation. Furthermore, the bigger the PM the more likely to experience one of these processes. Diffusion mechanism appears in particles smaller than 0.5 µm, which behave similar to gas molecules. Particles within this size follow a Brownian motion, and they deposit by chance (Bakand et al., 2012).

In the first part of the respirator tract, speed of inhaled air reaches the highest velocity within the respiratory tract. Furthermore, as soon as the activity intensity increases, so does the air velocity. Consequently, impaction phenomenon is the dominant deposition mechanism in head region, affecting especially those particles of bigger size during high intensity activities (Hussain et al., 2011). Air passing through tracheobronchial region experiences a deceleration, provoking the sedimentation of the heaviest particles. When reaching terminal areas of the respiratory tract the air's speed is minimum, which apparently could favor sedimentation. But at this point, most of the coarse PM has been already deposited, and diffusion mechanism becomes majoritarian (CCOHS, 2010).

Having into account these results, after 72 h the amount of $PM_{2.5\text{-}0.25}$ and $PM_{0.25}$ deposited into the lungs were 30.75 and 80.11 µg respectively. These doses correspond to $2.69{\cdot}10^{-4}$ and $7.01{\cdot}10^{-4}$ µg of particles per mL of culture media for $PM_{2.5\text{-}0.25}$ and $PM_{0.25}$ respectively.

### *3.3. Cytotoxicity:*

Dose-response plot graph, as well as fitting equations for both PM fractions can be seen in Figure 4. Biphasic decay was the best fitting equation for our data, so it was chosen to calculate the concentration corresponding to 5% of mortality ($LC_5$). In our case it is possible to see that the smaller PM fraction provokes a higher toxicity, especially when applying doses ranging from 0.5 to 10 µg/mL. Consequently, $LC_5$ for $PM_{0.25}$ was lower than for $PM_{2.5\text{-}0.25}$ (0.00808 and 0.07370 µg/mL respectively). This trend of a higher toxicity of smaller PM has been reported before (L. Cao et al., 2015b; Guan et al., 2016; Zou et al., 2017). In fact, this reduction in the size is related with a greater surface area, which can, independently from chemical composition, induce higher damage to cells (Kelly and Fussell, 2012).

Comparing our result with previous research is complicate. Few studies have been developed to evaluate the cytotoxicity of A549 cells after 72 h exposure to PM, and to our best knowledge, none of them has divided $PM_{2.5}$ into two fractions as we have done. Ho et al. (2016) obtained toxicity values (i.e. $LC_{50}$) similar to those found in the present study after exposing cells to $PM_{2.5}$ from coal burning origin. However, other studies using environmental or household $PM_{2.5}$ lower toxicity than ours (M. Huang et al., 2015; Q. Huang et al., 2015). Apart from differences in the PM fractions here assessed, differences between studies could be the result of different PM chemical composition and shape. Furthermore, the methods used to collect and extract PM, as well as the cell cultivation parameters differs among studies, making it difficult to compare results properly.

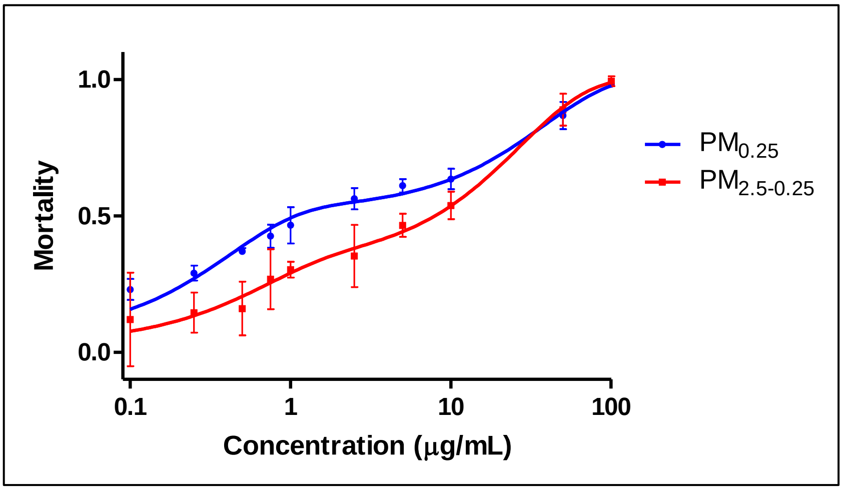

**Figure 4**: Dose-response graph. Two-phase decay was used as fitting curve.

### 3.4. *Metabolomics:*

Regardless of the experiment, around 2000 features were detected in our samples, which are superior to previously found in studies dealing with the same cell line and exposure time (Q. Huang et al., 2015).

#### 3.4.1. *$LC_5$ experiment:*

In the case of $LC_5$ dose we found that cells exposed to $PM_{0.25}$ showed significant differences in the content of 26 metabolites if compared to control cells. Similar number of features (25) showed significant differences after $PM_{2.5-0.25}$ exposition if compared to control. There were also 14 significant differences after the exposition to both fractions (Tables S1 and S2). Despite the number of significant changes in the metabolome is similar regardless of PM fraction exposed, it is important to notice that $LC_5$ values for $PM_{0.25}$ are lower.

Hierarchical clustering analysis of these features, as well as the samples, can be seen in Figure 5. According to this heat map, there is a grouping of samples into two marked groups: exposed and control. At the same time, there are a couple of clusters within the exposed group: one exclusively formed by 5 $PM_{0.25}$ replicates, and the other comprising $PM_{2.5-0.25}$ and the remaining $PM_{0.25}$ replicate. Regarding compounds, it is noted a grouping into two different clusters depending on the overall regulation pattern. The first group contains mostly downregulated features in exposed cells. It comprises cardiolipins (CLs), phosphatidylserines (PSs), and most of phosphatidylcholine (PCs). The second group is mainly formed by the upregulated features, and includes all the identified ceramides (CERs).

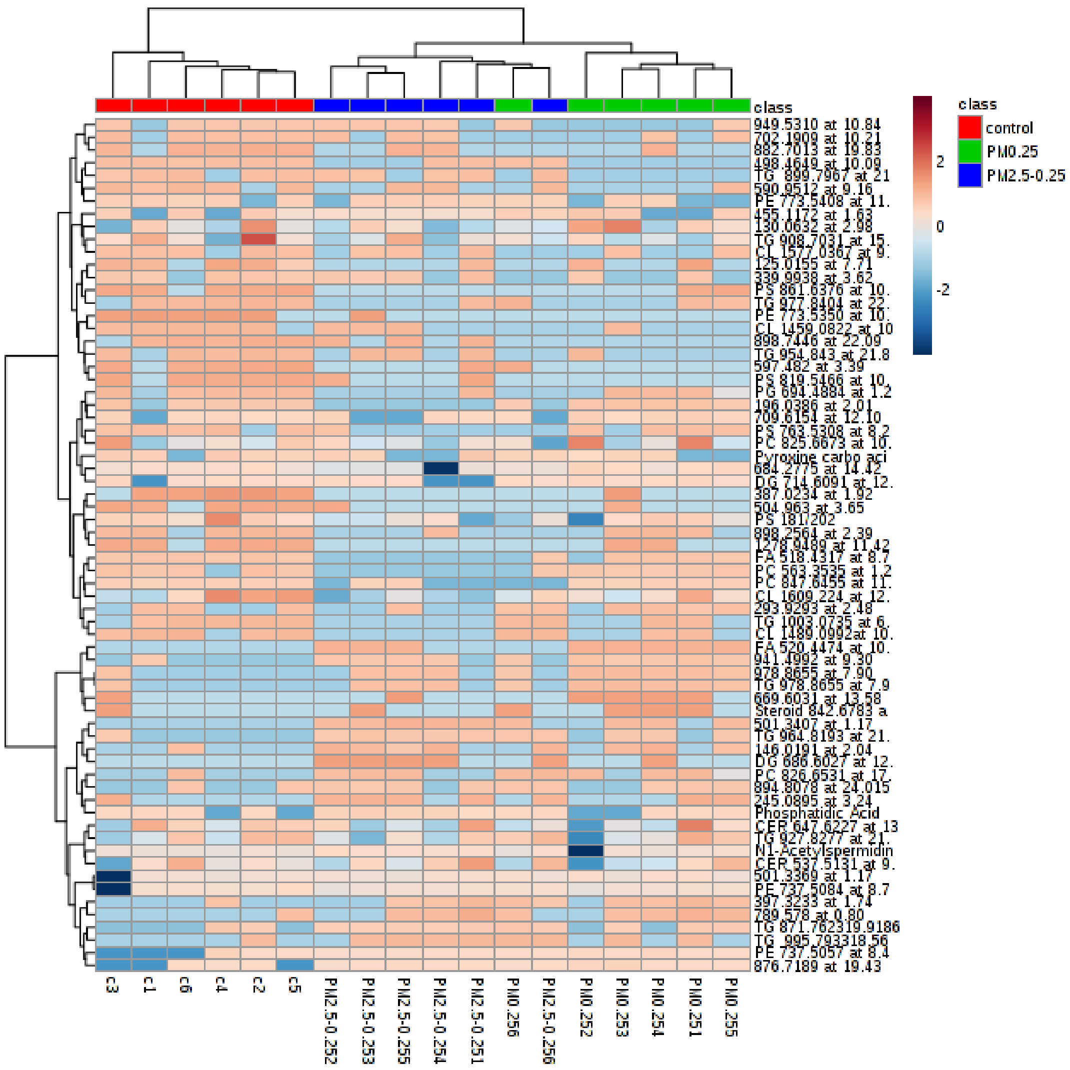

**Figure 5**: Hierarchical clustering heatmap analysis of significative differential metabolites after $LC_5$ exposition.

Regardless of PM fraction applied, most of the altered metabolites were apolar (Table S2). Most of them were triglycerides (TG), CERs, and phospholipids. More specifically, these changes have been detected in the content of PSs, phosphatidylcholines (PCs), PEs, and CLs. These components are majoritarian constituents of cells membranes (Stillwell, 2016). Triglycerides and PCs are also the main components of lung surfactant, a protein-lipid mixture essential to reduce tension at the alveoli air-liquid interphase (Bernhard et al., 2001; Lopez-Rodriguez and Pérez-Gil, 2014).

Under normal conditions, PSs are located in the inner part of the plasma membrane. But in cells undergoing the apoptosis process, these lipids turn to the external face of the cell membrane, sending an "eat-me" signal to macrophages in order to be phagocyted (Segawa and Nagata, 2015). Consequently, these substances have been studied as biomarkers of different diseases, such as cancer (Sharma and Kanwar, 2017). Although we were not able to locate where in the cell membrane PSs were, we noticed a downregulation of this group of compounds in both ($PM_{2.5-0.25}$ and $PM_{0.25}$) exposed groups.

Phosphatidylethanolamines (PEs) play a significant role in membrane fusion and division, apoptosis, and autophagy (Pavlovic and Bakovic, 2013). As in the case of PSs, our results show significant downregulation in the content of most PEs regardless of PM fraction applied. However, a different trend was showed for PCs, the main component of lung surfactant (Bernhard et al., 2001). In our study, changes in the contents of these substances are variable. While cells exposed to $PM_{0.25}$ showed an overall upregulation in PC content, those cells exposed to $PM_{2.5-0.25}$ showed an overall downregulation. This size related response in PC regulation has been previously reported in other studies (Chen et al., 2014; Juvin et al., 2002; Wang et al., 2017).

PCs and PEs are mainly generated via a couple of mechanisms: de novo or from PS decarboxylation (Figure 6)(Bleijerveld et al., 2007; Vance, 2008). In de-novo pathway, PEs and PCs are generated from ethanolamine and choline respectively after undergone three subsequent steps (phosphorylation, combination with cytidine diphosphate, and a final addition of two fatty acids) known as the Kennedy pathway (Gibellini and Smith, 2010). The other pathway consists on the transformation of PS to PE via decarboxylation. This PE can be then transformed into PC by the action of phosphatidylethanolamine N-methyltransferase (PEMT) (Zinrajh et al., 2014).

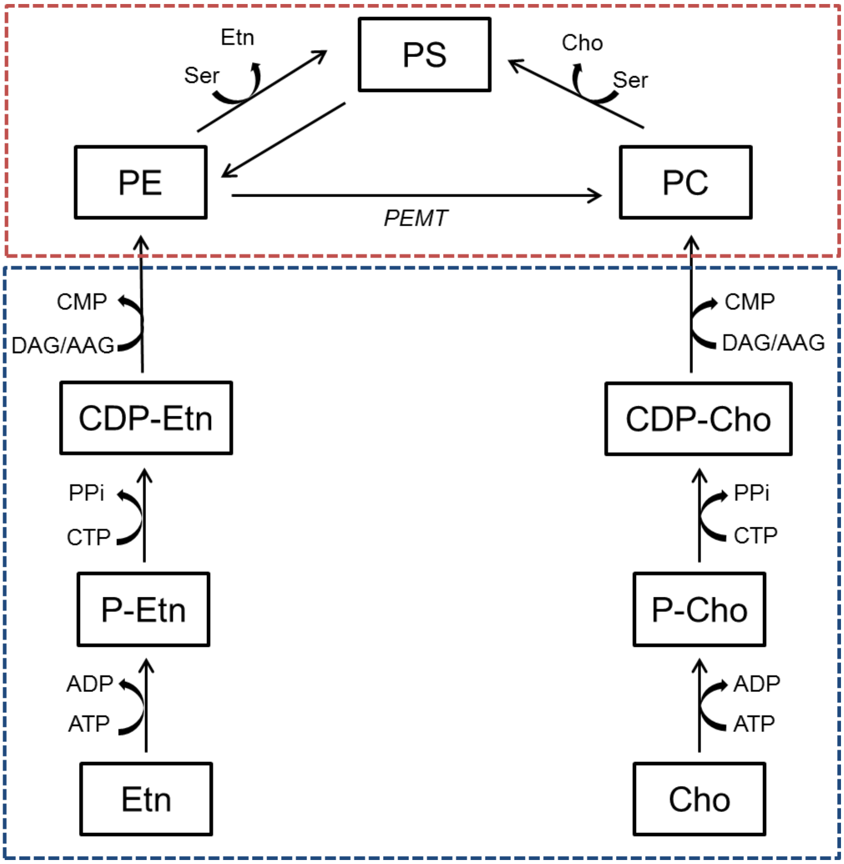

**Figure 6**: PS, PE, and PC metabolism in mammalian cells. Blue dotted line enclose the de-novo synthesis of PE and PC, while red dotted line encompasses the transformations between PE, PS, and PC. Key: Cho, choline; P-Cho, phosphocholine; CDP-Cho, cytidine-diphosphocholine; Etn, ethanolamine; P-Etn, phosphoethanolamine; CDP-Etn, cytidine-diphosphoethanolamine; PC, phosphatidylcholine; PE, phosphatidylethanolamine; PS, phosphatidylserine; DAG, diacylglycerol; AAG, alkyl-acyglycerol; CMP, cytidine-monophosphocholine; PEM, phosphatidylethanolamine N-methyltransferase; PPi, Pyrophosphate; ATP, adenosine triphosphate; ADP, adenosine diphosphate; CTP, cytidine triphosphate; Ser, serine.

According to our results, $PM_{2.5\text{-}0.25}$ seems to have a bigger effect on de novo pathway, affecting the synthesis of PCs and PEs, which consequently affects the levels of PSs. On the other hand, $PM_{0.25}$ is more likely to affect the PS decarboxylation pathway, increasing the levels of PCs by transforming PSs to PEs, and PEs into PCs. These differences in the way of action between $PM_{2.5\text{-}0.25}$ and $PM_{0.25}$ could be due to differences in physicochemical characteristics between these two fractions.

A downregulation in CLs was patent in this study, regardless of the PM fraction exposed. CLs are almost exclusively localized in the inner mitochondrial membrane (Houtkooper and Vaz, 2008). It improves the ATP generation via oxidative phosphorylation within this organelle, apart from being involved in other mitochondrial processes (Claypool and Koehler, 2012). Particulate matter, and more specifically, its polar toxic constituents have been recognized previously as disruptors of mitochondrial functions (Xia et al., 2004). Although using different kind of cells, Hiura et al. (2000) also recorded a decrease in mitochondrial CLs after exposing mice macrophages to PM. This damage in the mitochondrial membrane could be generated by the particle surface (mechanical damage), or by some of the constituents, leading to a reactive oxygen species generation (von Moos and Slaveykova, 2014).

Ceramides are highly concentrated in cell membranes, and play a significant role in the response to stress stimuli (Bikman and Summers, 2011). The upregulation of these compounds is recognized as a signal of apoptosis, and has been related to several lung diseases (Lee et al., 2015; Petrache et al., 2005). In fact, previous studies have found a clear upregulation in CER content after PM exposures (Peuschel et al., 2012; Zhang et al., 2017). However, in the present study regulations of these substances were variable, and fold changes were slight. Apart from variances in the experiment design (i.e. cell line, PM composition), PM doses applied in the present study were lower than the previously reported papers.

Regarding polar constituents (Table S2), cells exposed to $PM_{2.5-0.25}$ showed an upregulation in N1-Acetylspermidine, a precursor of spermidine (Wishart et al., 2013). Spermidine is involved in regulation of inflammatory reactions, and has been recognized as defense line against reactive oxygen species and DNA protector in lungs (Hoet and Nemery, 2000). On the other hand, cells exposed to $PM_{0.25}$ showed and upregulation in 1-Pyrroline-5-carboxylic acid. This compound is a precursor, among others, of L-proline, which is able to generate specific reactive oxygen species (ROS) acting as signals for tumor suppression, apoptosis and cell survival (Liang et al., 2013; Wishart et al., 2013). Furthermore, proline metabolism can be used as a source of energy under stress conditions within cells (Phang et al., 2015).

### 3.4.2. *Real dose experiment:*

In case of those cultures exposed to PM real dose, we found that the number of total features had been reduced to next numbers: 10 for $PM_{0.25}$ and 5 for $PM_{2.5-0.25}$ (Tables S3 and S4). The number of features affected after LC5 exposure was higher, which is expectable if we have into account that $LC_5$ dose was two orders of magnitude higher than real dose. It is also important to note, that number of significant features after $LC_5$ application were similar for the two PM fractions, while after applying real dose this number is higher for $PM_{0.25}$. Since $LC_5$ dose is response dependent it is plausible that under same responses, similar changes are expected. However, under real conditions, $PM_{0.25}$ doses are higher than $PM_{2.5\text{-}0.25}$, and consequently it is expected a higher effect of these particles onto the cells.

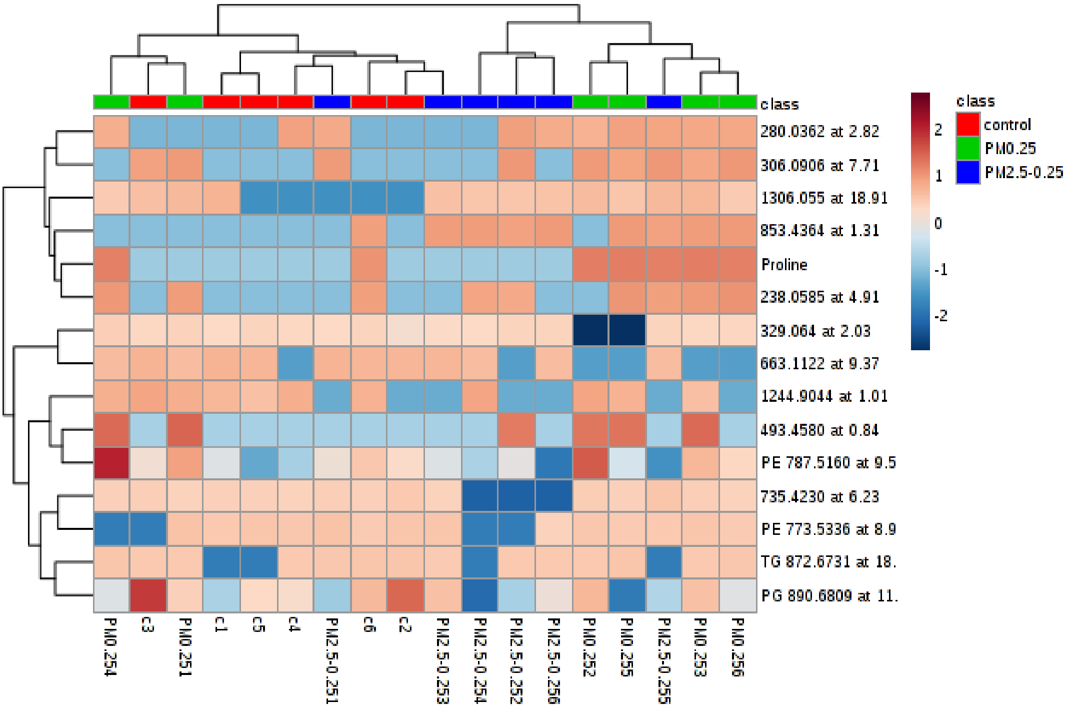

**Figure 7**: Hierarchical clustering heatmap analysis of significative differential metabolites after real dose exposition.

As shown in Figure 7, hierarchical grouping of replicates is not as marked as after $LC_5$ application. Replicates are distributed into two groups: the first comprising exposed cells of both PM fractions, while the second comprises a mix of exposed and control cells. Nevertheless, a plausible tendency in sample distribution can be drawn: $PM_{0.25}$ trend to stay at right, $PM_{2.5\text{-}0.25}$ remain in the center, and control to the left. There is also a grouping in compounds: in a first group it is possible to differentiate those features upregulated in the exposed cells, while the second group comprises those compounds showing more timid fold changes.

Contrary to the LC5 experiment, number of affected features after PM0.25 exposure was higher for polar (7) than for non-polar (3), which could reveal less intensive effects on cell membranes. Cells exposed to $PM_{0.25}$ experienced an upregulation in the content of most altered metabolites, such as proline, TGs, and PEs. These results could indicate that cells are undergoing a hormesis phase, in which cells are activated as a consequence of being exposed to low doses of toxic agents (Zimmermann et al., 2014). Cells exposed to $PM_{2.5-0.25}$ showed an overall decrease in the altered metabolites. Slight downregulations were noticed for PEs and phosphatidylglycerols (PGs), one of the constituents of lung surfactant and also present at small scale in cell membranes (Stillwell, 2016). However, as pointed out previously, the number of altered metabolites in this experiment was small, showing a higher fold change variability among same exposure group replicates.

Finally, it should be pointed out the effect of the dosage strategy into cell response. In the present study we decided to apply a single dose, instead of applying several time-distributed doses, at could be the case under real conditions. Previous in-vivo studies exposing rats to nickel oxides PM found that single dose effects were less toxic, while others applying silica PM did not find significant differences between different dosing strategies (Reasor and Antonini, 2000; Senoh et al., 2017). However, to the best of our knowledge, there are not papers studying this issue for A549 cells, and the possible effects derived from dosage strategy in this paper should be assessed in future research.

## 4. Conclusions

Three fractions of PM ($PM_{0.25}$, $PM_{2.5-0.25}$, and $PM_{10-2.5}$) were collected in three environments (outdoor, classroom, and home) within a village located nearby a petrochemical complex. At the same time, time activity pattern of 20 students attending to the aforementioned school were obtained to study the exposure and depositon of PM within the children's respiratory tract. Afterwards, these particles were extracted from filters and put in contact with alveolar cells (A549) to study the cytotoxicity and changes in the metabolic profile after 72 h exposure. Classroom microenvironment registered the highest levels of every PM fraction collected, due to its higher occupancy. Regardless of PM fraction, the upper respiratory tract (head) was the region that retained most of the overall deposited mass, especially when performing heavy intensity activities. Since the mass of $PM_{10-2.5}$ reaching the pulmonary region was minor, it was decided to perform toxicity assays with $PM_{2.5-0.25}$ and $PM_{0.25}$. The finest fraction ($PM_{0.25}$) elicited a higher cytotoxicity than $PM_{2.5-0.25}$. The number of metabolites affected by particles exposure was similar for both fractions in $LC_5$ doses, while after applying real doses changes were mainly due to $PM_{0.25}$. These changes were mostly in compounds dealing with cell and mitochondrial membrane functions, revealing the potential of PM to elicit both extracellular and intracellular damage. The methodology here described has proven to be powerful to elicit toxicity of environmental pollutants under real life conditions.

## References

Akhtar, U.S., McWhinney, R.D., Rastogi, N., Abbatt, J.P.D., Evans, G.J., Scott, J.A., 2010. Cytotoxic and proinflammatory effects of ambient and source-related particulate matter (PM) in relation to the production of reactive oxygen species (ROS) and cytokine adsorption by particles. Inhal. Toxicol. 22 Suppl 2, 37–47. doi:10.3109/08958378.2010.518377

ARA, 2014. ARA :: Products :: MPPD [WWW Document]. URL http://www.ara.com/products/mppd.htm (accessed 8.24.15).

Bakand, S., Hayes, A., Dechsakulthorn, F., 2012. Nanoparticles: a review of particle toxicology following inhalation exposure. Inhal. Toxicol. 24, 125–135.

Bernhard, W., Hoffmann, S., Dombrowsky, H., Rau, G.A., Kamlage, A., Kappler, M., Haitsma, J.J., Freihorst, J., von der Hardt, H., Poets, C.F., 2001. Phosphatidylcholine Molecular Species in Lung Surfactant. Am. J. Respir. Cell Mol. Biol. 25, 725–731. doi:10.1165/ajrcmb.25.6.4616

Bikman, B.T., Summers, S.A., 2011. Ceramides as modulators of cellular and whole-body metabolism. J. Clin. Invest. doi:10.1172/JCI57144

Bleijerveld, O.B., Brouwers, J.F.H.M., Vaandrager, A.B., Helms, J.B., Houweling, M., 2007. The CDP-ethanolamine Pathway and Phosphatidylserine Decarboxylation Generate Different Phosphatidylethanolamine Molecular Species. J. Biol. Chem. 282, 28362–28372. doi:10.1074/jbc.M703786200

Brown, J.S., Gordon, T., Price, O., Asgharian, B., 2013. Thoracic and respirable particle definitions for human health risk assessment. Part. Fibre Toxicol. 10, 12. doi:10.1186/1743-8977-10-12

Cao, L., Zeng, J., Liu, K., Bao, L., Li, Y., 2015a. Characterization and Cytotoxicity of PM<0.2, PM0.2-2.5 and PM2.5-10 around MSWI in Shanghai, China. Int. J. Environ. Res. Public Health 12, 5076–5089. doi:10.3390/ijerph120505076

Cao, L., Zeng, J., Liu, K., Bao, L., Li, Y., 2015b. Characterization and Cytotoxicity of PM<0.2, PM0.2–2.5 and PM2.5–10 around MSWI in Shanghai, China. Int. J. Environ. Res. Public Health 12, 5076–5089. doi:10.3390/ijerph120505076

Cao, X., Lin, H., Muskhelishvili, L., Latendresse, J., Richter, P., Heflich, R.H., 2015. Tight junction disruption by cadmium in an in vitro human airway tissue model. Respir. Res. 16, 30. doi:10.1186/s12931-015-0191-9

CCOHS, 2010. How Do Particulates Enter the Respiratory System? [WWW Document]. Can. Cent. Occup. Heal. Saf. URL https://www.ccohs.ca/oshanswers/chemicals/how_do.html (accessed 1.4.18).

Chen, W.-L., Lin, C.-Y., Yan, Y.-H., Cheng, K.T., Cheng, T.-J., 2014. Alterations in rat pulmonary phosphatidylcholines after chronic exposure to ambient fine particulate matter. Mol. BioSyst. 10, 3163–3169. doi:10.1039/C4MB00435C

Claypool, S.M., Koehler, C.M., 2012. The complexity of cardiolipin in health and disease. Trends Biochem. Sci. 37, 32–41. doi:10.1016/j.tibs.2011.09.003

Cohen Hubal, E.A., Sheldon, L.S., Burke, J.M., McCurdy, T.R., Berry, M.R., Rigas, M.L., Zartarian, V.G., Freeman, N.C., 2000. Children's exposure assessment: a review of factors influencing Children's exposure, and the data available to characterize and assess that exposure. Environ. Health Perspect. 108, 475–486.

Cuykx, M., Mortelé, O., Rodrigues, R.M., Vanhaecke, T., Covaci, A., 2017a. Optimisation of in vitro sample preparation for LC-MS metabolomics applications on HepaRG cell cultures. Anal. Methods 9, 3704–3712. doi:10.1039/C7AY00573C

Cuykx, M., Negreira, N., Beirnaert, C., Van den Eede, N., Rodrigues, R., Vanhaecke, T., Laukens, K., Covaci, A., 2017b. Tailored liquid chromatography–mass spectrometry analysis improves the coverage of the intracellular metabolome of HepaRG cells. J. Chromatogr. A 1487, 168–178. doi:10.1016/j.chroma.2017.01.050

Di Veroli, G.Y., Fornari, C., Goldlust, I., Mills, G., Koh, S.B., Bramhall, J.L., Richards, F.M., Jodrell, D.I., 2015. An automated fitting procedure and software for dose-response curves with multiphasic features. Sci. Rep. 5, 14701. doi:10.1038/srep14701

Donahue, N.M., Posner, L.N., Westervelt, D.M., Li, Z., Shrivastava, M., Presto, A.A., Sullivan, R.C., Adams, P.J., Pandis, S.N., Robinson, A.L., Donahue, N.M., Posner, L.N., Westervelt, D.M., Li, Z., Shrivastava, M., Presto, A.A., Sullivan, R.C., Adams, P.J., Pandis, S.N., Robinson, A.L., 2016. Where Did This Particle Come From? Sources of Particle Number and Mass for Human Exposure Estimates, in: Hester, R.E., Harrison, R.M., Querol, X. (Eds.), Airborne Particulate Matter: Sources, Atmospheric Processess and Health. pp. 35–71. doi:10.1039/9781782626589-00035

Dunnill, M.S., 1962. Postnatal Growth of the Lung. Thorax 17, 329–333. doi:10.1136/thx.17.4.329

EU Parliament, 2008. Directive 2008/50/EC of the European Parliament and of the Council of 21 May 2008 on ambient air quality and cleaner air for Europe. Off. J. Eur. Communities. 152, 1–44.

Fahy, E., Sud, M., Cotter, D., Subramaniam, S., 2007. LIPID MAPS online tools for lipid research. Nucleic Acids Res. 35, W606–12. doi:10.1093/nar/gkm324

Gibellini, F., Smith, T.K., 2010. The Kennedy pathway-De novo synthesis of phosphatidylethanolamine and phosphatidylcholine. IUBMB Life 62, n/a–n/a. doi:10.1002/iub.337

Guan, L., Rui, W., Bai, R., Zhang, W., Zhang, F., Ding, W., 2016. Effects of Size-Fractionated Particulate Matter on Cellular Oxidant Radical Generation in Human Bronchial Epithelial BEAS-2B Cells. Int. J. Environ. Res. Public Health 13, 483. doi:10.3390/ijerph13050483

Hiura, T.S., Li, N., Kaplan, R., Horwitz, M., Seagrave, J.-C., Nel, A.E., 2000. The Role of a Mitochondrial Pathway in the Induction of Apoptosis by Chemicals Extracted from Diesel Exhaust Particles. J. Immunol. 165, 2703–2711.

doi:10.4049/jimmunol.165.5.2703

Ho, K.F., Chang, C.C., Tian, L., Chan, C.S., Musa Bandowe, B.A., Lui, K.H., Lee, K.Y., Chuang, K.J., Liu, C.Y., Ning, Z., Chuang, H.C., 2016. Effects of polycyclic aromatic compounds in fine particulate matter generated from household coal combustion on response to EGFR mutations in vitro. Environ. Pollut. 218, 1262–1269. doi:10.1016/j.envpol.2016.08.084

Hoet, P.H., Nemery, B., 2000. Polyamines in the lung: polyamine uptake and polyamine-linked pathological or toxicological conditions. Am. J. Physiol. Lung Cell. Mol. Physiol. 278, L417–33.

Horgan, R.P., Kenny, L.C., 2011. "Omic" technologies: genomics, transcriptomics, proteomics and metabolomics. Obstet. Gynaecol. 13, 189–195. doi:10.1576/toag.13.3.189.27672

Houtkooper, R.H., Vaz, F.M., 2008. Cardiolipin, the heart of mitochondrial metabolism. Cell. Mol. Life Sci. 65, 2493–2506. doi:10.1007/s00018-008-8030-5

Huang, M., Kang, Y., Wang, W., Chan, C.Y., Wang, X., Wong, M.H., 2015. Potential cytotoxicity of water-soluble fraction of dust and particulate matters and relation to metal(loid)s based on three human cell lines. Chemosphere 135, 61–66. doi:10.1016/j.chemosphere.2015.04.004

Huang, Q., Zhang, J., Luo, L., Wang, X., Wang, X., Alamdar, A., Peng, S., Liu, L., Tian, M., Shen, H., 2015. Metabolomics reveals disturbed metabolic pathways in human lung epithelial cells exposed to airborne fine particulate matter. Toxicol. Res. 4, 939–947. doi:10.1039/C5TX00003C

Hussain, M., Madl, P., Khan, A., 2011. Lung deposition predictions of airborne particles and the emergence of contemporary diseases, Part-I. Health (Irvine. Calif). 2, 51–59.

Juvin, P., Fournier, T., Grandsaigne, M., Desmonts, J.-M., Aubier, M., 2002. Diesel particles increase phosphatidylcholine release through a NO pathway in alveolar type II cells. Am. J. Physiol. - Lung Cell. Mol. Physiol. 282, L1075–L1081. doi:10.1152/ajplung.00213.2001

Kelly, F., Fussell, J., 2016. Health Effects of Airborne Particles in Relation to Composition, Size and Source, in: Airborne Particulate Matter: Sources, Atmospheric Processess and Health. pp. 344–372.

Kelly, F.J., Fussell, J.C., 2012. Size, source and chemical composition as determinants of toxicity attributable to ambient particulate matter. Atmos. Environ. 60, 504–526. doi:10.1016/j.atmosenv.2012.06.039

Kim, K.H., Kabir, E., Kabir, S., 2015. A review on the human health impact of airborne particulate matter. Environ. Int. 74, 136–143.

Lee, J., Yeganeh, B., Ermini, L., Post, M., 2015. Sphingolipids as cell fate regulators in lung development and disease. Apoptosis 20, 740–757. doi:10.1007/s10495-015-1112-6

Liang, X., Zhang, L., Natarajan, S.K., Becker, D.F., 2013. Proline mechanisms of stress survival. Antioxid. Redox Signal. 19, 998–1011. doi:10.1089/ars.2012.5074

Líbalová, H., Uhlířová, K., Kléma, J., Machala, M., Šrám, R.J., Ciganek, M., Topinka, J., 2012. Global gene expression changes in human embryonic lung fibroblasts induced by organic extracts from respirable air particles. Part. Fibre Toxicol. 9, 1. doi:10.1186/1743-8977-9-1

Longhin, E., Capasso, L., Battaglia, C., Proverbio, M.C., Cosentino, C., Cifola, I., Mangano, E., Camatini, M., Gualtieri, M., 2016. Integrative transcriptomic and protein analysis of human bronchial BEAS-2B exposed to seasonal urban particulate matter. Environ. Pollut. 209, 87–98. doi:10.1016/j.envpol.2015.11.013

Lopez-Rodriguez, E., Pérez-Gil, J., 2014. Structure-function relationships in pulmonary surfactant membranes: From biophysics to therapy. Biochim. Biophys. Acta - Biomembr. 1838, 1568–1585. doi:10.1016/j.bbamem.2014.01.028

Matz, C.J., Stieb, D.M., Brion, O., 2015. Urban-rural differences in daily time-activity patterns, occupational activity and housing characteristics. Environ. Heal. 14, 88. doi:10.1186/s12940-015-0075-y

Nemmar, A., Holme, J. a, Rosas, I., Schwarze, P.E., Alfaro-Moreno, E., 2013. Recent advances in particulate matter and nanoparticle toxicology: a review of the in vivo and in vitro studies. Biomed Res. Int. 2013, 279371. doi:10.1155/2013/279371

Pavlovic, Z., Bakovic, M., 2013. Regulation of Phosphatidylethanolamine Homeostasis—The Critical Role of CTP:Phosphoethanolamine Cytidylyltransferase (Pcyt2). Int. J. Mol. Sci. 14, 2529–50. doi:10.3390/ijms14022529

Petrache, I., Natarajan, V., Zhen, L., Medler, T.R., Richter, A.T., Cho, C., Hubbard, W.C., Berdyshev, E. V, Tuder, R.M., 2005. Ceramide upregulation causes pulmonary cell apoptosis and emphysema-like disease in mice. Nat. Med. 11, 491–498. doi:10.1038/nm1238

Peuschel, H., Sydlik, U., Grether-Beck, S., Felsner, I., Stöckmann, D., Jakob, S., Kroker, M., Haendeler, J., Gotić, M., Bieschke, C., Krutmann, J., Unfried, K., 2012. Carbon nanoparticles induce ceramide- and lipid raft-dependent signalling in lung epithelial cells: A target for a preventive strategy against environmentally-induced lung inflammation. Part. Fibre Toxicol. 9, 48. doi:10.1186/1743-8977-9-48

Phang, J.M., Liu, W., Hancock, C.N., Fischer, J.W., 2015. Proline metabolism and cancer. Curr. Opin. Clin. Nutr. Metab. Care 18, 71–77. doi:10.1097/MCO.0000000000000121

Reasor, M.J., Antonini, J.M., 2000. Pulmonary responses to single versus multiple intratracheal instillations of silica in rats. J. Toxicol. Environ. Heal. - Part A 62, 9–21. doi:10.1080/00984100050201631

Roig, N., Sierra, J., Rovira, J., Schuhmacher, M., Domingo, J.L., Nadal, M., 2013. In vitro tests to assess toxic effects of airborne PM(10) samples. Correlation with metals and chlorinated dioxins and furans. Sci. Total Environ. 443, 791–797. doi:10.1016/j.scitotenv.2012.11.022

Romagnoli, P., Balducci, C., Perilli, M., Vichi, F., Imperiali, a., Cecinato, a., 2015. Indoor air quality at life and work environments in Rome, Italy. Environ. Sci. Pollut. Res. 23, 3503–3516. doi:10.1007/s11356-015-5558-4

Salma, I., Füri, P., Németh, Z., Balásházy, I., Hofmann, W., Farkas, Á., 2015. Lung burden and deposition distribution of inhaled atmospheric urban ultrafine particles as the first step in their health risk assessment. Atmos. Environ. 104, 39–49.

doi:10.1016/j.atmosenv.2014.12.060

Sánchez-Soberón, F., Lawson, M., Wlodarczyk, A.J., Prytherch, Z.C., Jones, T.P., Schuhmacher, M., Bérubé., K.A., Avenue, M., Place, P., 2018. Physicochemistry and toxicity of inhalable particulate matter collected proximal to cement plants. Toxicol. Vitr. in press.

Sánchez-Soberón, F., Mari, M., Kumar, V., Rovira, J., Nadal, M., Schuhmacher, M., 2015. An approach to assess the Particulate Matter exposure for the population living around a cement plant: modelling indoor air and particle deposition in the respiratory tract. Environ. Res. 143, 10–18. doi:10.1016/j.envres.2015.09.008

Segawa, K., Nagata, S., 2015. An Apoptotic “Eat Me” Signal: Phosphatidylserine Exposure. Trends Cell Biol. 25, 639–650. doi:10.1016/j.tcb.2015.08.003

Senoh, H., Kano, H., Suzuki, M., Ohnishi, M., Kondo, H., Takanobu, K., Umeda, Y., Aiso, S., Fukushima, S., 2017. Comparison of single or multiple intratracheal administration for pulmonary toxic responses of nickel oxide nanoparticles in rats. J. Occup. Health 59, 112–121. doi:10.1539/joh.16-0184-OA

Serfozo, N., Chatoutsidou, S.E., Lazaridis, M., 2014. The effect of particle resuspension during walking activity to PM10 mass and number concentrations in an indoor microenvironment. Build. Environ. 82, 180–189. doi:http://dx.doi.org/10.1016/j.buildenv.2014.08.017

Sharma, B., Kanwar, S.S., 2017. Phosphatidylserine: A cancer cell targeting biomarker. Semin. Cancer Biol. doi:10.1016/j.semcancer.2017.08.012

Smith, C.A., O’Maille, G., Want, E.J., Qin, C., Trauger, S.A., Brandon, T.R., Custodio, D.E., Abagyan, R., Siuzdak, G., 2005. METLIN: a metabolite mass spectral database. Ther. Drug Monit. 27, 747–51.

Stillwell, W., 2016. Membrane Polar Lipids, in: An Introduction to Biological Membranes. Elsevier, pp. 63–87. doi:10.1016/B978-0-444-63772-7.00005-1

US EPA, 2016. Basic Information | Particulate Matter | Air & Radiation | US EPA [WWW Document]. URL https://www.epa.gov/pm-pollution/particulate-matter-pm-basics#PM (accessed 5.31.15).

Vaccari, M., Mascolo, M.G., Rotondo, F., Morandi, E., Quercioli, D., Perdichizzi, S., Zanzi, C., Serra, S., Poluzzi, V., Angelini, P., Grilli, S., Colacci, A., 2015. Identification of pathway-based toxicity in the BALB/c 3T3 cell model. Toxicol. Vitr. 29, 1240–1253. doi:10.1016/j.tiv.2014.10.002

Vance, J.E., 2008. Thematic Review Series: Glycerolipids. Phosphatidylserine and phosphatidylethanolamine in mammalian cells: two metabolically related aminophospholipids. J. Lipid Res. 49, 1377–1387. doi:10.1194/jlr.R700020-JLR200

Viana, M., Rivas, I., Querol, X., Alastuey, A., Álvarez-Pedrerol, M., Bouso, L., Sioutas, C., Sunyer, J., 2014. Partitioning of trace elements and metals between quasi-ultrafine, accumulation and coarse aerosols in indoor and outdoor air in schools. Atmos. Environ. 106, 392–401. doi:10.1016/j.atmosenv.2014.07.027

von Moos, N., Slaveykova, V.I., 2014. Oxidative stress induced by inorganic nanoparticles in bacteria and aquatic microalgae – state of the art and knowledge gaps.

Nanotoxicology 8, 605–630. doi:10.3109/17435390.2013.809810

Wang, X., Jiang, S., Liu, Y., Du, X., Zhang, W., Zhang, J., Shen, H., 2017. Comprehensive pulmonary metabolome responses to intratracheal instillation of airborne fine particulate matter in rats. Sci. Total Environ. 592, 41–50. doi:10.1016/j.scitotenv.2017.03.064

Wheelock, C.E., Goss, V.M., Balgoma, D., Nicholas, B., Brandsma, J., Skipp, P.J., Snowden, S., Burg, D., D'Amico, A., Horvath, I., Chaiboonchoe, A., Ahmed, H., Ballereau, S., Rossios, C., Chung, K.F., Montuschi, P., Fowler, S.J., Adcock, I.M., Postle, A.D., Dahlén, S.-E., Rowe, A., Sterk, P.J., Auffray, C., Djukanovic, R., 2013. Application of 'omics technologies to biomarker discovery in inflammatory lung diseases. Eur. Respir. J. 42, 802–825. doi:10.1183/09031936.00078812

WHO, 2014. WHO | Ambient (outdoor) air quality and health [WWW Document]. WHO. URL http://www.who.int/mediacentre/factsheets/fs313/en/ (accessed 6.21.16).

Wishart, D.S., Jewison, T., Guo, A.C., Wilson, M., Knox, C., Liu, Y., Djoumbou, Y., Mandal, R., Aziat, F., Dong, E., Bouatra, S., Sinelnikov, I., Arndt, D., Xia, J., Liu, P., Yallou, F., Bjorndahl, T., Perez-Pineiro, R., Eisner, R., Allen, F., Neveu, V., Greiner, R., Scalbert, A., 2013. HMDB 3.0--The Human Metabolome Database in 2013. Nucleic Acids Res. 41, D801–D807. doi:10.1093/nar/gks1065

Xia, J., Wishart, D.S., 2016. Using metaboanalyst 3.0 for comprehensive metabolomics data analysis. Curr. Protoc. Bioinforma. 2016, 14.10.1–14.10.91. doi:10.1002/cpbi.11

Xia, T., Korge, P., Weiss, J.N., Li, N., Venkatesen, M.I., Sioutas, C., Nel, A., 2004. Quinones and Aromatic Chemical Compounds in Particulate Matter Induce Mitochondrial Dysfunction: Implications for Ultrafine Particle Toxicity. Environ. Health Perspect. 112, 1347–1358. doi:10.1289/ehp.7167

Xu, W., Jiang, J., Yang, B., Mei, D., Dai, B., 2013. o. Huanjing Kexue Xuebao/Acta Sci. Circumstantiae 33, 3407–3412.

Zhang, S.-Y., Shao, D., Liu, H., Feng, J., Feng, B., Song, X., Zhao, Q., Chu, M., Jiang, C., Huang, W., Wang, X., 2017. Metabolomics analysis reveals that benzo[a]pyrene, a component of PM 2.5 , promotes pulmonary injury by modifying lipid metabolism in a phospholipase A2-dependent manner in vivo and in vitro. Redox Biol. 13, 459–469. doi:10.1016/j.redox.2017.07.001

Zimmermann, A., Bauer, M.A., Kroemer, G., Madeo, F., Carmona-Gutierrez, D., 2014. When less is more : hormesis against stress and disease. Microb. Cell 1, 150–153. doi:doi:

Zinrajh, D., Hörl, G., Jürgens, G., Marc, J., Sok, M., Cerne, D., 2014. Increased phosphatidylethanolamine N-methyltransferase gene expression in non-small-cell lung cancer tissue predicts shorter patient survival. Oncol. Lett. 7, 2175–2179. doi:10.3892/ol.2014.2035

Zou, Y., Wu, Y., Wang, Y., Li, Y., Jin, C., 2017. Physicochemical properties, in vitro cytotoxic and genotoxic effects of PM1.0 and PM2.5 from Shanghai, China. Environ. Sci. Pollut. Res. 24, 19508–19516. doi:10.1007/s11356-017-9626-9

# OVERALL DISCUSSION

# Overall discussion

In the present thesis, characterization, toxicity, exposure, and human health risk assessment was performed for PM collected around a cement plant located in Montcada i Reixac (Barcelona, Spain) in different periods of the year. The first step in our analysis was to obtain the chemical characterization of the three fractions of PM ($PM_{10}$, $PM_{2.5}$, and $PM_1$) collected nearby the cement plant in different seasons (Chapter 1). A subsequent study was performed to elucidate the partition of different organic compounds during winter, the season registering highest levels of carbonaceous materials (Chapter 2). Chemical characterization was completed by microscopic imaging in a third study (Chapter 3). To study the hazardous activity of these particles and deduce their way of action, several toxicity tests were carried out exposing human respiratory cells to PM (Chapter 3). To assess human health risks, EPA methodology was followed to evaluate inhalation risks for metals and PAHs. To get a more accurate insight into the exposure to this contaminant, an infiltration model and a dosimetry model were coupled (Chapter 4). The former model was used to obtain levels of outdoor PM within indoor environments, while the latter to know the size distribution of PM within the human respiratory system. To reveal the contribution of different sources to the environmental levels of PM several receptor modelling techniques were applied together (Chapter 5). Finally, Chapter 6 depicts an improved methodology to study exposure and toxicity of PM based on the results obtained from Chapter 1, 3, and 4.

## Chemical characterization

### PM levels and primary compounds

Highest levels of PM were measured in winter, being in some cases above the thresholds established by the European air quality standards (daily limit of 50 μg/m$^3$ for $PM_{10}$ and annual limit of 40 and 25 μg/m$^3$ for $PM_{10}$ and $PM_{2.5}$ respectively) (European Commission and EU Parliament, 2008). It was also observed that in this season, shares of carbonaceous materials reached its maximum for the two fine PM fractions. This trend has been observed in several papers focused on urban/industrial environments, explained by the higher contribution from combustion sources (i.e. traffic and domestic heating) and air stagnation generated by anticyclonic episodes typically occurring in Mediterranean winters (Galindo et al., 2010; Pey et al., 2010; Reche et al., 2012). Source apportionment results corroborate this origin.

Most of the major elements were present in the coarse fraction, except K and Mg. In our samples K is mainly located in the fine fraction. This singularity is explained by the fact that potassium has been related to biomass combustion (Li et al., 2014). In our source apportionment exercise this element's loading reached the highest value for the cement plant/industry component, the main source of biomass combustion in the area. Mg is one of the most abundant elements in the earth crust, and its most plausible origin in PM is soil resuspension (Housecroft and Sharpe, 2012). However, in our samples we observed high contributions of Mg in the finest fractions. The origin of this fine Mg could be also the combustion process in the cement kiln. Some alternative fuels and/or materials used in the kiln, such as scrap, fly ash, or coal, could be the source of this Mg (Xie et al., 2005).

Aluminum, Fe and Ca are elements highly related to mineral particles resuspension. However, our results suggest two different origins for them. Al and Ca are highly related to the cement industry, while Fe is more linked to soil resuspension. These three elements have similar loading in the traffic component, suggesting a minor contribution from road dust to their contents. As expressed in Chapter 1 sea salt is the main source of Na in particles. This origin is corroborated by Principal Component Analysis (PCA) in Chapter 5, where $Cl^-$ shows its maximum loading for the marine component. Cu is originated from the wear of brake discs (Badaloni et al., 2017). Therefore it is expected to be found in the coarse fraction, and related to traffic, as confirmed in Chapters 1 and 5.

Distributions of toxic metals and As are variable. Be, Co, V, Mn, Cr and Ni, appeared mainly within the coarse fraction, while U is part of the fine fraction. Arsenic, Pb, and Cd showed a bimodal distribution, being present in both fractions (coarse and fine). However, these depicted distributions could shift towards fine fractions in winter, as happened to Pb, Mn and Cr. Chromium and lead have been reported to be originated from plating surfaces and combustion of fossil fuels and lubricants (Taiwo et al., 2014; Widory et al., 2010; Yu et al., 2014). Manganese has usually been related to mineral fraction of PM and, to a lesser extent, engine abrasion (Moreno et al., 2011; Schauer et al., 2006). The three of them have been reported to be part of cement dust and stack emissions from cement facilities (Gupta et al., 2012; Ogunbileje et al., 2013). The greater concentration of these metals within the fine fraction in winter could be related to the aforementioned higher influence of combustion sources within this season, especially the cement plant.

As expected from the results in Chapter 1, most of the organic compounds analyzed were present in the finest fraction ($PM_1$). Only saccharides and derivates were located in the coarse fraction. As discussed in the Chapter 2, the origin of this group of compounds is mainly soil resuspension and biological, which is corroborated by microscopic images and loading factors of organic dust (Chapters 3 and 5 respectively). PAHs were highly related to combustion processes, and, consequently, they were mostly present in the $PM_1$ fraction. The prevalent PAHs were those formed by six rings (benzo[b + j]fluoranthene and benzo[ghi]perylene). They were both related to combustion of biomass and fossil fuels, but results from source apportionment suggested that the latter had a greater contribution from traffic. Although levels of PAHs were higher than previously recorded in Barcelona their toxic potential, expressed as BaP equivalents, was below the threshold established in the European directive (European Commission and EU Parliament, 2008; Mesquita et al., 2014). The remaining organic compounds (hopanes, biomass combustion products) are especially useful when assessing the source apportionment. The great contribution of biomass combustion products confirms the importance of biomass burning within the area, as suggested in Chapter 1 by the presence of K in fine PM. The occurrence of hopanes confirmed the contribution of traffic, which, as seen by the contents of elemental carbon, Cu, and Pb, are lower in winter.

### Secondary compounds

Regarding secondary compounds, it is possible to distinguish a duality in distribution: sulfate, ammonium and secondary organic aerosols (SOA) are present mainly in the fine fraction of PM, while nitrate is mostly present in the coarse fraction. This phenomenon is related with the two main processes influencing the formation of these particles: nucleation and condensation. The first process deals with the formation of new cores of PM by chemical reactions from gaseous compounds. This process is favored by low temperatures, and high concentrations of precursor gases and humidity. Secondary particles can then stick together and form bigger particles by the phenomenon of agglomeration. Finally, condensation occurs when gases or small particles get in contact with greater particles, getting merged and increasing the size of the particle (Clement and Ford, 1999).

Nucleation is the process driving the formation of secondary sufate, ammonium, and SOA. Gaseous ammonia and sulfate react among them to form sulfate ammonium, which is especially favored under cold conditions (Gong et al., 2013). SOA are formed from photochemical reactions onto other organic precursors (Borrás and Tortajada-Genaro, 2012). On the other hand, nitrates mainly occur through condensation. Nitric acid and ion nitrate present in the air are able to react with coarse particles of $CaCO_3$ (soil resuspension in case of limestones areas) or sea salt particles to form calcium nitrate and sodium nitrate respectively in the coarse fraction (Pakkanen, 1996). This trend in size-distribution of secondary compounds has been witnessed in previous manuscripts (Plaza et al., 2011; Tsai et al., 2005).

### Toxicity

As stated in the introduction, hazardous potential of PM depends on physicochemical characteristics of particles. To study the influence of these characteristics on toxicity, two fractions of PM ($PM_{2.5}$ and $PM_{10}$) and cement dust (CD) were subjected to several *in-vitro* assays. In a first approach, bacterial DNA was exposed to different doses of PM and CD to study their oxidative potential. Subsequently, bronchial epithelial tissues were exposed to the same materials to evaluate protein secretion, mortality, and integrity of the epithelial barrier in the tissue. The results showed that $PM_{2.5}$ elicited a higher oxidative potential, mortality, and protein secretion than $PM_{10}$, but $PM_{10}$ triggers more affection to cell junction. Cement dust elicited also significant damage in the epithelial barrier and increased protein secretion, but exhibited higher vitality than controls, which could be related to the hormesis phenomenon. Histology imaging revealed the presence of vacuoles, condensed nuclei, and a higher thickness of the epithelial barrier on those tissues exposes to PMs and CD, confirming thus the inflammation and cytotoxicity.

In Chapter 3 it was already discussed how the differences in chemical composition between the two PM fractions could explain the aforementioned results, but also size plays an important role in overall toxicity. Since $PM_{10}$ includes coarse particles, overall surface area of this fraction is lower than $PM_{2.5}$. Consequently potential mechanical damage from $PM_{2.5}$ will be higher at an equal mass of PM. Besides, the lower content of mineral compounds and biological debris of $PM_{2.5}$ makes this fraction more soluble. Therefore, toxic components of $PM_{2.5}$ could get inside the cells more easily than in case $PM_{10}$. In this process, we also hypothesized that entrance of coarse components inside cells is more difficult, although we did not find any study confirming or rejecting this theory. Hence, it seems plausible that coarse components could elicit a higher extracellular toxicity, as is the case of tissue integrity. Histology imaging showed a clear influence of both PM fractions onto tracheobronchial epithelial cells. In line with the results from toxicity test, effects of a higher mucus release and a greater density and size of vacuoles was seen after exposure to $PM_{2.5}$.

According to the results exposed in the aforementioned paragraph it was decided to get a deeper insight into toxicity of fine PM trying to overtake some of the limitations of toxicity test described in Chapter 3. To have a better understanding of PM way of action, an untargeted metabolomic assay was conducted onto human alveolar epithelial cells (A549) (Chapter 6). These cells were exposed to two fractions of fine PM ($PM_{2.5-0.25}$ and $PM_{0.25}$) under more realistic conditions. These conditions consisted in applying real dose and lethal dose to get 5% mortality ($LC_5$) for 72 hours. Although this assay was not performed with PM collected in areas influenced by cement plants, we wanted to include this material in this thesis to better understand hazardous potential and of PM.

In this study it was seen that $LC_5$ was one order of magnitude lower for $PM_{0.25}$ than for $PM_{2.5-0.25}$ (i.e. 0.008 and 0.07 µg PM/mL respectively). The number of altered metabolites after exposure was similar regardless of the PM fraction assessed when applying $LC_5$, but when applying real dose more metabolites were altered fro $PM_{0.25}$. Most of these changes were performed on lipid content, and with substances dealing with the cell membrane functioning and inflammatory process. Thus, these results showed also a bigger influence from smaller particles in toxicity. Also, it exhibits the potential of PM as agent able to make changes in the metabolic profile, even at environmental doses.

## Exposure and risk assessment

To assess exposure and risks, general approaches are usually based on environmental levels of PM and focused on a single population group (MAGRAMA, 2007; US EPA, 2005). Some authors have criticized this methodology, stating that it can be setting unrealistics scenarios (Sarigiannis et al., 2015). In this thesis we wanted to go further, and improve the standard risk assessment methodologies by exploring the possibilities that software modelling could offer. Instead of focusing in just adults, it was decided to pay attention to three population groups (kids, adults, and elders). Since their routines were different, time activity patterns of the different population groups were taken from previous studies (Cohen Hubal et al., 2000; IEC, 2012; INSEE, 2010). Being aware that most of the time in developed countries is spent indoors, it was decided to simulate the concentrations in two indoor environments through the use of the infiltration software IAQX (Schweizer et al., 2007; US EPA, 2000). After studying the time-activity pattern of the groups two indoor environments were simulated: home and classroom/office. Physiological characteristics of the three population groups were also taken into account, and through the use of a dosimetry model it was possible to study the deposition patterns of three PM fractions ($PM_{10}$, $PM_{2.5}$, and $PM_1$) onto the respiratory system. Risks assessment can be then calculated according to the PM richness in toxic components (i.e. heavy metals and PAHs).

The highest overall exposure was experienced in winter, as consequence of the higher PM levels experienced during this season (Chapter 1). After using the infiltration model, it was noticed that highest levels of PM were experienced outdoors, since we considered indoor environment as absent of PM sources. Accordingly, ventilation was the dominant process defining indoor levels of PM. However, a couple of considerations should be taken into account for future simulations. Even considering an indoor environment lacking indoor PM sources, dust resuspension should be taken into consideration, since it is recognized as an important process influencing indoor PM concentrations (Serfozo et al., 2014). Also, when assessing mechanical ventilation, as could be the case of the office microenvironment, it is important to consider if the ventilation mechanism has any kind of filters favoring the presence of certain PM fraction inside (F. Wang et al., 2016).

About dosimetry model, it was observed that the head region was the one retaining most of the PM mass, regardless the fraction. Tracheobronchial region captured the smallest contributions, but retained most of coarse PM escaping from head region. Consequently, lung region retained middling masses of particles, composed almost exclusively by $PM_{2.5}$ and $PM_1$. Similar amounts of these two fractions reached the lungs regardless the population group. This fact is especially disturbing for kids, since their body weight is significantly lower, and their immunity system is still under development. Regarding activities, deposition while sleeping was very low despite the high share of time of this activity. This is a direct consequence of the low levels of PM calculated indoors and the lower breathing frequency during this activity. On the other hand, light and heavy intensity activities performed outdoor are the main contributors to overall PM deposition in the respiratory tract as a whole. Having into consideration these results, we decided to improve this model focused on children, since they were the population group experiencing higher mass of PM per body mass. The main improvements were to measure PM indoors and obtaining their time-activity pattern. Indoor measurements were higher than those simulated in Chapter 4, highlighting the influence of indoor resuspension. Regarding their activity pattern, children evaluated in Chapter 6 were slightly more active. Consequently, deposited doses in Chapter 6 were higher than in Chapter 4. However, the trends in the two chapters (i.e. the heavier the exercise the greater the deposited mass at a given PM concentration) were the same.

This trend has been reported in previous studies, and could lead to contradictory conclusions, such as exercising outdoors could be hazardous to health (Winter-Sorkina and Cassee, 2002). In the present thesis we focused on exposure, without addressing the benefits of exercising. Nevertheless, several papers have dealt with this issue, concluding that benefits from exercise overtake exposure damages even in highly polluted places (Mueller et al., 2015; Tainio et al., 2016). Furthermore, in order to simplify calculations, we considered daily average PM levels as constant for every microenvironment, but reality is that PM concentrations are highly variable in time and space (Steinle et al., 2015). Thus, choosing a convenient time and place could help to reduce inhaled PM dose when exercising outdoors.

Non-carcinogenic and carcinogenic risks for PAHs and most of metals were below the safety thresholds established in the Spanish legislation (MAGRAMA, 2007). Only carcinogenic risks from Cr (VI) showed values above carcinogenic threshold of 1 case of cancer for every $10^5$ inhabitants. Inhalation of this metal was calculated to be responsible of between 2 and 3 cases of cancer for every $10^5$ inhabitants. However, as explained in Chapter 1 Cr (VI), has been estimated from total Cr following the findings in previous studies (R. J. C. Brown et al., 2014). A proper measure of this metal in our samples could generate different results. It is also important to note that following the changing distribution of this metal, risks are associated to different PM fractions. In autumn, cancer risks were elicited as a consequence of the inhalation of coarse PM, while in winter they were related with $PM_1$. As seen from Chapter 4 the deposition pattern within the human respiratory tract is different for these two PM fractions, and so could be target area of these cases of cancer. However, once retained, toxicants are embedded on airway mucus, whose fate could affect this spatial distribution. The vast majority of this mucus is drained into the stomach, where the appearance of hazardous effects should also be assessed (Fahy and Dickey, 2010).

### Source apportionment

Three different tools were used to evaluate the contributions from different sources to environmental PM. Two of them were based on statistical techniques of variable reduction, while the third one was based on carbon isotopic content. Principal Component Analysis (PCA) has been widely used in source apportionment studies (Taiwo et al., 2014). This methodology was used in the dataset published in Chapter 1. Results indicate that sources contributions are variable among seasons, but also between years for the same season. Thus, in line with Chapter 1, combustion sources are the main contributors to $PM_{10}$ in autumn and winter 2013, while they have a smaller share in summer. As discussed previously, a decrease in traffic and heating use, joint to specific meteorological conditions could be the explanation to these results. As remarked in the

Chapter 5, during autumn/winter 2014 contributions from cement industry decreased drastically, related to the reduction in the production of the cement plant.

Since winter was the season reaching the highest levels of PM and organics, it was necessary to have a deeper idea of the contributions during this period. To do so, a Multivariate Curve Resolution by Alternating Least Squares (MCR-ALS) was applied. This technique has been historically applied to clarify the composition of complex mixtures in analytical chemistry. However, some studies have applied this tool for PM source apportionment (Alier et al., 2013; Tauler et al., 2009). In line with Chapter 1, contribution from combustion sources (i.e. fossil fuels and biomass) increased with decreasing PM size. According to last available data, more than 70% of the heating system used in Montcada i Reixac are gas driven technologies (IDESCAT, 2001). Consequently, fossil fuel component will be highly related with combustion in car's engines, domestic heating systems, and use of conventional fuels in the cement kiln. On the other hand, alternative fuel burning in the kiln seems to be the main contributor to biomass burning component, having some minor contribution from agricultural waste burning and biomass heating systems. From MCR-ALS analysis it is also notable the influence of SOA on fine PM ($PM_{2.5}$ and $PM_1$). Finally, organic dust component presented high loadings of hopanes, which claims the influence of traffic in the processes of organic coarse PM resuspension (Aryal et al., 2015; Gunawardana et al., 2012).

Isotopic ratios were used to complete the analysis. As in the previous statistical tools, $\delta^{13}C$ in collected samples were within the range of combustion processes (fossil fuels, biomass, and waste water sludge). A decrease in $\delta^{13}C$ is noticed when decreasing PM size, which revealed the influence of mineral components (calcite) in the coarse fraction $\delta^{13}C$. Furthermore, the influence of SOA in fine PM could lower $^{13}C$ content of $PM_1$ and $PM_{2.5}$ (Pavuluri and Kawamura, 2016). However, impact from the cement plant was difficult to estimate using this technique. Samples collected during not operational days were in the same range as working days, due to the overlapping in $\delta^{13}C$ among the sources influencing the area.

As in every study, this thesis has faced some limitations. First, sampling was developed during representative but short periods of time. In order to better understand the dynamics of PM in the area it is necessary to perform continuous long-term measurements. Finally, having access to the chemical characterization of the different sources of PM within the area would improve the accuracy of the source apportionment exercise. Future studies dealing with the aforementioned issues could help to broaden our understanding in this field.

# CONCLUSIONS

# Conclusions

Three fractions of PM ($PM_{10}$, $PM_{2.5}$, and $PM_1$) were collected in the surrounding of a cement plant in different seasons. Once collected, chemical characterization of these PM fractions was performed. Since winter was the season reaching highest levels of PM and carbonaceous compounds, a subsequent study was focused on elucidating the content of different organic species. To complete the physicochemical determination of particles, $PM_{10}$ and $PM_{2.5}$ were subjected to microscopy imaging. Human tracheobronchial were exposed to these two fractions in order to study their toxicity. Integrating environmental levels and composition of PM, and time activity pattern of population, inhalation exposure to PM were calculated and derived human health risks were assessed. Lastly, to reveal the contribution from cement plant, different source apportionment techniques were used. The main conclusions drawn from the present study are:

1. Regardless the season, $PM_1$ accounted over 60% of total $PM_{10}$ mass. Highest levels of the three PM fractions ($PM_{10}$, $PM_{2.5}$, and $PM_1$) were reached in winter, in some cases overtaking limits set by the European directives. During this season, the greatest levels of carbonaceous materials and toxic metals were registered for every PM fraction. Most of these substances were present within the $PM_1$ fraction.

2. Excepting saccharides, organic compounds were predominantly found in $PM_1$. Biomass combustion products were the most prevalent organic compounds, reaching higher levels than those found in Barcelona metropolitan area. The most predominant PAHs were five and six rings species with a PAH profile characteristic of a mixture of urban and industrial environments. The concentrations of benzo[a]pyrene were relatively high (0.6 ng/$m^3$), but below the limit set by the European Union (1 ng/$m^3$).

3. Greater contribution of soot and fly ash was found in $PM_{2.5}$ than in $PM_{10}$. Fine fraction ($PM_{2.5}$) also accounted for the highest oxidative potential and overall toxicity. However, $PM_{10}$ could elicit higher extracellular damage (i.e. barrier integrity). Consequently, density and size of vacuoles and condensed nuclei (i.e. indicators of inflammation and cytotoxixty) were higher on those tissues exposed to $PM_{2.5}$ than those exposed to $PM_{10}$.

4. The damage pattern described for the cement industry (i.e. the smaller the PM the greater the damage) was also observed with PM collected in environments influenced by a petrochemical complex. Cells exposed to $PM_{0.25}$ exhibited a bigger cytotoxicity and more changes in the metabolic profile than cells exposed to $PM_{2.5\text{-}0.25}$. Most of the altered features were lipids involved in the functioning of cell and mitochondrial membranes.

5. Highest levels of PM were reached outdoors. Despite sleeping was the most time demanding activity, deposited PM mass during this activity was minor. On the other hand, although outdoor activities accounted for 15% of time, these activities were responsible for the retention of 50-75% of overall PM mass. Most of this mass was addressed in the upper part of the respiratory tract, regardless of PM size, due to sedimentation processes. Tracheobronchial region registered the lowest values of deposited particles, while PM retained in the lung was mostly $PM_{2.5}$ and $PM_1$. Deposited mass in lungs was almost equal for kids, adults and retired.

6. Non-carcinogenic and carcinogenic inhalation risks for most metals and PAHs were below the safety thresholds. Cr (VI) was the only metal registering risk levels above the safety threshold (less than 3 cases of cancer per 100,000 inhabitants).

7. Contribution of the cement plant to total PM in the nearby is patent. This contribution depends on the working schedule of the plant, and could reach shares over 60%, depending on the season. Contribution from natural sources could also be majoritarian during summer and autumn in $PM_{10}$. When decreasing the PM size, shares from combustion sources (i.e. traffic, cement plant, heating) increases. Study of isotopic ratios has been useful to confirm the aforementioned results.

The general conclusion of this thesis is that physicochemical characteristics of coarse ($PM_{10\text{-}2.5}$), fine ($PM_{2.5}$) and quasi-ultrafine particles ($PM_1$) in areas influenced by cement plants are different, and depend profoundly on PM size and seasonality. Consequently, toxicity and human health risks derived from these particles are variable, and are determined by the PM fraction and the contribution from cement plant and other sources.

# REFERENCES

# References

Abdul-Wahab, S.A., 2006. Impact of fugitive dust emissions from cement plants on nearby communities. Ecol. Modell. 195, 338–348. doi:10.1016/j.ecolmodel.2005.11.044

Adar, S.D., Filigrana, P.A., Clements, N., Peel, J.L., 2014. Ambient Coarse Particulate Matter and Human Health: A Systematic Review and Meta-Analysis. Curr. Environ. Heal. reports 1, 258–274. doi:10.1007/s40572-014-0022-z

Addo, M.A., Darko, E.O., Gordon, C., Davor, P., Ameyaw, F., Affum, H., Gbadago, J.K., Dzide, S., 2016. Human health risk assessment of airborne trace elements for human receptors in the vicinity of the diamond cement factory, Volta region, Ghana. Int. J. Sustain. Dev. Plan. 11, 522–536. doi:10.2495/SDP-V11-N4-522-536

Akhtar, U.S., McWhinney, R.D., Rastogi, N., Abbatt, J.P.D., Evans, G.J., Scott, J.A., 2010. Cytotoxic and proinflammatory effects of ambient and source-related particulate matter (PM) in relation to the production of reactive oxygen species (ROS) and cytokine adsorption by particles. Inhal. Toxicol. 22 Suppl 2, 37–47. doi:10.3109/08958378.2010.518377

Aleksandar, J., Zoran, K., Dejan, R., Dragoslava, S., Marko, O., Dusan, T., Miroslav, S., 2010. The emission of particulate matters and heavy metals from cement kilns - case study: co-incineration of tires in Serbia. Chem. Ind. Chem. Eng. Q. 16, 213–217. doi:10.2298/CICEQ090902010J

Alier, M., van Drooge, B.L., Dall'Osto, M., Querol, X., Grimalt, J.O., Tauler, R., 2013. Source apportionment of submicron organic aerosol at an urban background and a road site in Barcelona (Spain) during SAPUSS. Atmos. Chem. Phys. 13, 10353–10371. doi:10.5194/acp-13-10353-2013

Amandus, H.E., 1986. Mortality from stomach cancer in United States cement plant and quarry workers, 1950-80. Br. J. Ind. Med. 43, 526–8. doi:10.1136/oem.43.8.526

Aryal, R., Lee, B.-K., Beecham, S., Kandasamy, J., Aryal, N., Parajuli, K., 2015. Characterisation of Road Dust Organic Matter as a Function of Particle Size: A PARAFAC Approach. Water, Air, Soil Pollut. 226, 24. doi:10.1007/s11270-014-2289-y

Asamany, E.A., Gibson, M.D., Pegg, M.J., 2017. Evaluating the potential of waste plastics as fuel in cement kilns using bench-scale emissions analysis. Fuel 193, 178–186. doi:10.1016/j.fuel.2016.12.054

Badaloni, C., Cesaroni, G., Cerza, F., Davoli, M., Brunekreef, B., Forastiere, F., 2017. Effects of long-term exposure to particulate matter and metal components on mortality in the Rome longitudinal study. Environ. Int. 109, 146–154.

doi:10.1016/j.envint.2017.09.005

Bauer, M., Gräbsch, C., Gminski, R., Ollmann, A.I.H., Borm, P., Dietz, A., Herbarth, O., Wichmann, G., 2012. Cement-related particles interact with proinflammatory IL-8 chemokine from human primary oropharyngeal mucosa cells and human epithelial lung cancer cell line A549. Environ. Toxicol. 27, 297–306. doi:10.1002/tox.20643

Beelen, R., Raaschou-Nielsen, O., Stafoggia, M., Andersen, Z.J., Weinmayr, G., Hoffmann, B., Wolf, K., Samoli, E., Fischer, P., Nieuwenhuijsen, M., Vineis, P., Xun, W.W., Katsouyanni, K., Dimakopoulou, K., Oudin, A., Forsberg, B., Modig, L., Havulinna, A.S., Lanki, T., Turunen, A., Oftedal, B., Nystad, W., Nafstad, P., De Faire, U., Pedersen, N.L., Östenson, C.-G., Fratiglioni, L., Penell, J., Korek, M., Pershagen, G., Eriksen, K.T., Overvad, K., Ellermann, T., Eeftens, M., Peeters, P.H., Meliefste, K., Wang, M., Bueno-de-Mesquita, B., Sugiri, D., Krämer, U., Heinrich, J., de Hoogh, K., Key, T., Peters, A., Hampel, R., Concin, H., Nagel, G., Ineichen, A., Schaffner, E., Probst-Hensch, N., Künzli, N., Schindler, C., Schikowski, T., Adam, M., Phuleria, H., Vilier, A., Clavel-Chapelon, F., Declercq, C., Grioni, S., Krogh, V., Tsai, M.-Y., Ricceri, F., Sacerdote, C., Galassi, C., Migliore, E., Ranzi, A., Cesaroni, G., Badaloni, C., Forastiere, F., Tamayo, I., Amiano, P., Dorronsoro, M., Katsoulis, M., Trichopoulou, A., Brunekreef, B., Hoek, G., 2014. Effects of long-term exposure to air pollution on natural-cause mortality: an analysis of 22 European cohorts within the multicentre ESCAPE project. Lancet 383, 785–795. doi:10.1016/S0140-6736(13)62158-3

Bonetta, S., Gianotti, V., Bonetta, S., Gosetti, F., Oddone, M., Gennaro, M.C., Carraro, E., 2009. DNA damage in A549 cells exposed to different extracts of PM2.5 from industrial, urban and highway sites. Chemosphere 77, 1030–1034. doi:10.1016/j.chemosphere.2009.07.076

Borrás, E., Tortajada-Genaro, L.A., 2012. Secondary organic aerosol formation from the photo-oxidation of benzene. Atmos. Environ. 47, 154–163. doi:10.1016/j.atmosenv.2011.11.020

Brockhaus, A., Dolgner, R., Ewers, U., Krämer, U., Soddemann, H., Wiegand, H., 1981. Intake and health effects of thallium among a population living in the vicinity of a cement plant emitting thallium containing dust. Int. Arch. Occup. Environ. Health 48, 375–389. doi:10.1007/BF00378686

Brown, D., Sadiq, R., Hewage, K., 2014. An overview of air emission intensities and environmental performance of grey cement manufacturing in Canada. Clean Technol. Environ. Policy 16, 1119–1131. doi:10.1007/s10098-014-0714-y

Brown, R.J.C., Van Aswegen, S., Webb, W.R., Goddard, S.L., 2014. UK concentrations of chromium and chromium (VI), measured as water soluble chromium, in PM10. Atmos. Environ. 99, 385–391. doi:10.1016/j.atmosenv.2014.10.008

Calvano, J.E., Agnese, D.M., Um, J.Y., Goshima, M., Singhal, R., Coyle, S.M., Reddell, M.T., Kumar, A., Calvano, S.E., Lowry, S.F., 2003. Modulation of the lipopolysaccharide receptor complex (CD14, TLR4, MD-2) and toll-like receptor 2 in systemic inflammatory response syndrome-positive patients with and without infection: relationship to tolerance. Shock 20, 415–419. doi:10.1097/01.shk.0000092269.01859.44

Cassee, F.R., Héroux, M.-E., Gerlofs-Nijland, M.E., Kelly, F.J., 2013. Particulate matter beyond mass: recent health evidence on the role of fractions, chemical constituents and sources of emission. Inhal. Toxicol. 25, 802–812. doi:10.3109/08958378.2013.850127

Cembureau, 2017. The story of cement manufacture [WWW Document]. URL https://cembureau.eu/media/1544/cementmanufacturing.pdf (accessed 9.26.17).

CEMBUREAU, 2016. Cement, concrete, and the circular economy. Brussels.

Clement, C.F., Ford, I.J., 1999. Gas-to-particle conversion in the atmosphere: I. Evidence from empirical atmospheric aerosols. Atmos. Environ. 33, 475–487. doi:10.1016/S1352-2310(98)00264-7

Cohen Hubal, E.A., Sheldon, L.S., Burke, J.M., McCurdy, T.R., Berry, M.R., Rigas, M.L., Zartarian, V.G., Freeman, N.C., 2000. Children’s exposure assessment: a review of factors influencing Children's exposure, and the data available to characterize and assess that exposure. Environ. Health Perspect. 108, 475–486.

CPRAC, 2008. Manual of pollution prevention in the cement industry. Regional Activity Centre for Cleaner Production (CP/RAC), Barcelona.

Dan, Z., Li, Z., GangCai, C., ZhiEn, Z., BaoHui, Y., Yuan, R., LiHong, R., 2015. The particle size distribution characteristics of different combustion sources. China Environ. Sci. 35, 3239–3246.

Degobbi, C., Saldiva, P.H.N., Rogers, C., 2011. Endotoxin as modifier of particulate matter toxicity: a review of the literature. Aerobiologia (Bologna). 27, 97–105. doi:10.1007/s10453-010-9179-6

Delgado-Buenrostro, N.L., Freyre-Fonseca, V., Cuéllar, C.M.G., Sánchez-Pérez, Y., Gutierrez-Cirlos, E.B., Cabellos-Avelar, T., Orozco-Ibarra, M., Pedraza-Chaverri, J., Chirino, Y.I., 2013. Decrease in respiratory function and electron transport chain induced by airborne particulate matter (PM10) exposure in lung mitochondria. Toxicol. Pathol. 41, 628–638. doi:10.1177/0192623312463784

Directive 2010/75/EU, 2010. Directive 2010/75/EU of the European Parliament and of the

Council on industrial emissions (integrated pollution prevention and control), Official Journal of the European Union. doi:10.3000/17252555.L_2010.334.eng

Dolgner, R., Brockhaus, A., Ewers, U., Wiegand, H., Majewski, F., Soddemann, H., 1983. Repeated surveillance of exposure to thallium in a population living in the vincinity of a cement plant emitting dust containing thallium. Int. Arch. Occup. Environ. Health 52, 79–94. doi:10.1007/BF00380610

Donahue, N.M., Posner, L.N., Westervelt, D.M., Li, Z., Shrivastava, M., Presto, A.A., Sullivan, R.C., Adams, P.J., Pandis, S.N., Robinson, A.L., Donahue, N.M., Posner, L.N., Westervelt, D.M., Li, Z., Shrivastava, M., Presto, A.A., Sullivan, R.C., Adams, P.J., Pandis, S.N., Robinson, A.L., 2016. Where Did This Particle Come From? Sources of Particle Number and Mass for Human Exposure Estimates, in: Hester, R.E., Harrison, R.M., Querol, X. (Eds.), Airborne Particulate Matter: Sources, Atmospheric Processess and Health. pp. 35–71. doi:10.1039/9781782626589-00035

Donato, F., Garzaro, G., Pira, E., Boffetta, P., 2016. Mortality and cancer morbidity among cement production workers: a meta-analysis. Int. Arch. Occup. Environ. Health 89, 1155–1168. doi:10.1007/s00420-016-1167-x

Dong, Z., Bank, M.S., Spengler, J.D., 2015. Assessing metal exposures in a community near a cement plant in the northeast U.S. Int. J. Environ. Res. Public Health 12, 952–969. doi:10.3390/ijerph120100952

Dorato, M.A., Engelhardt, J.A., 2005. The no-observed-adverse-effect-level in drug safety evaluations: Use, issues, and definition(s). Regul. Toxicol. Pharmacol. 42, 265–274. doi:10.1016/J.YRTPH.2005.05.004

EEA, 2017. European Union emission inventory report 1990–2015 under the UNECE Convention on Long-range Transboundary Air Pollution (LRTAP) — European Environment Agency. Luxembourg.

EEA, 2015. Particulate matter [WWW Document]. URL http://www.eea.europa.eu/themes/air/air-quality/resources/glossary/particulate-matter#parent-fieldname-title (accessed 4.19.17).

EEA, 2012. Particulate matter from natural sources and related reporting under the EU Air Quality Directive in 2008 and 2009 — European Environment Agency. Copenhaguen.

Ehrlich, C., Noll, G., Kalkoff, W.D., Baumbach, G., Dreiseidler, A., 2007. PM10, PM2.5 and PM1.0-Emissions from industrial plants-Results from measurement programmes in Germany. Atmos. Environ. 41, 6236–6254. doi:10.1016/j.atmosenv.2007.03.059

Enciclopædia Britannica, 2007. Cement [WWW Document]. URL https://www.britannica.com/technology/cement-building-material (accessed 9.26.17).

Ercan, Ö., Dinçer, F., 2016. Atmospheric concentrations of PCDD/Fs, PAHs, and metals in the vicinity of a cement plant in Istanbul. Air Qual. Atmos. Heal. 9, 159–172. doi:10.1007/s11869-015-0314-y

EU Parliament, 2005. Directive 2004/107/EC of the European Parliament and of the Council of 15 December 2004 relating to arsenic, cadmium, mercury, nicker and polyciclic aromatic hydrocarbons in ambient air. Off. J. Eur. Communities. 23, 3–16.

European Commission, EU Parliament, 2008. Directive 2008/50/EC of the European Parliament and of the Council of 21 May 2008 on ambient air quality and cleaner air for Europe. Off. J. Eur. Communities. 152, 1–44.

Fahy, J. V., Dickey, B.F., 2010. Airway Mucus Function and Dysfunction. N. Engl. J. Med. 363, 2233–2247. doi:10.1056/NEJMra0910061

Faiola, C., Johansen, A.M., Rybka, S., Nieber, A., Thomas, C., Bryner, S., Johnston, J., Engelhard, M., Nachimuthu, P., Owens, K.S., 2011. Ultrafine Particulate Ferrous Iron and Anthracene Associations with Mitochondrial Dysfunction. Aerosol Sci. Technol. 45, 1109–1122. doi:10.1080/02786826.2011.581255

Fell, A.K.M., Thomassen, T.R., Kristensen, P., Egeland, T., Kongerud, J., 2003. Respiratory symptoms and ventilatory function in workers exposed to portland cement dust. J. Occup. Environ. Med. 45, 1008–1014. doi:10.1097/01.jom.0000083036.56116.9d

Galindo, N., Varea, M., Gil-Moltó, J., Yubero, E., Nicolás, J., 2010. The Influence of Meteorology on Particulate Matter Concentrations at an Urban Mediterranean Location. Water, Air, Soil Pollut. 215, 365–372. doi:10.1007/s11270-010-0484-z

Generalitat de Catalunya, 2008. Resolució BA20060162 de 29 Abril 2008.

Gilmore, T., 2009. NF-kB Transcription Factors | Boston University [WWW Document]. URL http://www.bu.edu/nf-kb/ (accessed 3.30.16).

Ginns, S.E., Gatrell, A.C., 1996. Respiratory health effects of industrial air pollution: a study in east Lancashire, UK. J. Epidemiol. Community Health 50, 631–5. doi:10.1136/JECH.50.6.631

Giordano, F., Dell'Orco, V., Fantini, F., Grippo, F., Perretta, V., Testa, A., Figà-Talamanca, I., 2012a. Mortality in a cohort of cement workers in a plant of Central Italy. Int. Arch. Occup. Environ. Health 85, 373–379. doi:10.1007/s00420-011-0678-8

Giordano, F., Grippo, F., Perretta, V., Figa-Talamanca, I., 2012b. Impact of cement production emissions on heatlh: effects on the mortality patterns of the population living in the vicinity of acement plant. Fresenius Environ. Bull. 21, 1905–1909.

Gong, L., Lewicki, R., Griffin, R.J., Tittel, F.K., Lonsdale, C.R., Stevens, R.G., Pierce, J.R., Malloy, Q.G.J., Travis, S.A., Bobmanuel, L.M., Lefer, B.L., Flynn, J.H., 2013. Role of atmospheric ammonia in particulate matter formation in Houston during summertime. Atmos. Environ. 77, 893–900. doi:10.1016/j.atmosenv.2013.04.079

Guan, L., Rui, W., Bai, R., Zhang, W., Zhang, F., Ding, W., 2016. Effects of Size-Fractionated Particulate Matter on Cellular Oxidant Radical Generation in Human Bronchial Epithelial BEAS-2B Cells. Int. J. Environ. Res. Public Health 13, 483. doi:10.3390/ijerph13050483

Guevara, M., 2016. Emissions of Primary Particulate Matter, in: Hester, R.E., Harrison, R.M., Querol, X. (Eds.), Airborne Particulate Matter: Sources, Atmospheric Processess and Health. Royal Society of Chemistry, pp. 1–34.

Gunawardana, C., Goonetilleke, A., Egodawatta, P., Dawes, L., Kokot, S., 2012. Source characterisation of road dust based on chemical and mineralogical composition. Chemosphere 87, 163–170. doi:10.1016/j.chemosphere.2011.12.012

Gupta, R.K., Majumdar, D., Trivedi, J.V., Bhanarkar, A.D., 2012. Particulate matter and elemental emissions from a cement kiln. Fuel Process. Technol. 104, 343–351. doi:10.1016/j.fuproc.2012.06.007

Hallquist, M., Wenger, J.C., Baltensperger, U., Rudich, Y., Simpson, D., Claeys, M., Dommen, J., Donahue, N.M., George, C., Goldstein, A.H., Hamilton, J.F., Herrmann, H., Hoffmann, T., Iinuma, Y., Jang, M., Jenkin, M.E., Jimenez, J.L., Kiendler-Scharr, A., Maenhaut, W., McFiggans, G., Mentel, T.F., Monod, A., Prévôt, A.S.H., Seinfeld, J.H., Surratt, J.D., Szmigielski, R., Wildt, J., 2009. The formation, properties and impact of secondary organic aerosol: current and emerging issues. Atmos. Chem. Phys. 9, 5155–5236. doi:10.5194/acp-9-5155-2009

Haxhiu, M.A., Begraca, M., Radotic, M., Fehmiu, E., 1979. The interaction of multiple factors affecting respiratory function in cement workers. Bull. Int. Union Tuberc. 54, 424.

Hou, L., Zhu, Z.-Z., Zhang, X., Nordio, F., Bonzini, M., Schwartz, J., Hoxha, M., Dioni, L., Marinelli, B., Pegoraro, V., Apostoli, P., Bertazzi, P., Baccarelli, A., 2010. Airborne particulate matter and mitochondrial damage: a cross-sectional study. Environ. Heal. 9, 48. doi:10.1186/1476-069X-9-48

Housecroft, C.E., Sharpe, A.G., 2012. Inorganic chemistry, 4th ed. Pearson Prentice Hall, Harlow.

Huang, M., Kang, Y., Wang, W., Chan, C.Y., Wang, X., Wong, M.H., 2015. Potential cytotoxicity of water-soluble fraction of dust and particulate matters and relation to metal(loid)s based on three human cell lines. Chemosphere 135, 61–66. doi:10.1016/j.chemosphere.2015.04.004

I.N.E., 2017. Distribución porcentual de los activos por sector económico y provincia(3994) [WWW Document]. URL http://www.ine.es/jaxiT3/Tabla.htm?t=3994 (accessed 10.2.17).

IARC, 2012. Chemical agents and related ocupations: A review of human carcinogens. Lyon.

IDESCAT, 2001. Idescat. Cens de població i habitatges. Habitatges principals amb calefacció segons el tipus de combustible. Montcada i Reixac [WWW Document]. URL https://www.idescat.cat/pub/?geo=mun%3A081252&id=censph&n=357#Plegable=geo (accessed 11.20.17).

IEC, 2012. Enquesta de l’ús del temps 2010-2011 : principals resultats. – (Estadística Social). Institut d'Estadística de Catalunya.

INSEE, 2010. Conditions de vie-Société - Depuis 11 ans, moins de tâches ménagères, plus d’Internet. Insee. Available at: http://www.insee.fr/fr/themes/document.asp?ref_id=ip1377.

Işikli, B., Demir, T.A., Akar, T., Berber, A., Ürer, S.M., Kalyoncu, C., Canbek, M., 2006. Cadmium exposure from the cement dust emissions: A field study in a rural residence. Chemosphere 63, 1546–1552. doi:10.1016/j.chemosphere.2005.09.059

Jakobsson, K., Attewell, R., Hultgren, B., Sjöland, K., 1990. Gastrointestinal cancer among cement workers - A case-referent study. Int. Arch. Occup. Environ. Health 62, 337–340. doi:10.1007/BF00640844

Jakubowski, M., PałczyŃski, C., 2015. Beryllium, in: Handbook on the Toxicology of Metals. Elsevier, pp. 635–653. doi:10.1016/B978-0-444-59453-2.00030-5

Jiang, J., Oberdörster, G., Biswas, P., 2008. Characterization of size, surface charge, and agglomeration state of nanoparticle dispersions for toxicological studies. J. Nanoparticle Res. 11, 77–89. doi:10.1007/s11051-008-9446-4

Kelly, F., Fussell, J., 2016. Health Effects of Airborne Particles in Relation to Composition, Size and Source, in: Airborne Particulate Matter: Sources, Atmospheric Processess and Health. pp. 344–372.

Kelly, F.J., Fussell, J.C., 2012. Size, source and chemical composition as determinants of toxicity attributable to ambient particulate matter. Atmos. Environ. 60, 504–526. doi:10.1016/j.atmosenv.2012.06.039

Khwedim, K., Meza-Figueroa, D., Hussien, L.A., Del Río-Salas, R., 2015. Trace metals in topsoils near the Babylon Cement Factory (Euphrates River) and human health risk assessment. Environ. Earth Sci. 74, 665–673. doi:10.1007/s12665-015-4071-x

Kim, H., Kim, J.Y., Kim, J.S., Jin, H.C., 2015. Physicochemical and optical properties of combustion-generated particles from a coal-fired power plant, automobiles, ship engines, and charcoal kilns. Fuel 161, 120–128. doi:10.1016/j.fuel.2015.08.035

Kim, K.H., Choi, G.H., Kang, C.H., Lee, J.H., Kim, J.Y., Youn, Y.H., Lee, S.R., 2003. The chemical composition of fine and coarse particles in relation with the Asian Dust events. Atmos. Environ. 37, 753–765. doi:10.1016/S1352-2310(02)00954-8

Lafarge, 2016. Fábrica de Montcada [WWW Document]. URL http://www.lafarge.com.es/wps/portal/es/fabrica-de-montcada (accessed 6.23.16).

Lafarge, 2011. Health and Safety Information Portland cement. Birmingham.

Li, J., Song, Y., Mao, Y., Mao, Z., Wu, Y., Li, M., Huang, X., He, Q., Hu, M., 2014. Chemical characteristics and source apportionment of PM2.5 during the harvest season in eastern China’s agricultural regions. Atmos. Environ. 92, 442–448. doi:10.1016/j.atmosenv.2014.04.058

Li, K., Chen, Y., Zhang, W., Pu, Z., Jiang, L., Chen, Y., 2012. Surface interactions affect the toxicity of engineered metal oxide nanoparticles toward Paramecium. Chem. Res. Toxicol. 25, 1675–1681. doi:10.1021/tx300151y

Li, R., Kou, X., Geng, H., Xie, J., Yang, Z., Zhang, Y., Cai, Z., Dong, C., 2015. Effect of ambient PM2.5 on lung mitochondrial damage and fusion/fission gene expression in rats. Chem. Res. Toxicol. 28, 408–418. doi:10.1021/tx5003723

Li, Y., Zhu, T., Zhao, J., Xu, B., 2012. Interactive enhancements of ascorbic acid and iron in hydroxyl radical generation in quinone redox cycling. Environ. Sci. Technol. 46, 10302–10309. doi:10.1021/es301834r

Liao, C.-M., Chio, C.-P., Chen, W.-Y., Ju, Y.-R., Li, W.-H., Cheng, Y.-H., Liao, V.H.-C., Chen, S.-C., Ling, M.-P., 2011. Lung cancer risk in relation to traffic-related nano/ultrafine particle-bound PAHs exposure: a preliminary probabilistic assessment. J. Hazard. Mater. 190, 150–158. doi:10.1016/j.jhazmat.2011.03.017

Lin, M., Chen, Y., Burnett, R.T., Villeneuve, P.J., Krewski, D., 2002. The influence of ambient coarse particulate matter on asthma hospitalization in children: case-crossover and time-series analyses. Environ. Health Perspect. 110, 575–81.

MAGRAMA, 2007. Guía Técnica de aplicación del RD 9/2005, de 14 de enero, por el que se establece la relación de actividades potencialmente contaminantes del suelo y los criterios y estándares para la declaración de suelos contaminados. [WWW Document]. URL http://www.magrama.gob.es/es/calidad-y-evaluacion-ambiental/temas/suelos-contaminados/guia_tecnica_contaminantes_suelo_declaracion_suelos_tcm7-3204.pdf (accessed 9.25.14).

Marcon, A., Pesce, G., Girardi, P., Marchetti, P., Blengio, G., de Zolt Sappadina, S., Falcone, S., Frapporti, G., Predicatori, F., de Marco, R., 2014. Association between PM10 concentrations and school absences in proximity of a cement plant in northern Italy. Int. J. Hyg. Environ. Health 217, 386–391. doi:10.1016/j.ijheh.2013.07.016

Mesquita, S.R., van Drooge, B.L., Reche, C., Guimarães, L., Grimalt, J.O., Barata, C., Piña, B., 2014. Toxic assessment of urban atmospheric particle-bound PAHs: relevance of composition and particle size in Barcelona (Spain). Environ. Pollut. 184, 555–562. doi:10.1016/j.envpol.2013.09.034

Mirzaee, R., Kebriaei, A., Hashemi, S.R., Sadeghi, M., Shahrakipour, M., 2008. Effects of exposure to Portland cement dust on lung function in Portland cement factory workers in Khash, Iran. Iran. J. Environ. Heal. Sci. Eng. 5, 201–206.

MohseniBandpi, A., Eslami, A., Shahsavani, A., Khodagholi, F., Alinejad, A., 2017. Physicochemical characterization of ambient PM2.5 in Tehran air and its potential cytotoxicity in human lung epithelial cells (A549). Sci. Total Environ. 593, 182–190. doi:10.1016/j.scitotenv.2017.03.150

Molinelli, A.R., Santacana, G.E., Madden, M.C., Jiménez, B.D., 2006. Toxicity and metal content of organic solvent extracts from airborne particulate matter in Puerto Rico. Environ. Res. 102, 314–325. doi:10.1016/j.envres.2006.04.010

Moorthy, B., Chu, C., Carlin, D.J., 2015. Polycyclic aromatic hydrocarbons: from metabolism to lung cancer. Toxicol. Sci. 145, 5–15. doi:10.1093/toxsci/kfv040

Moreno, T., Pandolfi, M., Querol, X., Lavín, J., Alastuey, A., Viana, M., Gibbons, W., 2011. Manganese in the urban atmosphere: identifying anomalous concentrations and sources. Environ. Sci. Pollut. Res. 18, 173–183. doi:10.1007/s11356-010-0353-8

Mueller, N., Rojas-Rueda, D., Cole-Hunter, T., de Nazelle, A., Dons, E., Gerike, R., Götschi, T., Int Panis, L., Kahlmeier, S., Nieuwenhuijsen, M., 2015. Health impact assessment of active transportation: A systematic review. Prev. Med. (Baltim). 76, 103–114. doi:10.1016/j.ypmed.2015.04.010

Mwaiselage, J., Bråtveit, M., Moen, B.E., Masalla, Y., 2005. Respiratory symptoms and chronic obstructive pulmonary disease among cement factory workers. Scand. J. … 31, 316–323. doi:10.5271/sjweh.888

Nemmar, A., Holme, J. a, Rosas, I., Schwarze, P.E., Alfaro-Moreno, E., 2013. Recent advances in particulate matter and nanoparticle toxicology: a review of the in vivo and in vitro studies. Biomed Res. Int. 2013, 279371. doi:10.1155/2013/279371

Nkhama, E., Ndhlovu, M., Timothy Dvonch, J., Siziya, S., Voyi, K., 2015. Prevalence and determinants of mucous membrane irritations in a community near a cement factory in Zambia: A cross sectional study. Int. J. Environ. Res. Public Health 12, 871–887. doi:10.3390/ijerph120100871

Nordby, K.C., Fell, A.K.M., Notø, H., Eduard, W., Skogstad, M., Thomassen, Y., Bergamaschi, A., Kongerud, J., Kjuus, H., 2011. Exposure to thoracic dust, airway symptoms and lung function in cement production workers. Eur. Respir. J. 38, 1278–1286. doi:10.1183/09031936.00007711

Oficemen, 2017. Proceso de fabricación del cemento [WWW Document]. URL https://www.oficemen.com/el-cemento/proceso-de-fabricacion/ (accessed 9.26.17).

Oficemen, 2016a. Anuario del sector cementero español. Madrid.

Oficemen, 2016b. Economía circular mediante eficiencia y reutilización [WWW Document]. URL https://www.oficemen.com/sostenibilidad/economia-circular/# (accessed 10.9.17).

Ogunbileje, J.O., Sadagoparamanujam, V.-M., Anetor, J.I., Farombi, E.O., Akinosun, O.M., Okorodudu, A.O., 2013. Lead, mercury, cadmium, chromium, nickel, copper, zinc, calcium, iron, manganese and chromium (VI) levels in Nigeria and United States of America cement dust. Chemosphere 90, 2743–2479. doi:10.1016/j.chemosphere.2012.11.058

Oss, H.G., Padovani, A.C., 2003. Cement Manufacture and the Environment Part II: Environmental Challenges and Opportunities. J. Ind. Ecol. 7, 93–126. doi:10.1162/108819803766729212

Pakkanen, T.A., 1996. Study of formation of coarse particle nitrate aerosol. Atmos. Environ. 30, 2475–2482. doi:10.1016/1352-2310(95)00492-0

Pavuluri, C.M., Kawamura, K., 2016. Enrichment of 13C in diacids and related compounds during photochemical processing of aqueous aerosols: New proxy for organic aerosols aging. Sci. Rep. 6, 36467. doi:10.1038/srep36467

Pey, J., Pérez, N., Querol, X., Alastuey, A., Cusack, M., Reche, C., 2010. Intense winter atmospheric pollution episodes affecting the Western Mediterranean. Sci. Total Environ. 408, 1951–1959. doi:10.1016/j.scitotenv.2010.01.052

Plaza, J., Pujadas, M., Gómez-Moreno, F.J., Sánchez, M., Artíñano, B., 2011. Mass size distributions of soluble sulfate, nitrate and ammonium in the Madrid urban aerosol. Atmos. Environ. 45, 4966–4976. doi:10.1016/j.atmosenv.2011.05.075

Popoola, L.T., Adebanjo, S.A., Adeoye, B.K., 2017. Assessment of atmospheric particulate matter and heavy metals: a critical review. Int. J. Environ. Sci. Technol. 1–14. doi:10.1007/s13762-017-1454-4

Raaschou-Nielsen, O., Andersen, Z.J., Beelen, R., Samoli, E., Stafoggia, M., Weinmayr, G., Hoffmann, B., Fischer, P., Nieuwenhuijsen, M.J., Brunekreef, B., Xun, W.W., Katsouyanni, K., Dimakopoulou, K., Sommar, J., Forsberg, B., Modig, L., Oudin, A., Oftedal, B., Schwarze, P.E., Nafstad, P., De Faire, U., Pedersen, N.L., Ostenson, C.-G., Fratiglioni, L., Penell, J., Korek, M., Pershagen, G., Eriksen, K.T., Sørensen, M., Tjønneland, A., Ellermann, T., Eeftens, M., Peeters, P.H., Meliefste, K., Wang, M., Bueno-de-Mesquita, B., Key, T.J., de Hoogh, K., Concin, H., Nagel, G., Vilier, A., Grioni, S., Krogh, V., Tsai, M.-Y., Ricceri, F., Sacerdote, C., Galassi, C., Migliore, E., Ranzi, A., Cesaroni, G., Badaloni, C., Forastiere, F., Tamayo, I., Amiano, P., Dorronsoro, M., Trichopoulou, A., Bamia, C., Vineis, P., Hoek, G., 2013. Air pollution and lung cancer incidence in 17 European cohorts : prospective analyses from the European Study of Cohorts for Air Pollution Effects ( ESCAPE ). Lancet Oncol. 2045, 813–822. doi:10.1016/S1470-2045(13)70279-1

Reche, C., Moreno, T., Amato, F., Viana, M., van Drooge, B.L., Chuang, H.-C., Bérubé, K., Jones, T., Alastuey, A., Querol, X., 2012. A multidisciplinary approach to characterise exposure risk and toxicological effects of $PM_{10}$ and $PM_{2.5}$ samples in urban environments. Ecotoxicol. Environ. Saf. 78, 327–335. doi:10.1016/j.ecoenv.2011.11.043

Richard, E.E., Augusta Chinyere, N.-A., Jeremaiah, O.S., Opara, U.C.A., Henrieta, E.M., Ifunanya, E.D., 2016. Cement Dust Exposure and Perturbations in Some Elements and Lung and Liver Functions of Cement Factory Workers. J. Toxicol. 2016, 1–7. doi:10.1155/2016/6104719

Roig, N., Sierra, J., Rovira, J., Schuhmacher, M., Domingo, J.L., Nadal, M., 2013. In vitro tests to assess toxic effects of airborne PM(10) samples. Correlation with metals and chlorinated dioxins and furans. Sci. Total Environ. 443, 791–797. doi:10.1016/j.scitotenv.2012.11.022

Rovira, J., 2013. Impacte de la utilització de combustibles alternatius en fàbriques de ciment sobre la salut humana. TDX (Tesis Dr. en Xarxa). Universitat Rovira i Virgili.

Rovira, J., Flores, J., Schuhmacher, M., Nadal, M., Domingo, J.L., 2015. Long-Term Environmental Surveillance and Health Risks of Metals and PCDD/Fs Around a Cement Plant in Catalonia, Spain. Hum. Ecol. Risk Assess. An Int. J. 21, 514–532. doi:10.1080/10807039.2014.930620

Rovira, J., Mari, M., Schuhmacher, M., Nadal, M., Domingo, J.L., 2011. Monitoring environmental pollutants in the vicinity of a cement plant: a temporal study. Arch. Environ. Contam. Toxicol. 60, 372–384. doi:10.1007/s00244-010-9628-9

Rovira, J., Nadal, M., Schuhmacher, M., Domingo, J.L., 2016. Alternative Fuel Implementation in a Cement Plant: Human Health Risks and Economical Valuation. Arch. Environ. Contam. Toxicol. 71, 473–484. doi:10.1007/s00244-016-0308-2

Rovira, J., Nadal, M., Schuhmacher, M., Domingo, J.L., 2014. Environmental levels of PCDD/Fs and metals around a cement plant in Catalonia, spain, before and after alternative fuel implementation. Assessment of human health risks. Sci. Total Environ. 485-486, 121–129. doi:10.1016/j.scitotenv.2014.03.061

Sánchez-Soberón, F., Mari, M., Kumar, V., Rovira, J., Nadal, M., Schuhmacher, M., 2015. An approach to assess the Particulate Matter exposure for the population living around a cement plant: modelling indoor air and particle deposition in the respiratory tract. Environ. Res. 143, 10–18. doi:10.1016/j.envres.2015.09.008

Santacatalina, M., Reche, C., Minguillón, M.C., Escrig, A., Sanfelix, V., Carratalá, A., Nicolás, J.F., Yubero, E., Crespo, J., Alastuey, A., Monfort, E., Miró, J. V, Querol, X., 2010. Impact of fugitive emissions in ambient PM levels and composition: a case study in Southeast Spain. Sci. Total Environ. 408, 4999–5009. doi:10.1016/j.scitotenv.2010.07.040

Sarigiannis, D.A., Karakitsios, S.P., Zikopoulos, D., Nikolaki, S., Kermenidou, M., 2015. Lung cancer risk from PAHs emitted from biomass combustion. Environ. Res. 137, 147–156. doi:10.1016/j.envres.2014.12.009

Schauer, J.J., Lough, G.C., Shafer, M.M., Christensen, W.F., Arndt, M.F., DeMinter, J.T., Park, J.-S., 2006. Characterization of metals emitted from motor vehicles. Res. Rep. Health. Eff. Inst. 1–76; discussion 77–88.

Schorcht, F., Kourti, I., Scalet, B.M., Roudier, S., Delgado Sancho, L., 2013. Best Available Techniques (BAT) Reference Document for the Production of Cement, Lime and Magnesium Oxide. Seville. doi:10.2788/12850

Schuhmacher, M., Domingo, J.L., Garreta, J., 2004. Pollutants emitted by a cement plant: Health risks for the population living in the neighborhood. Environ. Res. 95, 198–206. doi:10.1016/j.envres.2003.08.011

Schuhmacher, M., Nadal, M., Domingo, J.L., 2009. Environmental monitoring of PCDD/Fs and metals in the vicinity of a cement plant after using sewage sludge as a secondary fuel. Chemosphere 74, 1502–1508. doi:10.1016/j.chemosphere.2008.11.055

Schweizer, C., Edwards, R.D., Bayer-Oglesby, L., Gauderman, W.J., Ilacqua, V., Jantunen, M.J., Lai, H.K., Nieuwenhuijsen, M., Künzli, N., 2007. Indoor time–microenvironment–activity patterns in seven regions of Europe. J. Expo. Sci. Environ. Epidemiol. 17, 170–181.

Senthilkumar, S., Manju, A., Muthuselvam, P., Shalini, D., Indhumathi, V., Kalaiselvi, K., Palanivel, M., Chandrasekar, P.P., Rajaguru, P., 2014. Characterization and genotoxicity evaluation of particulate matter collected from industrial atmosphere in Tamil Nadu state, India. J. Hazard. Mater. 274C, 392–398. doi:10.1016/j.jhazmat.2014.04.017

Serfozo, N., Chatoutsidou, S.E., Lazaridis, M., 2014. The effect of particle resuspension during walking activity to PM10 mass and number concentrations in an indoor microenvironment. Build. Environ. 82, 180–189. doi:http://dx.doi.org/10.1016/j.buildenv.2014.08.017

Shang, Y., Zhang, L., Jiang, Y., Li, Y., Lu, P., 2014. Airborne quinones induce cytotoxicity and DNA damage in human lung epithelial A549 cells: The role of reactive oxygen species. Chemosphere 100, 42–49. doi:10.1016/j.chemosphere.2013.12.079

Sheng, K., Lu, J., 2017. Typical airborne quinones modulate oxidative stress and cytokine expression in lung epithelial A549 cells. J. Environ. Sci. Heal. - Part A Toxic/Hazardous Subst. Environ. Eng. 52, 127–134. doi:10.1080/10934529.2016.1237127

Steinle, S., Reis, S., Sabel, C.E., Semple, S., Twigg, M.M., Braban, C.F., Leeson, S.R., Heal, M.R., Harrison, D., Lin, C., Wu, H., 2015. Personal exposure monitoring of PM2.5 in indoor and outdoor microenvironments. Sci. Total Environ. 508, 383–394. doi:10.1016/j.scitotenv.2014.12.003

Tainio, M., de Nazelle, A.J., Götschi, T., Kahlmeier, S., Rojas-Rueda, D., Nieuwenhuijsen, M.J., de Sá, T.H., Kelly, P., Woodcock, J., 2016. Can air pollution negate the health benefits of cycling and walking? Prev. Med. (Baltim). 87, 233–236. doi:10.1016/j.ypmed.2016.02.002

Tainio, M., Kukkonen, J., Nahorski, Z., 2010. Impact of airborne particulate matter on human health: an assessment framework to estimate exposure and adverse health effects in Poland. Arch. Environ. Prot. 36, 95–115.

Taiwo, A.M., Harrison, R.M., Shi, Z., 2014. A Review of Receptor Modelling of Industrially Emitted Particulate Matter. Atmos. Environ. 97, 109–120. doi:10.1016/j.atmosenv.2014.07.051

Tauler, R., Viana, M., Querol, X., Alastuey, A., Flight, R.M., Wentzell, P.D., Hopke, P.K., 2009. Comparison of the results obtained by four receptor modelling methods in aerosol source apportionment studies. Atmos. Environ. 43, 3989–3997. doi:10.1016/j.atmosenv.2009.05.018

Thomson, E.M., Breznan, D., Karthikeyan, S., MacKinnon-Roy, C., Charland, J.-P., Dabek-Zlotorzynska, E., Celo, V., Kumarathasan, P., Brook, J.R., Vincent, R., 2015. Cytotoxic and inflammatory potential of size-fractionated particulate matter collected repeatedly within a small urban area. Part. Fibre Toxicol. 12, 24. doi:10.1186/s12989-015-0099-z

Thorn, J., 2001. The inflammatory response in humans after inhalation of bacterial endotoxin: A review. Inflamm. Res. doi:10.1007/s000110050751

Thurston, G.D., Ahn, J., Cromar, K.R., Shao, Y., Reynolds, H.R., Jerrett, M., Lim, C.C., Shanley, R., Park, Y., Hayes, R.B., 2016. Ambient particulate matter air pollution exposure and mortality in the NIH-AARP diet and health cohort. Environ. Health Perspect. 124, 484–490. doi:10.1289/ehp.1509676

Tobiszewski, M., Namieśnik, J., 2012. PAH diagnostic ratios for the identification of pollution emission sources. Environ. Pollut. 162, 110–119. doi:10.1016/j.envpol.2011.10.025

Tokyay, M., 2016. Effects of mineral admixtures on hydration of portland cement, in: Cement and Concrete Mineral Admixtures.

Tsai, J.-H., Chang, K.-L., Lin, J.J., Lin, Y.-H., Chiang, H.-L., 2005. Mass-Size Distributions of Particulate Sulfate, Nitrate, and Ammonium in a Particulate Matter Nonattainment Region in Southern Taiwan. J. Air Waste Manage. Assoc. 55, 502–509. doi:10.1080/10473289.2005.10464640

US EPA, 2016a. Basic Information | Particulate Matter | Air & Radiation | US EPA [WWW Document]. URL https://www.epa.gov/pm-pollution/particulate-matter-pm-basics#PM (accessed 5.31.15).

US EPA, 2016b. Conducting a Human Health Risk Assessment [WWW Document]. URL https://www.epa.gov/risk/conducting-human-health-risk-assessment (accessed 10.18.17).

US EPA, 2009. Risk Assessment Guidance for Superfund Volume I: Human Health

Evaluation Manual (Part F, Supplemental Guidance for Inhalation Risk Assessment). Off. Superfund Remediat. Technol. Innov. Environ. Prot. Agency I, 1–68. doi:EPA-540-R-070-002

US EPA, 2005. Guidelines for Carcinogen risk assessment, Risk Assessment Forum.

US EPA, 2000. Indoor Air Quality Modeling [WWW Document]. URL https://www.epa.gov/air-research/simulation-tool-kit-indoor-air-quality-and-inhalation-exposure-iaqx (accessed 1.1.17).

US EPA, R. 01, 2017. How Does PM Affect Human Health? | Air Quality Planning Unit | Ground-level Ozone | New England | US EPA [WWW Document]. URL https://www3.epa.gov/region1/airquality/pm-human-health.html (accessed 9.25.17).

USEPA, 2016. Health and Environmental Effects of Particulate Matter (PM) [WWW Document]. US Environ. Prot. Agency. URL https://www.epa.gov/pm-pollution/health-and-environmental-effects-particulate-matter-pm (accessed 9.14.17).

van Berlo, D., Haberzettl, P., Gerloff, K., Li, H., Scherbart, A.M., Albrecht, C., Schins, R.P.F., 2009. Investigation of the cytotoxic and proinflammatory effects of cement dusts in rat alveolar macrophages. Chem. Res. Toxicol. 22, 1548–1558. doi:10.1021/tx900046x

Van Den Heuvel, R., Den Hond, E., Govarts, E., Colles, A., Koppen, G., Staelens, J., Mampaey, M., Janssen, N., Schoeters, G., 2016. Identification of PM10 characteristics involved in cellular responses in human bronchial epithelial cells (Beas-2B). Environ. Res. 149, 48–56. doi:10.1016/j.envres.2016.04.029

Vestbo, J., Rasmussen, F. V., 1990. Long-term exposure to cement dust and later hospitalization due to respiratory disease. Int. Arch. Occup. Environ. Health 62, 217–220. doi:10.1007/BF00379436

von Moos, N., Slaveykova, V.I., 2014. Oxidative stress induced by inorganic nanoparticles in bacteria and aquatic microalgae – state of the art and knowledge gaps. Nanotoxicology 8, 605–630. doi:10.3109/17435390.2013.809810

Wang, B., Li, N., Deng, F., Buglak, N., Park, G., Su, S., Ren, A., Shen, G., Tao, S., Guo, X., 2016. Human bronchial epithelial cell injuries induced by fine particulate matter from sandstorm and non-sandstorm periods: Association with particle constituents. J. Environ. Sci. (China) 47, 201–210. doi:10.1016/j.jes.2015.12.015

Wang, F., Meng, D., Li, X., Tan, J., 2016. Indoor-outdoor relationships of PM 2.5 in four residential dwellings in winter in the Yangtze River Delta, China. Environ. Pollut. 215, 280–289. doi:10.1016/j.envpol.2016.05.023

WHO, 2013. Health effects of Particulate Matter. Policy implications for countries in eastern Europe, Caucasus and central Asia. Copenhagen.

WHO, 2010. Polycyclic aromatic hydrocarbons, in: WHO Guidelines for Indoor Air Quality: Selected Pollutants. p. 484. doi:10.1186/2041-1480-2-S2-I1

WHO, 2000. Chapter 7.3 Particulate matter, in: Air Quality Guidelines for Europe. pp. 186–193.

Widory, D., Liu, X., Dong, S., 2010. Isotopes as tracers of sources of lead and strontium in aerosols (TSP & PM2.5) in Beijing. Atmos. Environ. 44, 3679–3687. doi:10.1016/j.atmosenv.2010.06.036

Winter-Sorkina, R., Cassee, F.R., 2002. From concentration to dose: factors influencing airborne particulate matter deposition in humans and rats. RIVM Rep. 650010031/2002.

Xie, R.K., Seip, H.M., Leinum, J.R., Winje, T., Xiao, J.S., 2005. Chemical characterization of individual particles (PM10) from ambient air in Guiyang City, China. Sci. Total Environ. 343, 261–272. doi:10.1016/j.scitotenv.2004.10.012

Yang, L., Liu, G., Lin, Z., Wang, Y., He, H., Liu, T., Kamp, D.W., 2016. Pro-inflammatory response and oxidative stress induced by specific components in ambient particulate matter in human bronchial epithelial cells. Environ. Toxicol. 31, 923–936. doi:10.1002/tox.22102

Yu, C.H., Huang, L., Shin, J.Y., Artigas, F., Fan, Z. (Tina), 2014. Characterization of concentration, particle size distribution, and contributing factors to ambient hexavalent chromium in an area with multiple emission sources. Atmos. Environ. 94, 701–708. doi:10.1016/j.atmosenv.2014.06.004

Yubero, E., Carratalá, A., Crespo, J., Nicolás, J., Santacatalina, M., Nava, S., Lucarelli, F., Chiari, M., 2011. PM10 source apportionment in the surroundings of the San Vicente del Raspeig cement plant complex in southeastern Spain. Environ. Sci. Pollut. Res. 18, 64–74. doi:10.1007/s11356-010-0352-9

# ANNEX I

# Annex I: Supplementary materials for Chapter 1

Supplementary materials for the paper entitled:

# Main components and human health risks assessment of $PM_{10}$, $PM_{2.5}$, and $PM_1$ in two areas influenced by cement plants

Francisco Sánchez-Soberón [a,b], Joaquim Rovira [a,b], Montse Marí [a,b] Jordi Sierra [b,c], Martí Nadal [a], José L. Domingo [a], Marta Schuhmacher [a,b *]

## Content

- Supplementary materials and methods
- Tables

## 1. Materials and Methods

### *2.1. Area of Study*

The two studied facilities are located in Catalonia (Northeast Spain). The first one (A) is placed in Barcelona metropolitan area, within an urban sector profoundly affected by a number of different industries. This settlement is crossed by two highways with an average daily traffic of 49,199 and 160,558 vehicles per day, respectively (Ministerio de Fomento, 2012). According to the company ruling the installation, the plant has an annual production of 900,000 metric tons of cement annually. Non-conventional fuels (sewage sludge, animal flours, refuse derived fuels, biomass) account 20% of the total energy consumed. The second plant (B) is set in the coastline of southern Catalonia, integrated in a rural background. Apart from the cement manufacture process, limestone mining activities are performed in the nearby of the plant. Close to the cement plant there is a road with an average daily traffic of 12,380 vehicles per day, being 34.4 % of them considered as heavy vehicles (Ministerio de Fomento, 2012). In 2012 the plant reached a production of 867,353 metric tons of cement annually. During the same year 31.9% of the total energy consumption came from alternative fuels, which means more than 85.5 thousands metric tons yearly. Half of this number is composed by biomass, while the other half is made from refuse derived fuels. Both plants are 165 km away from each other, and both present same air cleaning devices i.e. electrostatic precipitator for cleaning the exhaust gases from kiln and oil mill, and a baghouse for gases coming from stone crusher, cement mill and coal mill.

### *2.2. Analytical methods*

Before sampling, filters were heated at 200ºC for 4 h. PM levels were calculated by gravimetric determination. Filters were acclimated and weighted at constant humidity (40%) and temperature (20ºC) during consecutive days until constant weight before and after sampling campaign. Subsequently, filters were divided into three portions to perform different analytical determinations.

The first portion of filter was used for elemental analysis. It was treated with a mixture of 2 mL of $HNO_3$ (65% Suprapur, E.Merck) and 3 mL of HF (37.5%, Panreac) in hermetic Teflon bombs for 8 h at room temperature, and 8 additional hours at 80°C. After cooling, extracts were filtered and made up to 25 mL with ultrapure water. They were kept frozen at -20 °C until further analysis (Mari et al., 2009). Aluminium (Al), arsenic (As), beryllium (Be), bismuth (Bi), cadmium (Cd), cerium (Ce), cobalt (Co), chromium (Cr), caesium (Cs), copper (Cu), dysprosium (Dy), erbium (Er), europium (Eu), gadolinium (Gd), germanium (Ge), hafnium (Hf), holmium (Ho), lanthanum (La), lithium (Li) mercury (Hg), manganese (Mn), molybdenum (Mo), niobium (Nb), neodymium (Nd), nickel (Ni), lead (Pb), praseodymium (Pr), rubidium (Rb), antimony (Sb), scandium (Sc), selenium (Se), samarium (Sm), tin (Sn), strontium (Sr), Tantalum (Ta), terbium (Tb), thorium (Th), titanium (Ti), thallium (Tl), uranium (U), vanadium (V), wolfram (W), yttrium (Y), ytterbium (Yb), and zirconium (Zr) were determined by means of Inductively Coupled Plasma Mass Spectrometry (ICP-MS, Perkin Elmer Elan 6000). Calcium (Ca), iron (Fe), potassium (K), magnesium (Mg), sodium (Na) and phosphorus (P) concentrations were determined by Inductively Coupled Plasma Optical Emission Spectrometry techniques

(ICP-OES, Perkin Elmer, Optima 3200RL). Detection limits, in ng/m$^3$, were; 0.01 for Bi, Ce, Cs, Dy, Er, Eu, Gd, Ho, La, Nb, Nd, Rb, Sm, Ta, Tb, Tl, U, Y, Yb, and W; 0.02 for Rb; 0.03 for Cd and Pb; 0.06 for Co, Cu, Mn, Mo, Sn, Sr, Th, and Zr; 0.12 for As, Be, Hf, and Li; 0.13 for Hg; 0.31 for Cr and V; 0.59 for Ge; 0.63 for Se; 1.18 for Sc and Ti; 3.13 for Fe; 5.88 for B; 6.25 for Mn and Zn; 15.7 for Ca; 29.4 for Mg; 31.3 for Al; 156 for K, P, and Na.

Another portion of filter was used for the determination of soluble inorganic ions ($Cl^-$, $SO_4^{2-}$, $NO_3^-$, and $NH_4^+$). The piece of filter was cut in smaller portions and mixed with 15 mL of deionised water in a falcon tube. Then, it was shaken during 4 hours and submerged in a sonication bath at 60ºC during 1 hour. The extract was then filtered with a 250 µm sieve, and the filtered liquid analyzed by means of Ionic Chromatography and specific electrode (DX-300 Dionex) to elucidate the ionic content. For obtaining the total carbon (TC) content, the last portion of filter was submitted to pyrolysis with oxygen at 1,000 ºC. Resulting gases ($CO_2$ and $NO_X$) were driven by a helium flow, which was subsequently analyzed by means of gas chromatography (Thermo EA 1108 CHNS-O Carlo Erba Instruments) (Tiessen and Moir, 2000a, 2000b). To address the joint content of organic carbon (OC) and elemental carbon (EC), sample was previously exposed to a HCl enriched atmosphere in order to remove the carbon from carbonates. After that it was analyzed following the same methodology described for TC.

Laboratory reagents blanks and duplicates were performed in order to control the quality of the process. As external standard, Loamy clay soil (National Institute of Standards and Technology) was used for metal and sulphanilamide for carbonic content.

**References**

Ministerio de Fomento, 2012. Mapa de Tráfico [WWW Document]. URL http://www.fomento.gob.es/NR/rdonlyres/6B349269-A03D-45CA-8AEC-0AF11A7EA168/119364/MapaIntensidad2012.pdf (accessed 4.17.14).

Tiessen, H., Moir, J., 2000a. Total nitrogen., in: Carter, M.R., Gregorich, E.G. (Eds.), Soil Sampling and Methods of Soil Analysis. Canadian Society of Soil Science.

Tiessen, H., Moir, J., 2000b. Total and organic carbon., in: Carter, M.R., Gregorich, E.G. (Eds.), Soil Sampling and Methods of Soil Analysis. Canadian Society of Soil Science.

**Table S1:** Levels of elements, in ng/m$^3$, for both cement plants (A and B), and sampling periods: autumn (A), winter (W), and summer (S).

AA

| | $PM_{10}$ | | $PM_{2.5}$ | | $PM_1$ | |
|---|---|---|---|---|---|---|
| | Mean | Stan. Dev. | Mean | Stan. Dev. | Mean | Stan. Dev. |
| Al | 624 | 114 | 83.5 | 42.2 | 45.7 | 23.6 |
| As | 0.63 | 0.09 | 0.38 | 0.07 | 0.36 | 0.01 |
| Be | 0.09 | 0.03 | ND | - | ND | - |
| Bi | 1.59 | 0.50 | 0.37 | 0.11 | 3.54 | 0.30 |
| Ca | 2142 | 1108 | 1586 | 844 | 1631 | 2239 |
| Cd | 0.68 | 0.35 | 0.31 | 0.13 | 0.26 | 0.05 |
| Ce | 1.30 | 0.48 | 0.69 | 0.36 | 1.11 | 1.01 |
| Co | 0.33 | 0.00 | 0.09 | 0.03 | 0.08 | 0.07 |
| Cr | 7.29 | 0.06 | ND | - | ND | 1.45 |
| Cs | 0.11 | 0.04 | 0.03 | 0.01 | 0.06 | 0.04 |
| Cu | 42.6 | 9.50 | 18.9 | 2.51 | 6.80 | 3.73 |
| Dy | 0.06 | 0.02 | 0.03 | 0.00 | 0.06 | 0.06 |
| Er | 0.05 | 0.02 | 0.02 | 0.00 | 0.05 | 0.06 |
| Eu | 0.11 | 0.05 | ND | - | ND | - |
| Fe | 407 | 103 | 131 | 42.0 | 106 | 72.5 |
| Gd | 0.21 | 0.07 | 0.04 | 0.00 | 0.12 | 0.14 |
| Ge | ND | - | ND | - | ND | - |
| Hf | 0.30 | 0.11 | 0.23 | 0.06 | 0.34 | 0.35 |
| Hg | ND | - | ND | - | ND | - |
| Ho | 0.01 | 0.01 | ND | - | ND | - |

| | | | | | | |
|---|---|---|---|---|---|---|
| K | 1600 | 662 | 1304 | 60.9 | 1107 | 1843 |
| La | 0.48 | 0.17 | 0.20 | 0.02 | 0.34 | 0.46 |
| Li | 0.64 | 0.31 | ND | - | 1.45 | 1.77 |
| Mg | 64.3 | 52.9 | 45.0 | 18.6 | 103 | 96.7 |
| Mn | 6.98 | 3.94 | 4.38 | 1.02 | 3.32 | 3.67 |
| Mo | 1.06 | 0.22 | ND | - | 0.24 | 0.19 |
| Na | 904 | 473 | 45.2 | 29.8 | 39.4 | 17.7 |
| Nb | 0.25 | 0.04 | ND | - | 0.22 | 0.10 |
| Nd | 0.36 | 0.15 | 0.15 | 0.02 | 0.29 | 0.39 |
| Ni | 4.07 | 0.91 | 1.74 | 0.14 | 1.60 | 0.18 |
| P | 118 | 59.9 | 123 | 47.5 | 117 | 37.7 |
| Pb | 11.9 | 3.19 | 4.96 | 1.76 | 4.07 | 2.64 |
| Pr | 0.10 | 0.04 | 0.04 | 0.00 | 0.08 | 0.09 |
| Rb | 3.55 | 1.57 | 0.32 | 0.07 | ND | 3.73 |
| Sb | 3.88 | 0.90 | 1.29 | 0.17 | 1.47 | 0.32 |
| Sc | 2.90 | 2.41 | 2.33 | 2.80 | 1.57 | 0.32 |
| Se | ND | - | ND | - | ND | - |
| Sm | 0.08 | 0.03 | 0.04 | 0.01 | ND | - |
| Sn | 4.76 | 1.37 | 1.81 | 0.36 | 0.98 | 1.42 |
| Sr | 9.00 | 2.77 | 5.44 | 0.31 | 6.16 | 8.34 |
| Ta | 0.05 | 0.01 | ND | - | ND | - |
| Tb | 0.01 | 0.01 | ND | - | ND | - |
| Th | 0.14 | 0.04 | 0.09 | 0.01 | 0.16 | 0.13 |
| Ti | 46.8 | 14.4 | 7.69 | 2.97 | ND | - |
| Tl | 0.05 | 0.03 | 0.03 | 0.01 | 0.07 | 0.05 |

| | | | | | | |
|---|---|---|---|---|---|---|
| U | 0.11 | 0.01 | 0.10 | 0.01 | 0.10 | 0.06 |
| V | 6.87 | 3.03 | 3.15 | 0.57 | 2.22 | 0.85 |
| W | 0.33 | 0.34 | 0.03 | 0.01 | 0.14 | 0.10 |
| Y | 0.24 | 0.10 | 0.05 | 0.01 | ND | - |
| Yb | 0.03 | 0.01 | ND | - | ND | - |
| Zr | 10.4 | 4.19 | 9.04 | 2.88 | 0.07 | 14.4 |

| | AW | | | | | |
|---|---|---|---|---|---|---|
| | $PM_{10}$ | | $PM_{2.5}$ | | $PM_1$ | |
| | Mean | Stan. Dev. | Mean | Stan. Dev. | Mean | Stan. Dev. |
| Al | 2596 | 539 | 355 | 434 | 195 | 108 |
| As | 0.62 | 0.13 | 0.59 | 0.06 | 0.39 | 0.21 |
| Be | ND | - | ND | - | ND | - |
| Bi | 3.97 | 2.06 | 0.30 | 0.43 | 1.33 | 1.23 |
| Ca | 4743 | 1076 | 319 | 347 | 351 | 533 |
| Cd | 0.47 | 0.01 | 0.20 | 0.01 | 0.20 | 0.01 |
| Ce | 2.12 | 0.75 | 1.31 | 0.83 | 0.40 | 0.42 |
| Co | 0.45 | 0.27 | 0.15 | 0.09 | 0.10 | 0.02 |
| Cr | 8.50 | 3.09 | 4.20 | 1.32 | 4.18 | 3.26 |
| Cs | 0.12 | 0.04 | ND | - | ND | - |
| Cu | 41.4 | 18.2 | 28.6 | 9.84 | 12.38 | 4.85 |
| Dy | 0.15 | 0.03 | ND | - | ND | - |
| Er | 0.11 | 0.03 | ND | - | ND | - |
| Eu | 0.42 | 0.11 | ND | - | ND | - |
| Fe | 627 | 197 | 168 | 69.0 | 121 | 76.0 |

| | | | | | | |
|---|---|---|---|---|---|---|
| Gd | 0.29 | 0.07 | ND | - | ND | - |
| Ge | ND | - | ND | - | ND | - |
| Hf | 0.71 | 0.10 | ND | - | 0.49 | 0.30 |
| Hg | ND | - | ND | - | ND | - |
| Ho | 0.03 | 0.01 | ND | - | ND | - |
| K | 3093 | 871 | 1892 | 236 | 1593 | 1272 |
| La | 1.04 | 0.22 | 0.07 | 0.05 | 0.16 | 0.20 |
| Li | 0.84 | 0.28 | ND | - | ND | - |
| Mg | 85.6 | 26.0 | 38.2 | 25.5 | 49.3 | 69.1 |
| Mn | 8.13 | 2.82 | 7.48 | 1.38 | 5.29 | 2.47 |
| Mo | 2.04 | 0.61 | 0.11 | 0.17 | 0.94 | 0.52 |
| Na | 1495 | 451 | 96.0 | 49.1 | 47.8 | 364 |
| Nb | 0.30 | 0.08 | ND | - | 0.13 | 0.07 |
| Nd | 0.89 | 0.19 | ND | - | ND | |
| Ni | 6.96 | 2.42 | 5.94 | 4.33 | 1.69 | 0.94 |
| P | ND | - | ND | - | ND | |
| Pb | 16.8 | 3.03 | 13.2 | 4.89 | 13.11 | 3.88 |
| Pr | 0.25 | 0.06 | 0.01 | 0.01 | ND | 0.04 |
| Rb | 4.90 | 1.23 | ND | - | 0.31 | 0.02 |
| Sb | 5.76 | 1.95 | 2.89 | 0.55 | 2.29 | 0.77 |
| Sc | 2.68 | 1.15 | ND | - | ND | - |
| Se | ND | - | ND | - | ND | - |
| Sm | 0.18 | 0.04 | ND | - | 0.04 | 0.03 |
| Sn | 8.05 | 2.39 | 3.56 | 1.38 | 1.75 | 0.84 |
| Sr | 21.2 | 3.67 | 7.84 | 1.97 | 5.00 | 9.45 |

| | | | | | | |
|---|---|---|---|---|---|---|
| Ta | 0.25 | 0.35 | ND | - | ND | - |
| Tb | 0.03 | 0.01 | ND | - | ND | - |
| Th | 0.34 | 0.10 | ND | - | 0.10 | 0.04 |
| Ti | 71.0 | 20.3 | 26.4 | 11.9 | 10.5 | 13.6 |
| Tl | 0.07 | 0.01 | 0.11 | 0.05 | 0.06 | 0.02 |
| U | 0.15 | 0.04 | 0.15 | 0.03 | 0.15 | 0.07 |
| V | 23.5 | 8.95 | 9.09 | 8.95 | 4.44 | 1.02 |
| W | 0.62 | 0.39 | ND | - | 0.41 | 0.24 |
| Y | 0.60 | 0.17 | ND | - | ND | - |
| Yb | 0.08 | 0.02 | ND | - | ND | - |
| Zr | 21.3 | 3.75 | 7.06 | 2.84 | 7.32 | 8.81 |

AS

| | $PM_{10}$ | | $PM_{2.5}$ | | $PM_1$ | |
|---|---|---|---|---|---|---|
| | Mean | Stan. Dev. | Mean | Stan. Dev. | Mean | Stan. Dev. |
| Al | 428 | 58.7 | 390 | 146 | 328 | 49.2 |
| As | 0.19 | 0.07 | ND | - | ND | - |
| Be | ND | - | ND | - | ND | - |
| Bi | 0.24 | 0.16 | 0.20 | 0.05 | 0.14 | 0.05 |
| Ca | 391 | 142 | 285 | 153 | 169 | 71.4 |
| Cd | 5.88 | 0.12 | ND | - | ND | - |
| Ce | 0.19 | 0.09 | 1.48 | 1.94 | ND | - |
| Co | 0.15 | 0.02 | ND | - | ND | - |
| Cr | 3.26 | 0.53 | ND | - | ND | - |
| Cs | 0.02 | 0.01 | 0.02 | 0.01 | ND | - |

| | | | | | | |
|---|---|---|---|---|---|---|
| Cu | 9.62 | 14.8 | 10.2 | 3.55 | ND | - |
| Dy | 0.02 | 0.01 | ND | - | ND | - |
| Er | 0.01 | 0.00 | ND | - | ND | - |
| Eu | 0.01 | 0.00 | ND | - | ND | - |
| Fe | 314 | 84.2 | 53.2 | 27.1 | 28.4 | 10.7 |
| Gd | 0.02 | 0.01 | 0.01 | 0.01 | ND | - |
| Ge | 0.29 | 0.00 | ND | - | ND | - |
| Hf | ND | - | ND | - | ND | - |
| Hg | ND | - | ND | - | ND | - |
| Ho | ND | - | ND | - | ND | - |
| K | 309 | 202 | ND | - | ND | - |
| La | 0.15 | 0.04 | 0.11 | 0.03 | 0.09 | 0.02 |
| Li | 0.29 | 0.07 | 0.25 | 0.15 | 0.33 | 0.14 |
| Mg | 54.1 | 42.5 | 48.7 | 32.1 | 35.7 | 17.6 |
| Mn | 7.85 | 2.30 | 1.91 | 0.91 | 1.89 | 0.46 |
| Mo | 2.39 | 0.35 | ND | - | 3.91 | 1.41 |
| Na | 1539 | 285 | 1471 | 265 | 116 | 98.71 |
| Nb | ND | - | ND | - | ND | - |
| Nd | 0.11 | 0.03 | 0.04 | 0.05 | 0.10 | 0.04 |
| Ni | 7.00 | 0.00 | ND | - | ND | - |
| P | ND | - | ND | - | ND | - |
| Pb | 3.16 | 1.62 | 1.70 | 2.21 | 1.29 | 0.86 |
| Pr | 0.03 | 0.01 | 0.02 | 0.01 | ND | - |
| Rb | 0.51 | 0.13 | 0.19 | 0.12 | 0.30 | 0.07 |
| Sb | 1.62 | 0.59 | 1.15 | 1.25 | ND | - |

| | | | | | | |
|---|---|---|---|---|---|---|
| Sc | 3.94 | 1.71 | 3.32 | 2.16 | 3.54 | 1.52 |
| Se | 0.59 | 0.00 | ND | - | ND | - |
| Sm | 0.02 | 0.01 | 0.01 | 0.01 | ND | - |
| Sn | 1.86 | 0.74 | 0.48 | 0.14 | 0.43 | 0.16 |
| Sr | 3.03 | 0.12 | ND | - | ND | - |
| Ta | ND | - | ND | - | ND | - |
| Tb | ND | - | ND | - | ND | - |
| Th | ND | - | ND | - | ND | - |
| Ti | 24.1 | 8.12 | 6.33 | 11.53 | 8.79 | 5.90 |
| Tl | 0.02 | 0.00 | ND | - | ND | - |
| U | 0.02 | 0.02 | ND | - | ND | - |
| V | 6.57 | 3.79 | 3.04 | 0.05 | 2.85 | 0.15 |
| W | 0.08 | 0.03 | 0.01 | 0.01 | 0.03 | 0.03 |
| Y | 0.10 | 0.03 | ND | - | 0.20 | 0.06 |
| Yb | ND | - | ND | - | ND | - |
| Zr | 2.60 | 1.35 | 2.42 | 1.76 | 4.88 | 2.92 |

BA

| | $PM_{10}$ | | $PM_{2.5}$ | | $PM_1$ | |
|---|---|---|---|---|---|---|
| | Mean | Stan. Dev. | Mean | Stan. Dev. | Mean | Stan. Dev. |
| Al | 390 | 312 | 197 | 31.6 | 425 | 252 |
| As | 0.36 | 0.16 | 0.30 | 0.02 | 0.15 | 0.10 |
| Be | ND | - | ND | - | ND | - |
| Bi | ND | - | ND | - | ND | - |
| Ca | 1941 | 1279 | 1511 | 664 | 200 | 70.0 |

| | | | | | | |
|---|---|---|---|---|---|---|
| Cd | ND | - | ND | - | ND | - |
| Ce | 1.40 | 1.56 | 0.28 | 0.07 | 0.19 | 0.14 |
| Co | 0.20 | 0.10 | 0.11 | 0.02 | 0.08 | 0.01 |
| Cr | 6.05 | 0.70 | 6.02 | 2.84 | ND | - |
| Cs | 0.09 | 0.12 | 0.08 | 0.09 | 0.04 | 0.02 |
| Cu | 32.0 | 31.6 | 27.2 | 24.4 | 11.8 | 7.26 |
| Dy | 0.05 | 0.00 | 0.05 | 0.02 | ND | - |
| Er | 0.02 | 0.01 | 0.02 | 0.02 | 0.01 | 0.00 |
| Eu | ND | - | ND | - | ND | - |
| Fe | 221 | 201 | 104 | 52.3 | 11.6 | 1.86 |
| Gd | 0.05 | 0.03 | 0.03 | 0.02 | ND | - |
| Ge | ND | 0.00 | 0.63 | 0.04 | ND | - |
| Hf | ND | - | ND | 0.14 | ND | - |
| Hg | ND | - | ND | - | ND | - |
| Ho | ND | - | ND | - | ND | - |
| K | 702 | 84.2 | 415 | 163 | 350 | 152 |
| La | 0.19 | 0.15 | 0.12 | 0.04 | 0.10 | 0.03 |
| Li | 0.39 | 0.23 | 0.32 | 0.13 | 0.43 | 0.11 |
| Mg | 154 | 15.5 | 264 | 70.9 | ND | - |
| Mn | 5.10 | 3.32 | 2.83 | 1.23 | 1.33 | 0.70 |
| Mo | 6.30 | 4.53 | 15.10 | 4.52 | 5.37 | 1.89 |
| Na | 3985 | 1043 | 4320 | 379 | ND | - |
| Nb | 0.06 | 0.05 | ND | - | 0.07 | 0.03 |
| Nd | 0.16 | 0.14 | 0.10 | 0.05 | 0.09 | 0.02 |
| Ni | 3.44 | 0.47 | 3.23 | 0.66 | 2.88 | 0.69 |

| | | | | | | |
|---|---|---|---|---|---|---|
| P | ND | - | ND | - | ND | - |
| Pb | 3.57 | 2.57 | 2.88 | 1.93 | 1.61 | 0.96 |
| Pr | 0.06 | 0.03 | 0.02 | 0.01 | 0.02 | 0.01 |
| Rb | 0.71 | 0.69 | 0.46 | 0.45 | 0.42 | 0.22 |
| Sb | 0.88 | 0.36 | 2.08 | 0.65 | 1.52 | 0.31 |
| Sc | 11.2 | 8.85 | 8.97 | 7.54 | 20.2 | 12.7 |
| Se | ND | - | ND | - | ND | - |
| Sm | 0.16 | 0.15 | 0.02 | 0.01 | ND | - |
| Sn | 0.54 | 0.21 | 0.54 | 0.17 | 0.39 | 0.20 |
| Sr | 3.44 | 3.49 | 1.78 | 0.89 | 0.77 | 0.04 |
| Ta | ND | - | ND | - | ND | 0.02 |
| Tb | ND | - | ND | - | ND | - |
| Th | ND | - | ND | - | ND | - |
| Ti | 21.8 | 21.5 | 8.95 | 6.21 | 7.29 | 2.97 |
| Tl | 0.29 | 0.29 | 0.06 | 0.09 | 0.03 | 0.03 |
| U | 0.08 | 0.06 | 0.08 | 0.06 | ND | - |
| V | 7.28 | 1.02 | 6.36 | 2.52 | 6.07 | 1.85 |
| W | 0.03 | 0.00 | 0.02 | 0.01 | 0.04 | 0.02 |
| Y | 0.21 | 0.17 | 0.15 | 0.09 | 0.13 | 0.04 |
| Yb | 0.03 | 0.01 | ND | - | ND | - |
| Zr | 5.00 | 3.13 | 7.08 | 4.73 | 7.96 | 4.79 |

ND:not detected. Values Ander the limit of detection

**Table S2**: Levels of PM, carbon and ions in location A during Autumn period (AA). Results are expressed in µg/m$^3$.

| | AA | | | | | |
|---|---|---|---|---|---|---|
| | $PM_{10}$ | | $PM_{2.5}$ | | $PM_1$ | |
| | Mean | Stan. Dev. | Mean | Stan. Dev. | Mean | Stan. Dev. |
| PM | 26.7 | 1.85 | 17.0 | 0.95 | 16.8 | 1.91 |
| TC | 8.01 | 1.09 | 5.51 | 0.87 | 5.69 | 0.96 |
| OC+EC | 7.38 | 1.33 | 5.45 | 0.70 | 5.59 | 0.88 |
| $Cl^-$ | 0.69 | 0.35 | 0.01 | 0.00 | 0.04 | 0.02 |
| $SO_4^{2-}$ | 2.48 | 0.74 | 2.55 | 0.63 | 2.06 | 0.76 |
| $NH_4^+$ | 0.08 | 0.07 | 0.11 | 0.09 | 0.01 | 0.01 |
| $NO_3^-$ | 3.31 | 0.97 | 1.10 | 0.14 | 1.19 | 0.17 |

TC: total carbón; OC + EC: organic carbon and elemental carbon

**Table S3**: Levels of PM, carbon and ions in location A during winter period (AW). Results are expressed in µg/m$^3$.

| | AW | | | | | |
|---|---|---|---|---|---|---|
| | $PM_{10}$ | | $PM_{2.5}$ | | $PM_1$ | |
| | Mean | Stan. Dev. | Mean | Stan. Dev. | Mean | Stan. Dev. |
| PM | 51.2 | 13.9 | 31.9 | 9.94 | 31.3 | 7.12 |
| TC | 17.5 | 5.61 | 14.9 | 3.98 | 15.3 | 3.72 |
| OC+EC | 13.9 | 5.48 | 11.4 | 2.43 | 11.8 | 3.52 |
| $Cl^-$ | 0.05 | 0.03 | 0.01 | 0.01 | 0.02 | 0.03 |
| $SO_4^{2-}$ | 2.47 | 0.42 | 2.85 | 0.39 | 1.90 | 0.24 |
| $NH_4^+$ | 0.24 | 0.09 | 0.70 | 0.22 | 0.20 | 0.17 |
| $NO_3^-$ | 5.02 | 1.29 | 2.11 | 0.43 | 3.38 | 2.51 |

TC: total carbón; OC + EC: organic carbon and elemental carbon

**Table S4**: Levels of PM, carbon and ions in location A during summer period (AS). Results are expressed in μg/m$^3$.

| | AS | | | | | |
|---|---|---|---|---|---|---|
| | $PM_{10}$ | | $PM_{2.5}$ | | $PM_1$ | |
| | Mean | Stan. Dev. | Mean | Stan. Dev. | Mean | Stan. Dev. |
| PM | 20.5 | 1.28 | 19.5 | 5.02 | 13.0 | 5.22 |
| TC | 3.04 | 0.47 | 1.36 | 0.58 | 1.32 | 1.19 |
| OC+EC | 3.69 | 0.43 | 3.51 | 0.57 | 3.26 | 1.14 |
| $Cl^-$ | 0.34 | 0.50 | 0.09 | 0.04 | 0.04 | 0.00 |
| $SO_4^{2-}$ | 2.46 | 0.44 | 1.88 | 0.26 | 1.80 | 0.27 |
| $NH_4^+$ | 0.27 | 0.05 | 0.23 | 0.06 | 0.08 | 0.06 |
| $NO_3^-$ | 1.00 | 0.26 | 0.37 | 0.03 | 0.14 | 0.01 |

TC: total carbón; OC + EC: organic carbon and elemental carbon

**Table S5**: Levels of PM, carbon and ions in location B during autumn period (BA). Results are expressed in μg/m$^3$.

| | BA | | | | | |
|---|---|---|---|---|---|---|
| | $PM_{10}$ | | $PM_{2.5}$ | | $PM_1$ | |
| | Mean | Stan. Dev. | Mean | Stan. Dev. | Mean | Stan. Dev. |
| PM | 29.9 | 15.9 | 14.9 | 6.98 | 6.10 | 3.67 |
| TC | 2.18 | 1.30 | 2.20 | 0.85 | 1.46 | 0.06 |
| OC+EC | 2.26 | 1.17 | 2.16 | 0.83 | 1.40 | 0.06 |
| $Cl^-$ | 0.52 | 0.54 | 0.07 | 0.05 | 0.03 | 0.00 |
| $SO_4^{2-}$ | 2.53 | 1.06 | 1.74 | 0.78 | 1.06 | 0.65 |
| $NH_4^+$ | 0.28 | 0.16 | 0.23 | 0.22 | 0.10 | 0.11 |
| $NO_3^-$ | 2.42 | 1.99 | 0.34 | 0.19 | 0.09 | 0.02 |

TC: total carbón;OC + EC: organic carbon and elemental carbon

# ANNEX II

# Annex II: Supplementary materials for Chapter 3

Supporting information for the paper entitled

## Physicochemistry and toxicity of inhalable particulate matter collected proximal to cement plants.

Francisco Sánchez-Soberón[1], Matthew Lawson[2], Anna J. Wlodarczyk[2], Zoë C. Prytherch[2],

Tim P. Jones[3], Kelly A. Bérubé[2], Marta Schuhmacher[1*],

*Correspondence: marta.schuhmacher@urv.cat; Telephone: +44 (0)29 2087 6012.

### Supporting information

1. *PM levels and meteorological data while sampling*

*“Average PM concentrations during the sampling period were 31.17 and 17.40 µg/m$^3$ for PM10 and PM2.5 respectively. PM10 concentrations ranged between 60.05 and 18.35 µg/m$^3$, while PM2.5 ranged between 38.75 and 10.60 µg/m$^3$. The highest concentrations were found in the beginning of the sampling period (mornings of 03/11 and 03/12 for), while the lowest values were experienced by the mid sampling period (03/26 morning and 03/27 night for PM10 and PM2.5 respectively). No statistical differences (P>0.05) in PM levels were found among the different daily sampling periods (i.e. morning, afternoon and night).*

*Temperature during sampling period ranged between 25.5 and 0.6 ºC, with the average temperature 11.05 ºC. No rain was registered during sampling interval. All meteorological data was provided by the Meteorological Service of Catalonia.”*

### Supporting Figures and Tables

**Figure S 1:** Cement plant (blue) and sampling location (green).

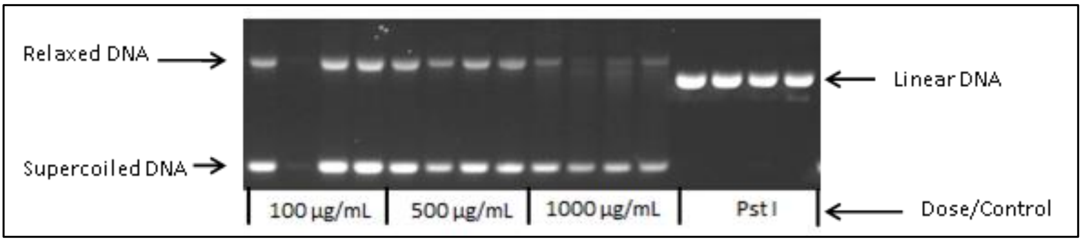

**Figure S 2:** Aspect of an agarose gel showing the different forms of DNA.

**Table S 6:** Description of alternative raw materials and fuels used in the cement kiln.

| **Raw materials** | | |
|---|---|---|
| **Material** | **European Waste Catalogue Code** | **Tons*$10^3$/yr.** |
| Mineral admixture | 190902 ; 100906 ;101304; 101313; 010409; 191209 | 100 |
| Lime admixture | 050113; 060201; 060314; 060316; 100104; 101110; 101120; 101208; 101311; 101314; 150203; 160304; 161103; 161104; 161106; 170101; 170103; 170107; 170504; 190206;191209; | 30 |
| Grinding aid | 070599; 161004 | 12 |
| Paper mill sludge | 030305; 030307; 030309; 030310; 030311 | 30 |
| Sewage sludge | 020502; 070112; 040220; 070312; 070512 ; 070612; 110110; 110114 ; 190813; 190814 ; 070712; 110109 | |
| Gypsum | 070610; 100105 | 40 |
| Coal fly ash | 100102 | 150 |
| Iron slag | 100201; 100202; 100210; 100299; 100903; 100908; 101006; 120117;100399; 100906 | 20 |
| **Total** | | **382** |
| **Fuels** | | |
| **Material** | **European Waste Catalogue Number** | **Tons*$10^3$/yr.** |
| Spent coffee grounds | 020301 | 40 |
| Dry sewage sludge | 190805 | |
| Meat and bone mill | 020203 | |
| Biodiesel | 130703 | 10 |
| Pruning and wood wastes | 170201; 030101; 030105; 030301; 020103 | 20 |
| Refuse derived fuel | 191210 | 30 |
| **Total** | | **100** |

# ANNEX III

# Annex III: Supplementary materials for Chapter 5:

Supplementary materials fro the paper entitled:

## Source apportionment of inorganic and organic PM in the ambient air around a cement plant: assessment of complementary tools.

Montse Mari, Francisco Sánchez-Soberón, Carme Audí-Miró, Barend L. van Drooge, Albert Soler, Joan O. Grimalt, Marta Schuhmacher (2016). Aerosol and Air Quality Research 16 (12) 3230-3242.

Figure S1: Location of the cement plant and the sampling point.

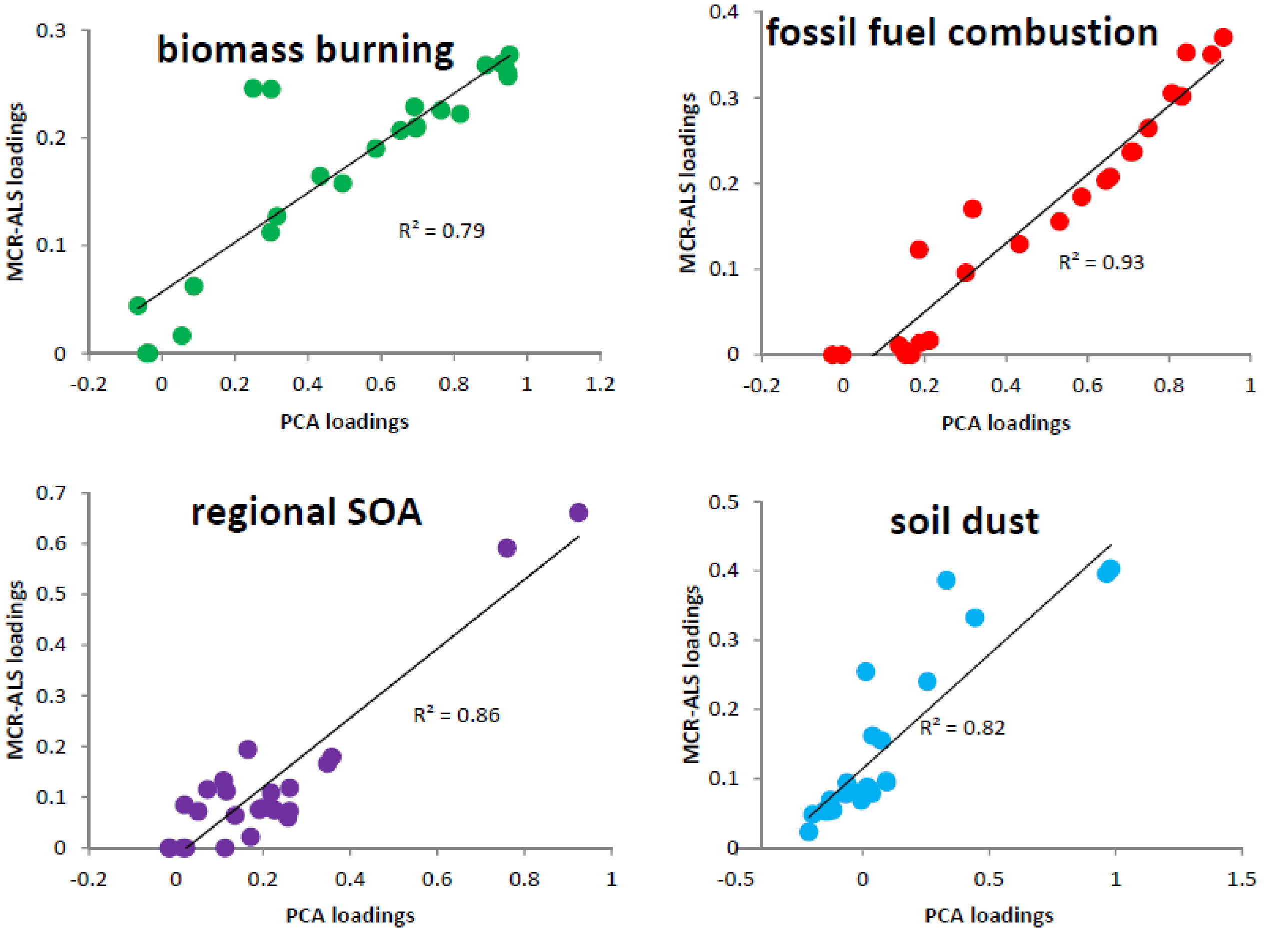

Figure S2: Correlations between loadings obtained by means of PCA and MCR-ALS in organic species.

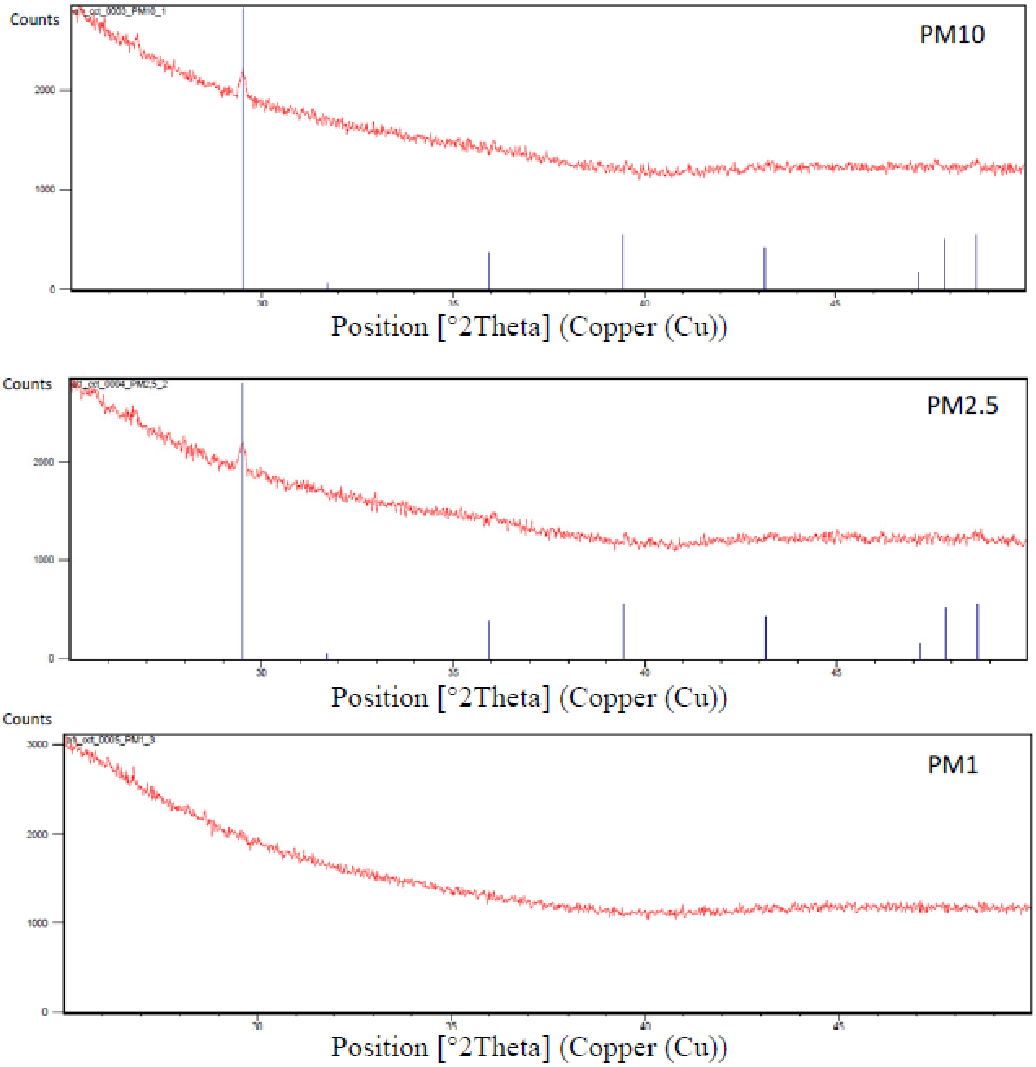

Figure S3: X-ray diffraction chromatograph of $PM_{10}$, $PM_{2.5}$, and $PM_1$. $PM_{2.5}$ and $PM_{10}$ shopw a peak of calcite.

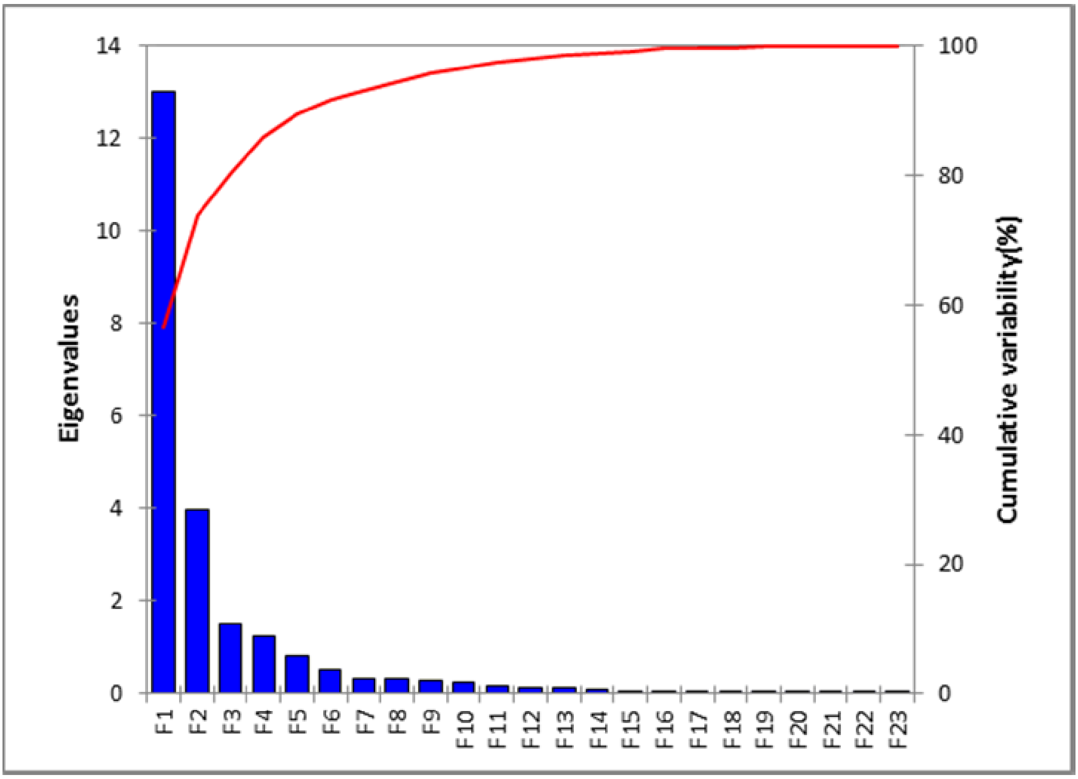

Figure S4: Sedimentation graph.

**Description of the points indicated in Fig. 1 of the main text**:

**Mineral fraction:** *1.* Cement*; *2.* Kiln dust*; *3.* PM 10 street dust (López-Veneroni et al., 2009). **Combusted biomass fuels from C3 plants:** *4.* Sunflower stalk; *5.* Agricultural waste; *6.* Wood pellets; *7.* Grain screening; *8.* Straw pellets; *9.* Buckwheat shell (4-9 from Garbaras et al., 2015). **Combusted fossil fuels:** *10. 16.* Range of natural gas; *11. 14.* Range of coal for heating; *12.* Coal (Andres et al., 1994); *13.* Unleaded fuel from exhaust pipe; *15.* Regular fuel from exhaust pipe; *17.* Domestic fuel oil; *18.* Diesel from exhaust pipe (10, 11 and 13-18 from Widory et al., 2004); *19.20.* Range of petroleum (Andres et al., 1994). **Combusted sewage sludge:** *21.* Sewage sludge (Garbaras et al., 2015). **Fuels analysed in this study:** *22.* Unleaded fuel from exhaust pipe*; *23.* Diesel from exhaust pipe*. **Deposited:** *24.* Deposited material on a Petri dish in the school sampling point (Montcada)*. **Montcada samples:** *25.* PM10 average from December 2014, school sampling point (cement plant turned on); *26.* PM10 cement plant turned on, close to the school sampling point, December 2014; *27.* PM10 cement plant turned off, close to the school sampling point, December 2014; *28.* PM2.5 average July 2014, school sampling point (cement plant turned on); *29.* PM2.5 average December2014, school sampling point (cement plant turned on); *30.* PM1 average December 2014, school sampling point (cement plant turned on). * samples analyzed in this study.

| | MEAN | SD | MIN | MAX |
|---|---|---|---|---|
| Al | 689 | 945 | 61 | 3322 |
| As | 0.46 | 0.23 | 0.06 | 1.00 |
| Ca | 1707 | 1689 | 31 | 5881 |
| Cd | 0.37 | 0.32 | 0.06 | 1.20 |
| Ce | 0.87 | 0.79 | 0.06 | 3.39 |
| Co | 0.25 | 0.18 | 0.03 | 0.94 |
| Cr | 5.35 | 3.35 | 1.23 | 13.20 |
| Cu | 29.14 | 18.51 | 1.23 | 63.60 |
| Fe | 575 | 327 | 152 | 1455 |
| K | 1045 | 1176 | 147 | 4547 |
| Li | 0.47 | 0.30 | 0.06 | 1.31 |
| Mn | 10.70 | 7.27 | 2.08 | 32.34 |
| Ni | 3.62 | 2.54 | 0.59 | 11.52 |
| Pb | 11.48 | 6.43 | 1.10 | 25.05 |
| Sb | 3.53 | 1.96 | 0.72 | 8.13 |
| Sn | 4.80 | 2.80 | 0.58 | 11.10 |
| Sr | 7.07 | 7.29 | 0.61 | 24.90 |
| Ti | 45.34 | 29.69 | 4.83 | 123.37 |
| V | 10.25 | 7.84 | 3.00 | 37.10 |
| OC+EC | 8.06 | 4.79 | 2.02 | 20.61 |
| Cl- | 0.32 | 0.42 | 0.02 | 1.77 |
| SO42- | 1.88 | 0.70 | 0.90 | 3.38 |
| NO3- | 2.33 | 1.69 | 0.41 | 6.78 |

Table S1: Statistics of inorganic PM10 species collected around the cement plant. N: 34 samples
Note: Metals are given in ng/m$^3$; OC+EC and anions are given in µg/m$^3$.

.

| | $PM_1$ | | | | $PM_{2.5}$ | | | | $PM_{10}$ | | | |
|---|---|---|---|---|---|---|---|---|---|---|---|---|
| | MEAN | SD | MIN | MAX | MEAN | SD | MIN | MAX | MEAN | SD | MIN | MAX |
| phen | 0.12 | 0.05 | 0.05 | 0.17 | 0.1 | 0.05 | 0.04 | 0.16 | 0.07 | 0.07 | 0.06 | 0.25 |
| anthr | 0.02 | 0 | 0.01 | 0.02 | 0.02 | 0 | 0.01 | 0.03 | 0.01 | 0.01 | 0.01 | 0.03 |
| fluo | 0.24 | 0.09 | 0.11 | 0.38 | 0.23 | 0.12 | 0.09 | 0.42 | 0.16 | 0.16 | 0.15 | 0.6 |
| pyrene | 0.42 | 0.21 | 0.17 | 0.72 | 0.29 | 0.17 | 0.1 | 0.53 | 0.23 | 0.23 | 0.17 | 0.82 |
| retene | 0.15 | 0.11 | 0.06 | 0.42 | 0.19 | 0.15 | 0.05 | 0.47 | 0.22 | 0.22 | 0.07 | 0.71 |
| benz[a]anthracene | 0.49 | 0.33 | 0.11 | 0.93 | 0.45 | 0.31 | 0.1 | 0.87 | 0.4 | 0.4 | 0.16 | 1.15 |
| chrysene | 0.59 | 0.39 | 0.16 | 1.34 | 0.49 | 0.29 | 0.14 | 0.84 | 0.31 | 0.31 | 0.2 | 1.1 |
| benzo[b+j]fluoranthene | 1.08 | 0.51 | 0.39 | 1.65 | 0.93 | 0.5 | 0.29 | 1.62 | 0.82 | 0.82 | 0.46 | 2.72 |
| benzo[k]fluoranthene | 0.29 | 0.14 | 0.12 | 0.46 | 0.23 | 0.11 | 0.08 | 0.34 | 0.2 | 0.2 | 0.1 | 0.62 |
| benzo[e]pyrene | 0.5 | 0.23 | 0.19 | 0.72 | 0.42 | 0.2 | 0.14 | 0.64 | 0.31 | 0.31 | 0.21 | 1.07 |
| benzo[a]pyrene | 0.6 | 0.34 | 0.19 | 1.06 | 0.43 | 0.24 | 0.15 | 0.73 | 0.37 | 0.37 | 0.18 | 1.16 |
| indeno[123cd]pyrene | 0.91 | 0.51 | 0.29 | 1.62 | 0.72 | 0.4 | 0.19 | 1.19 | 0.47 | 0.47 | 0.34 | 1.69 |
| benzo[ghi]perylene | 1.15 | 0.58 | 0.42 | 1.89 | 0.84 | 0.42 | 0.27 | 1.28 | 0.51 | 0.51 | 0.42 | 1.75 |
| dibenz[ah]anthracene | 0.03 | 0.01 | 0.02 | 0.05 | 0.03 | 0.01 | 0.02 | 0.06 | 0.02 | 0.02 | 0.02 | 0.07 |
| coronene | 0.2 | 0.12 | 0.06 | 0.42 | 0.14 | 0.08 | 0.03 | 0.26 | 0.08 | 0.08 | 0.06 | 0.31 |
| 17(H)α-21(H)β-29-norhopane | 0.13 | 0.04 | 0.08 | 0.18 | 0.12 | 0.05 | 0.07 | 0.18 | 0.09 | 0.09 | 0.12 | 0.37 |
| 17(H)α-21(H)β-hopane | 0.09 | 0.04 | 0.06 | 0.14 | 0.1 | 0.04 | 0.06 | 0.15 | 0.05 | 0.05 | 0.09 | 0.21 |
| galactosan | 46.71 | 38.06 | 14.85 | 126.57 | 43.76 | 32.81 | 13.93 | 102.86 | 45.19 | 45.19 | 19.77 | 150.3 |
| mannosan | 44.77 | 31.68 | 15.92 | 109.23 | 39.28 | 26.61 | 13.65 | 88.57 | 37.02 | 37.02 | 19.27 | 128.95 |
| levoglucosan | 343 | 271 | 129 | 952 | 350 | 278 | 107 | 887 | 422 | 422 | 148 | 1342 |
| dehydrabietic acid | 47.32 | 33.69 | 11.45 | 113.68 | 42.77 | 30.58 | 11.11 | 96.28 | 43.14 | 43.14 | 13.23 | 145.1 |
| α-glucose | 4.52 | 1.66 | 2.61 | 6.58 | 7.8 | 6.28 | 3.51 | 23 | 31.5 | 31.5 | 19.71 | 115.39 |
| β-glucose | 5.36 | 1.33 | 3.6 | 6.88 | 10.34 | 7.59 | 5.17 | 28.29 | 38.93 | 38.93 | 23.87 | 143.67 |
| mannitol | 3.63 | 1.44 | 1.89 | 5.93 | 9 | 7.72 | 4.24 | 27.9 | 26.65 | 26.65 | 25.58 | 103.24 |
| succinic acid | 14 | 4.96 | 9.79 | 24.68 | 13.61 | 2.51 | 9.85 | 17 | 4.2 | 4.2 | 10.29 | 23.09 |
| glutaric acid | 3.14 | 0.71 | 2.41 | 4.13 | 3.02 | 0.82 | 1.48 | 4.03 | 0.83 | 0.83 | 2.6 | 5.14 |
| isotopic | -26.76 | 0.11 | -26.92 | -26.64 | -26.32 | 0.3 | -26.64 | -25.68 | 0.38 | 0.38 | -26.4 | -25.48 |

Table S2: Statistics of organic compounds (ng/m$^3$) δ$^{13}$C values in $PM_{10}$, $PM_{2.5}$ and $PM_1$ fractions.

|  | Al | As | Ca | Cd | Ce | Co | Cr | Cu | Fe | K | Li | Mn | Ni | Pb | Sb | Sn | Sr | Ti | V | OC+EC | $Cl^-$ | $SO_4^{2-}$ | $NO_3^-$ |
|---|---|---|---|---|---|---|---|---|---|---|---|---|---|---|---|---|---|---|---|---|---|---|---|
| Al | 1.00 | 0.24 | 0.94 | 0.54 | 0.85 | 0.57 | 0.49 | 0.39 | 0.11 | 0.90 | 0.71 | -0.20 | 0.70 | 0.46 | 0.56 | 0.55 | 0.95 | 0.50 | 0.82 | 0.54 | -0.22 | 0.47 | 0.80 |
| As | 0.24 | 1.00 | 0.34 | 0.59 | 0.45 | 0.57 | 0.69 | 0.75 | 0.64 | 0.31 | 0.43 | 0.51 | 0.65 | 0.67 | 0.71 | 0.63 | 0.20 | 0.60 | 0.24 | 0.63 | -0.19 | 0.00 | 0.50 |
| Ca | 0.94 | 0.34 | 1.00 | 0.58 | 0.89 | 0.59 | 0.56 | 0.52 | 0.18 | 0.92 | 0.66 | -0.15 | 0.72 | 0.55 | 0.61 | 0.62 | 0.94 | 0.55 | 0.79 | 0.55 | -0.15 | 0.49 | 0.81 |
| Cd | 0.54 | 0.59 | 0.58 | 1.00 | 0.66 | 0.52 | 0.65 | 0.75 | 0.23 | 0.63 | 0.57 | -0.01 | 0.59 | 0.61 | 0.69 | 0.63 | 0.52 | 0.49 | 0.34 | 0.65 | 0.05 | 0.30 | 0.76 |
| Ce | 0.85 | 0.45 | 0.89 | 0.66 | 1.00 | 0.77 | 0.61 | 0.60 | 0.26 | 0.84 | 0.72 | -0.04 | 0.77 | 0.50 | 0.67 | 0.62 | 0.84 | 0.66 | 0.73 | 0.62 | -0.06 | 0.51 | 0.83 |
| Co | 0.57 | 0.57 | 0.59 | 0.52 | 0.77 | 1.00 | 0.79 | 0.68 | 0.63 | 0.47 | 0.54 | 0.46 | 0.79 | 0.52 | 0.76 | 0.69 | 0.58 | 0.84 | 0.57 | 0.70 | -0.16 | 0.31 | 0.64 |
| Cr | 0.49 | 0.69 | 0.56 | 0.65 | 0.61 | 0.79 | 1.00 | 0.82 | 0.66 | 0.45 | 0.50 | 0.47 | 0.86 | 0.78 | 0.90 | 0.86 | 0.48 | 0.73 | 0.45 | 0.79 | -0.19 | 0.20 | 0.66 |
| Cu | 0.39 | 0.75 | 0.52 | 0.75 | 0.60 | 0.68 | 0.82 | 1.00 | 0.62 | 0.44 | 0.37 | 0.36 | 0.70 | 0.75 | 0.89 | 0.83 | 0.42 | 0.63 | 0.30 | 0.76 | -0.03 | 0.19 | 0.67 |
| Fe | 0.11 | 0.64 | 0.18 | 0.23 | 0.26 | 0.63 | 0.66 | 0.62 | 1.00 | 0.05 | 0.20 | 0.88 | 0.54 | 0.63 | 0.65 | 0.69 | 0.10 | 0.74 | 0.22 | 0.58 | -0.20 | -0.19 | 0.18 |
| K | 0.90 | 0.31 | 0.92 | 0.63 | 0.84 | 0.47 | 0.45 | 0.44 | 0.05 | 1.00 | 0.74 | -0.26 | 0.63 | 0.47 | 0.53 | 0.53 | 0.90 | 0.48 | 0.73 | 0.52 | -0.13 | 0.48 | 0.78 |
| Li | 0.71 | 0.43 | 0.66 | 0.57 | 0.72 | 0.54 | 0.50 | 0.37 | 0.20 | 0.74 | 1.00 | 0.11 | 0.66 | 0.43 | 0.46 | 0.39 | 0.61 | 0.60 | 0.53 | 0.33 | -0.07 | 0.29 | 0.52 |
| Mn | -0.20 | 0.51 | -0.15 | -0.01 | -0.04 | 0.46 | 0.47 | 0.36 | 0.88 | -0.26 | 0.11 | 1.00 | 0.30 | 0.42 | 0.36 | 0.37 | -0.23 | 0.59 | -0.06 | 0.26 | -0.16 | -0.37 | -0.18 |
| Ni | 0.70 | 0.65 | 0.72 | 0.59 | 0.77 | 0.79 | 0.86 | 0.70 | 0.54 | 0.63 | 0.66 | 0.30 | 1.00 | 0.71 | 0.79 | 0.78 | 0.66 | 0.70 | 0.75 | 0.76 | -0.23 | 0.28 | 0.75 |
| Pb | 0.46 | 0.67 | 0.55 | 0.61 | 0.50 | 0.52 | 0.78 | 0.75 | 0.63 | 0.47 | 0.43 | 0.42 | 0.71 | 1.00 | 0.80 | 0.82 | 0.41 | 0.62 | 0.39 | 0.77 | -0.27 | -0.05 | 0.55 |
| Sb | 0.56 | 0.71 | 0.61 | 0.69 | 0.67 | 0.76 | 0.90 | 0.89 | 0.65 | 0.53 | 0.46 | 0.36 | 0.79 | 0.80 | 1.00 | 0.94 | 0.54 | 0.65 | 0.49 | 0.88 | -0.29 | 0.18 | 0.72 |
| Sn | 0.55 | 0.63 | 0.62 | 0.63 | 0.62 | 0.69 | 0.86 | 0.83 | 0.69 | 0.53 | 0.39 | 0.37 | 0.78 | 0.82 | 0.94 | 1.00 | 0.52 | 0.63 | 0.56 | 0.89 | -0.34 | 0.06 | 0.66 |
| Sr | 0.95 | 0.20 | 0.94 | 0.52 | 0.84 | 0.58 | 0.48 | 0.42 | 0.10 | 0.90 | 0.61 | -0.23 | 0.66 | 0.41 | 0.54 | 0.52 | 1.00 | 0.52 | 0.80 | 0.54 | -0.11 | 0.56 | 0.79 |
| Ti | 0.50 | 0.60 | 0.55 | 0.49 | 0.66 | 0.84 | 0.73 | 0.63 | 0.74 | 0.48 | 0.60 | 0.59 | 0.70 | 0.62 | 0.65 | 0.63 | 0.52 | 1.00 | 0.46 | 0.60 | -0.05 | 0.23 | 0.51 |
| V | 0.82 | 0.24 | 0.79 | 0.34 | 0.73 | 0.57 | 0.45 | 0.30 | 0.22 | 0.73 | 0.53 | -0.06 | 0.75 | 0.39 | 0.49 | 0.56 | 0.80 | 0.46 | 1.00 | 0.56 | -0.35 | 0.38 | 0.66 |
| OC+EC | 0.54 | 0.63 | 0.55 | 0.65 | 0.62 | 0.70 | 0.79 | 0.76 | 0.58 | 0.52 | 0.33 | 0.26 | 0.76 | 0.77 | 0.88 | 0.89 | 0.54 | 0.60 | 0.56 | 1.00 | -0.30 | 0.15 | 0.76 |
| $Cl^-$ | -0.22 | -0.19 | -0.15 | 0.05 | -0.06 | -0.16 | -0.19 | -0.03 | -0.20 | -0.13 | -0.07 | -0.16 | -0.23 | -0.27 | -0.29 | -0.34 | -0.11 | -0.05 | -0.35 | -0.30 | 1.00 | 0.37 | -0.08 |
| $SO_4^{2-}$ | 0.47 | 0.00 | 0.49 | 0.30 | 0.51 | 0.31 | 0.20 | 0.19 | -0.19 | 0.48 | 0.29 | -0.37 | 0.28 | -0.05 | 0.18 | 0.06 | 0.56 | 0.23 | 0.38 | 0.15 | 0.37 | 1.00 | 0.62 |
| $NO_3^-$ | 0.80 | 0.50 | 0.81 | 0.76 | 0.83 | 0.64 | 0.66 | 0.67 | 0.18 | 0.78 | 0.52 | -0.18 | 0.75 | 0.55 | 0.72 | 0.66 | 0.79 | 0.51 | 0.66 | 0.76 | -0.08 | 0.62 | 1.00 |

Table S3: Correlation matrix (Pearson (n)) for inorganic PCA.

| | |
|---|---|
| Al | 0.668 |
| As | 0.614 |
| Ca | 0.729 |
| Cd | 0.745 |
| Ce | 0.753 |
| Co | 0.815 |
| Cr | 0.752 |
| Cu | 0.677 |
| Fe | 0.726 |
| K | 0.748 |
| Li | 0.716 |
| Mn | 0.67 |
| Ni | 0.74 |
| Pb | 0.76 |
| Sb | 0.667 |
| Sn | 0.726 |
| Sr | 0.846 |
| Ti | 0.85 |
| V | 0.751 |
| OC+EC | 0.763 |
| Cl- | 0.301 |
| SO42- | 0.397 |
| NO3- | 0.718 |
| **KMO** | **0.718** |

Table S4:Kaiser-Meyer-Olkin measure of sampling adequacy of the PCA analysis.

# ANNEX IIII

## Supplementary materials for Chapter 6:

# In-vitro metabolomics to evaluate toxicity of PM nearby a petrochemical complex

Francisco Sánchez-Soberón, Matthias Cuykx, Noemi Serra, Victoria Linares, Montserrat Bellés, Adrian Covaci, Marta Schuhmacher

**Table S 1**: Apolar features showing significant changes in A549 cells when exposed to real doses of the two assessed fractions. F: major fragment; NA: not acquired; NL: neutral loss.

| Fraction | Mass (amu) | Retention time (min) | Regulation | Fold change | Precursor Ion | Average mass error (ppm) | Molecular formula | Major fragments and neutral loses | Identification |
|---|---|---|---|---|---|---|---|---|---|
| $PM_{2.5-0.25}$ | 293.2827 | 2.48 | Down | 0.57 | (M+H)+ | | No matches | NA | |
| $PM_{0.25}$ | | | Up | 1.43 | | | | | |
| $PM_{2.5-0.25}$ | 498.4649 | 10.09 | Down | 0.53 | (M+H)+ | 4.71 | C30 H62 N2 O S | F 298.3268 [C20 H42 O]+ | |
| $PM_{0.25}$ | | | Down | 0.15 | | | | | |
| $PM_{2.5-0.25}$ | 501.3369 | 1.17 | Up | $>10^4$ | (M-H)- | 5.98 | C29 H47 N3 O2 S | | |
| $PM_{0.25}$ | | | Up | $>10^4$ | | | | | |
| $PM_{2.5-0.25}$ | 518.4317 | 8.75 | Down | 0.11 | (M+H)+ | 4.50 | C33 H58 O4 | NA | Fatty acid |
| $PM_{2.5-0.25}$ | 520.4474 | 10.08 | Up | $>10^5$ | (M+H)+ | 3.71 | C33 H60 O4 | | Fatty acid |
| $PM_{0.25}$ | | | Up | $>10^5$ | | | | | Fatty acid |
| $PM_{2.5-0.25}$ | 537.5131 | 9.14 | Up | 1.05 | (M+H)+ | 2.02 | C34 H67 N O3 | NL 404.4028 | Ceramide |
| | | | | | (M+Na)+ | 3.43 | C34 H67 N O3 | | |
| $PM_{2.5-0.25}$ | 563.3535 | 1.28 | Down | 0.89 | (M+H)+ | 4.21 | C30 H49 N3 O7 | F 133.0842 [C5 O4 H9]+ | Phosphatidylcholines |
| | | | | | (M+H)+ | 4.27 | C34 H49 N3 O2 S | | |
| $PM_{2.5-0.25}$ | 597.482 | 3.39 | Down | 0.19 | (M+H)+ | 2.96 | C35 H67 N O4 S | NL 315.3236 | |
| $PM_{2.5-}$ | 647.6204 | 13.79 | Down | 0.95 | (M+H)+ | 0.48 | C42 H81 N O3 | NA | Ceramide |

| | | | | | | | | | |
|---|---|---|---|---|---|---|---|---|---|
| 0.25 | | | | | | | | | |
| $PM_{0.25}$ | | | Down | 0.94 | (M+H)+ | 4.86 | C38 H77 N7 O | | |
| $PM_{2.5-0.25}$ | 667.6207 | 12.41 | Up | 1.39 | (M+H)+ | | No matches | NA | |
| $PM_{0.25}$ | 669.6031 | 13.58 | Up | 4.34 | (M+H)+ | 5.69 | C38 H79 N5 O2 S | NA | |
| $PM_{2.5-0.25}$ | 686.6027 | 12.88 | Up | $>10^4$ | (M-H)- | 2.84 | C37 H78 N6 O5 | NA | Diglycerol |
| | | | | | (M-H)- | 1.04 | C45 H82 O2 S | | |
| | | | | | (M-H)- | 3.83 | C48 H78 O2 | | |
| | | | | | (M-H)- | 4.74 | C41 H82 O7 | | |
| $PM_{2.5-0.25}$ | 694.4884 | 1.26 | Down | 0.25 | (M+2H)+2 | 0.12 | C40 H71 O7 P | NA | Phosphatidylglycerol |
| | | | | | (M+H)+ | 4.29 | C31 H66 N8 O9 | | |
| | | | | | (M+H)+ | 3.09 | C47 H66 O4 | | |
| | | | | | (M+2H)+2 | 2.56 | C42 H66 N2 O6 | | |
| $PM_{0.25}$ | 702.1909 | 10.21 | Down | 0.30 | (M-H)- | | No matches | NA | |
| $PM_{2.5-0.25}$ | 709.6154 | 12.10 | Down | 0.62 | (M-H)- | 10.29 | No matches | F 662.6019 | |
| $PM_{0.25}$ | 709.6154 | 12.10 | Up | 1.43 | (M-H)- | 10.29 | No matches | F 662.6019 | |
| $PM_{2.5-0.25}$ | 714.6091 | 12.74 | Down | 0.77 | (M-H)- | | No matches | NA | Diglycerol |
| $PM_{2.5-0.25}$ | 737.5057 | 8.42 | Up | 1.28 | (M+H)+ | 1.28 | C35 H72 N5 O9 P | F 313.2726 [C17 H35 N3 O2]+ | Phosphatidylethanolamine |
| $PM_{0.25}$ | | | Up | 1.68 | (M+H)+ | 1.03 | C37 H67 N7 O8 | | |
| | | | | | (M+H)+ | 2.94 | C36 H68 N9 O5 P | | |
| $PM_{2.5-0.25}$ | 737.5084 | 8.74 | Down | 0.80 | (M+H)+ | 0.74 | C35 H72 N5 O9 P | F 184.0747 [C6 H11 N5 P]+ or [C10 H8 N4]+ | Phosphatidylethanolamine or Phosphatidylcholine |
| $PM_{0.25}$ | | | Down | 0.84 | (M+H)+ | 1.46 | C34 H71 N7 O8 S | | |
| $PM_{0.25}$ | 762.5616 | 7.53 | Up | 1.90 | (M-H)- | 5.19 | C45 H79 O7 P | NA | Phosphatidic acid |

| | | | | | | | | | |
|---|---|---|---|---|---|---|---|---|---|
| | | | | | (M-H)- | 5.19 | C45 H79 O7 P | | |
| | | | | | (M-H)- | 6.05 | C45 H79 O7 P | | |
| $PM_{2.5-0.25}$ | 763.5308 | 8.23 | Down | 0.13 | (M-H)- | 5.87 | C49 H69 N3 O4 | F 255.2324 [C16 H31 O2]+ | Phosphatidylserine |
| | | | | | (M-H)- | 4.36 | C54 H69 N O2 | or [C14 H29 N3 O]+ | |
| | | | | | (M-H)- | 5.05 | C47 H74 N O5 P | | |
| $PM_{2.5-0.25}$ | 773.535 | 10.75 | Down | 0.23 | (M+H)+ | 3.41 | C45 H76 N O7 P | NA | Phosphatidylethanolamine |
| $PM_{0.25}$ | | | Down | $<10^{-5}$ | (M+H)+ | 3.71 | C47 H71 N3 O6 | | |
| | | | | | (M+H)+ | 5.29 | C44 H75 N3 O6 S | | |
| $PM_{0.25}$ | 773.5408 | 11.88 | Down | 0.53 | (M+H)+ | 0.44 | C46 H71 N5 O5 | NA | Phosphatidylethanolamine |
| $PM_{2.5-0.25}$ | 813.5496 | 10.39 | Down | 0.84 | (M-H)- | 0.83 | C40 H76 N7 O8 P | F 281.2504 [C18 H33 O2]+ | |
| $PM_{0.25}$ | | | Down | 0.86 | (M-H)- | 1.51 | C42 H71 N9 O7 | | |
| | | | | | (M-H)- | 1.38 | C39 H80 N3 O12 P | | |
| | | | | | (M-H)- | 2.99 | C41 H75 N5 O11 | | |
| | | | | | (M-H)- | 4.23 | C44 H80 N O10 P | | Phosphatidylserine (18:1/20:2) |
| $PM_{0.25}$ | 819.5466 | 10.71 | Down | $<10^{-5}$ | (M-H)- | 2.29 | C42 H73 N7 O9 | F 303.2291 [C16 H27 N6]+ | Phosphatidylserine |
| | | | | | (M-H)- | 5.86 | C41 H74 N9 O6 P | | |
| $PM_{2.5-0.25}$ | 825.6673 | 10.90 | Down | 0.84 | (M-H)- | 6.44 | C48 H92 N O7 P | NA | Phosphatidylcholine |
| | | | | | (M-H)- | 0.14 | C44 H87 N7 O7 | | |
| | | | | | (M-H)- | 0.49 | C52 H91 N O4 S | | |
| | | | | | (M-H)- | 6.97 | C51 H83 N7 O2 | | |
| | | | | | (M-H)- | 4.44 | C47 H91 N3 O6 S | | |
| $PM_{0.25}$ | 826.6531 | 17.45 | Up | 4.65 | (M+H)+ | 1.98 | C43 H87 N8 O5 P | NA | Phosphatidylcholines |
| | | | | | (M+H)+ | 1.83 | C48 H90 O10 | | |

| | | | | | | | | | |
|---|---|---|---|---|---|---|---|---|---|
| | | | | | (M+H)+ | 3.34 | C49 H86 N4 O6 | | |
| $PM_{0.25}$ | 842.6783 | 20.01 | Up | 3.98 | (M+H)+ | 1.08 | C56 H90 O5 | | Steroid |
| | | | | | (M+H)+ | 1.30 | C57 H86 N4 O | | |
| | | | | | (M+H)+ | 1.98 | C49 H90 N6 O3 S | | |
| | | | | | (M+H)+ | 3.91 | C52 H86 N6 O3 | | |
| $PM_{2.5-0.25}$ | 847.6455 | 11.03 | Down | 0.29 | (M+H)+ | 4.45 | Many candidates | NA | Phosphatidylcholines |
| $PM_{2.5-0.25}$ | 861.6376 | 10.47 | Down | 0.30 | (M-H)- | | No matches | NA | Phosphatidylserine |
| $PM_{0.25}$ | | | Down | 0.81 | | | | | |
| $PM_{0.25}$ | 871.7623 | 19.92 | Up | 1.88 | (M+H)+ | 0.92 | C56 H97 N5 O2 | F 575.5099 | Triglyceride |
| | | | | | (M+H)+ | 0.86 | C55 H101 N O6 | | |
| $PM_{0.25}$ | 876.5564 | 17.21 | Up | 2.34 | (M+H)+ | 0.81 | Many candidates | F 549.427 [C36 H57 N2 S]+ | |
| $PM_{2.5-0.25}$ | 882.7013 | 19.83 | Down | 0.36 | (M+H)+ | 4.36 | C56 H90 N4 O4 | NA | |
| $PM_{0.25}$ | | | | 0.22 | | | | | |
| $PM_{2.5-0.25}$ | 894.8078 | 24.01 | Up | 2.02 | (M+H)+ | 3.42 | Many candidates | F 509.4583 [C32 H61 O4]+ or [C30 H59 N3 O3]+ | |
| $PM_{0.25}$ | | | Up | 1.73 | | | | | |
| $PM_{0.25}$ | 898.7446 | 22.09 | Down | $<10^{-5}$ | (M+H)+ | 1.09 | C56 H94 N6 O3 | NA | |
| | | | | | (M+H)+ | 1.22 | C53 H103 O8 P | | |
| | | | | | (M+H)+ | 2.58 | C54 H99 N4 O4 P | | |
| | | | | | (M+H)+ | 1.61 | C55 H98 N2 O7 | | |
| $PM_{0.25}$ | 899.7967 | 21.25 | Down | $<10^{-5}$ | (M+H)+ | 1.30 | C57 H105 N O6 | F 577.5169 [C40 H67 N O]+ | Triglyceride |

| | | | | | | | | | |
|---|---|---|---|---|---|---|---|---|---|
| | | | | | (M+H)+ | 0.16 | C58 H101 N5 O2 | | |
| PM$_{0.25}$ | 908.7031 | 15.56 | Down | 0.92 | (M+H)+ | | No matches | NA | Triglyceride |
| PM$_{0.25}$ | 927.8277 | 21.82 | Down | 0.99 | (M+H)+ | | No matches | F 605.5549 | Triglyceride |
| PM$_{0.25}$ | 941.4992 | 9.30 | Up | 7.67 | (M-H)- | 1.83 | Many candidates | NA | |
| PM$_{0.25}$ | 949.5310 | 10.84 | Down | 0.33 | (M-H)- | 4.37 | C46 H76 N7 O12 P | NA | |
| PM$_{0.25}$ | 954.843 | 21.85 | Down | 0.23 | (M+H)+ | | No matches | F 657.5652[C39 H74 N6 P]+ or [C40 H74 N4 O P]+ | Triglyceride |
| PM$_{2.5-0.25}$ | 964.8193 | 21.10 | Up | 8.11 | (M+H)+ | 0.78 | C55 H109 N6 O5 P | NA | Triglyceride |
| | | | | | (M+H)+ | 2.08 | C54 H113 N2 O9 P | | |
| | | | | | (M+H)+ | 0.45 | C59 H113 O7 P | | |
| PM$_{2.5-0.25}$ | 977.8404 | 22.21 | Down | 0.15 | (M+H)+ | | No matches | NA | Triglyceride |
| PM$_{2.5-0.25}$ | 995.7933 | 18.56 | Up | 5.37 | (M+H)+ | 1.34 | C58 H105 N7 O4 S | NA | Triglyceride |
| PM$_{0.25}$ | 1033.9099 | 24.08 | Down | 0.24 | (M+H)+ | | No matches | F 689.6497[C48 H83 N O]+ | Triglyceride |
| PM$_{2.5-0.25}$ | 1278.9489 | 11.43 | Down | $>10^{-4}$ | (M+H)+ | 0.14 | C79 H122 N8 O6 | NA | |
| | | | | | (M+H)+ | 1.00 | C80 H131 N2 O6 P S | | |
| PM$_{0.25}$ | 1459.0822 | 10.78 | Down | 0.16 | (M+H)+ | | No matches | NA | Cardiolipin |
| PM$_{2.5-0.25}$ | 1489.09 | 10.84 | Down | 0.21 | (M+H)+ | | No matches | NA | Cardiolipin |
| PM$_{0.25}$ | 1577.0367 | 9.65 | Down | 0.34 | (M+H)+ | | No matches | NA | Cardiolipin |
| PM$_{2.5-0.25}$ | 1609.2238 | 12.94 | Down | 0.72 | (M+H)+ | | No matches | NA | Cardiolipin |

**Table S 2**: Polar features showing significant changes in A549 cells when exposed to LC5 doses of the two assessed fractions. F: major fragment; NA: not acquired; NL: neutral loss

| Fraction | Mass (amu) | Retention time (min) | Regulation | Fold change | Precursor Ion | Average mass error (ppm) | Molecular formula | Major fragments and neutral loses | Identification |
|---|---|---|---|---|---|---|---|---|---|
| PM$_{0.25}$ | 113.0477 | 2.34 | Down | 0.51 | (M-H)- | 8.00 | C5 H7 N O2 | NA | Pyrroline-carboxylic acid |
| | | | | | (M+HCOO)- | 2.03 | C5 H7 N O2 | | |
| PM$_{2.5\text{-}0.25}$ | 125.0155 | 7.71 | Down | 0.07 | (M+H)+ | | No matches | NA | |
| PM$_{0.25}$ | 130.0632 | 2.98 | Up | 1.16 | (M-H)- | 1.37 | C6 H10 O3 | NA | |
| PM$_{2.5\text{-}0.25}$ | 146.0191 | 2.04 | Up | 12.12 | (M-H)- | 7.21 | C6 H2 N4 O | NA | |
| PM$_{2.5\text{-}0.25}$ | 187.1635 | 12.46 | Up | 2.31 | (M+H)+ | 4.71 | C9 H21 N3 O | NA | N1-Acetylspermidine |
| PM$_{2.5\text{-}0.25}$ | 196.0386 | 2.01 | Down | $<10^{-4}$ | (M-H)- | 1.75 | C10 H4 N4 O | | |
| | | | | | (M-H)- | 6.90 | C9 H8 O5 | | |
| | | | | | (M-H)- | 7.18 | C6 H12 O5 S | | |
| PM$_{2.5\text{-}0.25}$ | 245.0895 | 3.24 | Up | 3.22 | (M-H)- | | No matches | NA | |
| | | | | | (M+H)+ | 18.43 | C14 H30 N2 O3 | | |
| PM$_{0.25}$ | 339.99 | 3.62 | Down | 0.38 | (M-H)- | 4.27 | C8 H9 N2 O11 P | NA | |
| | | | | | (M-H)- | 6.06 | C9 H5 N6 O7 P | | |
| | | | | | (M-H)- | 3.59 | C6 H14 O12 P2 | | |
| | | | | | (M-H)- | 5.80 | C7 H10 N4 O8 P2 | | |
| PM$_{0.25}$ | 387.0234 | 1.92 | Down | 0.23 | (M-H)- | 2.91 | C13 H14 Cl N5 O3 S2 | NA | |
| | | | | | (M-H)- | 4.67 | C12 H18 Cl N O7 S2 | | |
| PM$_{2.5\text{-}0.25}$ | 397.3233 | 1.74 | Up | 4.93 | (M+H)+ | | No matches | NA | |

| | | | | | | | | |
|---|---|---|---|---|---|---|---|---|
| $PM_{0.25}$ | | | Up | 7.10 | | | | |
| $PM_{2.5-0.25}$ | 455.1172 | 1.63 | Down | 0.41 | (M+H)+ | 2.98 | Many candidates | NA |
| $PM_{0.25}$ | 504.963 | 3.65 | Down | 0.15 | (M-H)- | 4.82 | C16 H3 N5 O15 | NA |
| | | | | | (M-H)- | 5.25 | C10 H14 N5 O11 P3 S | |
| $PM_{0.25}$ | 590.9512 | 9.16 | Down | 0.15 | (M+H)+ | 2.30 | C15 H16 N O18 P3 | NA |
| | | | | | (M+H)+ | 3.35 | C14 H15 N3 O17 P2 S | |
| | | | | | (M+H)+ | 4.84 | C8 H16 N7 O16 P3 S | |
| | | | | | (M+H)+ | 3.12 | C16 H22 N O11 P5 S | |
| | | | | | (M+H)+ | 4.39 | C17 H11 N3 O17 P2 | |
| $PM_{2.5-0.25}$ | 684.2775 | 14.42 | Down | 0.30 | (M+2H)+2 | 1.47 | C22 H45 N12 O9 S2 | NA |
| | | | | | (M+2H)+2 | 0.89 | C26 H53 O16 P S | |
| | | | | | (M+2H)+2 | 1.73 | C25 H52 N2 O15 S2 | |
| | | | | | (M+2H)+2 | 2.27 | C27 H59 O9 P3 S2 | |
| $PM_{0.25}$ | 789.578 | 0.80 | Up | 8.21 | (M+H)+ | 3.23 | C36 H71 N17 O S | NA |
| | | | | | (M+H)+ | 3636.50 | C39 H79 N7 O7 S | |
| | | | | | (M+H)+ | 3.78 | C35 H75 N13 O5 S | |
| | | | | | (M+H)+ | 5.37 | C42 H75 N7 O7 | |
| $PM_{2.5-0.25}$ | 898.2564 | 2.39 | Down | 0.18 | (M-H)- | 1.95 | C32 H44 N12 O15 P2 | NA |
| | | | | | (M-H)- | 1.83 | C37 H47 N4 O20 P | |
| | | | | | (M-H)- | 2.85 | C35 H50 N2 O23 S | |
| | | | | | (M-H)- | 2.79 | C26 H45 N16 O14 P3 | |
| $PM_{0.25}$ | 978.8655 | 7.90 | Up | 7.32 | (M+H)+ | 1.84 | Many candidates | NA |
| $PM_{2.5-0.25}$ | 1003.0735 | 6.84 | Down | 0.24 | NA | | | |

**Table S 3**: Apolar features showing significant changes in A549 cells when exposed to real doses of the two assessed fractions. F: major fragment; NA: not adquired; NL: neutral loss

| Fraction | Mass (amu) | Retention time (min) | Regulation | Fold change | Precursor Ion | Average Mass error (ppm) | Molecular formula | Major fragments and neutral loses | Identification |
|---|---|---|---|---|---|---|---|---|---|
| $PM_{2.5-0.25}$ | 735.4230 | 6.23 | Down | 0.58 | (M+H)+ | 1.57 | C39 H59 N7 O5 P | | |
| | | | | | (M+H)+ | 1.06 | C37 H64 N5 O6 P2 | | |
| | | | | | (M+H)+ | 1.04 | C36 H68 N O10 P2 | | |
| | | | | | (M+H)+ | 3.20 | C38 H63 N3 O9 P | | |
| | | | | | (M+H)+ | 2.45 | C43 H63 N O7 P | | |
| | | | | | (M+H)+ | 3.89 | C41 H54 N9 O4 | | |
| | | | | | (M+H)+ | 2.42 | C38 H58 N9 O4 S | | |
| | | | | | (M+H)+ | 2.62 | C37 H62 N5 O8 S | | |
| | | | | | (M+H)+ | 1.89 | C31 H50 N19 O3 | | |
| $PM_{2.5-0.25}$ | 773.5363 | 10.3 | Down | 0.74 | (M+H)+ | 1.11 | C45 H76 N O7 P | F 120.9681 [C2 H2 O4 P]+ | Phosphatidylethanolamine |
| $PM_{0.25}$ | 787.516 | 9.58 | Up | 1.09 | (M+H)+ | 0.76 | C36 H69 N9 O10 | F 441.233 [C23 H39 O4 P2]+, [C19 H35 N6 O2 P2]+ or [C19 H34 N6 O4 P]+ | Phosphatidylethanolamine |
| | | | | | (M+H)+ | 2.71 | C39 H75 N5 O7 P2 | | |
| | | | | | (M+H)+ | 0.72 | C38 H74 N7 O6 P S | | |
| $PM_{0.25}$ | 872.6890 | 18.34 | Up | 1.47 | (M+H)+ | 1.30 | C57 H92 O6 | NL 228.2089 [C14 H28 O2]+ | Triglyceride |
| $PM_{2.5-0.25}$ | 890.6809 | 11.58 | Down | 0.89 | (M-H)- | 0.75 | Many candidates | NA | Phosphatidylglycerol |

| | | | | | | | |
|---|---|---|---|---|---|---|---|
| $PM_{0.25}$ | 1306.055 | 18.91 | Up | 1.82 | (M+H)+ | 0.84 | C79 H135 N9 O6 |
| | | | | | (M+H)+ | 0.77 | C76 H144 N3 O11 P |

**Table S 4**: Polar features showing significant changes in A549 cells when exposed to real doses of the two assessed fractions. F: major fragment; NA: not adquired; NL: neutral loss

| Fraction | Mass (amu) | Retention time (min) | Regulation | Fold change | Precursor Ion | Average Mass error (ppm) | Molecular formula | Major fragments and neutral loses | Identification |
|---|---|---|---|---|---|---|---|---|---|
| $PM_{0.25}$ | 115.0652 | 7.87 | Up | 16.43 | (M+H)+ | 11.61 | C5 H9 N O2 | NA | Proline |
| $PM_{0.25}$ | 238.0585 | 4.91 | Up | 7.87 | (M+H)+ | 0.13 | C8 H15 O6 P | NA | |
| | | | | | (M+H)+ | 7.67 | C10 H10 N2 O5 | | |
| | | | | | (M+H)+ | 5.56 | C7 H14 N2 O5 S | | |
| $PM_{0.25}$ | 280.0363 | 2.82 | Up | 3.26 | (M-H)- | | | NA | |
| $PM_{0.25}$ | 306.0906 | 7.71 | Up | 5.81 | (M+H)+ | 2.06 | C11 H20 N2 O4 P2 | NA | |
| | | | | | (M+H)+ | 2.42 | C11 H18 N2 O6 S | | |
| | | | | | (M+H)+ | 8.99 | C8 H14 N6 O7 | | |
| | | | | | (M+H)+ | 7.09 | C12 H19 O7 P | | |
| | | | | | (M+H)+ | 7.95 | C8 H22 N2 O6 S2 | | |
| $PM_{0.25}$ | 329.064 | 2.03 | Down | 0.82 | (2M-H)- | 4.19 | C12 H16 N3 O8 P S | NA | |
| $PM_{0.25}$ | 493.458 | 0.84 | Up | $>10^4$ | (M+H)+ | 2.39 | C26 H55 N9 | NA | |
| | | | | | (M+H)+ | 8.27 | C30 H59 N3 O2 | | |
| $PM_{0.25}$ | 663.1122 | 9.37 | Down | 0.24 | (M+2H)+2 | 0.95 | C23 H19 N15 O6 P2 | NA | |
| | | | | | (M+2H)+2 | 3.70 | C32 H26 N O13 P | | |
| | | | | | (M+2H)+2 | 4.08 | C28 H34 N3 O6 P5 | | |
| | | | | | (M+2H)+2 | 5.46 | C29 H18 N11 O7 P | | |
| $PM_{2.5-0.25}$ | 853.4364 | 1.31 | Up | 5.44 | (M+NH4)+ | 0.00 | Many candidates | NA | |
| $PM_{2.5-0.25}$ | 1244.9044 | 1.01 | Down | 0.39 | (M+H)+ | 1.85 | C63 H19 N3 O15 P3 S3 | NA | |

UNIVERSITAT
ROVIRA i VIRGILI